N-Heterocyclic carbene ligands bearing redox-active and non-innocent moieties in combination with transition metals

Inauguraldissertation

zur Erlangung der Würde eines Doktors der Philosophie vorgelegt der Philosophisch- Naturwissenschaftlichen Fakultät der Universität Basel

von

Ewa Adela Miłopolska

aus Polen

Basel 2019

Genehmigt von der Philosophisch-Naturwissenschaftlichen Fakultät auf Antrag von:

Prof. Dr. Thomas R. Ward

Prof. Dr. Catherine Housecroft

Basel, den 21. März 2017

Prof. Dr. Martin Spiess
Dekan

In loving memory of my grandmother, Adela Miłopolska

“Thank you” to my beloved Mom-without her support and love it would be much harder.

If you do not know where you are going, you will not get there.

We breathe till we have hope.

I hereby declare that this doctoral dissertation

"N-Heterocyclic carbenes bearing redox-active and non-innocent moieties in combination with transition metals."

has been completed only with the assistance mentioned herein and that it has not been submitted for award to any other university nor to any other faculty at the University of Basel.

Table of Contents

Chapter 2

Synthesis and coordination chemistry of *N*- heterocyclic carbene ligands bearing quinone moiety

Chapter 3

Synthesis and coordination chemistry of *N*- heterocyclic carbene ligands bearing pyridinone moiety

Chapter 1

General introduction

1. Challenging reactions in Nature

Nature is an excellent architect that designed systems to perform very challenging reactions that require the rigorous shuttling of multiple electrons and protons over long distances. This challenge was overcome by highly evolved enzymes, which include both metals and organic cofactors (containing HAT- Hydrogen Atom Transfer Moieties). Multiple elementary reaction steps allow to avoid high activation barriers and carry out reactions with low energetic cost and precise management of electrons and protons.

Photosystem II is an excellent example of a natural enzyme that catalyzes a challenging reaction. During water oxidation four protons and electrons are produced. If not intercepted quickly, a radical-hydrogen atom would be formed. This deleterious side reaction would prevent the utilization of electrons and protons to create electrochemical power. Photosystem II is the most powerful water splitting system. Within millions of years Nature has created proton coupled electron transfer (PCET hereafter) that allows to transfer protons and electrons over long distances and prevent radical side reactions.[1-9] Photosystem II consists of two crucial structural elements, which involve hydrogen bond interactions and enable electron and proton transfer at each site (Scheme 1).

The process of water oxidation starts with light-induced sensitization of cytochrome P680 (Scheme 1). The sensitization is followed by rapid transfer of electron from P680 through pheophitin to benzoquinone. The oxidized P680 is a powerful oxidant and immediately oxidizes Tyr161-OH. It has been demonstrated that without His190, the formation of radical Tyr161-$O^{\cdot}$ is not

possible.[8] The second important structural element is located in the oxygen-evolving complex (OEC hereafter). The interaction between $MnOH_2$ in the OEC and Asp61-carbonyl allows proton transfer from the OEC to the chloroplast lumen which protects the system from charge accumulation.[8] Knowledge of he reaction mechanism of photosystem II stimulated the rational design of novel synthetic catalysts.

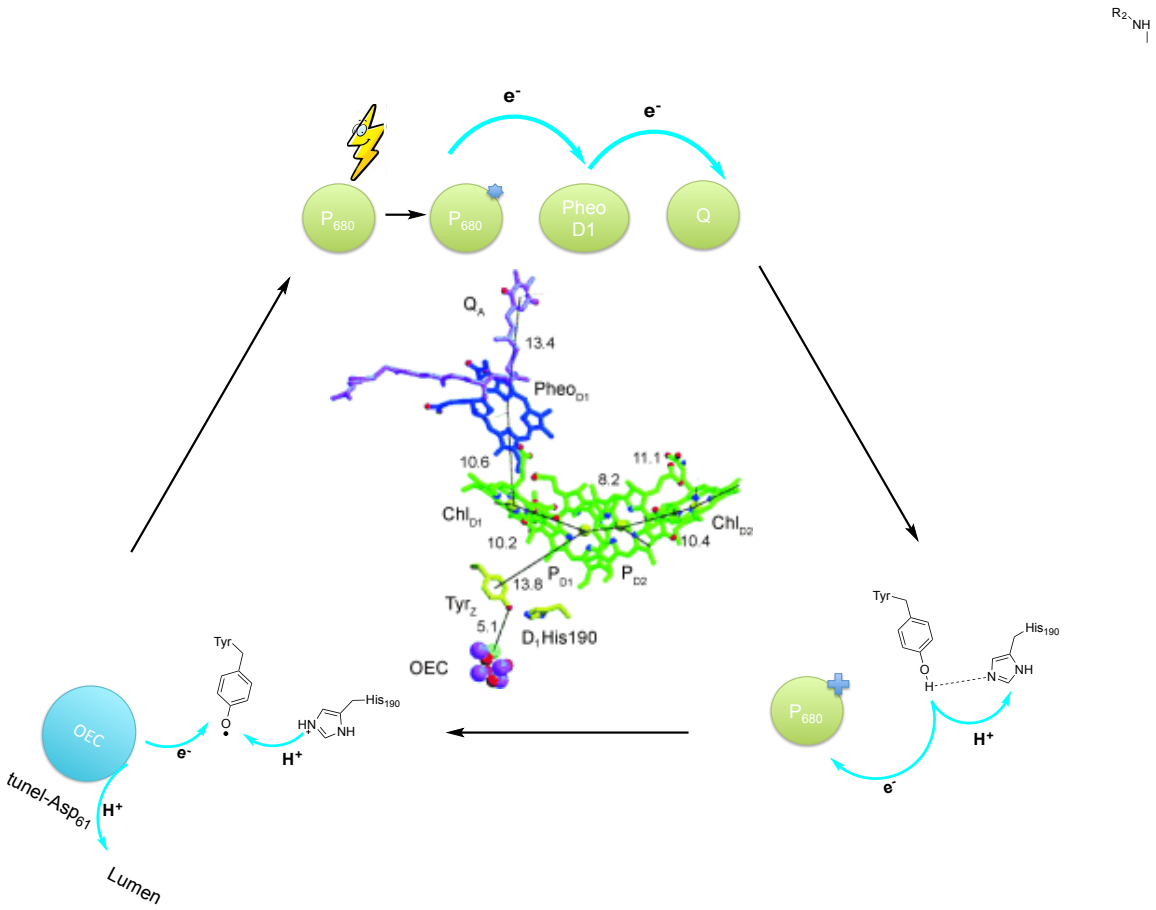

Scheme 1. Simplified mechanism of the crucial steps of water oxidation performed by photosystem II. The structure of the reaction centre of photosystem II was addapted from Meyer.[8]

Another example of a challenging natural reaction that involves a tyrosyl radical is galactose oxidase (GO hereafter). The GO active site contains a

Cu^{II}-ion and tyrosyl radical.[10] The galactose oxidation process involves three steps (Scheme 2). In the first step, the alcohol substrate coordinates to the metal center. In the second step, a β-hydrogen atom abstraction from the substrate by the tyrosyl radical occurs. Hydride abstraction followed by alcohol oxidation leads to aldehyde formation. The aldehyde is released from the active site and the tyrosyl radical and the copper II is recycled by reaction with dioxygen.[11-13]

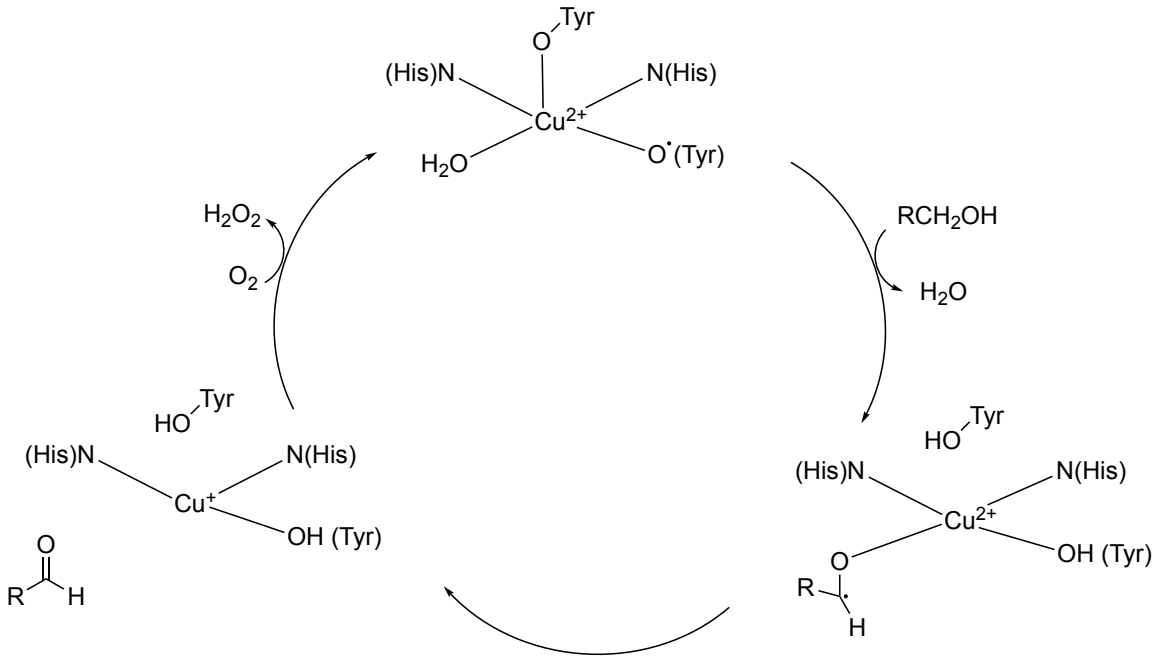

Scheme 2. Mechanism of alcohol oxidation performed by GO.

Hydrogenases constitute another family of enzymes that involve PCET. Iron-only hydogenase (HmD hereafter) contains in its active site an iron guanylylpyridinol (FeGP) cofactor and a non-iron sulfur cluster. The HmD splits hydrogen into H^+ and H^- while maintaining iron in the +II oxidation state.[14-17] This is possible due to the coordination of the pyridinol ligand that

can exist in two forms: a neutral and anionic form.[14] The catalytic center of iron-only hydrogenase is displayed in Figure 1.

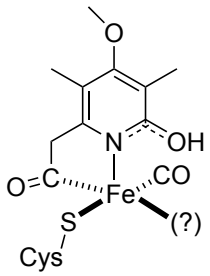

Figure 1. The catalytic centre in iron-only hydrogenase with non-innocent ligand.

Finally, in alcohol dehydrogenase the catalytic redox reaction occurs at cofactor NAD^+/NADH cofactor couple (Scheme 3).[18-19] The reaction belongs to the major pathways of alcohol metabolism. The role of the catalytic center, which contains a redox neutral zinc, is to bind and activate the substrate.[18]

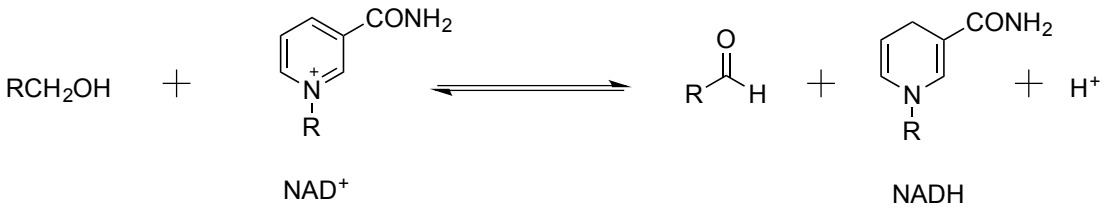

Scheme 3. The role of NAD^+ in alcohol oxidation, catalyzed by alcohol dehydrogenase.

2. Redox-active and non-innocent ligands

2.1. Introduction

All the mechanistically relevant structural elements described in section 1 such as: quinones, tyrosil-radical or NAD^+, can accept and release single protons and electrons. This allows the transport of electrons and protons over a long range. The mechanistic tools employed by Nature are a major source of inspiration to develop redox-active and non-innocent ligands in bio-inspired catalysis.

2.2. Redox-active ligands

2.2.1. Catechols

Catecholates exist in three oxidation states: quinone, semiquinone and catecholate (Scheme 3). Since they are part of many biological processes they are the most investigated group of redox active ligands.[20-21] The oxygen within catechols can be substituted by other heteroatoms, which opens possibilities to tune complex stability or activity.

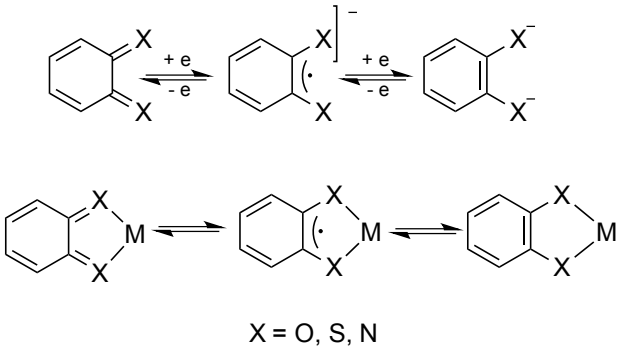

Scheme 4. The resonance structures of the catecholate-type redox active ligands.

Catechols are widely used in catalysis. Their remarkable features are highlighted by the following examples.

In 2005 Heyduk reported the d^0- complex **1** performing oxidative addition. The reaction occurs thanks to the redox active ligand.[22,23] Later catechols were replaced by *o*-phenyldiamines, which resulted in a higher stability of the complex with an oxidized ligand.[22] Similarly, 2-amidophenolate was employed as a ligand in dihydrogen oxidation by Rauchfuss.[24]

In contrast to Heyduk, Soper coordinated the ligand to Co(III).[25] During the reaction, the ligands in complex **2** undergo a one electron oxidation and form

the semiquinone imine complex (Scheme 5). The same complex **2** also found application in transformation of 1,2-diphenyl hydrazine. In both cases, the oxidation state of the metal remains unchanged throughout the reaction. This demonstrates that redox active ligands may serve as electron reservoirs and thus mimic the role of precious metals in 2 electrons transformations anymore.

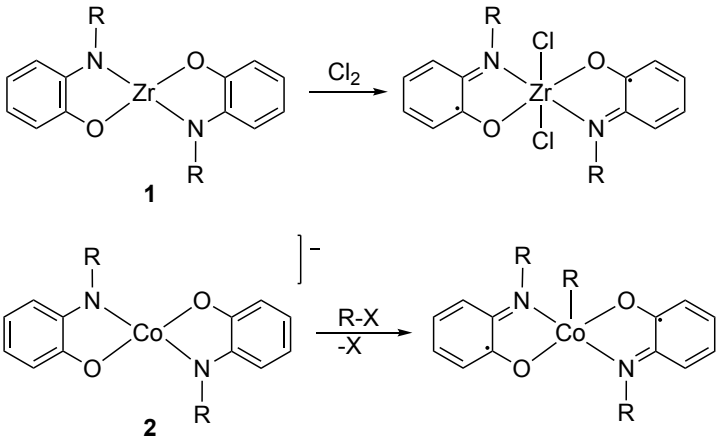

Scheme 5. Complexes introduced by Heyduk[23] and Soper,[25] allowing ligand mediated oxidative addition.

A noteworthy system for the oxidation of secondary amines to imines was designed by Stahl (Scheme 6).[26] The complex **3** is composed of redox neutral zinc coordinated to 1,10-phenanthroline-5,6-dione.

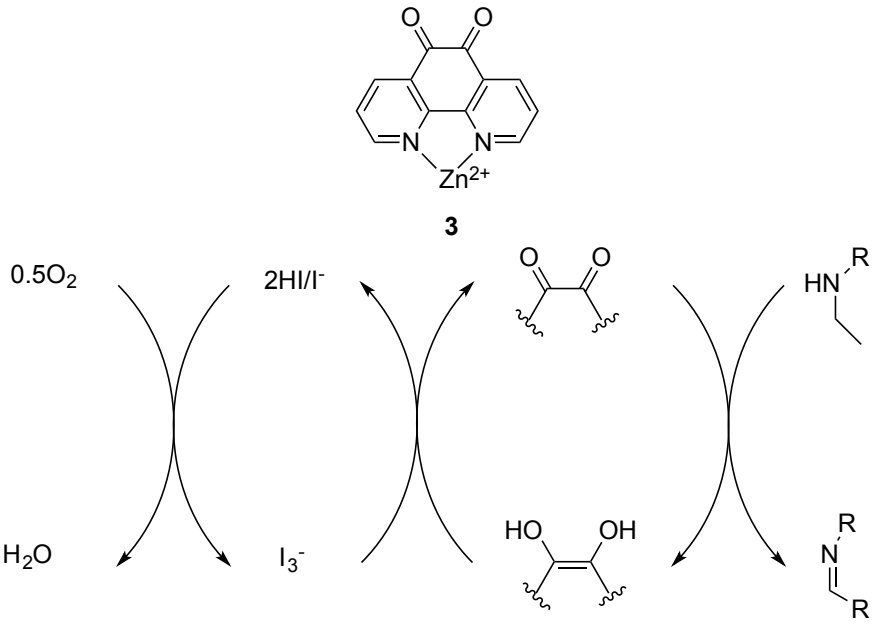

Scheme 6. Bioinspired system for oxidation of secondary amines and nitrogen heterocycles.

Oxidation reactions are crucial steps in many complex synthetic processes. Palladium(II) complexes found multiple applications in this area. It is important to mention that Pd belongs to the group of precious metals. It has been mentioned in section 2, that nature overcomes high-energy barriers by splitting reactions into several multielectron processes.

An illustrative example of such a system, acting in a biomimetic fashion is the Wacker oxidation of ethylene to acetaldehyde. In this process ethylene is oxidized to acetaldehyde by oxygen, catalyzed by $PdCl_2$ and $CuCl_2$ (Scheme 7a).[27] It has been discovered that electrons can easily be transferred from Pd(0) to $CuCl_2$ which is therefore protected from precipitation as palladium black.[28]

In Pd oxidation chemistry direct oxidation of Pd(0) to Pd(II) by oxygen is very often too slow in comparison to decomposition. The use of polar solvents in the Wacker reaction requires addition of chloride ions to stabilize system $PdCl_2/CuCl_2/O_2$ that results in the formation of chlorinated by-products.[29-30] Due to that pitfall, industry developed a new chloride-free Wacker reaction relying on a catalytic system composed of $Pd(OAc)_2$/BQ and a macrocyclic iron complex, shuttling electrons between BQ and O_2.[31-32]

Further investigation improved the results by replacing the iron macrocyclic complex with Co(salophen}$_2$ complex **4**.[31,33] Quinones were also successfully employed in reactions such us: methane oxidation (Scheme 7c)[34], palladium C-H activation of benzoic acids[35] or 1,4 oxidation of 1,3-dienes (Scheme 7d).[31]

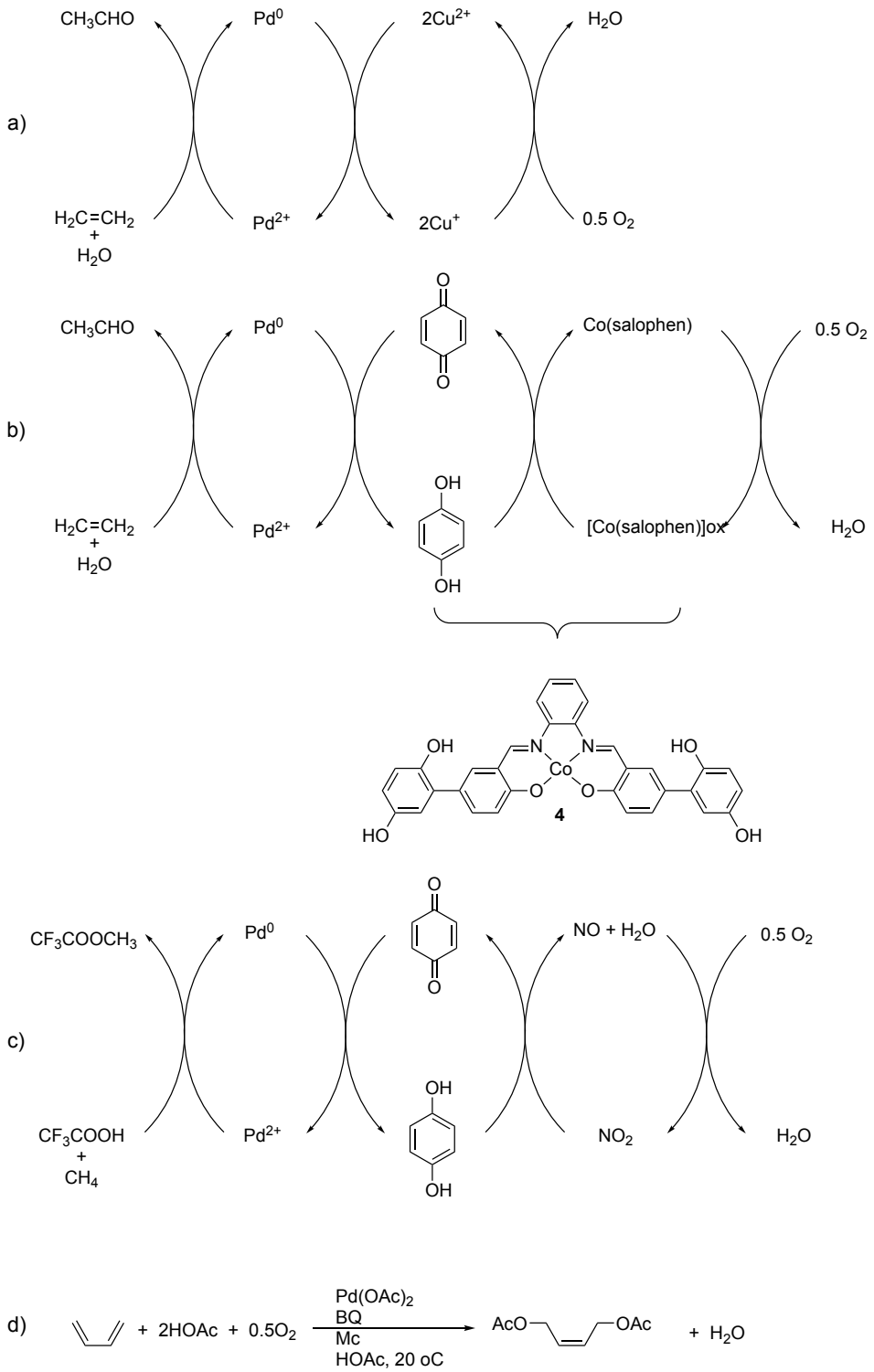

Scheme 7. Oxidations performed by biomimetic catalytic system: a) Wacker oxidation b) Wacker oxidation with hybrid Electron Transfer Mediator c) Bao's Methane oxidation d) 1,4 oxidation of 1,3 dienes.

Ruthenium complexes poses the ability to act as dehydrogenation as well as hydrogenation catalysts.[36-38] It is known that during alcohol oxidation ruthenium forms {RuH} species. To increase the catalytic rate, oxidation of alcohols can be performed with the assistance of well-documented HAT such as quinones and TEMPO radical, which readily react with hydride species. The idea was successfully employed by Sheldon and Bäckvall.[37,39,40]

Water oxidation is a very active field. Newly designed systems recognize the importance of hydrogen bonding and the necessity of introducing groups which are able to release and accept protons and electrons. The first highly potent system was developed by Meyer[41] with a so-called ruthenium blue dimer **5**. The complex displays remarkable activity in water oxidation, which is probably based on high-valent ruthenium intermediates. This success was followed by Tanaka's[42-44] complex **6** which in contrast to Meyer's blue dimer **5** involves shuttling between Ru^{II} and Ru^{III}, attached with two (semiquinone/ quinone) redox couples. Interesting results were also presented by Akermark[45] who combined ruthenium with benzimidazole and phenol motifs (complexes **7** and **8**).

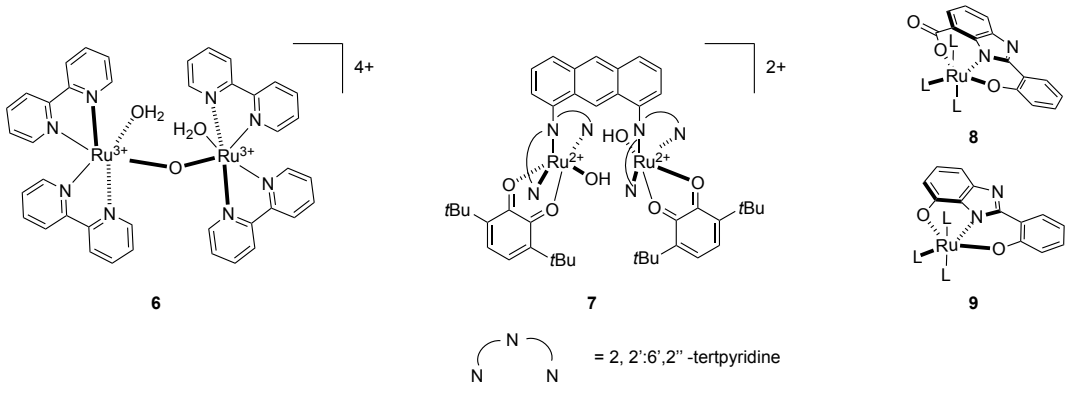

Figure 2. Four catalysts employed in water oxidation: 6-Meyer's blue dimmer, 7- Tanaka's complex, 8,9- Akemark's complexes.

2.2.2. Imino pyridines

The first complexes of Co(II), Ni(II) and Fe(II) with bis-hydrazone pyridine were reported in 1950 by Busch and Stoufer.[46] In 1998 complexes with sterically hindered bisimino pyridines were reported for their high activity towards polymerization reactions.[47] The new group of hindered bisimino pyridines was pioneered by Brookhardt[48] and Gibson.[49]

The ligands can be synthesized by reacting two equivalents of aniline with 2,6- diacetyl pyridine.[50] The complexation reaction of the ligand with MX_2 ($M=Co^{II}$, Fe^{II}, Ni^{II}, X=Cl or Br) occurs in THF or *n*-butanol. Those complexes are in fact precatalysts. In case of ethylene polymerization, the complex is activated *in situ* in the presence of MAO.[50] Complex **9** with a redox active ligand is obtained by reduction with sodium amalgam under nitrogen atmosphere.[51] Complex **9** exists in three mesomeric structures (Scheme 8).

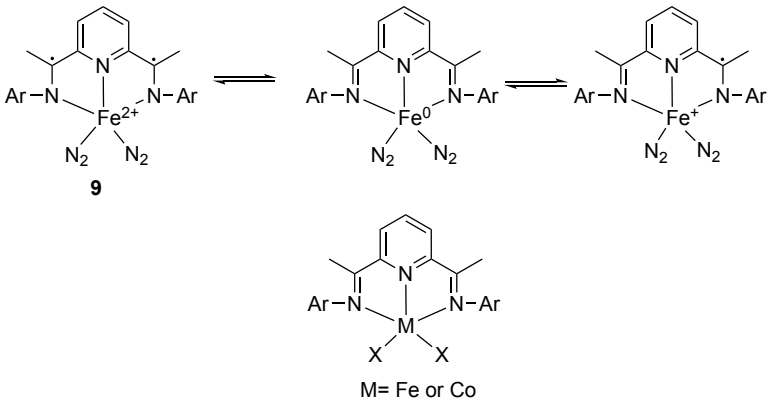

Scheme 8. Pyridine-bis-imine ligands as a redox-active ligands.

The complex **10** was successfully employed in the [2+2] cycloaddition of dienes (Scheme 9a). It has been shown that the reaction does not proceed without the redox-active ligand. The complex **10** also found an application in

the hydrosilylation reaction for inactivated olefins with tertiary olefins (Scheme 9b).

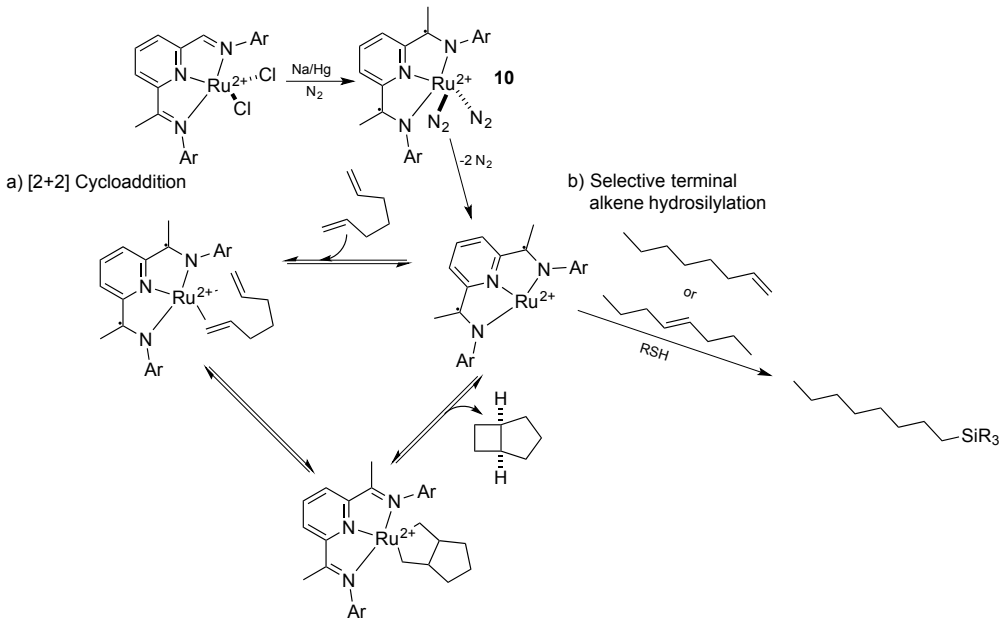

Scheme 9. a)The mechanism of the [2+2] cycloaddition b) selective terminal alkene hydrosilylation.

2.3. Non-innocent ligands

As mentioned in section 2.1, non-innocent ligands can exist in two forms, neutral and ionic. This feature is especially interesting in the context of designing a pH responsive catalyst.

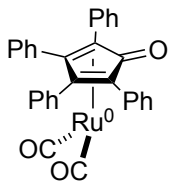

11

Figure 2. Shvo's ruthenium complex.

Probably the most famous catalyst bearing a non-innocent ligand is Shvo's ruthenium complex **11** (Figure 2).[52-53] The complex found utility in organic synthesis as a very versatile catalyst with interesting features. In contrast to $[RuCl_2(PPh_3)_3]$, catalyst **11** in Oppenauer oxidation or allylic alcohols isomerization, does not require the use of base.[52] Its iron analogue **12** introduced by Knölker attracted attention as a hydrogenation catalyst and is very interesting because of the low price and toxicity.[54] The two forms of complex **12** again suggest that the ligand acts as an electron reservoir (Scheme 11).

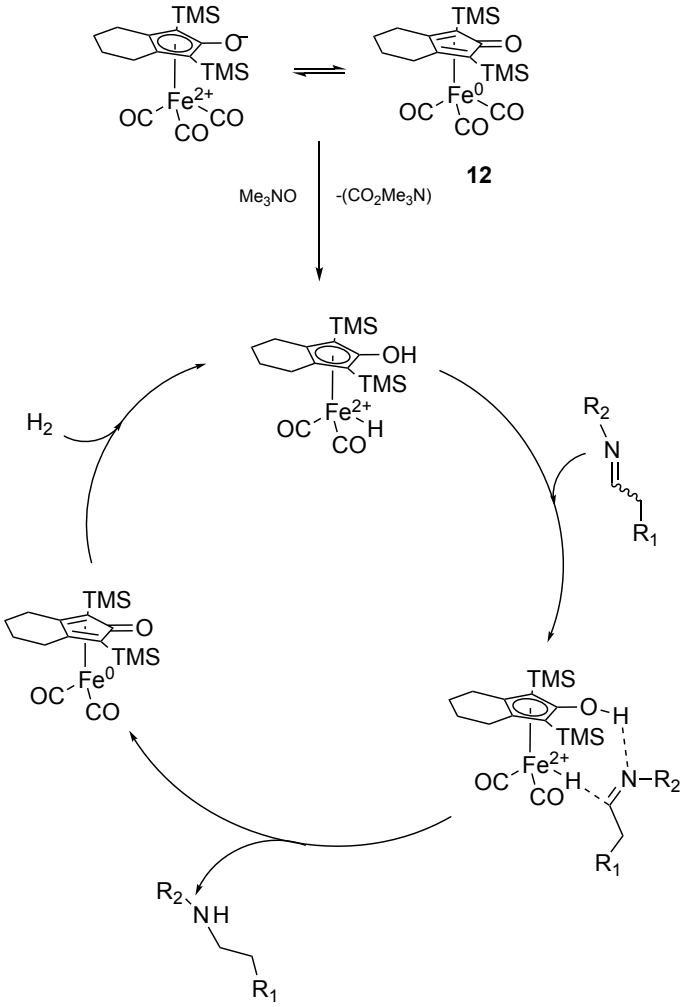

Scheme 11. Reductive amination of aliphatic aldehydes and imines with the use of Knölker's complex as a catalyst.

Another important functional group worth mentioning is the pyridone moiety. Milstein and co-workers have exploited several pincer complexes catalyzing challenging reactions.[55-64] One of them, ruthenium pincer complex **13** presents an fascinating ability to split water.[65]

Complex **13** was previously also used as a powerful catalyst for the esterification of alcohols,[66] dehydrogenative coupling of alcohols with amines to give amides[67] and coupling of alcohols with amines to form imines.[68]

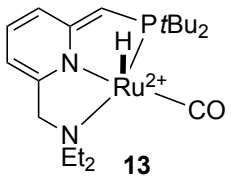

13

Figure 4. Ruthenium complex bearing a non-innocent ligand.[66]

To slow down global warming, the attention of many researchers was drawn towards carbon capturing by transforming CO_2 into formic acid. Formic acid is widely used in organic synthesis, has a high potency to release H_2 and is a liquid at ambient temperature.[69-71]

Nozaki,[72,73] Hazari[74] and Peris[75] have shown a strong enhancement effect of NHC and PNP ligands in Ir(III) catalysis performing hydrogenation of carbon dioxide. In 2007 Himeda[76] reported hydrogenation proceeding at very mild conditions: water, 30 °C with a TOF of 3.5 h^{-1}. Following the results of Himeda, Fukuzumi[77] achieved a TOF of 6.8 h^{-1} at the same conditions. In 2012 Himeda in cooperation with Fujita achieved the reaction proceeding at room temperature and under atmospheric pressure. The strong improvement of the catalysis resulted from the application of the non-innocent ligand Thbpym (4,4',6,6'-tetrahydroxy-2,2'-bipyrimidine).[78] The ligand is flanked with hydroxyl groups positioned close to the catalytic centre, therefore they can behave as a base to facilitate H_2-heterolysis. Because of that, the energetic barrier of the Ir-H_2 adduct formation is lowered and this results in milder reaction conditions.[78] The entries 1 and 4 in Table 1 illustrate the significant role of the second coordination sphere in the reaction of carbondioxide hydrogenation.

Besides iridium, Himeda and Fujita combined a non-innocent ligand with Co(III), performing carbon dioxide hydrogenation in water.[79] Table 1 summarizes the catalysts and conditions used for the reactions mentioned above.

Bispyridinol ligands were also employed by Fujita and Yamaguchi in several other transformations, including: acceptorless alcohol dehydrogenation (AAD),[80-84] water oxidation,[85,86] transfer hydrogenation[87] or reversible dehydrogenation-hydrogenation reaction of nitrogen heterocycles.[88,89]

	Year	Name	Catalyst	Conditions	TOF [h^{-1}]
1	2007	Himeda	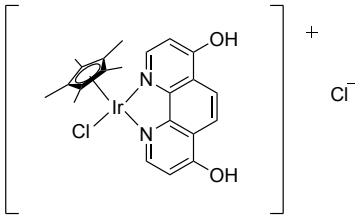 **14**	30 °C, 0.1 MPa, 0.1M K_2CO_3	3.5
2	2012	Fukuzumi	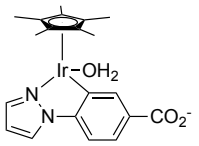 **15**	30 °C, 0.1 MPa, 0.1 M K_2CO_3	6.8
3	2012	Fujita and Himeda	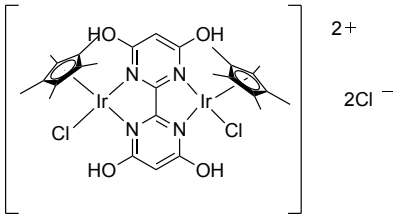 **16**	25 °C, 0.1 MPa, 1 M $NaHCO_3$	64
4	2012	Fujita and Himeda	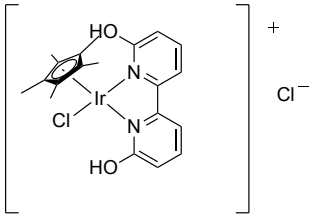 **17**	25 °C, 0.1 MPa, 1 M $NaHCO_3$	7
5	2013	Himeda and Fujita	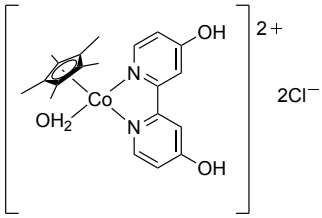 **18**	80 °C, 4 MPa, 1 M $NaHCO_3$	39

Table 1. The table summarizing improvement of the iridium(III) catalyst with non-innocent ligand in the reaction of carbon dioxide hydrogenation.

3. *N*-Heterocyclic carbenes

3.1. Introduction

Carbenes are neutral compounds with a divalent carbon and six valence electrons. The divalent carbon is covalently bound to two adjacent groups and has two nonbonding electrons that can exist either as a singlet or as triplet.

N-heterocyclic carbenes constitute a special group of carbenes, which are an important subject of this thesis.

For a very long time carbenes were considered as extremely reactive and not possible to isolate. Pioneering work in the use of NHCs as ligands for metal complexes came from Wanzlik and Öfel in 1968.[90,91]

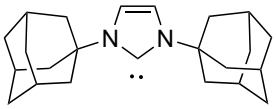

Figure 5. First synthesized and isolated NHC carbene described by Arduengo.

In 1991 Arduengo published crystalline, stable and storable NHC with two adamantyl groups (Figure 5).[92] Since then, the field has been developing exponentially.[93-96]

3.2. Carbenes as a ligands

Persistent carbenes can exist either in a singlet or a triplet state. As singlet carbenes can be isolated and stored under inert atmosphere, triplet carbenes can only be observed at most.[92,94,96-98]

Steric hindrance, which is still a topic of discussion, undoubtly plays a role in stabilizing carbenes by protecting them from dimerization.

Another important stabilizing factor is conjugation. Unsaturated NHC carbenes are much more stable than unsaturated, which is also predicted by the aromaticy rule of Hückel.[96,99,100]

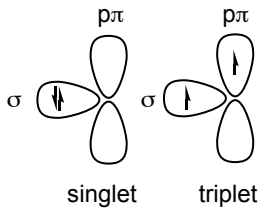

Figure 6. Electronic configurations of carbenes.

Whether the carbene is in a singlet or a triplet state is determinated by the relative energy gap between two orbitals σ-p_π (Figure 6). If the energy gap is higher than 40 kcal/mol, the singlet state is preferred and electrons are paired in one orbital. Carbenes in a triplet state have two electrons in different orbitals and are described as diradicals. The σ-orbital is stabilized by electron withdrawing substituents which force the carbene into a singlet state. The opposite situation appears when σ-donating substituents are used. In this case the σ orbital is destabilized which

decreases the energy gap and the triplet state becomes accessible. In case of NHC carbenes, especially the ones having two nitrogens in the ring, the energy gap between singlet and triplet state is 65-68 kcal/mol. This explains why they adopt a singlet state.[97] The observed stability stems from the inductive effect of the electron withdrawing substituents that stabilize the σ -orbital[97] and p_π -donation from the nitrogen atoms into empty orbital p_π of the carbon atom.[95]

3.3. Comparison of phosphines with NHCs

Very often NHCs are described as mimics of phosphines, which is not fully true. Phosphines are geometrically very different than NHCs. Substituents on P are pointed away from the metal and create a cone (Figure 7). The steric demand of these ligands can be described by Tolman's cone angle. In the case of NHCs the situation appears more complicated. The substituents are pointed towards the metal centre and additionally can rotate, which changes their steric and electronic properties. To describe the steric demand of these ligands, Nolan introduced the parameter $\%V_{bur}$ -percent volume burried.[101] In his model he assumes that the bond between metal and NHC has always the same length for all ligands. The bulkier the NHC, the larger the part ofthe sphere $\%V_{bur}$ which will be occupied by the ligand. As substituents in phosphines are bound to the coordinating atom, the electronic and steric properties cannot be tuned separately as in the case of NHCs. Another very important difference is that NHCs are much stronger σ donors[102] than

phosphines and they can act as π-acceptors in a number of complexes,[103-104] that result in stronger bonds.

Figure 7. Comparison of the steric effect of phosphine's and NHCs as ligands for metals.

N-heterocyclic carbenes have found a wide use in catalysis. They opened up new possibilities to organometallic chemistry as the NHC complexes turned out to be prone to oxidative addition. This feature found wide application in Heck reactions[98,102,105-108]

NHCs bearing quinones were described by Colbran **19**, and Bielawski **20**-**21** and Their catalytic properties are still beeing explored. Colbran also presented complex **22** in which the NHC is functionalized with nicotinamide.[109] Recently a new, interesting Ru complex **23** was described. It contains an NHC ligand, capable of accepting a proton during a catalytic cycle.[110] Several groups have exploited the use of NHCs in switchable catalysis. For example Bielawski and Nelson presented a photo-modulated transestrification.[111] In another example the electron donating abilities of NHCs were modified by a change of pH in ring opening metathesis polymerization.[112]

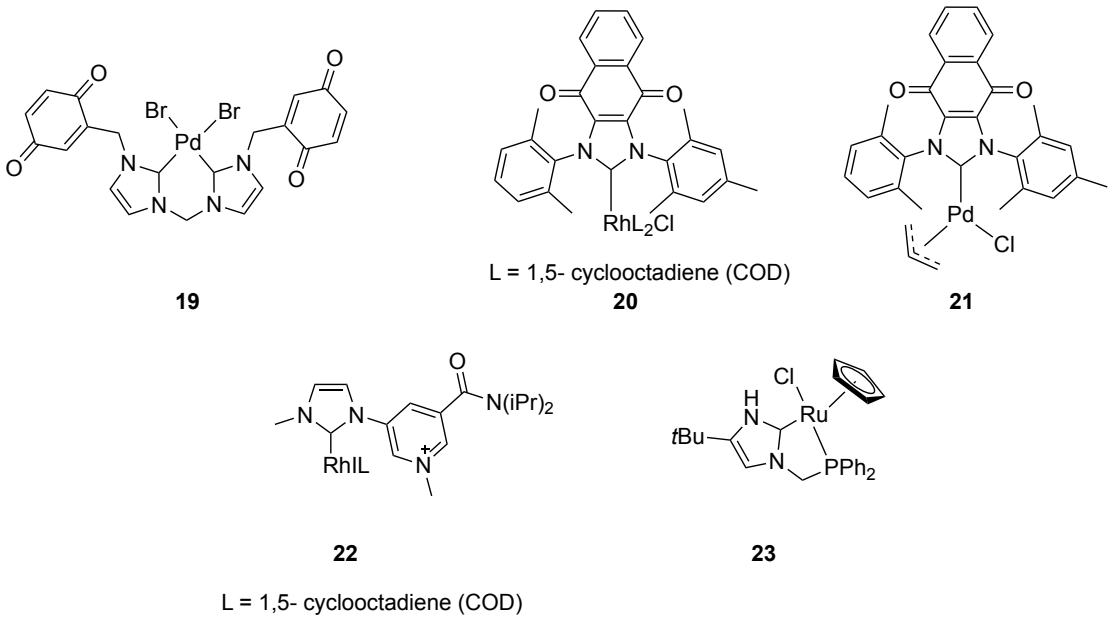

Figure 8. Complexes with NHCs bearing quinones and redox-active ligands.

In contrast to other ligands, NHCs form very stable complexes with early and late transition metals as well as with low and high oxidation state metals. This feature is particularly attractive in the context of multi-electron redox processes.

4. Outlook

In this introduction, we highlighted progress achieved in the field of redox-active and non-innocent ligands. In certain examples they can be temporarily bound to the metal centre like in the modified Wacker[27,113] process where quinone binds to Pd^0 to reoxidize the metal. In other cases they can constitute the backbone of the complex. Most of these complexes still employ precious second- and third-row transition metals. This raises the main focus on connecting these ligands with earth aboundant first-row metals such as: Fe, Mn, Co, Ni etc. As it has been shown by Heyduk[23] they can serve as an electron reservoir and facilitate the an oxidative addition step in connection with zirconium in its highest oxidation state. They can also support metals in delivering or accepting additional electrons, therefore allowing processes requiring 2 electron redox reactions to occur.

Some computational results highlight the role of non-innocent ligands in catalysis[80] but some of the mechanistic steps still remain unclear. For a deeper understanding of the electronic balance between the metal and the ligand, which is responsible for the catalytic activity of the complex, further spectroscopic and computational studies are needed.

5. References

[1] M. H. V. Huynh, T. J. Meyer, *Chem. Rev.* **2007**, *107*, 5004.

[2] J. M. Mayer, *Annu. Rev. Phys. Chem.* **2004**, *55*, 363.

[3] C. W. Hoganson, G. T. Babcock, Science **1977**, *277*, 1953.

[4] R. I. Cukier, D.G. Nocera, *Annu. Rev. Phys. Chem.* **1998**, *49*, 337.

[5] M. Sjödin, S. Styring, B. Åkermark, A. L. Sun, L. Hammarström, *J. Am. Chem. Soc.* **2000**, *122*, 3932.

[6] D. R. Weinberg, C. J. Gagliardi, J. F. Hull, C. F. Murphy, C. A. Kent, B. C. Westlake, *Chem. Rev.* **2012**, *112*, 4016.

[7] J. M. Mayer, D. A. Hrovat, J. L. Thomas, W. T. Borden, *J. Am. Chem. Soc.* **2002**, *124*, 11142.

[8] T. J. Meyer, M. H. V. Huynh, H. H. Thorp, *Angew. Chem. Int. Ed.* **2007**, *46*, 5284.

[9] S. Hammes-Schiffer, *Acc. Chem. Res*. **2001**, *34*, 273.

[10] N. Ito, S. E. V. Phillips, C. Stevens, Z. B. Ogel, M. J. McPherson, J. N. Keen, *Nature* **1991***, 350*, 87.

[11] L. Que, W. B. Tolman, *Nature* 2008, *455*, 333.

[12] P. Gamez, I. A. Koval, J. Reedijk, *Dalton Trans.* **2004**, 4079.

[13] A. J. Baron, C. Stevens, C. Wilmot, K. D. Senevirante, V. Blakelay, D. Dooley, *J. Biol. Chem*. **1994**, *269*, 25093.

[14] V. K. K. Praneeth, M. R. Ringenberg, T. R. Ward, *Angew. Chem. Int. Ed. Engl.* **2012**, *51*, 10228.

[15] T. R. Simmons, G. Berggren, M. Bacchi, M. Fontecave, V. Artero, *Coord .Chem. Rev.* **2014,** *270*, 127.

[16] M. J. Corr, J. A. Murphy, *Chem. Soc. Rev.* **2011**, *40*, 2279.

[17] D. Chen, R. Scopelliti, X. Hu, *Angew. Chem. Int. Ed.* **2010**, *49*, 7512.

[18] J. F. Biellmann, *Acc. Chem. Res.* **1986**, 321.

[19] S. Hammes-Schiffer, S. Benkovic, *Annu. Rev. Biochem.* **2006**, *75*, 519.

[20] W. Kaim, B. Schwederski, *Coord. Chem. Rev.* **2010**, *254*, 1580.

[21] D. X. L. L. J. Broere, R. Plessius, J. I. van der Vlugt, *Chem. Soc. Rev.* **2015**, *44*, 6886.

[22] N. A. Ketterer, H. Fan, K. J. Blackmore, X. Yang, J.W. Ziller, M.-H. Baik, *J. Am. Chem. Soc.* **2008**, *130*, 4364.

[23] K.J. Blackmore, J.W. Ziller, A.F. Heyduk, *Inorg. Chem.* **2005**, *44*, 5559.

[24] M. R. Ringenberg, M. J. Nilges, T. B. Rauchfuss, S. R. Wilson, *Organometallics* **2010**, *29*, 1956.

[25] A. L. Smith, K. I. Hardcastle, *J. Am. Chem. Soc.* **2010**, *132*,14358.

[26] A. E. Wendlandt, S.S. Stahl, *J. Am. Chem. Soc.* **2014***, 136*, 506.

[27] J. K. Stille, R. Divakaruni, *J. Organomet. Chem.* **1979**, *169*, 239.

[28] J. Piera, J.-E. Bäckvall, *Angew. Chem. Int. Ed.* **2008,** *49,* 3506.

[29] P. M. Henry, *J. Am. Chem. Soc.* **1964,** *88*, 1595.

[30] P. M. Henry, *J. Am. Chem. Soc.* **1964**, *86*, 3246.

[31] A. K. Awasthi, M.M. Mader, H. Grennberg, R. B. Hopkins, J. E. Bäckvall, *J. Am. Chem. Soc.* **1990**, *112,* 5160.

[32] B. Hopkins, J.E. Bäckvall, *Tetrahedron Letters*. **1988**, *29*, 2885.

[33] E. V. Johnston, E. A. Karlsson, S. A. Lindberg, B. Åkermark, J.-E.

Bäckvall, *Chem. Eur. J.* **2009**, *15*, 6799.

[34] Z. An, X. Pan, X. Liu, X. Han, X. Bao, *J. Am. Chem. Soc.* **2006**, *128*, 16028.

[35] Y.-H. Zhang, J.-Q. Yu, *J. Am. Chem. Soc.* **2009**, *131*, 14654.

[36] J.-E. Bäckvall, R.L. Chowdhury, U. Karlsson, *J. Chem. Soc., Chem. Commun.***1991**, 473.

[37] Á. Zsigmond, F. Notheisz, G. Csjernyik, J.-E. Bäckvall, *Top. Catal.* **2002**, *19*, 119.

[38] G.-Z. Wang, U. Andreasson, J.-E. Bäckvall, *J. Chem. Soc., Chem. Commun.* **1994,** 1037.

[39] A. Dijksman, A. Marino-González, A. Mairata i Payeras, I. W. C. E. Arends, R.A. Sheldon, *J. Am. Chem. Soc.* **2001**, *123,* 6826.

[40] A. Dijksman, I. W. C. E. Arends, R.A. Sheldon, *Platin. Met. Rev.* **2001**, *45*, 15.

[41] J. J. Concepcion, J. W. Jurss, M. K. Brennaman, P. G. Hoertz, A. O. T. Patrocinio, N. Y. Murakami Iha, *Acc. Chem. Res*. **2009**, *42*, 1954.

[42] S. Ghosh, S. Ghosh, M.-H. Baik, M.-H. Baik, *Angew. Chem. Int. Ed.* **2011**, *51*, 1221.

[43] S. Ghosh, M.-H. Baik, *Inorg. Chem.* **2011**, *50,* 5946.

[44] J. T. Muckerman, D. E. Polyansky, T. Wada, K. Tanaka, E. Fujita, *Inorg. Chem.* **2008**, *47*, 1787.

[45] M. D. Kärkäs, T. Åkermark, E. V. Johnston, S. R. Karim, T. M. Laine, B.-L. Lee, *Angew. Chem. Int. Ed.* **2012**, *51*, 11589.

[46] R. C. Stoufer, D. H. Busch, *J. Am. Chem. Soc.* **1956**, *78*, 6018.

[47] V. C. Gibson, S. K. Spitzmesser, *Chem. Rev.* **2003**, *103,* 283.

[48] B. L. Small, M. Brookhart, A. M. A. Bennet, *J. Am. Chem. Soc.* **1998**, *120*, 4049.

[49] G. J. P. Britovsek, V. C. Gibson, S. J. McTavish, G. A. Solan, A. J. P. White, D. J. Williams, *Chem. Commun.* **1998**, 849.

[50] V. C. Gibson, C. Redshaw, G. A. Solan, *Chem. Rev.* **2007**, *107*, 1745.

[51] S. C. Bart, K. Chłopek, E. Bill, M.W. Bouwkamp, E. Lobkovsky, F. Neese, *J. Am. Chem. Soc.* **2006,** *128*, 1390.

[52] R. Karvembu, R. Prabhakaran, K. Natarajan, *Coord. Chem. Rev.* **2005**, *249*, 911.

[53] Y. Shvo, D. Czarkie, Y. Rahamim, *J. Am. Chem. Soc.* **1986**, *108*, 7402.

[54] H.-J. Knölker, E. Baum, H. Goesmann, R. Klauss, A*ngew. Chem. Int. Ed. Engl.* **1999**, *38*, 2064.

[55] R. Langer, G. Leitus, Y. Ben-David, D. Milstein, *Angew. Chem. Int. Ed.* **2011**, *50*, 2120.

[56] C. Gunanathan, D. Milstein, *Acc. Chem. Res.* **2011**, *44*, 588.

[57] R. Langer, Y. Diskin-Posner, G. Leitus, L. J. W. Shimon, Y. Ben-David, D. Milstein, *Angew. Chem. Int. Ed.* **2011**, *50*, 9948.

[58] M. Feller, E. Ben-Ari, M. A. Iron, Y. Diskin-Posner, G. Leitus, L. J. W. Shimon, *Inorg. Chem.* **2010**, *49*, 1615.

[59] E. Balaraman, B. Gnanaprakasam, L. J. W. Shimon, D. Milstein, *J. Am. Chem. Soc.* **2010**, *132*, 16756.

[60] B. Gnanaprakasam, Y. Ben-David, D. Milstein, *Adv. Synth. Catal.*

2010, *352*, 3169.

[61] T. Zell, R. Langer, M. A. Iron, L. Konstantinovski, L. J. W. Shimon, Y. Diskin-Posner, *Inorg. Chem.* **2013**, *52*, 9636.

[62] D. Srimani, Y. Ben-David, D. Milstein, *Chem. Commun*. **2013**, *49*, 6632.

[63] C. Gunanathan, D. Milstein, *Chem. Rev.* **2014**, *114*, 12024.

[64] J. Zhang, G. Leitus, Y. Ben-David, D. Milstein, *Angew. Chem. Int. Ed. Engl.* **2006**, *45*, 1113.

[65] S. W. Kohl, L. Weiner, L. Schwartsburd, L. Konstantinovski, L. J. W. Shimon, Y. Ben-David, Science **2009**, *324*, 74.

[66] J. Zhang, G. Leitus, Y. Ben-David, D. Milstein, *J. Am. Chem. Soc.* **2005**, *127*, 10840.

[67] C. Gunanathan, Y. Ben-David, D. Milstein, Science **2007**, *317*, 787.

[68] B. Gnanaprakasam, J. Zhang, D. Milstein, *Angew Che*m. **2010,** *122*, 1510.

[69] S. Enthaler, J. von Langermann, T. Schmidt, *Energy Environ. Sci.* **2010**, *3*, 1207.

[70] T. C. Johnson, D. J. Morris, M. Wills, *Chem. Soc. Rev.* **2010**, *39*, 81.

[71] B. Loges, A. Boddien, F. Gärtner, H. Junge, M. Beller, *Top. Catal.* **2010**, *53*, 902.

[72] R. Tanaka, M. Yamashita, K. Nozaki, *J. Am. Chem. Soc.* **2009**, *131*, 14168.

[73] R. Tanaka, M. Yamashita, L.W. Chung, K. Morokuma, K. Nozaki, Organometallics **2011**, *30*, 6742.

[74] T. J. Schmeier, G. E. Dobereiner, R. H. Crabtree, N. Hazari, *J. Am. Chem. Soc.* **2011**, *133*, 9274.

[75] A. Azua, S. Sanz, E. Peris, *Chem. Eur. J.* **2011**, *17*, 3963.

[76] Y. Himeda, N. Onozawa-Komatsuzaki, H. Sugihara, K. Kasuga, *Organometallics* **2007**, *26*, 702.

[77] Y. Maenaka, T. Suenobu, S. Fukuzumi, Energy Environ. Sci. **2012**, *5*, 7360

[78] W.-H. Wang, J. F. Hull, J. T. Muckerman, E. Fujita, Y. Himeda, *Energy Environ. Sci.* **2012**, *5*, 7923.

[79] Y. M. Badiei, W.-H. Wang, J. F. Hull, D. J. Szalda, J. T. Muckerman, Y. Himeda, *Inorg. Chem.* **2013**, *52*, 12576.

[80] G. Zeng, S. Sakaki, K.-I. Fujita, H. Sano, R. Yamaguchi, *ACS Catal.* **2014**, *4*, 1010.

[81] K.-I. Fujita, N. Tanino, R. Yamaguchi, *Org. Lett.* **2007**, *9*, 109.

[82] R. Kawahara, K.-I. Fujita, R. Yamaguchi, *J. Am. Chem. Soc.* **2012**, *134*, 3643.

[83] K.-I. Fujita, T. Yoshida, Y. Imori, R. Yamaguchi, *Org. Lett.* **2011**, *13*, 2278.

[84] R. Kawahara, K.-I. Fujita, R. Yamaguchi, *Angew. Chem. Int. Ed.* **2012**, *51*, 12790.

[85] J. DePasquale, I. Nieto, L.E. Reuther, C.J. Herbst-Gervasoni, J.J. Paul, V. Mochalin, *Inorg. Chem.* **2013**, *52*, 9175.

[86] T. Zhang, K.E. deKrafft, J.-L. Wang, C. Wang, L. Wenblin, *Eur. J. Inorg. Chem.* **2014**, *52*, 698.

[87] I. Nieto, M. S. Livings, J. B. Sacci, L.E. Reuther, M. Zeller,

E. T. Papish, *Organometallics* **2011**, *30*, 6339.

[88] R. Yamaguchi, C. Ikeda, Y. Takahashi, K.-I. Fujita, *J. Am. Chem. Soc.* **2009**, *131*, 8410.

[89] K.-I. Fujita, Y. Tanaka, M. Kobayashi, R. Yamaguchi, *J. Am. Chem. Soc.* **2014**, *136*, 4829.

[90] H. W. Wanzlick, H. J. Schonherr, *Angew*. *Chem. Int. Edit.* **1968**, *136*, 1.

[91] A. J. Arduengo, G. Jens, M. William, K. Roland, *Angew. Chem. Int. Edit.* **1998**, *37,* 1.

[92] A. J. Arduengo, R. L. Harlow, M. Kline, *J. Am. Chem. Soc.* **1991**, *113,* 361.

[93] L. Benhamou, E. Chardon, G. Lavigne, S. Bellemin-Laponnaz, V. César, *Chem. Rev.* **2011**, *111*, 2705.

[94] D. Bourissou, O. Guerret, F. P. Gabbaï, G. Bertrand, *Chem. Rev.* **2000**, *100*, 39.

[95] H. Jacobsen, A. Correa, A. Poater, C. Costabile, L. Cavallo, *Coord. Chem. Rev.* **2009**, *253,* 687.

[96] *W. A. Herman,* C. Kocher*, Angew. Chem. Int. Eng.* **1997**, *36*, 2162.

[97] H. Christoph, T. Walter, *Chem. Phys. Lett.* **1994**, *217*, 11.

[98] F. Glorius, N-Heterocyclic Carbenes in Transition Metal Catalysis, Volume *21* of the series Topics in Organometallic Chemistry, **2006**, 1.

[99] M. N. Hopkinson, Ch. Richter, M. Schedler, F. Glorius, *Nature* **2016**, *510*, 485.

[100] T. Dröge, F. Glorius, *Angew. Chem. Int. Ed.* **2010**, *49*, 6940.

[101] H. Clavier, S. P. Nolan, *Chem. Commun.* **2010**, *46*, 841.

[102] E. Peris, R. H. Crabtree, *Chem. Rev.* **2004**, *49*, 2239.

[103] U. Radius, F .M. Bickelhaupt, Organometallics **2008**, *27*, 3410.

[104] H. Jacobsen, A. Correa, C. Costabile, L. Cavallo, *J. Organomet. Chem.* **2006** , *691*, 4350.

[105] G. C. Fortman, S. P. Nolan, *Chem. Soc. Rev.* **2011**, *40*, 5151.

[106] K. Riener, S. Haslinger, A. Raba, M. P. Högerl, M. Cokoja, W. A. Herrmann, *Chem. Rev.* **2014**, *114*, 5215.

[107] M. J. Ingleson, M. J. Ingleson, R. A. Layfield, R. A. Layfield, *Chem. Commun.* **2012**, *48*, 3579.

[108] J. Czaban, B. M. Schertzer, K. Grela, *Adv. Synth. Catal.* **2013,** *355,* 1997.

[109] A. McSkimming, M. Bhadbhade, S. B. Colbran, *Dalton Trans.* **2010,** *39*, 10581.

[110] V. Miranda-Soto, D. B. Grotjahn, A. L. Cooksy, J. A. Golen, C. E. Moore, *Angew. Chem. Int. Ed.* **2010**, *50*, 631.

[111] B. M. Neilson, C. W. Bielawski, *J. Am. Chem. Soc.* **2012**, *134*, 12693.

[112] S.L. Balof, S.J. P'Pool, N.J. Berger, E.J. Valente, A.M. Shiller, H.-J. Schanz, *Dalton Trans.* **2008,** 5791.

[113] P. Teo, Z. K. Wickens, G. Dong, R. H. Grubbs, *Org. Lett.* **2012**, *14*, 3237.

Chapter 2

Synthesis and coordination chemistry of *N*- heterocyclic carbene ligands bearing a quinone moiety

1. Introduction

The functionalization of small molecule such as CO_2, CH_4, N_2, H_2O, etc., requires the orchestrated delivery of multiple protons and electrons. Nature has evolved several metalloenzymes that catalyze these challenging redox reactions with exquisite precision. These metalloenzymes achieve the activation of small molecule substrates with base metals, i.e. Fe, Cu, Mn, Ni, etc. often by combining the metal with a redox active organic cofactor, for example flavins, nicotinamide, quinones, etc.. The purpose of the metal is usually to bind the substrate and afford electron transfer, while the organic cofactor is used to shuttle protons and electrons.

The use of redox-active ligands metal complexes have attracted increasing attention in homogeneous catalysis because of their ability to address the challenges of multiple electron transfers.[1-16] In contrast, ligands capable of orchestrating the release and uptake both protons and electrons remain rare.[17-24] To address this challenge, and in view of its versatile bonding properties towards transition metals in all oxidation states, we selected an *N*-heterocyclic carbene (NHC) scaffold and set out to tether a quinone as H-atom transfer moiety.

Inspired by the ligands developed by Bielawski,[17] Heinicke,[21] Chen,[20] and Colbran[24] (Figure 1), we report on the synthesis, coordination, and characterization of transition metal complexes bearing an unsaturated NHC ligand. The NHC was tethered via a propylene linker to 1,4-naphthoquinone, **1** and will be discussed in section 2.1. In section 2.2 the synthesis and coordination properties of the NHC salts appended by methylene linker to quinones, will be discussed. In the final section, we focus on the synthesis of the NHC salts with quinones attached directly to the

imidazolium ring, the initial findings will be presented although the work is yet incomplete.

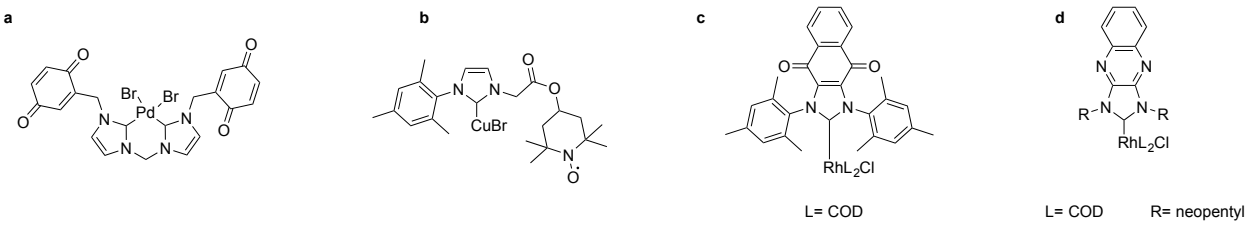

Figure 1. Metal complexes bearing NHC-ligands flanked with a HAT moiety reported by: a) Colbran[24] b) ; Chen[20]; c) Bielawski[17]; d) and Heinicke.[21]

2. Results and discussion

2.1. Synthesis and coordination properties of NHC salt with a propylene spacer between the naphthaquinone and the imidazolium ring

2.1.1. Synthesis

The imidazolium salt (H-**1**)$^{+}$Cl^{-} was synthesized in two steps by reacting *N*-mesitylimidazole with boc-protected 3-chloropropylamine. After the *in situ*-deprotection, the free amine was allowed react with 2,3-dichloro-1,4-naphthoquinone in the presence of triethylamine to afford (H-**1**)$^{+}$Cl^{-} in 48% overall yield. Stirring the imidazolium salt (H-**1**)$^{+}$Cl^{-} at RT in the presence of Ag_2O yielded the chloro-bridged complex [Ag(μ-Cl)(NHC-**1**)]$_2$ **2**.

The silver salt **2** was reacted with a series of (arene)metal dichloride dimer precursors; $[(\eta^6\text{-}C_6H_6)RuCl_2]_2$, $[(\eta^5\text{-}Cp^*)IrCl_2]_2$ and $[Pd(\eta^3\text{-allyl})Cl]_2$ to afford the corresponding complexes $[(\eta^6\text{-}C_6H_6)RuCl_2$(NHC-**1**)] **3**, $[(\eta^5\text{-}Cp^*)IrCl_2$(NHC-**1**)] **4** and $[PdCl(\eta^3\text{-allyl})$(NHC-**1**)] **5**, Scheme 1. For comparison purposes, the NHC-**2** lacking the naphthoquinone moiety and the corresponding complexes $[AgI$(NHC-**2**$)_2]$ **7**, $[(\eta^6\text{-}C_6H_6)RuCl_2$(NHC-**2**)] **8**, $[(\eta^5\text{-}Cp^*)IrCl_2$(NHC-**2**)] **9** and $[PdCl(\eta^3\text{-allyl})$(NHC-**2**)] **10** were prepared and characterized, Scheme 2.

The resulting organometallic complexes were characterized by ^{1}H and ^{13}CNMR spectroscopy. The overlaid ^{1}HNMR spectra of complexes **2-5** are presented in Figure 2. Upon deprotonation of (H-**1**)$^+Cl^-$ and complexation to Ru, Ir and Pd complexes,

the mesityl aromatic protons experience a deshielding which is also reflected by the shielding of the imidazole protons (H_i). The naphthoquinone protons are only moderately downfield shifted, suggesting that the interaction between the HAT moiety and the metal is minimal. Both methyl groups from mesityl moiety remain equivalent, except upon coordination of NHC-**1** to Pd.

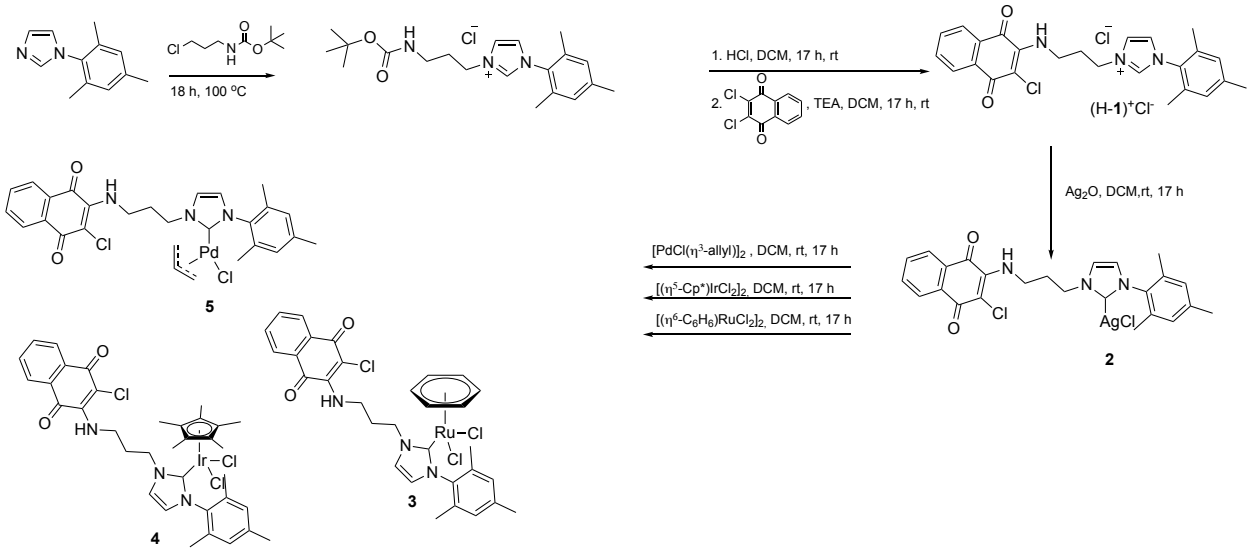

Scheme 1. Synthesis of an *N*-heterocyclic carbene ligand bearing a quinone moiety (NHC-**1**) and complexes thereof.

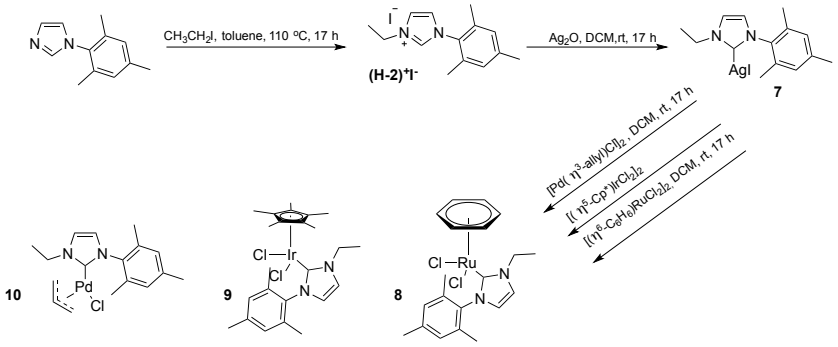

Scheme 2. Synthesis of reference complexes lacking the 1,4-naphthoquinone moiety.

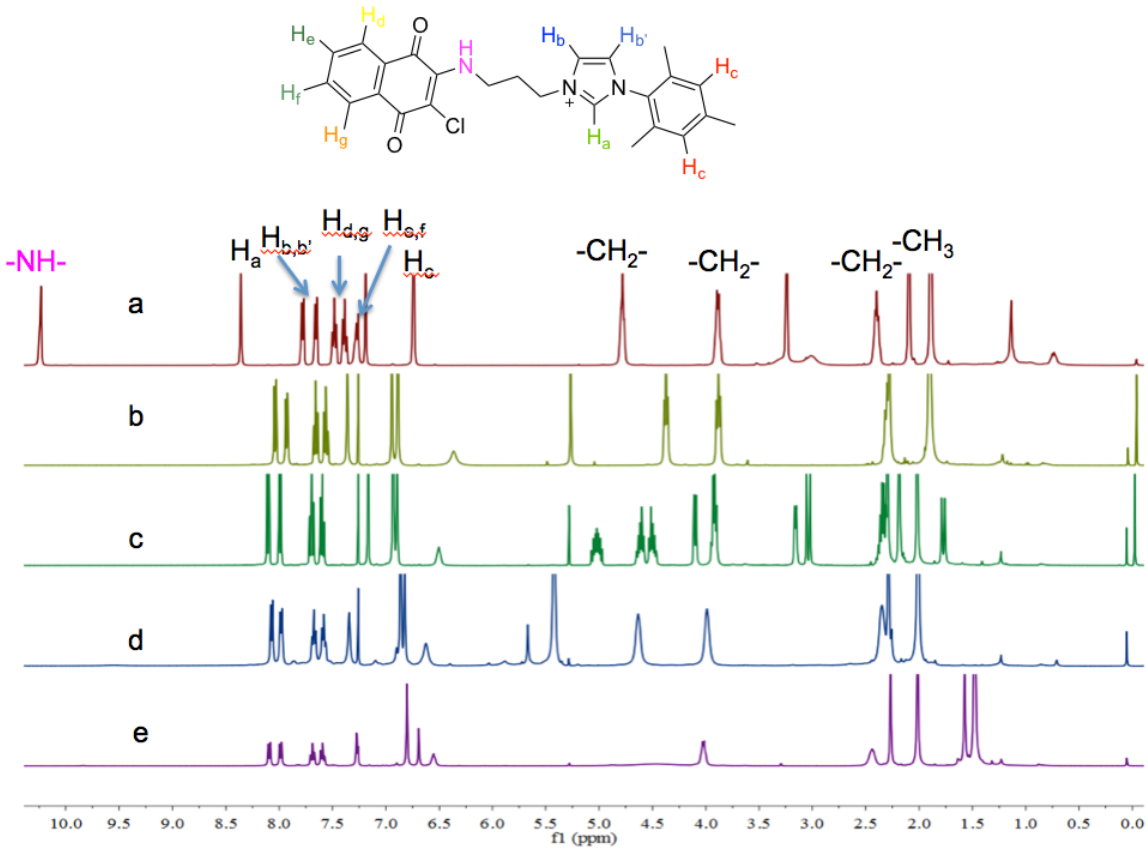

Figure 2. ^{1}HNMR spectra of a) (H-**1**)$^{+}$Cl^{-}, b) [Ag(μ-Cl)(NHC-**1**)]$_2$ **2**, c) [PdCl(η^3-allyl)(NHC-**1**)] **5**, d) [(η^6-C_6H_6)$RuCl_2$(NHC-**1**)] **3**, e) [(η^5-Cp*)$IrCl_2$(NHC-**1**)] **4.**

2.1.2. Cyclic voltammetry

The electrochemical behavior of the organometallic complexes bearing an H-atom transfer (HAT) moiety **2-5** as well as their reference compounds (H-**1**)$^{+}$Cl^{-} and complexes devoid of HAT **8-10** were investigated by cyclic voltammetry in dry, deoxygenated acetonitrile with of 0.1 M Bu_4NPF_6 as supporting electrolyte. The voltammograms are collected in Figure 3 and the corresponding reduction potentials are summarized in Table 1. For the NHC salt (H-**1**)$^{+}$Cl^{-}, the waves at -0.68

V and -1.13 V *vs.* SCE are assigned to the successive reductions steps of the naphthoquinone moiety. The first of these two potentials is cathodically shifted compared to 2,3-dichloronaphthoquinone, this is likely due to replacing an electron withdrawing chloride with a donating amine. The silver complex [Ag(μ-Cl)(NHC-**1**)]$_2$ **2** and the palladium complex [PdCl(η^3-allyl)(NHC-**1**)] **5** both display the two characteristic quinone-reduction waves. In addition, the [Ag(μ-Cl)(NHC-**1**)]$_2$ **2** exhibits an irreversible reduction wave at -1.11 V *vs.* SCE. A similar reduction is detected for the silver complex [AgI(NHC-**2**)$_2$] **7** at -1.16 V vs. SCE. We tentatively assign these irreducible reduction waves to Ag^+/Ag^0, leading to decomposition of the corresponding complexes. In the case of the iridium complex [(η^5-Cp*)IrCl$_2$(NHC-**1**)] **4** the quinone-based reductions occur at -0.67 and -1.24 V *vs.* SCE.

A presumably metal-based oxidation wave is present at 0.99 V *vs.* SCE. The first naphthoquinone reduction and the metal oxidation are irreversible, in contrast to their respective reference compounds [(η^5-Cp*)IrCl$_2$(NHC-**2**)] **9**. The ruthenium complex [(η^6-C$_6$H$_6$)RuCl$_2$(NHC-**1**)] **3** possesses two reversible naphthoquinone-based reduction

waves at -0.83 V and -1.37 V. An irreversible presumably metal-based oxidation wave occurs at 1.00 V. This stands in good agreement with the reference complex [(η^6-C$_6$H$_6$)RuCl$_2$(NHC-**2**)] **8**. The origin of the irreversible reduction wave in the cyclic voltammogram for the ruthenium complex [(η^6-C$_6$H$_6$)RuCl$_2$(NHC-**1**)] **3** at -0.65 V vs. SCE is unclear.

In general, the current associated with the first reduction wave of the quinone moiety of the complexes, except for the silver compound [Ag(μ-Cl)(NHC-**1**)]$_2$ **2**, is

significantly stronger than that associated with the second reduction wave. This reduction event was attributed to the adsorption of silver on the working electrode

	$E(M^{(n+1)+/n+})^a$	$E(NQ^{0/-})^a$	$E(NQ^{-/2-})^a$	additional waves[a]
(H-**1**)$^+$Cl$^-$		-0.68	-1.13	
2,3-dichloronaphthoquinone		-0.36	-1.04	
[Ag(μ-Cl)(NHC-**1**)]$_2$ **2**		-0.72	-1.29	-1.11[b]
[AgI(NHC-**2**)$_2$] **7**				-1.16[b]
[PdCl(η^3-allyl)(NHC-**1**)] **5**		-0.81	-1.34	
[PdCl(η^3-allyl)(NHC-**2**)] **10**				
[(η^5-Cp*)IrCl$_2$(NHC-**1**)] **4**	0.99[b]	-0.67[b]	-1.24	
[(η^5-Cp*)IrCl$_2$(NHC-**2**)] **9**	1.12			-0.88
[(η^6-C$_6$H$_6$)RuCl$_2$(NHC-**1**)] **3**	1.00[b]	-0.83	-1.37	-0.65[b]
[(η^6-C$_6$H$_6$)RuCl$_2$(NHC-**2**)] **8**	1.08[b]			

[a] half-wave potentials in V *vs.* SCE, measured in MeCN in presence of 0.1 M $TBAPF_6$; [b] irreversible

Table 1. Reduction potentials of the new compounds and their references extracted from the cyclic voltammograms (See Figure 3).

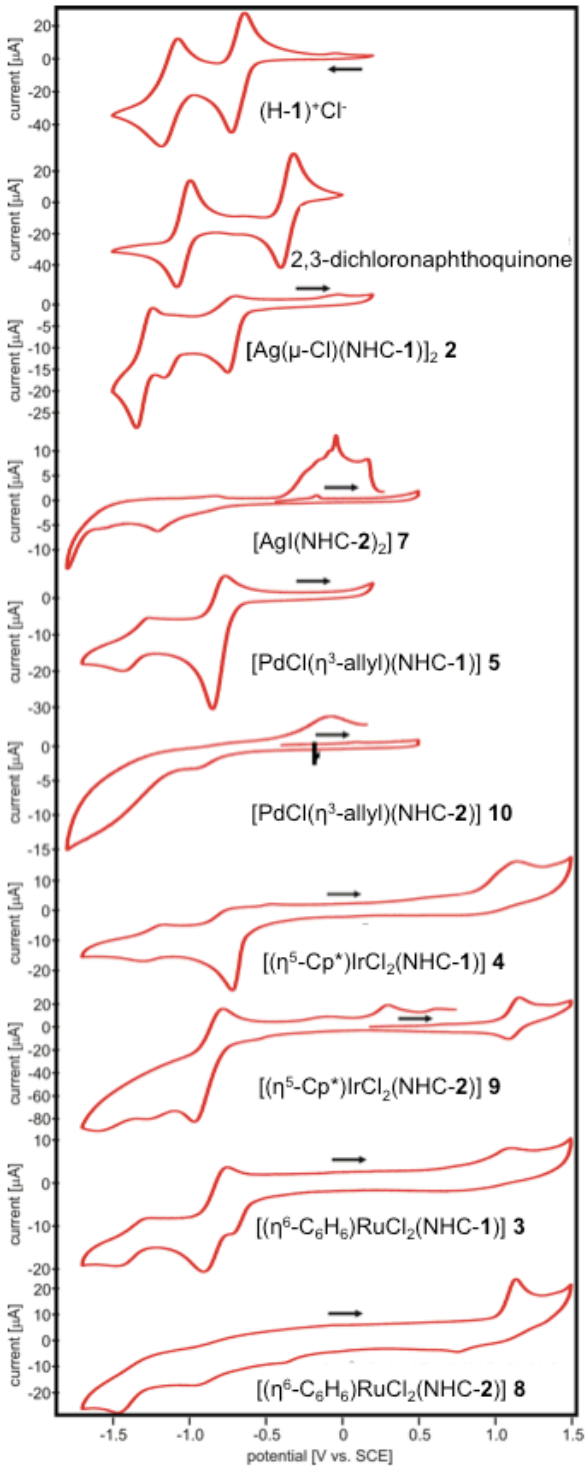

Figure 3. Cyclic voltammograms of the HAT-bearing complexes (containing NHC-**1)** and reference complexes devoid of the HAT moiety (containing NHC-**2**). (100mV/s scan rate; V vs. SCE).

2.1.3. Structural Characterization

In order to gain structural insight on the complexes bearing the NHC ligand **1**, both the silver complex [Ag(μ-Cl)(NHC-**1**)]$_2$ and the palladium complex [PdCl(η^3-allyl)(NHC-**1**)] were subjected to X-ray analysis. Suitable single crystals were obtained by slow diffusion of diethyl ether into a concentrated dichloromethane solution.

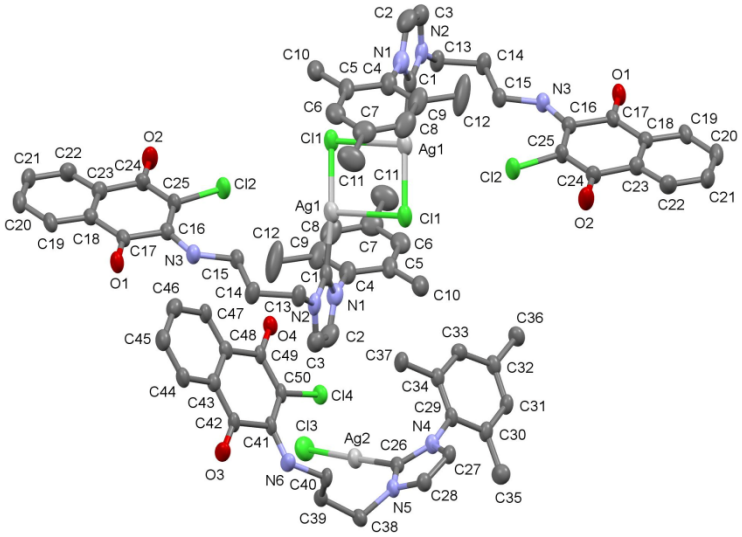

Figure 4. Crystal structure of [Ag(μ-Cl)(NHC-**1**)]$_2$ **2** displaying all non-hydrogen atoms. Solvents molecules were omitted.

The silver complex [Ag(μ-Cl)(NHC-**1**)]$_2$ **2** crystallizes in the centrosymmetric space group P-1. The asymmetric unit contains two formula units of the compound [Ag(μ-Cl)(NHC-**1**)]$_2$. One molecule is present as a monomer and the coordination geometry of the central Ag atom is linear. The second molecule has its Ag and Cl atoms located near one of the inversion centres of the P-1 space group. Although the distance between the Ag atom and the symmetry-generated Cl atom of the neighboring molecule is 2.9803(17) Å (i.e. longer than the Ag-Cl distance for the

monomeric building block (2.356 Å) a dimeric arrangement containing an Ag-Cl-Ag-Cl ring is present. Relevant angles and distances describing coordination around silver are collected in Table 2. No van-der-Waals contact between the HAT moiety and the silver ion is present: the quinone$_{centroid}$·····Ag distance is > 6.5 Å.

Distances [Å]		Angles [°]	
Ag_1-Cl_1^*	2.9803(17)	Cl_1^*-Ag_1-Ag_1^*	39.58(4)
Ag_1-Cl_1	2.356(2)	Cl_1 - Ag_1 -Cl_1	93.30(5)
Ag_1-C_1	2.084(8)	Ag_1^*-Ag_1-Cl_1	53.72(4)
Ag_2-Cl_3	2.3251(19)	Cl_1 - Ag_1 -Cl	95.19(18)
Ag_2-C_{26}	2.076(6)	Ag_1^*-Cl_1-Ag_1	86.70(5)
Ag_1 to quinone ring (centroid)	6.538	Cl_3-Ag_2-C_{26}	175.77(18)
Ag_2 to quinone ring (centroid)	6.787	Ag_1-Cl_1-C_1-Ag_1^* Cl_1^*-C_1^*	71.63

*symetry operator –x, -y+1, -z

Table 2. Selected geometrical parameters for complex [Ag(μ-Cl)(NHC-**1**)] **2**.

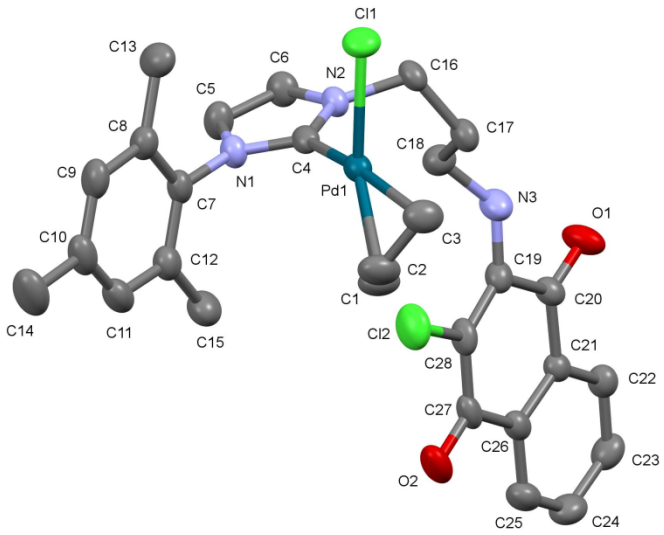

Figure 5. Crystal structure of [PdCl(η^3-allyl)(NHC-**1**)] **5** displaying all non-hydrogen atoms. Solvents molecules were omitted.

The palladium complex [PdCl(η^3-allyl)(NHC-**1**)] **5** crystallizes in the triclinic space group P-1. The coordination around the Pd site can be regarded as square planar with the allyl ligand occupying two coordination sites of the metal centre. The NHC-**1** moiety and one Cl atom occupy the two remaining coordination sites. Selected geometrical parameters for [PdCl(η^3-allyl)(NHC-**1**)] are collected in Table 3. In the propyl side-chain between N2 and N3, disorder is observed. The ratio of the site occupancy factors between the two disordered groups is about 5:1.

π-π- stacking is observed between the naphthoquinone and the neighbor in the lattice generated by the symmetry operator -x+1, -y+2, -z, the distance between the two best planes through the atoms C19 until C28 respectively is 3.450 Å. As for the silver complex [Ag(μ-Cl)(NHC-**1**)]$_2$ **2**, no van-der-Waals contact between the Pd ion and the naphthoquinone moiety is present.

A hydrogen bond is present between N3-H1...O1 where O1 is generated by the symmetry operator -x, -y+2, -z. Due to symmetry reasons, this hydrogen bond is present twice resulting in the formation of a ring

Distances [Å]		Angles [°]	
Pd-Cl1	2.370(8)	Cl1-Pd-C1	164.701(1)
Pd-C1	2.112(3)	Cl1-Pd-C2	130.291(1)
Pd-C2	2.152(3)	Cl1-Pd-C3	97.56(9)
Pd-C3	2.176(3)	Cl1-Pd-C4	92.65(8)
Pd-C4	2.036(3)	C1-Pd-C4	101.22(12)
Pd-quinone ring(centroid)	7.622	C2-Pd-C4	135.60(13)
		C3-Pd-C4	168.22(12)
		Pd1-Cl1-C4 to C4-N1-N2	71.28

Table 3. Selected Geometrical parameters for [PdCl(η^3-allyl)(NHC-**1**)] **5**.

2.2. Synthesis and coordination chemistry of *N*-heterocyclic carbene ligands bearing catechols or quinones with a methylene spacer

Next, we set out to synthesize NHC-ligands bearing a quinone moiety lying closer to the donor carbene C–atom. For this purpose, we exploited the quaternarization of a (substituted) imidazole by an activated halomethylene moiety: typically a benzylic halide (Scheme 3). Thanks to reasonable yield of the alkylation, further investigation of the corresponding imidazolium salts was possible

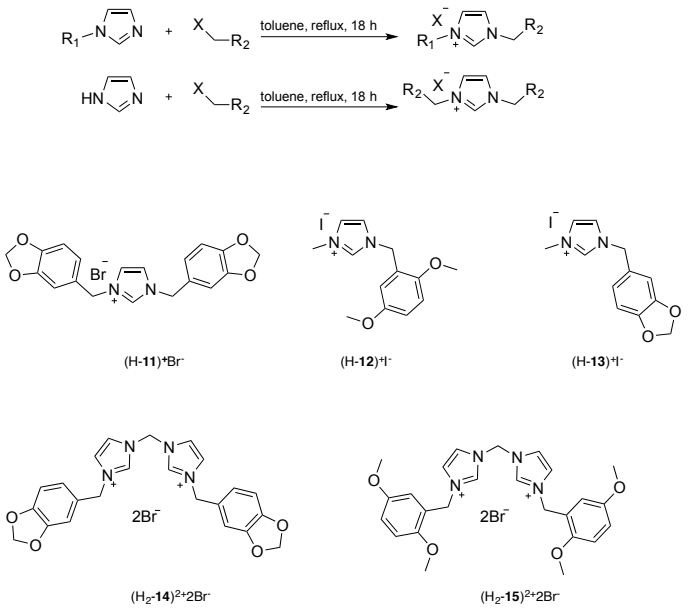

Scheme 3. Synthesis of the new imidazolium salts bearing a protected cathechol moiety. Salt (H-**13**)$^{+}$I^{-} and (H$_2$-**15**)$^{2+}$2Br^{-} were reproduced from literature protocols.[22]

Following Colbran's procedure,[24] we resynthesized complex **16** by reacting $Pd(OAc)_2$ with the imidazolium salt (H$_2$-**15**)$^{2+}$2Br^{-} and subsequent addition of BBr_3, The resulting precipitate was reacted in acetone with DDQ to yield complex **16**. All the analytical data confirmed the purity of the compound. Attempts to prepare the

analog compound **18** with an *o*-quinone moiety by reacting the salt $(H_2\text{-}\mathbf{14})^{2+}2Br^-$ with $Pd(OAc)_2$, lead to untractable mixtures. The MS analysis of the crude reaction did not reveal the presence of the fragment m/z 600, corresponding to the cationic complex **17**, therefore we could not proceed with synthesis of palladium complex **18**.

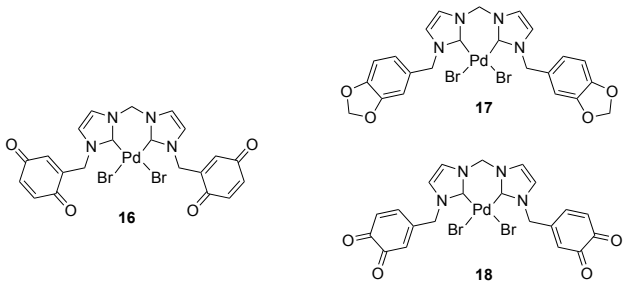

Figure 5. Palladium complexes with NHC bearing quinones. Complex **16**[24] served as a model for the synthesis of complexes **17** and **18**.

To obtain the palladium complex **20**, the salt $(H\text{-}\mathbf{11})^+Br^-$ was reacted with Ag_2O in CH_2Cl_2 and subsequently filtered into a solution containing $[Pd(\eta^3\text{-allyl})Cl]_2$. A white precipitate appeared. Filtration and subsequent addition of diethyl ether to the supernatant afforded the pure complex **19** in 66% yield. To deprotect the hydroxyl groups of the catechol, the complex **19** was reacted with BBr_3. Careful analysis of the ^{1}HNMR and ESI-MS revealed that during the deprotection step, complex $[PdCl(\eta^3\text{-allyl})(NHC\text{-}\mathbf{11})]$ **19** decomposes. As a main product, we observed deprotected salt $(H\text{-}\mathbf{22})^+Br^-$. In order to obtain complex **21**, we reacted the salt $(H\text{-}\mathbf{11})^+Br^-$ with $Pd(OAc)_2$. Analysis of the crude by ^{1}HNMR and ESI-MS however did not indicate any product formation.

All attempts to react the salt $(H\text{-}\mathbf{22})^+Br^-$ in the presence of 5.5 eq of *t*-BuOK and $[Pd(\eta^3\text{-allyl})Cl]_2$ resulted in a formation of palladium black.

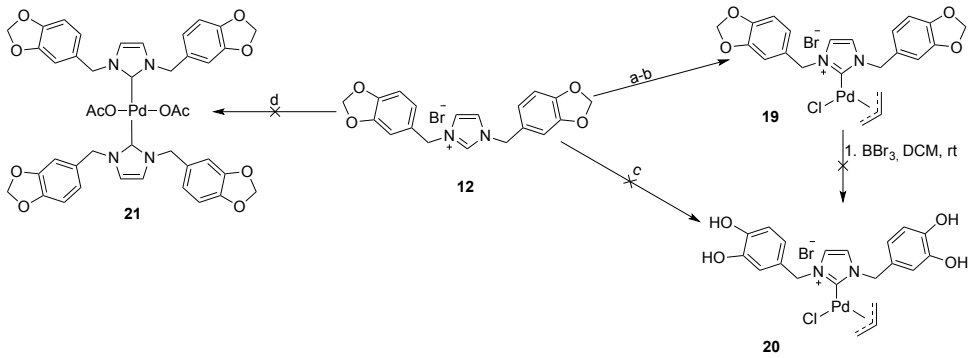

Scheme 6. Reagents and conditions: a) Ag_2O, DCM, rt, 17 h b) $[Pd(\eta^3\text{-allyl})Cl]_2$, DCM, rt, 5 h c) *t*-BuOK, THF,) $[Pd(\eta^3\text{-allyl})Cl]_2$, 8 h d) $Pd(OAc)_2$, MeCN, reflux, 12 h.

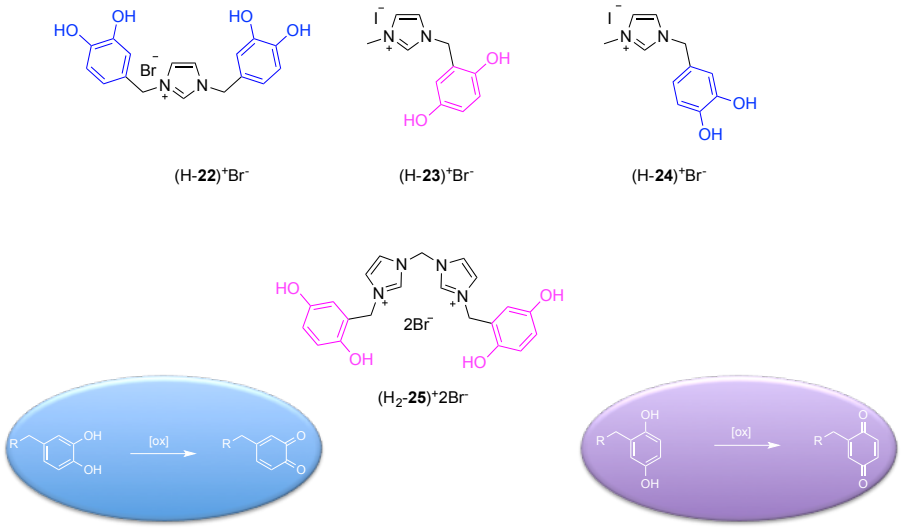

Scheme 7. Imidazolium salts with free catechols groups.

As catechols constitute good ligands for many transition metals and can behave as reducing agents, we attempted the oxidation of catechols to quinones (Scheme 7).

The methylethers ((H-**11**)$^+$Br$^-$, (H-**12**)$^+$I$^-$, (H-**13**)$^+$I$^-$, (H$_2$-**15**)$^{2+}$2Br$^-$) were deprotected upon reaction with BBr_3 in CH_2Cl_2 to form the corresponding catechols presented in Scheme 7. We anticipated to obtain the Ag(I) complex with NHC bearing quinone upon reacting the salts (H-**22**)$^+$Br$^-$, (H-**23**)$^+$I$^-$ or (H-**24**)$^+$I$^-$ with Ag_2O. Unfortunately, we only could observe ligand decomposition.

To use the Ag-NHC complex as a transmetallating agent, oxidants such as: DDQ, $PhI(OAc)_2$ were tested. In each case, the reactions were monitored by TLC and accomplished within 1 hour. However, upon isolation, decomposition of the products was observed. Due to the insolubility of the salt $(H_2\text{-}\mathbf{25})^{2+}2Br^-$, oxidation was unsuccessful. As attempts of catechols' oxidation failed, we were not able to proceed further with the synthesis of transmetallating block Ag-NHC.

Difficulties in coordination of the NHC's with appended catechols, required a change in synthetic strategy. We synthesized NHC salts bearing quinones (Figure 6) and reacted these with Ag_2O. The general reaction conditions for the imidazolium salts synthesis bearing a quinone moiety are identical to those used for the synthesis of NHCs bearing a protected catechol (Scheme 3).

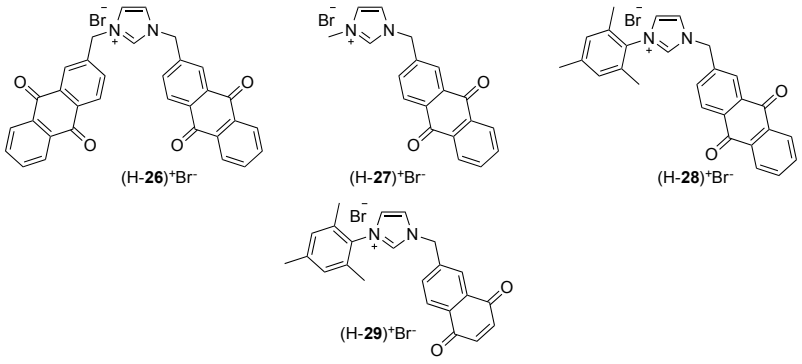

Figure 6. New class of imidazolium salts bearing Antraquinone and Naphthaquinone substituents.

The imidazolium salts $(H\text{-}\mathbf{26})^+Br^-$, $(H\text{-}\mathbf{27})^+Br^-$ and $(H\text{-}\mathbf{28})^+Br^-$ have poor solubility in common solvents used in organometallic synthesis (i.e. CH_2Cl_2, THF, MeCN, H_2O etc.). The reactions were thus performed in DMSO, which may be problematic in view of its coordinating ability. The reaction of the imidazolium salt $(H\text{-}\mathbf{26})^+Br^-$ with 0.65 eq. of Ag_2O resulted in the formation of a light green precipitate. Careful

analysis of the supernatant by ^{1}HNMR and ESI-MS did not reveal the presence of the substrate or [AgBr(NHC-**26**)] **30**. The green precipitate was not soluble in any solvent and analysis was therefore not possible. However over the course of the reaction, we observed silver oxide consumption and concomitant formation of the green precipitate. The observation and analysis of the supernatant led us to conclude that the reaction occurred with the formation of the desired [AgBr(NHC-**26**)] **30** (Figure 7). Due to its insolubility, its characterization was not possible. The reaction of the salts (H-**27**)$^{+}$Br^{-} and (H-**28**)$^{+}$Br^{-} with Ag_2O led to the formation of the complexes [AgBr(NHC-**27**)] **31** and [AgBr(NHC-**28**)] **32**. In the case of complex [AgBr(NHC-**27**)] **31**, the reaction was not complete. The ^{1}HNMR analysis indicated that reaction mixture contained the desired complex, substrate and unidentified impurities. To shift the equilibrium toward the product, 0.25 eq. of Ag_2O was added. The reaction was heated up to 80 ^{o}C and stirred for another 4 days. The HR-MS (DMSO) of the crude product showed fragment m/z 711.1157 [Ag(NHC-**27**)$_2$]$^{+}$ corresponding to the complex [AgBr(NHC-**27**)] **31** and m/z 303.1131 representing salt (H-**27**)$^{+}$Br^{-} (Figure 8). Isolation of the complex by crystallization was not possible. Direct reaction of (H-**26**)$^{+}$Br^{-}, (H-**27**)$^{+}$Br^{-} and (H-**28**)$^{+}$Br^{-} with $Pd(OAc)_2$ resulted in decomposition of the imidazolium salts. Compound (H-**29**)$^{+}$Br^{-} exhibit high instability. Full characterization of that compound was not possible due to its rapid decomposition.

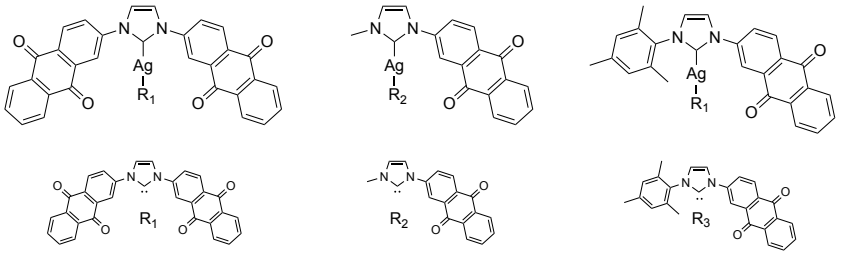

30 **31** **32**

Figure 7. New Ag-NHC complexes obtained from the reaction of imidazolium salts (H-**26**)$^{+}$Br^{-}, (H-**27**)$^{+}$Br^{-} and (H-**28**)$^{+}$Br^{-} with Ag_2O.

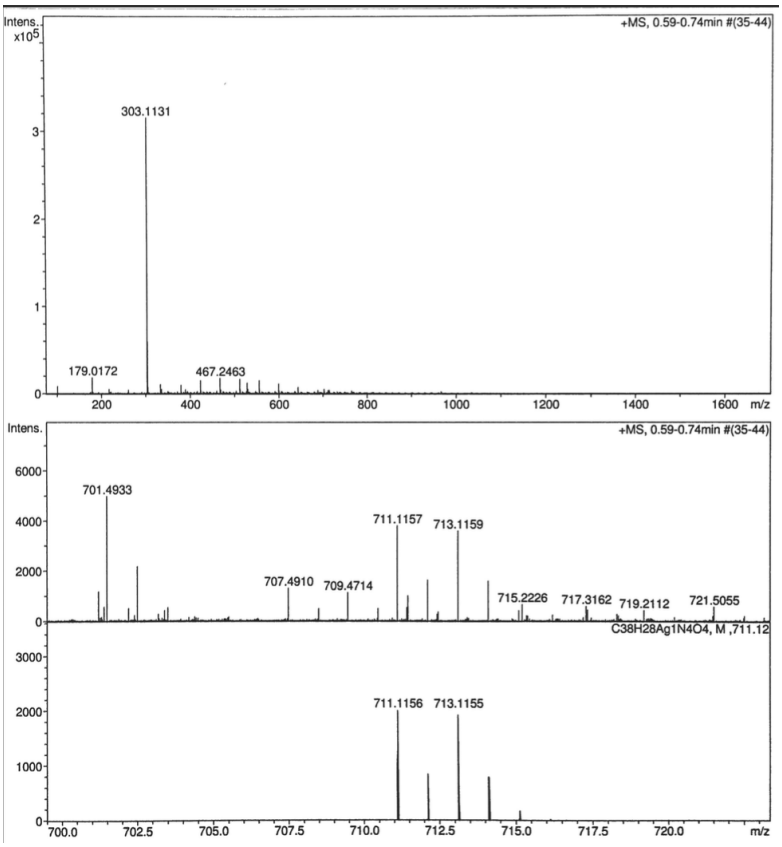

Figure 8. The ESI-MS spectrum of the [AgBr(NHC-**27**)] **31**.

2.3. Synthesis of the NHC without a linker between the imidazolium ring and the quinone moiety

Quinones and halogenated quinones undergo nucleophilic addition and nucleophilic substitution. Following this reactivity, we attempted to synthesize NHC salts with quinone or catechol directly attached to the imidazolium ring (Scheme 10).

For this purpose, we reacted 2,3-dichloronaphthaquinone with mesitylimidazole and methylimidazole. Detailed studies revealed that, after substitution of chloride by imidazole, hydrolysis of the chloride in position 3 occurs. The HR-MS spectrum of compounds (H-**33**)and (H-**34**) displayed peaks at m/z 255.0763 (molecule **34**) and m/z 359.1389 (molecule **33**). The isotope pattern of the peaks indicated that molecules do not contain chloride in the structure. Mass simulation of potential products led us to the conclusion that second chloride underwent hydrolysis. Slow evaporation of the solution of the (H-**33**) in CH_2Cl_2 yielded crystals suitable for X-ray analysis.

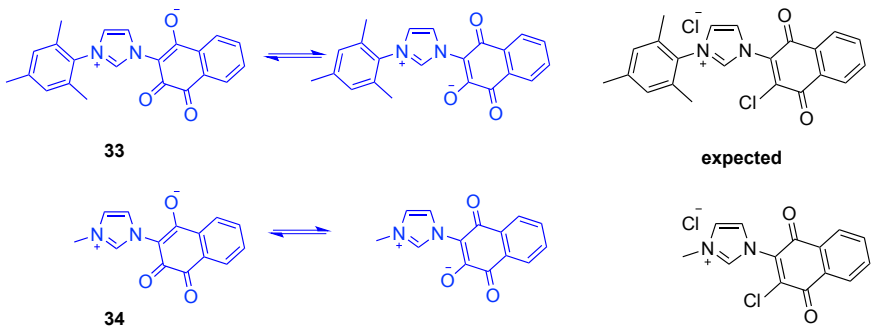

Scheme 10. New imidazolium salts displaying zwiterionic character.

The X-ray structure (Figure 9) of the imidazolium salt **33** does not contain any counter ion. The three C–O bond lengths vary between 1.215-1.246 Å, indicative of a double bond.[37,38] On that basis we suggest that the imidazolium salt **33** and **34** exists as a zwitterions (Scheme 10).

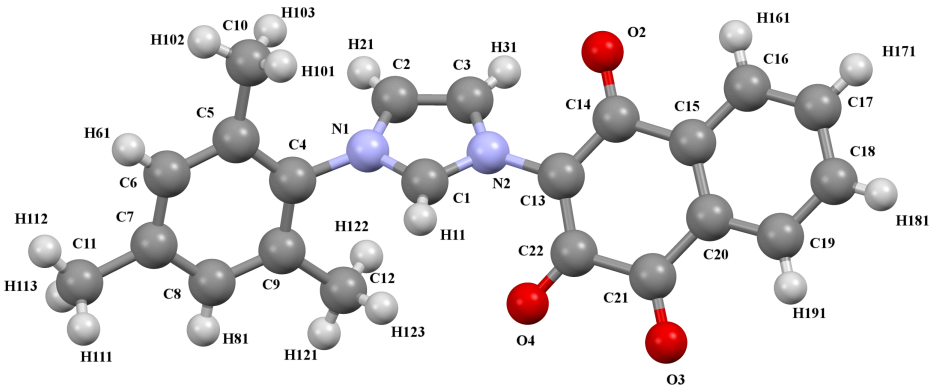

Figure 9. Crystal structure of imidazolium salt **33**. Solvents molecules are omitted for clarity.

Due to the lack of halide as a counterion, molecules **33** and **34** were unreactive towards Ag_2O. The lack of solubility in non-polar solvents such as toluene or THF made complexation to other metals not possible.

To prevent hydrolysis of the C–Cl bond, compounds containing an *o*-methyl group were employed (Figure 9).

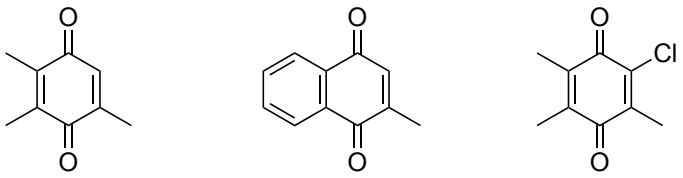

35 **36** **37**

Figure 9. Substrates used in reaction of nucleophilic addition and nucleophilic substitution.

Nucleophilic addition of methylimidazole and mesytylimidazole to compound **35** and **36** (Figure 9) in THF resulted in the formation of a dark brown solid and a black solution. Reactions were monitored by TLC and quenched after the disappearance of compound **35** and **36** from the TLC. The analysis of the ^{1}HNMR and ESI-MS spectra indicated that the desired product was not formed. In the reaction of methylimidazole with compound **37** in CH_2Cl_2, no product was obtained either. In all cases, substrate decomposition was observed. Similar observations were described by S.T. Lee in his doctoral thesis.[39] The reaction of compound **37** with mesytilimidazole gave an unexpected product (H-**38**)$^{+}Cl^{-=}$ in a 4% yield. The ESI-MS spectrum indicated a mass of m/z 371.3, close to the mass of desired product m/z= 370.1. The isotope pattern indicated that the product contains a chloride. Analysis of the ^{1}HNMR and ^{13}CNMR allowed to tentatively derived a structure where chloride was integrated to one of the methyl groups. ^{1}HNMR measured in DMSO and MeOD highlighted the presence of downfield protons at 9.03 and 8.65 ppm, characteristic for phenolic protons. No peaks above 160 ppm in ^{13}CNMR spectra suggest that the molecule likely does not contain carbonyl groups. Additionally, in the ^{1}HNMR spectra, one of the methyl groups is missing. Instead, we observe a singlet at 5.59 ppm corresponding to two protons and carbon peak 46.51 ppm. These data suggest

that the molecule contains methylene group with shift very similar to CH_2Cl_2. We thus hypothesized, that during the reaction a methyl group is chlorinated in *ortho* position to the imidazolium ring, corresponding to m/z=371.3 (Figure 11). Due to the low yield, no further coordination attempts were undertaken.

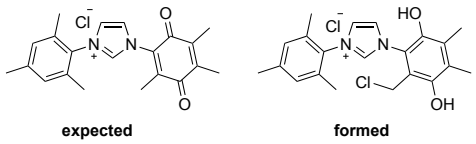

expected **formed**

38

Figure 11. Tentative structure of the imidazolium salt obtained during the nucleophilic substitution between mesytylimidazole and 2-chloro-3,5,6 trimethylquinone .

3. Catalysis

Inspired by the earlier connections of transition metals with quinones,[30,31,40] we set out to test Colbran's complex **16,** [(η^6-C_6H_6)$RuCl_2$(NHC-**1**)] **3**, [(η^5-Cp*)$IrCl_2$(NHC-**1**)] **4** and [PdCl(η^3-allyl)(NHC-**1**)] **5** in reaction of alcohol oxidation.

All catalysis reactions were performed in toluene, 1 mmol substrate concentration, 5% mmol catalyst loading, 80 °C, using benzyl alcohol as a model substrate. Unfortunately none of them turned out to be active for the alcohol oxidation. All attempts to enhance the activity of the complexes such as addition of: bases, Ag_2SO_4 or solvent changes failed. In the case of complex [(η^6-C_6H_6)$RuCl_2$(NHC-**1**)] **3** after 17 h of reaction we could observe an insoluble black precipitate. In the resulting ESI-MS spectrum, no peak-indicating presence of the complex was detected, suggestsing that during reaction the catalyst was decomposed. No further catalytic attempts were made with this system.

4. Experimental part

4.1. Synthesis and coordination properties of NHC salt with propylene spacer between naphthaquinone and imidazolium ring

4.1.1. Synthesis of imidazolium salts

N-mesitylimidazole and boc-protected 3-chloropropylamine were synthesized according to described procedures.[39-40]

4.1.2. Synthesis of imidazolium salt (H-1)$^+$Cl$^-$

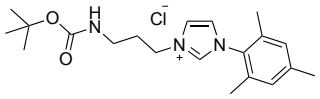

N-mesitylimidazole (770 mg, 4.13 mmol) was mixed with boc-protected 3-chloropropylamine (881 mg, 4.55 mmol). A few drops of toluene were added to facilitate stirring. The reaction mixture was brought to 100 °C and compounds were melted together over night. After 17 h, the reaction was stopped and cooled to yield a glassy orange solid. Purification by silica column chromatography using 5% methanol in CH_2Cl_2 yielded a white hygroscopic solid (811 mg, yield = 52%).

^{1}HNMR (400 MHz, $CDCl_3$) δ 10.38 (s, 1H), 8.11 (s, 1H), 7.15 (t, *J* = 1.8 Hz, 1H), 6.97 (s, 2H), 6.26 (t, *J* = 6.1 Hz, 1H), 4.70 (t, *J* = 6.4 Hz, 2H), 3.18 (q, *J* = 6.1 Hz, 2H), 2.31 (s, 3H), 2.22 (p, *J* = 6.2 Hz, 2H), 2.04 (s, 6H), 1.37 (s, 9H).

^{13}CNMR (101 MHz, $CDCl_3$) δ 156.91, 141.30, 138.59, 134.31, 130.88, 129.91, 123.59, 123.16, 79.23, 50.47, 47.91, 36.75, 31.14, 28.51, 21.16, 17.65.

HRMS (MeOH): m/z 344.2333 [M-Cl]

HRMS calculated: m/z 344.2338 [M-Cl]

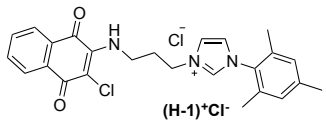

(H-1)$^+$Cl$^-$

The boc-protected propyl amine 3-mesitylimidazolium chloride (426 mg, 1.08 mmol) was dissolved in CH_2Cl_2 (10 ml) and a solution of HCl in dioxane (2,7 ml of 4M stock solution, 10.8 mmol) was slowly added via a syringe. The solution was stirred overnight at room temperature and the resulting white solid was collected by filtration (324 mg, 1 mmol). The crude solid was transferred into a flask containing dichloromethane (4 ml), triethylamine (0.57 ml, 4.1 mmol) and 2,3-dichloro-1,4-naphthoquinone (465 mg, 2 mmol). Upon stirring overnight at room temperature, a red precipitate formed. The suspension was evaporated and purified by column chromatography using a MeOH-CH_2Cl_2 gradient (0-10% MeOH). The fractions containing the product were washed with water followed with brine, dried over Na_2SO_4 and the solvent was evaporated. Compound (H-**1**)$^+$Cl was isolated as a red solid (217 mg, yield = 45%).

^{1}HNMR (400 MHz, $CDCl_3$) δ 10.89 (s, 1H), 8.08 (dd, *J* = 7.7, 1.3 Hz, 1H), 7.96 (dd, *J* = 7.7, 1.3 Hz, 1H), 7.84 – 7.81 (m, 1H), 7.69 (td, *J* = 7.6, 1.4 Hz, 1H), 7.60 (td, *J* = 7.5, 1.3 Hz, 1H), 7.17 (t, *J* = 1.8 Hz, 1H), 7.12 (d, *J* = 7.0 Hz, 1H), 7.00 – 6.95 (m, 2H), 4.98 (t, *J* = 6.6 Hz, 2H), 4.07 (q, *J* = 6.9 Hz, 2H), 2.48 (p, *J* = 6.7 Hz, 2H), 2.32 (s, 3H), 2.06 (s, 6H).

^{13}CNMR (101 MHz, $CDCl_3$) δ 179.83, 176.26, 144.39, 140.92, 137.84, 134.51, 134.02, 132.21, 132.02, 130.67, 129.56, 129.50, 126.45, 126.16, 123.93, 123.28, 49.79, 47.59, 40.93, 32.28, 29.50, 20.88, 17.37.

HRMS (MeOH): m/z 434.1627 [M-Cl]

HRMS calculated: m/z 434.1635 [M-Cl]

4.1.3. Synthesis of reference imidazolium salt (H-2)$^{+}$I^{-}

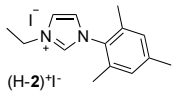

(H-**2**)$^{+}$I^{-}

N-mesitylimidazole (414 mg, 2.22 mmol) was dissolved in toluene (4 ml) and CH_3CH_2I (0.53 ml, 6.67 mmol) was added. After stirring overnight at reflux, the reaction was cooled and yellow oil was formed. The reaction mixture was decanted and diethyl ether (2 ml) was added. Sonification for 5 minutes resulted in the formation of a white solid, which was collected by filtration. The solid was redissolved in a small amount of CH_2Cl_2 and excess of diethyl ether was added, what resulted in formation of an oil. The sonification of the oil for 5 minutes in diethyl ether gave pure white compound (700 mg, yield =92%).

^{1}**HNMR** (400 MHz, $CDCl_3$) δ 10.01 (s, 1H), 8.04 (s, 1H), 7.24 – 7.20 (m, 1H), 6.97 (d, 2H), 4.73 (q, *J* = 7.3 Hz, 1H), 2.31 (s, 3H), 2.06 (s, 6H), 1.64 (td, *J* = 7.2, 2.7 Hz, 3H).
^{13}**CNMR** (101 MHz, $CDCl_3$) δ 141.43, 136.96, 134.29, 130.62, 129.94, 123.43, 123.18, 94.25, 46.05, 21.19, 17.96, 16.24.

HRMS (MeOH): m/z 215.1546 [M-I]

HRMS calculated: m/z 215.1548 [M-I]

4.1.4. Synthesis of metal complexes with NHC-1

The reactions and all subsequent operations were performed under nitrogen atmosphere

4.1.5. Synthesis of $[Ag(\mu\text{-}Cl)(NHC\text{-}1)]_2$ 2

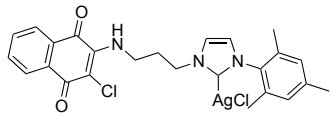

2

The imidazolium salt (H-**1**)$^+$Cl (88 mg, 0.187 mmol) and silver oxide (26 mg, 0.112 mmol) were placed in the Schlenk tube and dry CH_2Cl_2 (2 ml) was added. The reaction mixture was stirred protected from light for 18 hours at room temperature. The solution was filtered and the solvent was removed on a rotary evaporator yielding a dark red solid (123 mg, yield = 57%).

^{1}**HNMR** (400 MHz, $CDCl_3$) δ 7.99 (ddd, *J* = 40.0, 7.7, 1.3 Hz, 2H), 7.60 (dtd, *J* = 37.3, 7.5, 1.4 Hz, 2H), 7.23 (d, *J* = 1.8 Hz, 1H), 6.99 – 6.80 (m, 3H), 6.21 (s, 1H), 4.33 (t, *J* = 6.8 Hz, 2H), 3.84 (d, *J* = 7.8 Hz, 2H), 2.32 – 2.21 (m, 5H), 1.89 (s, 6H).

^{13}**CNMR** (101 MHz, $CDCl_3$) δ 180.06, 176.70, 143.93, 139.54, 135.30, 134.96, 134.69, 132.62, 132.42, 129.70, 129.42, 126.92, 126.73, 123.15, 121.41, 77.36, 53.55, 49.49, 41.73, 32.97, 21.10, 17.74.

HRMS (MeOH): m/z 973.6221 $[Ag(NHC\text{-}1)_2]^+$

HRMS calculated: m/z 973.2165 $[Ag(NHC\text{-}\mathbf{1})_2]^+$

4.1.6. Synthesis of [(η^6-C_6H_6)Ru(NHC-1)Cl_2] 3

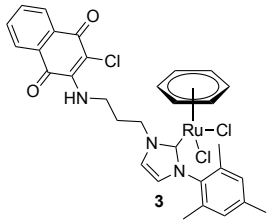

3

The silver complex **2** (77 mg, 0.067 mmol) was dissolved in CH_2Cl_2 (2 ml) and [(η^6-C_6H_6)$RuCl_2$]$_2$ (72 mg, 0.067 mmol) was added. Reaction was stirred in a room temperature for 17 hours. White precipitate was formed. The reaction mixture was filtered and condensed under vacuum. Addition of diethyl ether afforded a red precipitate which was filtered using a cannula and was washed several times with diethyl ether to yield a red solid (39 mg, yield = 91%)

^{1}**HNMR** (400 MHz, $CDCl_3$) δ 8.07 (d, *J* = 7.5 Hz, 3H), 7.98 (d, *J* = 7.3 Hz, 3H), 7.67 (t, *J* = 7.3 Hz, 3H), 7.58 (t, *J* = 7.2 Hz, 3H), 7.34 (s, 2H), 6.84 (d, *J* = 15.3 Hz, 7H), 6.62 (s, 2H), 5.67 (s, 1H), 5.42 (s, 11H), 4.63 (s, 5H), 3.99 (s, 5H), 2.32 (d, *J* = 24.4 Hz, 13H), 2.01 (s, 12H)

^{13}**CNMR** (101 MHz, $CDCl_3$) δ 180.34, 176.72, 172.13, 138.79, 136.95, 136.04, 134.81, 132.57, 132.46, 128.43, 126.87, 126.65, 125.46, 122.19, 86.67, 50.00, 42.26, 33.20, 21.22, 18.79

HRMS (MeOH): m/z 648.0766 [M-Cl]

HRMS calculated: m/z 648.0758 [M-Cl]

4.1.7. Synthesis of [(η^5-Cp*)Ir(NHC-1)Cl_2] 4

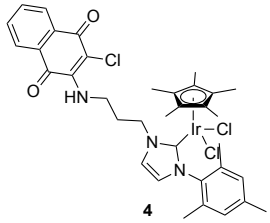

4

The silver complex **2** (77 mg, 0.067 mmol) was dissolved in CH_2Cl_2 (2 ml) and [(η^5-Cp*)$IrCl_2$]$_2$ (53 mg, 0.067 mmol) was added. The reaction was stirred at room temperature for 17 hours. A white precipitate formed and the reaction mixture was filtered and condensed under vacuum. Addition of diethyl ether resulted in red solid precipitate, which was. filtered using cannula technique and washed several times with diethyl ether to give a red solid (50 mg, yield = 90%).

^{1}**HNMR** (400 MHz, $CDCl_3$) δ 8.12 – 8.06 (m, 1H), 8.01 – 7.95 (m, 1H), 7.69 (td, *J* = 7.6, 1.4 Hz, 1H), 7.62 – 7.55 (m, 1H), 7.27 (d, *J* = 2.0 Hz, 1H), 6.80 (s, 2H), 6.69 (d, *J* = 1.9 Hz, 1H), 6.56 (d, *J* = 6.5 Hz, 1H), 4.47 (s, 2H), 4.02 (q, *J* = 6.7 Hz, 2H), 2.44 (t, *J* = 7.6 Hz, 2H), 2.27 (s, 3H), 2.01 (s, 6H), 1.48 (s, 15H).

^{13}**CNMR** (101 MHz, $CDCl_3$) δ 180.26, 176.73, 154.54, 144.53, 138.42, 136.72, 134.79, 132.54, 132.46, 129.92, 127.87, 126.83, 126.66, 125.87, 120.54, 89.02, 49.41, 42.25, 33.20, 21.31, 19.07, 9.23.

HRMS (MeOH): m/z 796.2049 [M-Cl], m/z 761.2295 [M-2Cl]

HRMS (MeOH): m/z 796.2048 [M-Cl], m/z 761.2360 [M-2Cl]

4.1.8. Synthesis of palladium complex [PdCl(η^3-allyl)(NHC-1)] 5

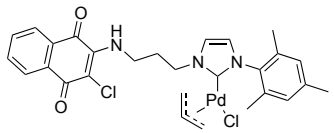

5

The silver complex **2** (117 mg, 0.101 mmol) was dissolved in CH_2Cl_2 (3 ml) and [Pd(η^3-allyl)Cl]$_2$ (37 mg, 0.101 mmol) was added. The reaction was stirred at room temperature for 17 hours, yielding a greenish precipitate. The reaction mixture was filtered and concentrated under vacuum. Addition of diethyl ether yielded a greenish solid, which was filtered using cannula technique and washed several times with diethyl ether to give greenish solid (60 mg, yield = 96%).

^{1}HNMR (400 MHz, $CDCl_3$) δ 8.10 (dd, *J* = 7.7, 1.3 Hz, 2H), 7.99 (dd, *J* = 7.7, 1.3 Hz, 2H), 7.70 (td, *J* = 7.5, 1.3 Hz, 2H), 7.60 (td, *J* = 7.5, 1.3 Hz, 2H), 7.17 (d, *J* = 1.9 Hz, 2H), 6.97 – 6.84 (m, 6H), 6.50 (d, *J* = 6.9 Hz, 1H), 5.09 – 4.95 (m, 2H), 4.62 (dt, *J* = 13.7, 6.8 Hz, 2H), 2.06 – 1.98 (m, 6H), 4.50 (dt, *J* = 13.8, 6.7 Hz, 2H), 4.13 – 4.07 (m, 2H), 3.92 (q, *J* = 6.5 Hz, 4H), 3.16 (dt, *J* = 6.8, 1.9 Hz, 2H), 3.04 (d, *J* = 13.6 Hz, 2H), 2.39 – 2.25 (m, 10H), 2.19 (s, 6H), 1.77 (d, *J* = 11.9 Hz, 2H)

^{13}CNMR (101 MHz, $CDCl_3$) δ 181.80, 180.28, 176.90, 144.17, 139.00, 136.31, 135.95, 135.14, 134.96, 132.66, 132.57, 129.87, 129.22, 128.80, 126.96, 126.84, 122.91, 120.97, 114.93, 73.18, 49.19, 48.20, 41.63, 41.52, 32.53, 21.17, 18.56, 18.11.

HRMS (MeOH): m/z 580.0979 [M-Cl]

HRMS calculated: m/z 580.0983 [M-Cl]

4.1.9. Synthesis of the reference complexes of Ru, Ir and Pd

Complexes were synthesized as described above upon reacting 1 equivalent of (H-**2**)$^{+}$I^{-} with 0.65 equivalent of Ag_2O followed by transmetalation of the silver complex with

$[(\eta^6\text{-}C_6H_6)RuCl_2]_2$ (0.55 equivalent vs. (H-**2)**$^{+}$I^{-}, $[(\eta^5\text{-}Cp^*)IrCl_2]_2$ and $[Pd(\eta^3\text{-allyl})Cl]_2$ respectively.

4.1.10. [Ag(NHC 2)$_2$I] 7

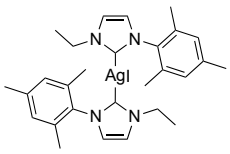

7

White solid, yield = 92%

^{1}**HNMR** (400 MHz, Acetonitrile-d_3) δ 7.37 (d, *J* = 1.8 Hz, 1H), 7.07 (d, *J* = 1.8 Hz, 1H), 7.04 – 6.94 (m, 2H), 4.09 (q, *J* = 7.3 Hz, 2H), 2.35 (s, 3H), 1.84 (s, 6H), 1.35 (t, *J* = 7.3 Hz, 3H).

^{13}**CNMR** (101 MHz, CD_3CN) δ 182.68, 140.03, 136.83, 135.92, 129.84, 123.48, 122.20, 118.22, 47.36, 21.17, 17.74, 17.49.

HRMS (CH_2Cl_2): m/z 535.2022 $[Ag(NHC)_2]^{+}$

HRMS calculated: m/z 535.1991 $[Ag(NHC)_2]^{+}$

4.1.11. [(η^6-C_6H_6)$RuCl_2$(NHC-2)]

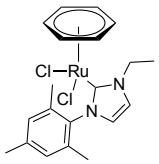

8

Light brown solid, yield = 93%

^{1}HNMR (400 MHz, Chloroform-d) 1.53 (t, *J* = 7.2 Hz, 3H), 2.03 (s, 6H), 2.3(s, 3H), 4.58 (q, *J* = 7.2 Hz, 2H),), δ 5.44 (s, 6H), 6.82 (d, *J* = 1.8 Hz, 1H), 6.87 (s, 2H), 7.26 – 7.26 (m, 1H).

^{13}CNMR (101 MHz, $CDCl_3$) δ 171.69, 138.64, 136.97, 136.12, 128.37, 125.49, 121.67, 86.51, 47.35, 21.27, 18.89, 17.45.

HRMS (MeOH): m/z 429.0671 [M-Cl]

HRMS calculated: m/z 429.0671 [M-Cl]

4.1.12. Reference iridium complex [(η^5-Cp*)$IrCl_2$(NHC-2)] 9

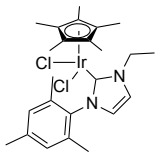

9

Complex [(η^5-Cp*)$IrCl_2$(NHC-**2**)] **9** was obtained as an orange solid (y = 89%)

^{1}**HNMR** (400 MHz, Chloroform-d) δ 7.18 (d, *J* = 2.0 Hz, 1H), 6.84 – 6.81 (m, 2H), 6.68 (d, *J* = 2.0 Hz, 1H), 4.41 (s, 2H), 2.29 (s, 3H), 2.04 (s, 6H), 1.58 (t, *J* = 7.3 Hz, 3H), 1.50 (s, 15H).

^{13}**CNMR** (101 MHz, $CDCl_3$) δ 154.10, 138.46, 137.05, 125.58, 120.21, 88.93, 46.75, 21.40, 19.26, 17.07, 9.28.

HRMS (MeOH): m/z 577.1951 [M-Cl], 542.2190 [M-2Cl]

HRMS calculated: m/z 577.1962 [M-Cl], 542.2273 [M-2Cl]

4.1.13. [PdCl(η^3-allyl)(NHC-2)] 10

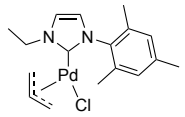

10

The complex [PdCl(η^3-allyl)(NHC-**2**)] **10** was obtained as yellow solid (y = 64%)

^{1}HNMR (400 MHz, $CDCl_3$) δ 7.11 (d, *J* = 1.9 Hz, 1H), 7.00 – 6.85 (m, 3H), 5.00 (ddt, *J* = 13.7, 11.7, 7.4 Hz, 1H), 4.45 (th, *J* = 14.0, 7.3 Hz, 2H), 4.07 (dd, *J* = 7.5, 2.0 Hz, 1H), 3.14 (dt, *J* = 6.6, 1.9 Hz, 1H), 3.00 (d, *J* = 13.5 Hz, 1H), 2.31 (s, 3H), 2.19 (s, 3H), 2.03 (s, 3H), 1.79 (d, *J* = 11.9 Hz, 1H), 1.50 (t, *J* = 7.3 Hz, 3H).

^{13}CNMR (101 MHz, $CDCl_3$) δ 181.07, 138.86, 136.57, 136.09, 135.33, 129.19, 128.78, 122.33, 120.60, 114.67, 72.71, 48.49, 46.20, 21.21, 18.57, 18.13, 16.67.

HRMS (MeOH): m/z 361.0974 [M-Cl]

HRMS calculated: m/z 361.0896 [M-Cl]

4.2. Synthesis of an *N*-heterocyclic carbene ligands bearing catechols or quinones without or with –CH_2– as a spacer

Compound **13**, **16**, **23**, **25** were synthesized according to literature protocols. Their characterization was in accordance with literature data.[24,37]

4.2.1. Salt (H-11)$^+$Br$^-$

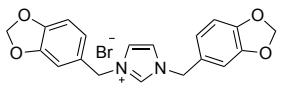

(H-**11**)$^+$Br$^-$

To a solution of sodium imidazole (6.82 mmol, 0.611 g) in THF (10 mL) 5-(bromomethyl)-1,3-benzodioxole (16 mmol, 3.45 g) was added. After refluxing for 46 hours, the reaction mixture was cooled to room temperature and filtered. The precipitate was washed several times with THF and dissolved in methanol. The volume was reduced under vacuum and diethyl ether was added. The product was recrystallized from MeOH/Et_2O three times to yield pure (H-**11**)$^+$Br$^-$ as a beige powder (3.36 g, yield = 83%).

^{1}**HNMR** (400 MHz, DMSO) δ 9.32 (t, *J* = 1.6 Hz, 1H), 7.79 (d, *J* = 1.6 Hz, 2H), 7.08 (dd, *J* = 1.6, 0.6 Hz, 2H), 7.00 – 6.93 (m, 4H), 6.04 (s, 4H), 5.29 (s, 4H).

^{13}**CNMR** (101 MHz, DMSO) δ 147.6, 135.7, 128.1, 109.0, 108.5, 101.3, 51.8.

HRMS (MeOH): m/z 337.1186 [M-Br]

HRMS calculated: m/z 337.1183 [M-Br]

4.2.2. Salt (H-13)$^{+}I^{-}$

a)

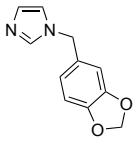

Imidazole (141 mg, 2.05 mmol) and NaH (52.6 mg, 2.19 mmol) were placed in a Schlenk tube and air was evacuated. Under a nitrogen atmosphere, dry DMF (3 mL) was added. The reaction mixture was stirred at room temperature for 3 hours and 5-(bromomethyl)-1,3-benzodioxole (300 mg, 1.4 mmol) in 2 mL of DMF was slowly added. The reaction was stirred overnight followed by DMF evaporation. To the residue water (10 mL) was added and extracted 5 times with DCM. The organic layers were collected and dried over $MgSO_4$ followed by filtration and evaporation. Purified by silica column chromatography (5% MeOH in EtOAc). The product was isolated as an yellow oil (170 mg, yield = 60%).

^{1}HNMR (400 MHz, Chloroform-d) δ 6.81 (t, *J* = 1.2 Hz, 1H), 6.63 (t, *J* = 1.4 Hz, 1H), 6.50 (d, *J* = 7.9 Hz, 1H), 6.44 – 6.33 (m, 2H), 5.65 (s, 2H), 4.71 (s, 2H).

^{13}CNMR (101 MHz, $CDCl_3$) δ 147.76, 147.12, 136.78, 129.58, 129.21, 120.60, 118.71, 107.99, 107.46, 100.88, 77.48, 77.16, 76.84, 50.06.

HRMS (MeOH): m/z 203.0814 [M+H]

HRMS calculated: m/z 203.0821 [M+H]

b)

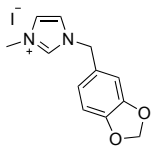

(H-**13**)$^{+}$I^{-}

186 mg of oil was collected and 3 ml of Methyliodide was added. Refluxed for 7 hours, cooled down and diethyl ether was added. Filtered off and dissolved in a small amount of CH_2Cl_2. Addition of diethyl ether caused precipitation and yielded pure product (H-**13**)$^{+}$I^{-}

^{1}HNMR (400 MHz, CD_3CN) δ 9.06 (d, *J* = 1.6 Hz, 1H), 7.52 (t, *J* = 1.8 Hz, 1H), 7.44 (t, *J* = 1.8 Hz, 1H), 7.05 – 6.97 (m, 2H), 6.83 (d, *J* = 7.9 Hz, 1H), 5.96 (s, 2H), 5.34 (s, 2H), 3.85 (d, *J* = 0.6 Hz, 3H).

^{13}CNMR (101 MHz, CD_3CN) δ 148.84, 148.71, 136.82, 128.16, 124.47, 123.67, 122.63, 118.05, 109.71, 109.05, 102.49, 52.83, 36.90, 1.94, 1.73, 1.53, 1.32, 1.11, 0.91, 0.70.

HRMS (MeOH): m/z 217.0973 [M-I]

HRMS calculated: m/z 217.0972 [M-I]

4.2.2. Salt $(H_2\text{-}14)^{2+}2Br^-$

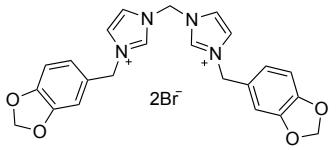

$(H_2\text{-}\mathbf{14})^{2+}2Br^-$

Compound **13a** (281 mg, 1.39 mmol) was dissolved in toluene and CH_2Br_2 (242 mg, 1.39 mmol, 0.09 ml) was added. The reaction mixture was refluxed for 2 days, cooled to room temperature and filtered. White precipitate was washed twice with toluene and dried under the vacuum. The product was obtained pure as a white solid of 22% (127 mg).

^{1}**HNMR** (400 MHz, DMSO) δ 9.52 (t, *J* = 1.6 Hz, 1H), 8.02 (t, *J* = 1.9 Hz, 1H), 7.87 (t, *J* = 1.9 Hz, 1H), 7.09 (d, *J* = 1.7 Hz, 1H), 7.05 – 6.95 (m, 2H), 6.62 (s, 1H), 6.05 (s, 2H), 5.37 (s, 2H).

HRMS (DMSO): m/z 497.0820 [M-Br], m/z 418.1690 [M-2Br]

HRMS calculated: m/z 497.0814 [M-Br], m/z 418.1630 [M-2Br]

4.2.3. Complex [PdCl(η^3-allyl)(NHC-11)] 19

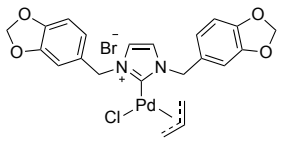

19

The salt (H-**11**)$^+$Br$^-$ (150 mg, 0.359 mmol) was reacted in dry CH_2Cl_2 with Ag_2O (54 mg, 0.233 mmol) and stirred protected from light for 6 hours. The precipitate was filtered off and injected to the flask containing allylpalladium(II) chloride dimer (65.7 mg, 0.18 mmol). The reaction mixture was stirred at room temperature for 2 hours and filtered. Subsequently Et_2O was added to the solution, resulting in the formation of white precipitate. The procedure was repeated twice to obtain a pure product in 48% yield.

^{1}**HNMR** (400 MHz, $CDCl_3$) δ 6.84 (s, 2H), 6.79 – 6.72 (m, 5H), 5.92 (s, 4H), 5.29 (q, *J* = 14.4 Hz, 5H), 4.39 – 4.17 (m, 1H), 3.21 (d, *J* = 12.6 Hz, 2H), 2.16 – 2.05 (m, 1H).
^{13}**CNMR** (101 MHz, $CDCl_3$) δ 180.76, 148.16, 147.62, 130.16, 121.82, 121.36, 114.94, 108.63, 108.42, 101.32, 54.74.

HRMS (H_2O): m/z 483.0535 [M-Cl], m/z 819.1652 [(η^3-allyl)Pd(NHC)$_2$]$^+$
HRMS calculated: m/z 483.0536 [M-Cl]

4.2.4. Salt (H-22)$^{+}$Br^{-}

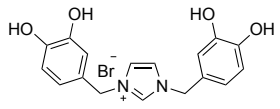

(H-**22**)$^{+}$Br^{-}

The dry salt (H-**11**)$^{+}$Br^{-} (0.9 mmol, 0.376 g) was placed in a Schlenk flask equipped with a magnetic stirrer. Under nitrogen atmosphere dry CH_2Cl_2 (5 mL) and boron tribromide (3.15 mmol, 395 µL) were added. The reaction was stirred overnight (controlled by TLC MeOH/DCM = 1:9, v/v) at room temperature.The, reaction mixture was cooled down to 0 °C and MeOH was added and stirred for an hour. The solvent was evaporated under reduced pressure and the compound was purified by reverse phase chromatography with a semipreparative Dr. Maisch Reprospher C18-DE column (150 x 20 mm, 5 µm particle size) using eluent A (water, 0.1% TFA) and B (acetonitrile). The following method was used: flow rate 15 mL/min, UV detection at 254 nm; 0-2 min (90% A, isocratic), 2-16 min (gradient 90 → 0% A).

Applied conditions were found with an analytical Dr. Maisch Reprospher C18-DE column (150 x 4,6 mm, 5 µm particle size). Compound was isolated as brown oil (0.3 g, 84.7%).

^{1}**HNMR** (400 MHz, DMSO) δ 9.20 (m, 3H), 9.05 (s, 2H), 7.71 (d, *J* = 1.6 Hz, 7H), 6.80 – 6.65 (m, 6H), 5.19 (s, 16H).

^{13}**CNMR** (101 MHz, DMSO) δ 145.9, 145.5, 135.4, 125.3, 122.5, 119.7, 115.9, 115.7, 51.9.

HRMS (MeOH): m/z 313.1187 [M-Br]

HRMS calculated: m/z 313.1183 [M-Br]

4.2.5. Salt (H-23)$^{+}$Br^{-}

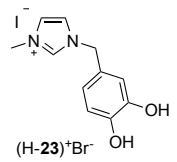

(H-**23**)$^{+}$Br^{-}

The salt (H-**13**)$^{+}$I^{-} (0.5 mmol, 172 mg) was placed in a Schlenk glass equipped with a magnetic stirrer. Under a nitrogen atmosphere dry CH_2Cl_2 (5 mL) and boron tribromide (1.5 mmol, 188 µL) were added. The reaction was stirred overnight at room temperature. The reaction mixture was then cooled down to 0 °C and MeOH was added. Stirred for another hour. The solvent was evaporated and the residue dissolved in a small amount of MeOH. Addition of Et_2O resulted in the formation of a brown oil, proved to be pure (H-**23**)$^{+}$Br^{-}.

^{1}**HNMR** (400 MHz, DMSO) δ 9.23 (s, 2H), 9.15 (s, 2H), 9.05 (s, 1H), 7.70 (dt, *J* = 16.1, 1.8 Hz, 3H), 6.86 – 6.63 (m, 5H), 5.20 (s, 3H), 3.84 (s, 5H).

^{13}**CNMR** (101 MHz, DMSO) δ 146.02, 145.63, 136.29, 125.46, 123.88, 122.26, 119.92, 116.06, 115.84, 51.95, 35.92.

HRMS(H_2O): m/z 205.0972 [M-I]

HRMS calculated: m/z 205.0972 [M-I]

4.2.6. Salt (H-26)$^{+}$Br^{-}

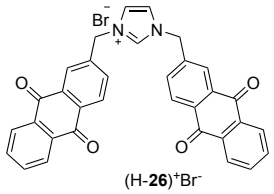

(H-**26**)$^{+}$Br^{-}

2-Bromomethyl-anthraquinone (2.21 mmol, 665 mg) and imidazole sodium derivative (1.1 mmol, 99.4 mg) were placed in round-bottomed flask equipped with a magnetic stirrer. After addition of toluene (15 mL), the solution was refluxed for two days and filtered using canula system. The precipitate was washed several times with hot toluene and methanol to yield pure (H-**26**)$^{+}$Br^{-} as a green powder (315 mg, 24%).

^{1}**HNMR** (400 MHz, DMSO) δ 9.57 (t, *J* = 1.6 Hz, 1H), 8.29 (d, *J* = 8.0 Hz, 2H), 8.26 – 8.22 (m, 4H), 8.21 – 8.16 (m, 2H), 8.00 – 7.92 (m, 8H), 5.72 (s, 4H).

HRMS (DMSO): m/z 509.1501 [M-Br]

HRMS calculated: m/z 509.1495 [M-Br]

4.2.7. Salt (H-27)$^{+}$Br^{-}

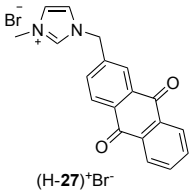

(H-**27**)$^{+}$Br^{-}

1-Methylimidazol (111 mg, 1.35 mmol, 4 eq) and 2-Bromomethyl- antraquinone (102 mg, 0.34 mmol, 1 eq) were placed in a round-bottomed flask and of toluene (5 mL) were added. The reaction mixture was refluxed for 18 hours. Cooled down to room temperature and filtered. Washing the precipitate several times with toluene and Et_2O yielded pure whitish compound (yield = 81%).

^{1}HNMR (400 MHz, DMSO) δ 9.31 (d, *J* = 1.7 Hz, 1H), 8.30 – 8.19 (m, 4H), 7.99 – 7.92 (m, 3H), 7.88 (t, *J* = 1.8 Hz, 1H), 7.77 (t, *J* = 1.8 Hz, 1H), 5.69 (s, 2H), 3.88 (s, 3H).

^{13}CNMR (101 MHz, DMSO) δ 182.24, 182.09, 141.31, 137.10, 134.78, 134.06, 133.44, 133.04, 127.63, 126.84, 126.57, 124.24, 122.50, 51.21, 35.99.

HRMS (DMSO): m/z 303.1130 [M-Br]

HRMS calculated: m/z 303.1128 [M-Br]

4.2.8. Salt (H-28)$^{+}$Br^{-}

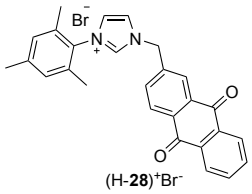

(H-**28**)$^{+}$Br^{-}

1-Mesytylimidazole (187 mg, 1.01 mmol, 3 eq) and 2-bromomethyl- antraquinone were placed in a round bottomed flask. Toluene (5 ml) was added and the reaction mixture was refluxed for 18 hours. The reaction mixture was cooled to room temperature and filtered. The precipitate was washed several times with hot toluene and Et_2O. The pure compound was obtained as yellowish solid (yield = 85%).

^{1}HNMR (400 MHz, DMSO) δ 9.76 (t, *J* = 1.6 Hz, 1H), 8.26 (d, *J* = 8.0 Hz, 1H), 8.22 – 8.12 (m, 4H), 8.06 – 7.98 (m, 2H), 7.94 (dt, *J* = 5.5, 3.8 Hz, 2H), 7.15 (s, 2H), 5.84 (s, 2H), 2.32 (s, 3H), 2.05 (s, 7H).

^{13}CNMR (101 MHz, DMSO) δ 182.22, 182.12, 141.28, 140.45, 138.18, 134.84, 134.78, 134.31, 133.92, 133.50, 133.02, 132.96, 132.95, 131.14, 129.37, 127.77, 126.89, 126.03, 124.57, 123.60, 51.79, 20.67, 17.03.

HRMS (DMSO): m/z 407.1758 [M-Br]

HRMS calculated: m/z 407.1754 [M-Br]

4.2.9. Salt (H-29)$^{+}$Br^{-}

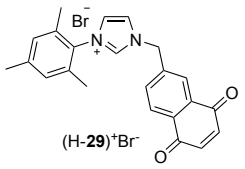

(H-**29**)$^{+}$Br^{-}

1-Mesytylimidazol (320 mg, 1.72 mmol, 3 eq) and 2-bromomethyl-naphthaquinone (144 mg, 0.57 mmol, 1 eq) were placed in round-bottomed flask and toluene (5 mL) were added. The reaction mixture was refluxed for 18 hours and subsquently cooled down to the room temperature and filtered. The precipitate was washed several times with hot toluene and Et_2O. The compound was purified by silica column chromatography (2% MeOH in CH_2Cl_2). The product was obtained as a beige solid (yield = 39%).

The product was fully decomposed after few hours when stored in the standard conditions. The decomposition process is slower when product is kept in the freezer. Due to the instability full characterization of the imidazolium salt (H-**29**)$^{+}$Br^{-} was not possible.

^{1}**HNMR** (400 MHz, $CDCl_3$) δ 10.51 (s, 1H), 8.17 – 8.03 (m, 4H), 7.96 (d, *J* = 7.9 Hz, 1H), 7.22 (s, 1H), 6.96 – 6.85 (m, 4H), 6.25 (s, 2H), 2.28 (s, 3H), 2.03 (s, 6H).

4.2.10. [AgBr(NHC-27)] 31

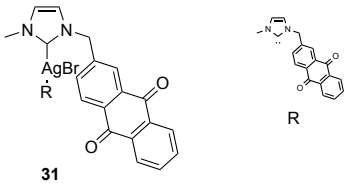

31

Silver oxide (25.6 mg, 0.111 mmol) and imidazolium salt **27** (65 mg, 0.17 mmol) were placed in Schlenk tube and air was evacuated. Under a nitrogen atmosphere deuterated DMSO (2 mL) was added. Reaction was stirred for 4 days protected from light. Progress of the reaction was monitored by ^{1}HNMR. Beside the desired complex, some unidentified impurities were formed. We also observed that imidazolium salt **27** was not completely reacted. The addition of 0.25 eq of Ag_2O did not drive the reaction to completion. All attempts to isolate the product were unsuccesful.

HRMS (DMSO): m/z 711.1157 $[Ag(NHC)_2]^+$

HRMS calculated: m/z 711.1161 $[Ag(NHC)_2]^+$

4.2.11. [AgBr(NHC-28)] 32

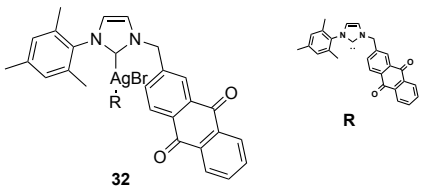

Silver oxide (36.2 mg, 0.156 mmol) and salt **28** (117 mg, 0.24 mmol) were placed in a Schlenk tube and air was evacuated. Under nitrogen atmosphere, deuterated DMSO (2 mL) was added. The reaction was stirred for 18 h protected from light and the progress of the reaction was monitored by ^{1}HNMR. The reaction mixture was filtered and ^{1}HNMR spectrum was recorded. The desired complex [AgBr(NHC-**27**)] **32** was obtained quantitatively.

^{1}HNMR (400 MHz, DMSO-d6) δ 8.07 (td, *J* = 7.5, 7.1, 3.6 Hz, 3H), 7.90 – 7.74 (m, 4H), 7.71 – 7.63 (m, 1H), 7.54 (d, *J* = 1.8 Hz, 1H), 6.93 (s, 2H), 5.58 (s, 2H), 2.29 (s, 3H), 1.79 (s, 6H).

^{13}CNMR (101 MHz, DMSO) δ 181.82, 181.75, 144.16, 138.51, 135.38, 134.59, 134.51, 134.23, 133.04, 132.71, 132.67, 132.49, 132.19, 128.83, 127.29, 126.66, 124.36, 123.76, 123.15, 53.16, 39.94, 39.73, 39.52, 39.31, 39.10, 38.89, 20.65, 17.11.

HRMS(DMSO): m/z 919.2414 $[Ag(NHC)_2]^+$

HRMS calculated: m/z 919.2413 $[Ag(NHC)_2]^+$

4.2.12. Salt (H-33)

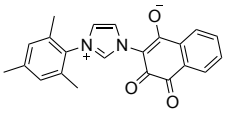

(H-**33**)

1-Mesytylimidazol (100 mg, 0.537 mmol) and 2,3-dichloronaphthaquinone (244 mg, 0.107 mmol) were placed in round-bottomed flask. The reaction mixture was refluxed in toluene (5 mL) for 2 days. An orange precipitate formed and was recovered by filtration and purified by reversed-phase chromatography.

Column: semipreparative Dr. Maisch Reprospher C18-DE column (150 x 20 mm, 5 µm particle size)

eluent A (water) and B (acetonitrile). The following method was used: flow rate 15 mL/min, UV detection at 254 nm; 0-1 min (90% A, isocratic), 1-10 min (gradient 90 → 0% A).

^{1}HNMR (400 MHz, $CDCl_3$) δ 9.30 (t, *J* = 1.6 Hz, 1H), 8.46 (dd, *J* = 2.0, 1.4 Hz, 1H), 8.16 (dd, *J* = 7.7, 1.2 Hz, 1H), 8.08 (dd, *J* = 7.7, 1.3 Hz, 1H), 7.69 (td, *J* = 7.6, 1.4 Hz, 1H), 7.58 (td, *J* = 7.5, 1.3 Hz, 1H), 7.14 (t, *J* = 1.9 Hz, 1H), 7.07 – 7.01 (m, 2H), 2.37 (s, 3H), 2.14 (s, 7H).

^{13}CNMR (101 MHz, $CDCl_3$) δ 184.05, 174.25, 166.48, 141.31, 136.01, 134.76, 134.37, 134.27, 131.49, 131.42, 131.14, 129.96, 126.83, 126.19, 124.70, 119.97, 21.26, 17.64.

HRMS(MeOH): m/z 359.1389 (M+H), m/z 381.1208 (M+Na)

HRMS calculated: m/z 359.1396 (M+H)

4.2.13. Salt (H-34)

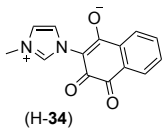

(H-**34**)

1-Methylimidazol (64 mg, 0.771 mmol) and 2,3-dichloronaphthaquinone were placed together in flask and toluene was added (5 mL). The reaction mixture was refluxed for 18 hours and then cooled to the room temperature. The suspension was filtered and the precipitate was purified on silica column using gradient system from 2-10% MeOH in CH_2Cl_2. The zwitterionic product **34** was obtained as orange solid (yield = 49%).

^{1}HNMR (400 MHz, DMSO) δ 9.18 (d, *J* = 1.6 Hz, 1H), 8.01 (dd, *J* = 7.7, 1.3 Hz, 1H), 7.90 (dd, *J* = 7.6, 1.4 Hz, 1H), 7.78 (td, *J* = 7.5, 1.4 Hz, 1H), 7.72 – 7.62 (m, 3H), 3.92 (s, 3H).

^{13}CNMR (101 MHz, DMSO) δ 184.29, 172.97, 165.95, 137.86, 134.45, 134.04, 131.51, 131.09, 125.99, 125.74, 124.81, 121.74, 115.74, 39.94, 39.73, 39.52, 39.31, 39.10, 35.69.

HRMS (MeOH): m/z 255.0763 [M+H]

HRMS calculated: m/z 255.0770 [M+H]

4.2.14. Salt (H-38)$^{+}$Cl^{-}

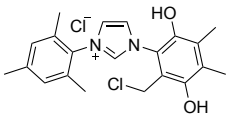

(H-**38**)$^{+}$Cl^{-}

2-Chloro-3,5,6 trimethylquinone(23.8 mg, 129 mmol) and mesytylimidazole (20 mg, 107 mmol) were placed in flask and CH_2Cl_2 (3 mL) was added. After stirring for 5 days at room temperature, a small amount of yellow precipitate appeared. After stirring for another 2 weeks the precipitate was filtered and washed with cold CH_2Cl_2 to yield pure compound **38** (4 mg, y = 12%).

^{1}**HNMR** (400 MHz, DMSO-d_6) δ 9.56 (q, *J* = 1.3 Hz, 1H), 9.02 (q, *J* = 2.9, 2.5 Hz, 1H), 8.65 (s, 0H), 7.89 (t, *J* = 1.6 Hz, 1H), 7.82 (dq, *J* = 2.4, 1.4 Hz, 1H), 7.13 (s, 2H), 5.59 (s, 2H), 2.32 (s, 3H), 2.15 (d, *J* = 2.3 Hz, 6H), 1.99 (s, 6H).

^{13}**CNMR** (101 MHz, DMSO) δ 147.45, 144.53, 140.12, 137.63, 134.28, 131.16, 129.13, 128.35, 124.22, 122.62, 119.35, 117.23, 46.51, 20.56, 16.88, 13.54, 13.27.

MS-ESI (MeOH): m/z 371.2

5. ^{1}HNMR ^{13}CNMR spectra

5.1. Boc protected propyl amine 3-mesitylimidazolium chloride

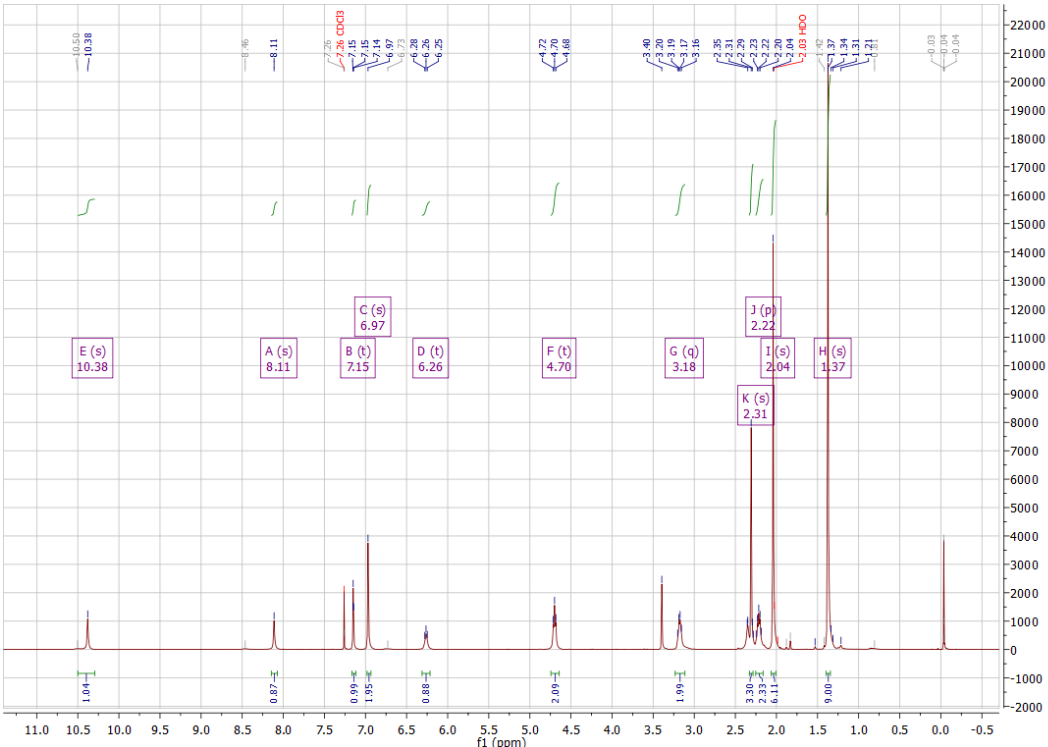

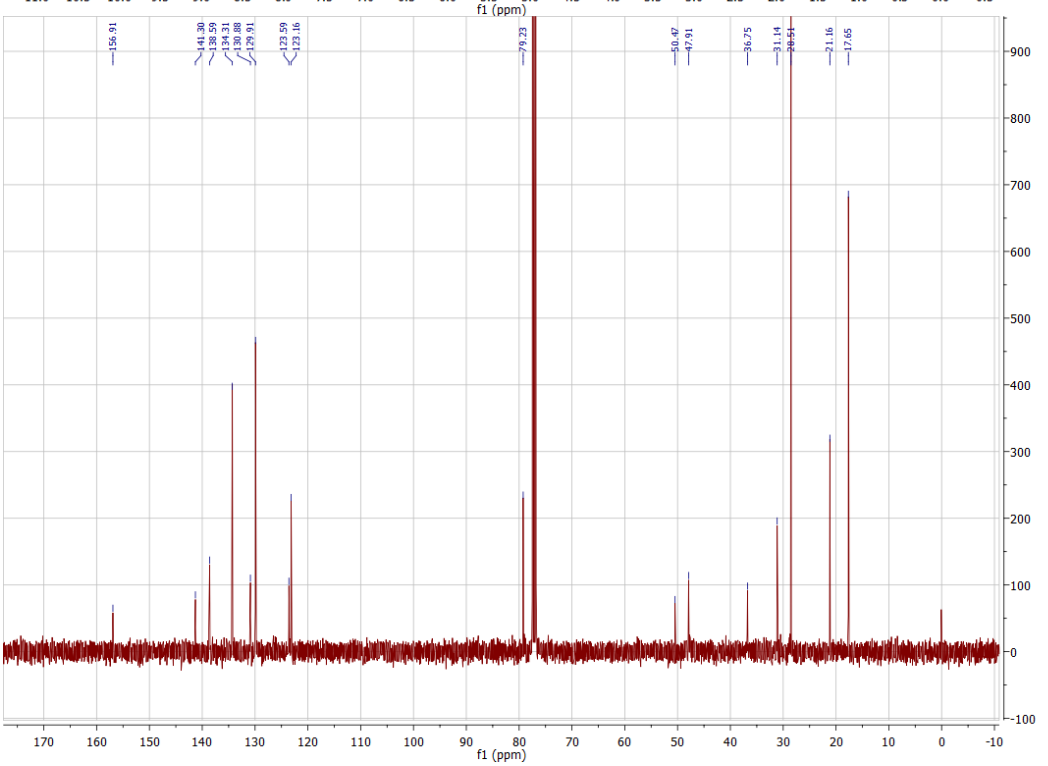

5.2. Salt $(H\text{-}1)^{+}Cl^{-}$

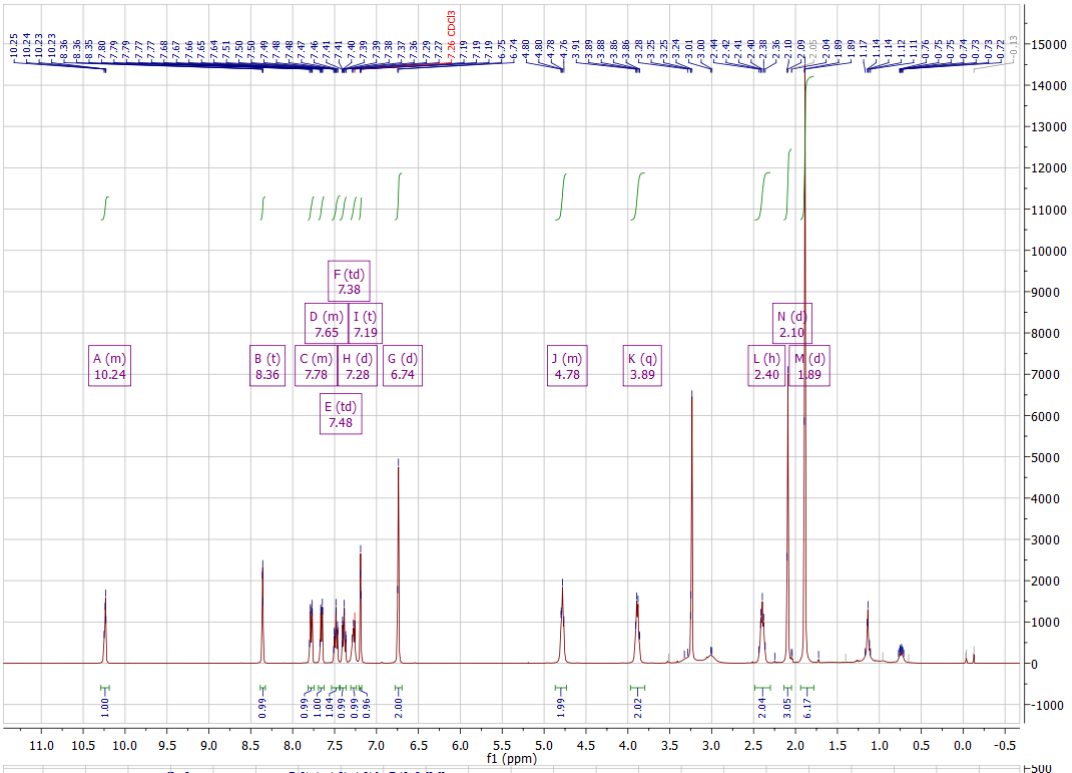

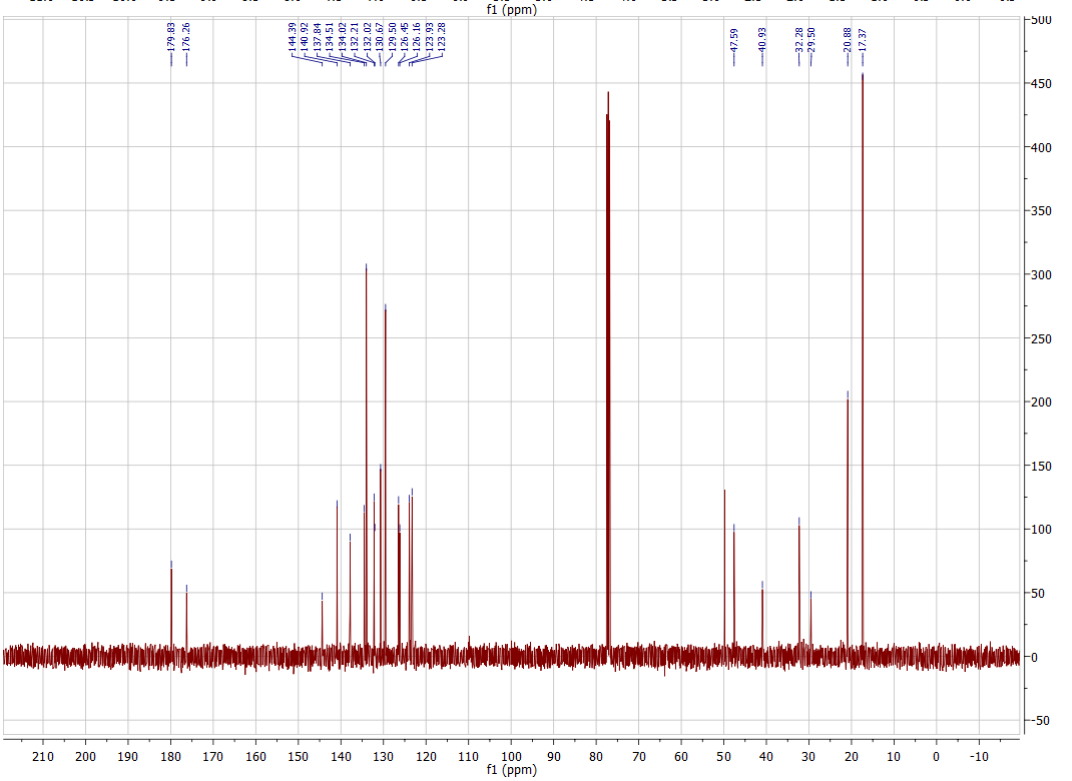

5.3. [Ag(μ-Cl)(NHC-1)$_2$] 2

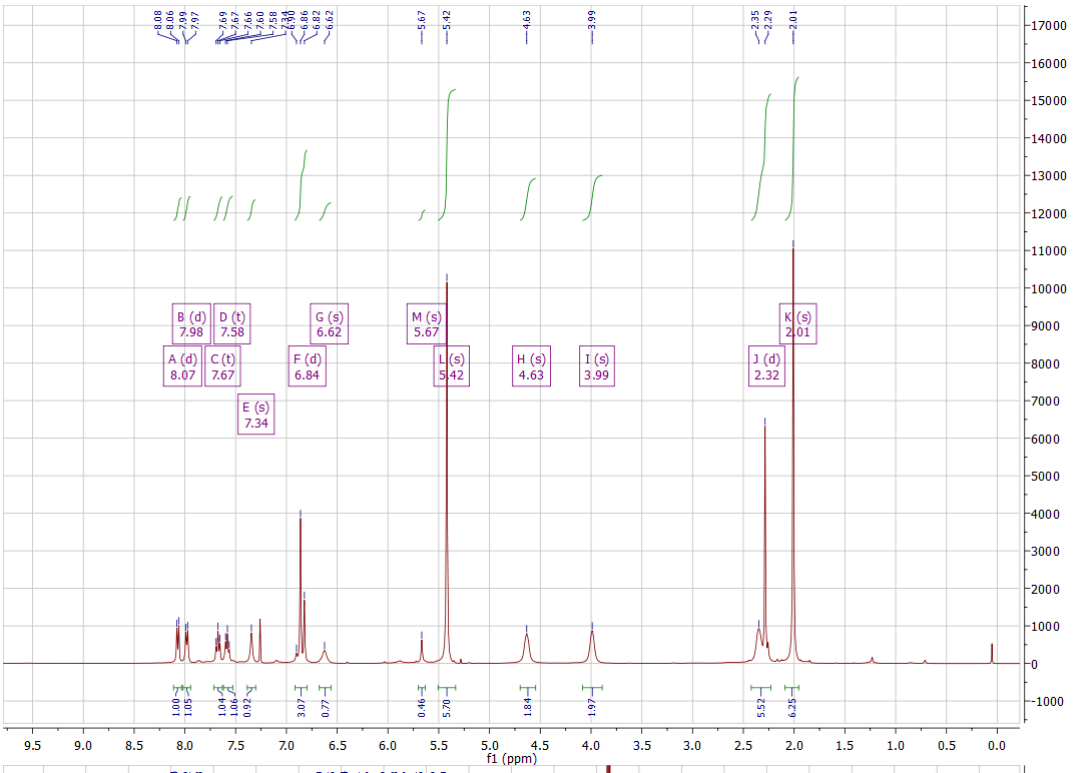

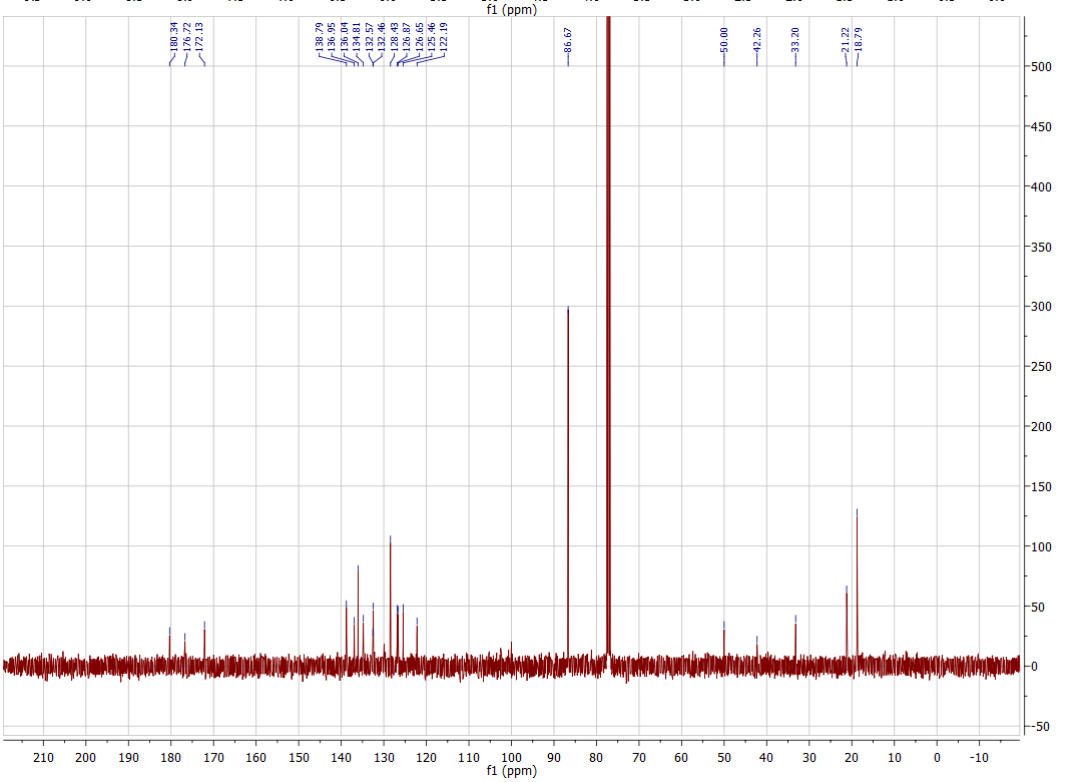

5.4. [(η^6-C_6H_6)$RuCl_2$(NHC-1)] 3

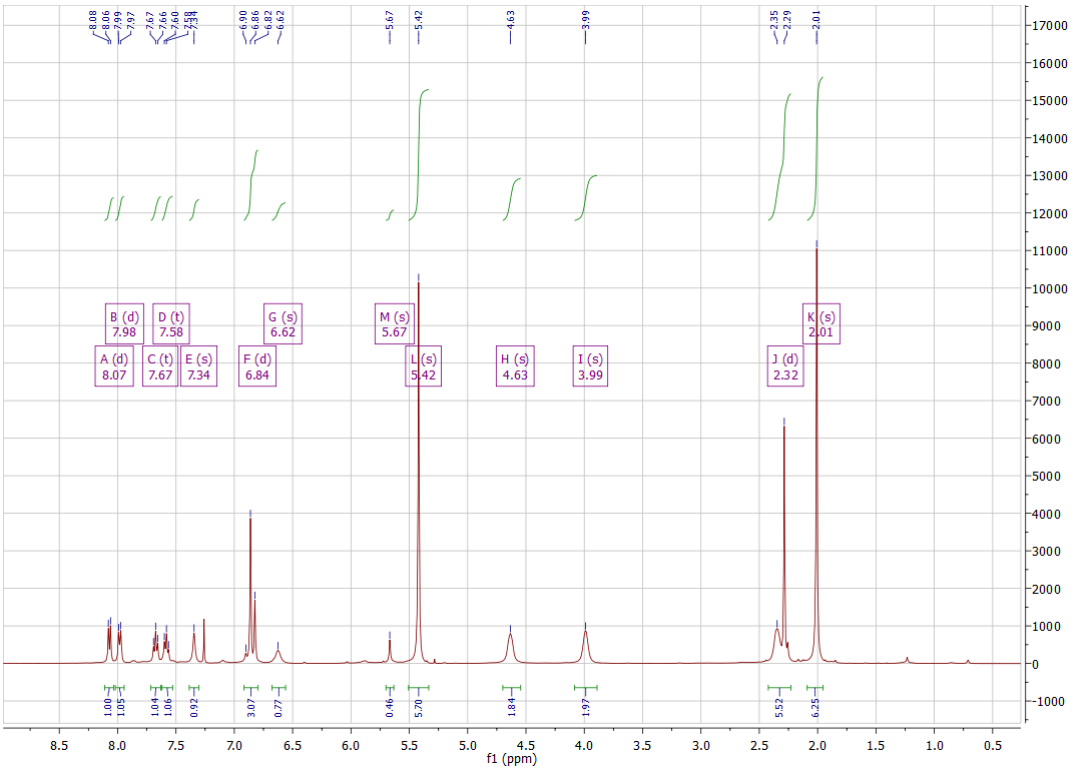

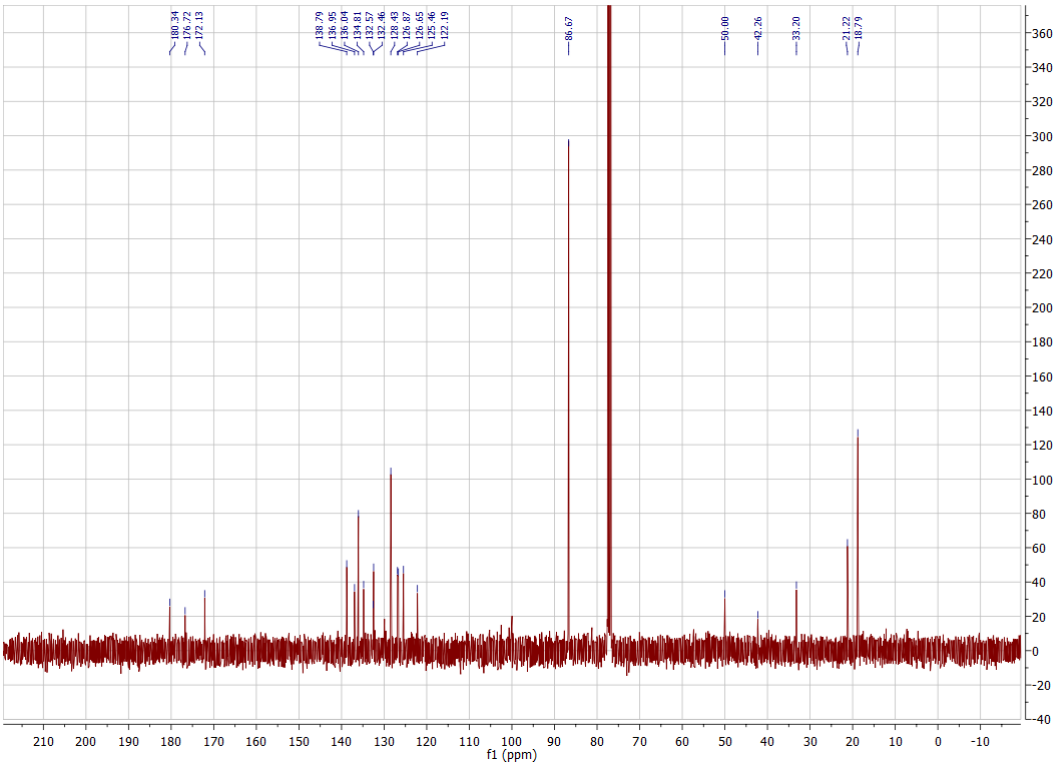

5.5. [(η^5-Cp*)$IrCl_2$(NHC-1)] 4

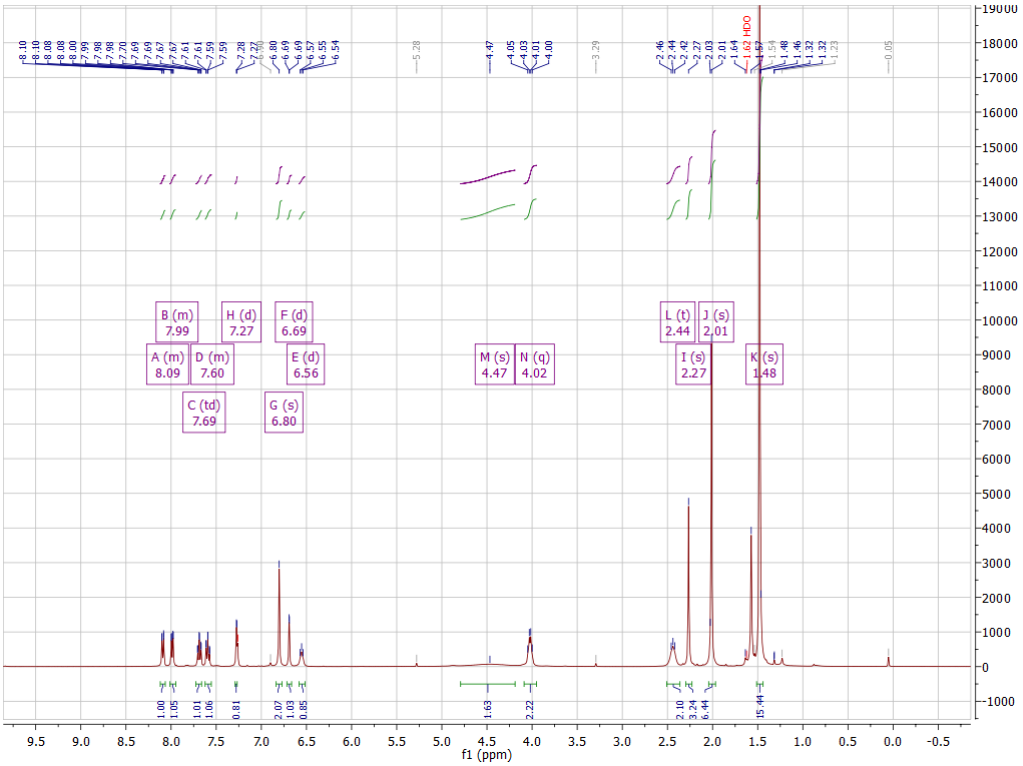

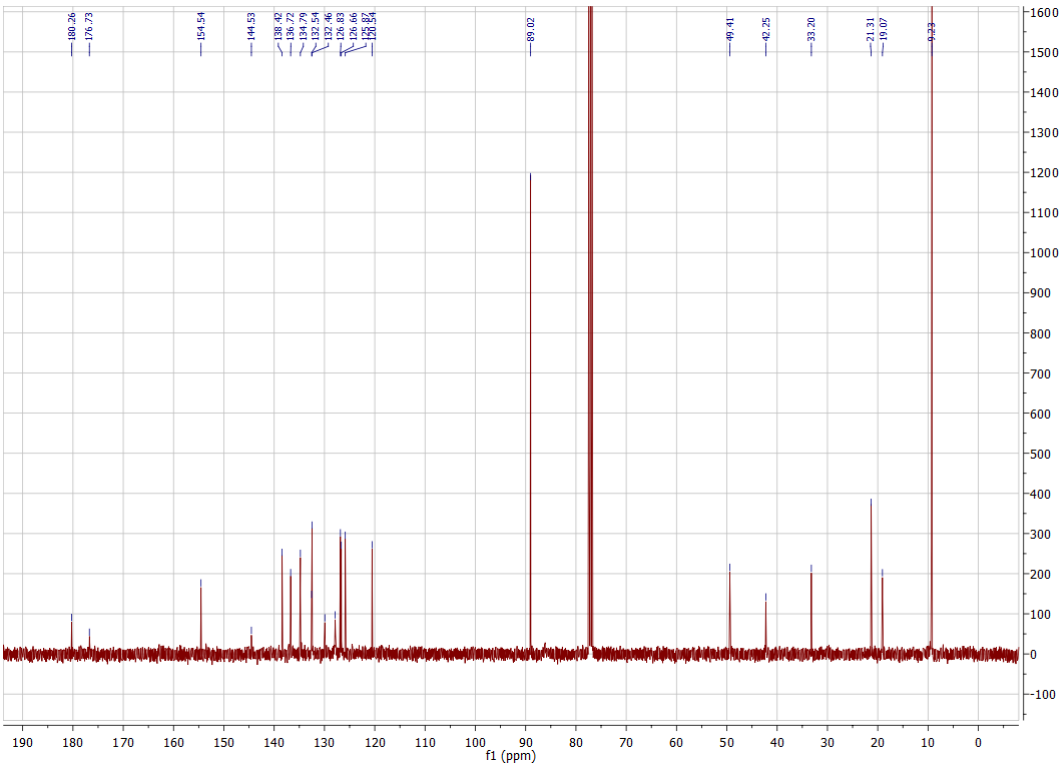

5.6. [PdCl(η^3-allyl)(NHC-1)] 5

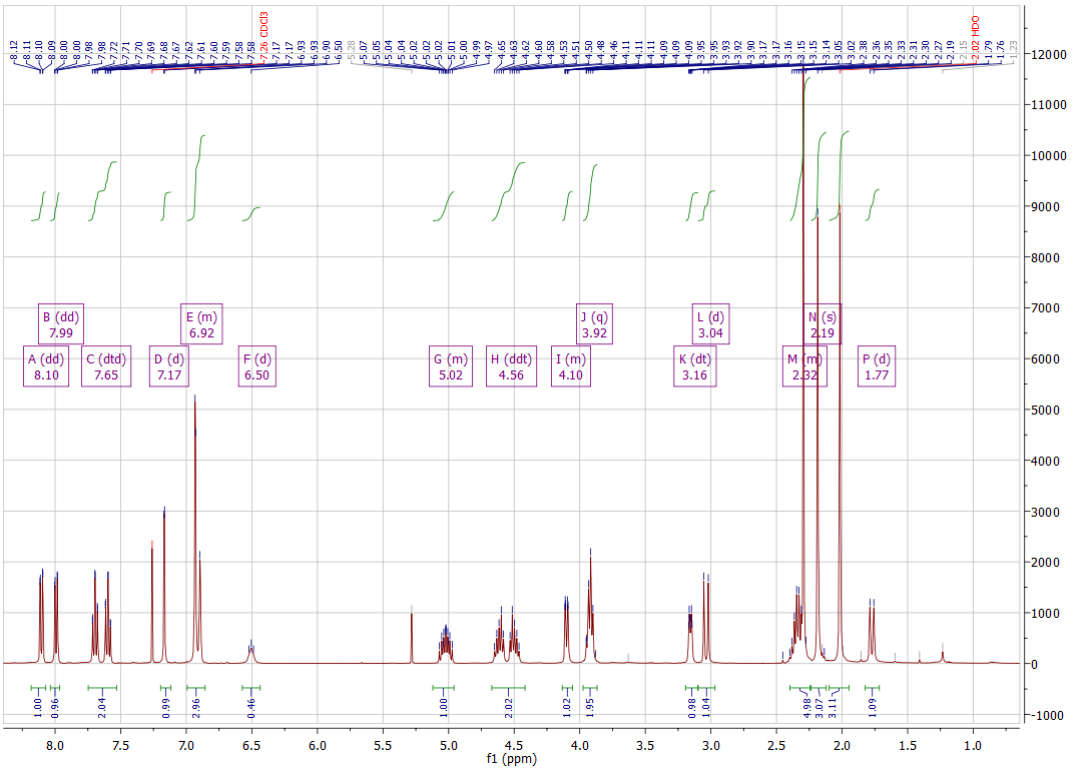

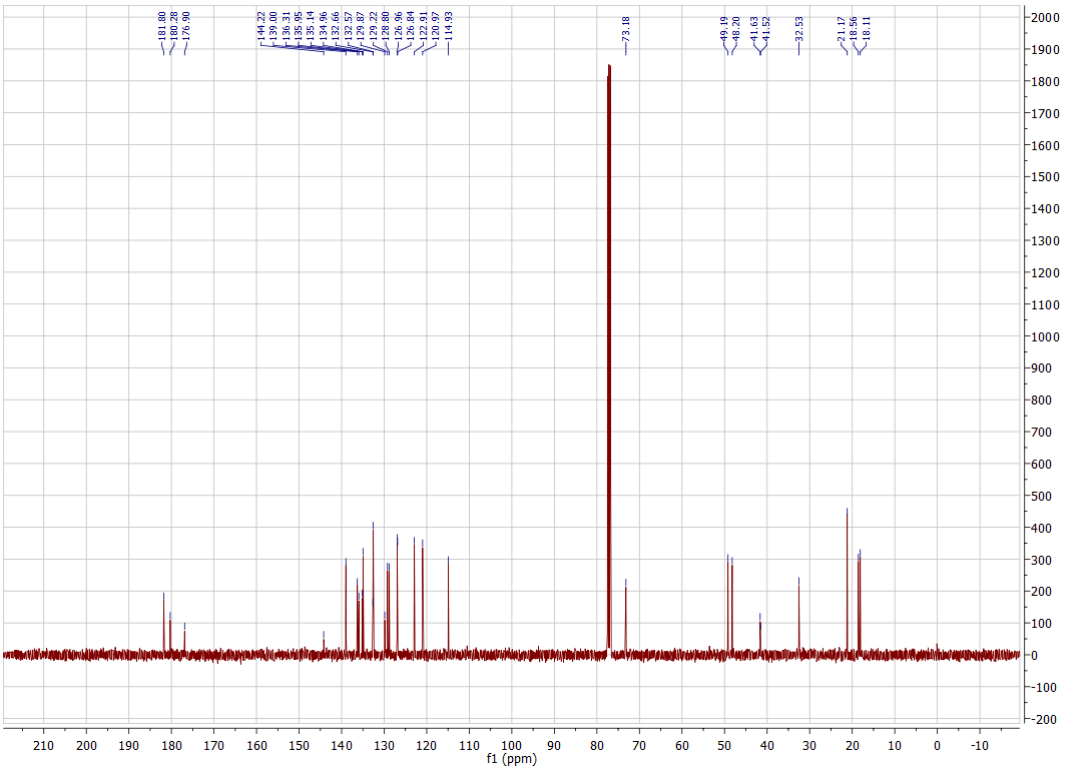

5.7. Reference imidazolium salt $(H\text{-}2)^{+}I^{-}$

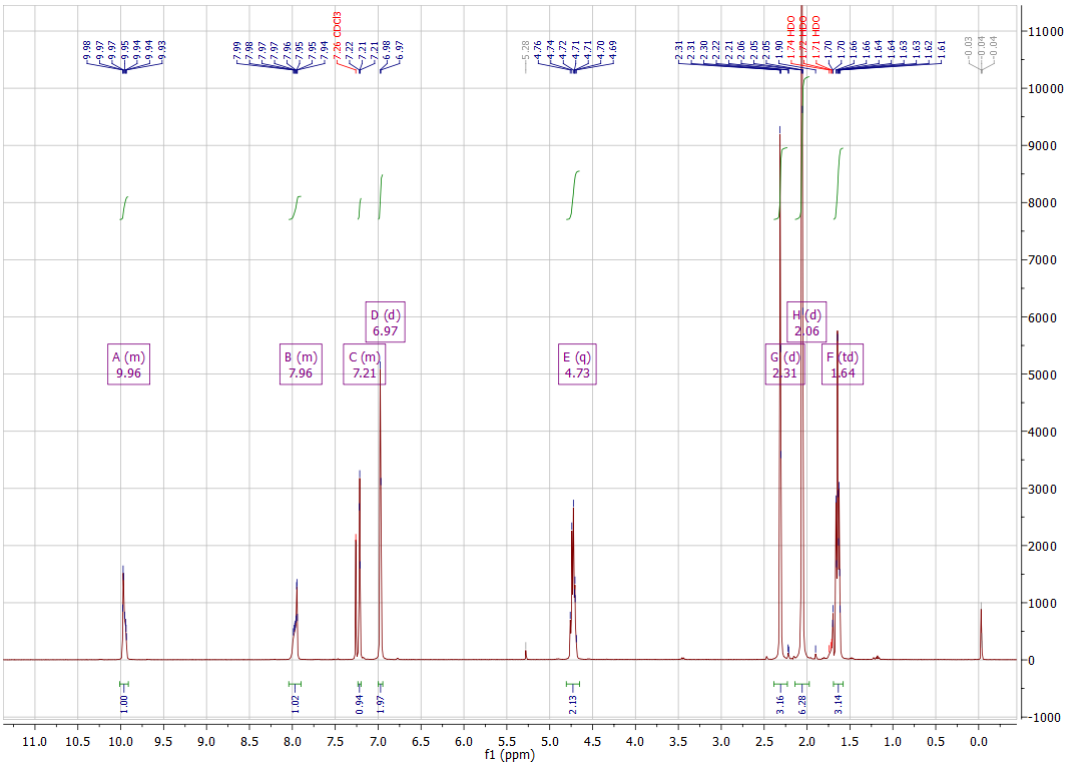

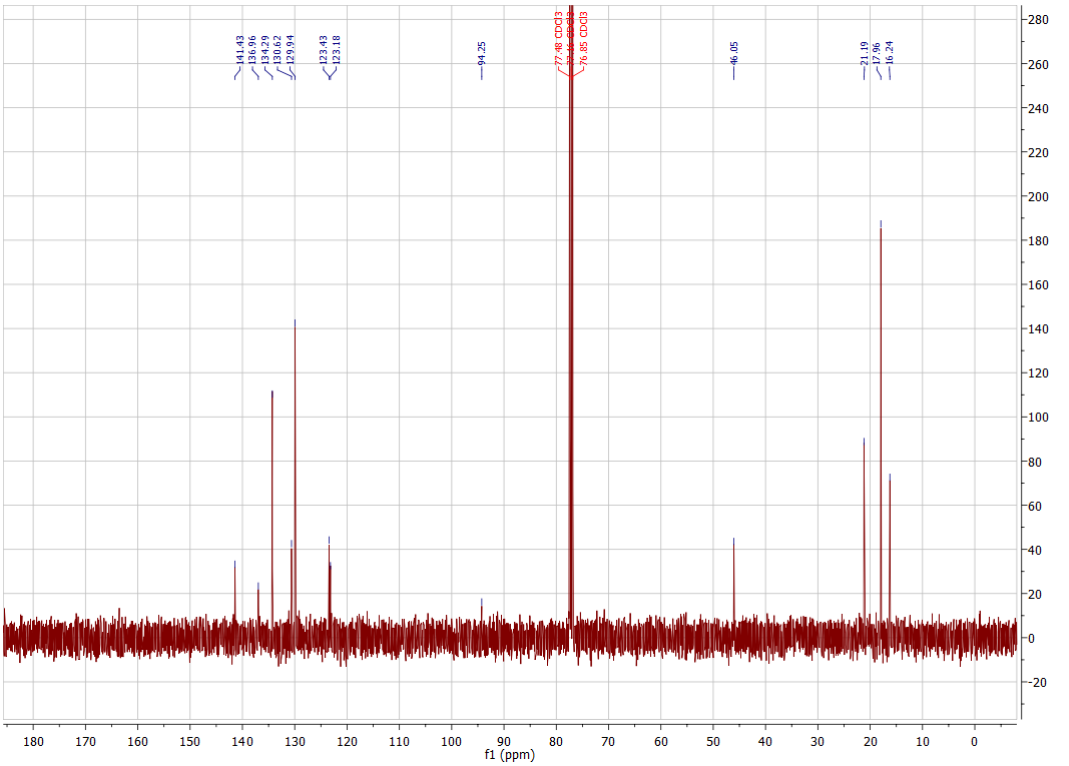

5.8. [AgI(NHC-2)$_2$] 7

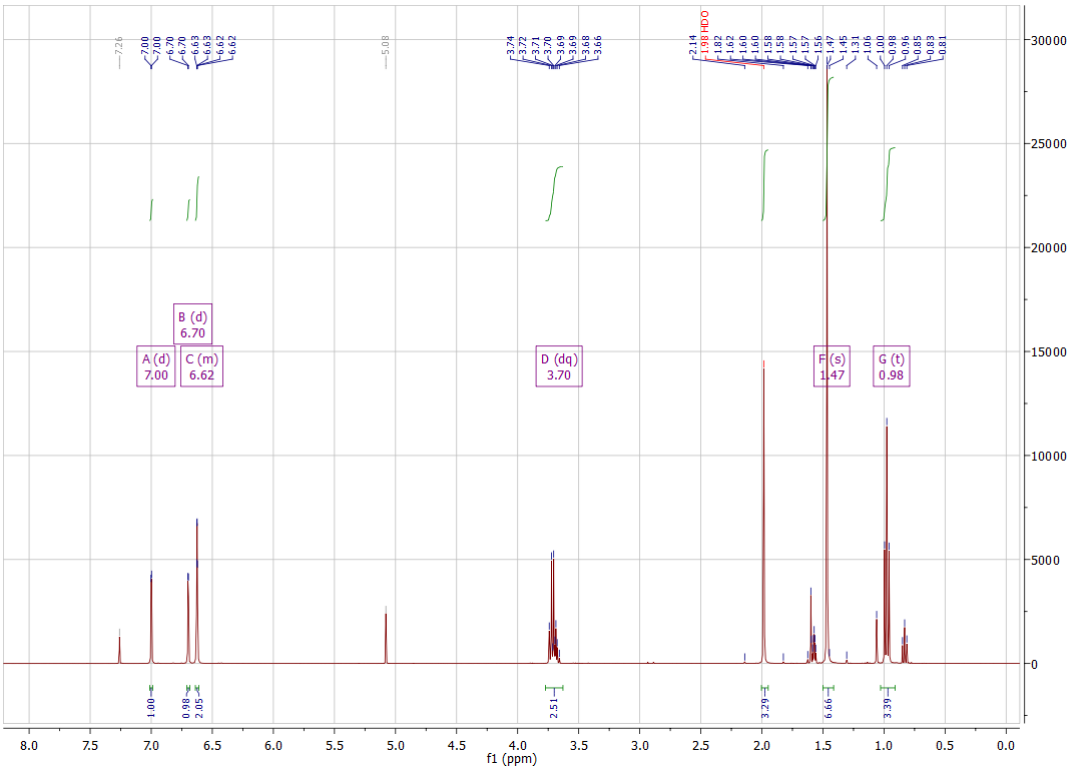

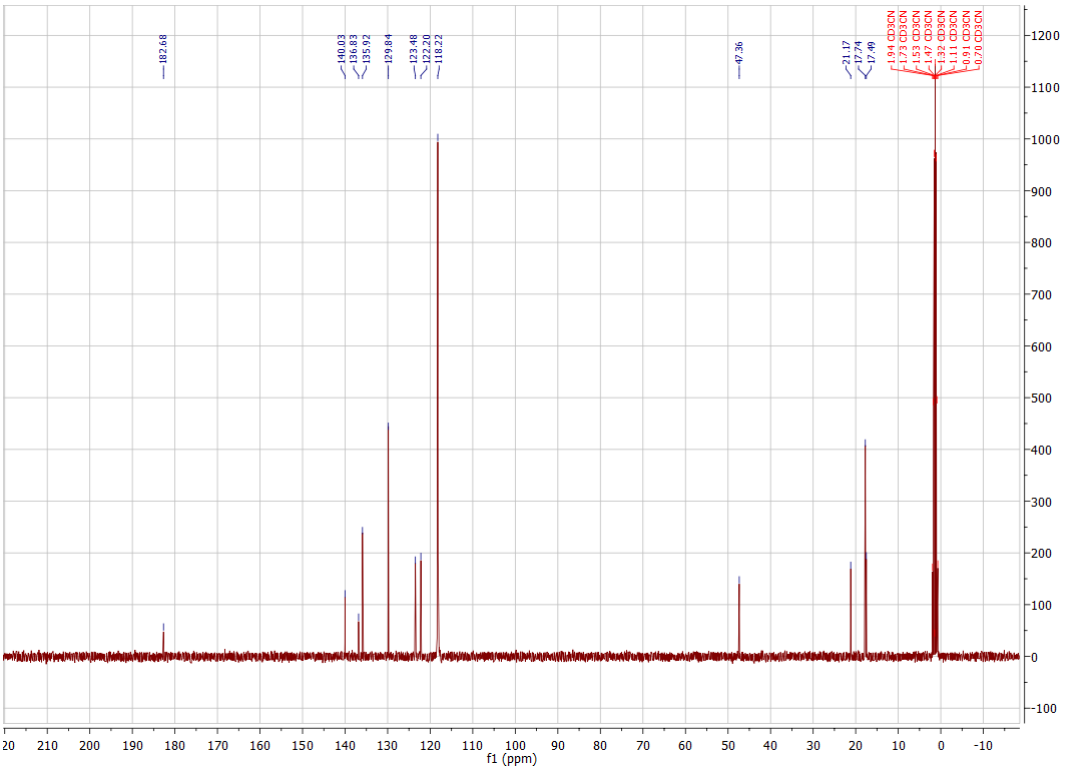

5.9. [(η^6-C_6H_6)$RuCl_2$(NHC-2)] 8

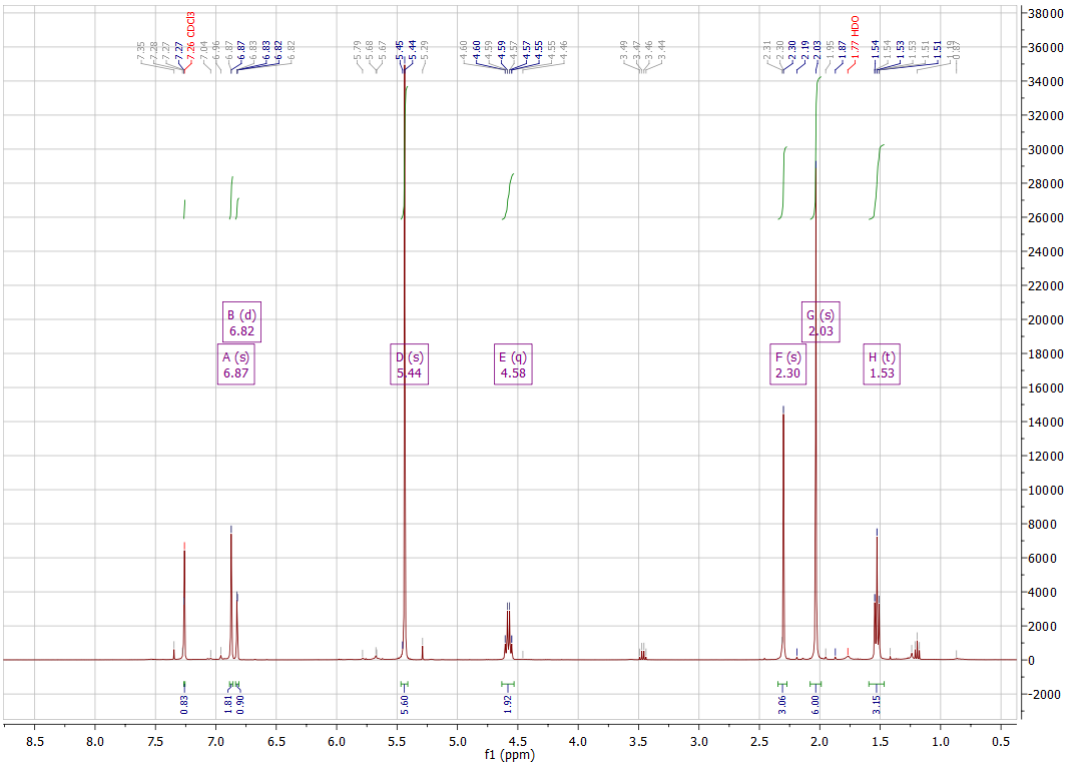

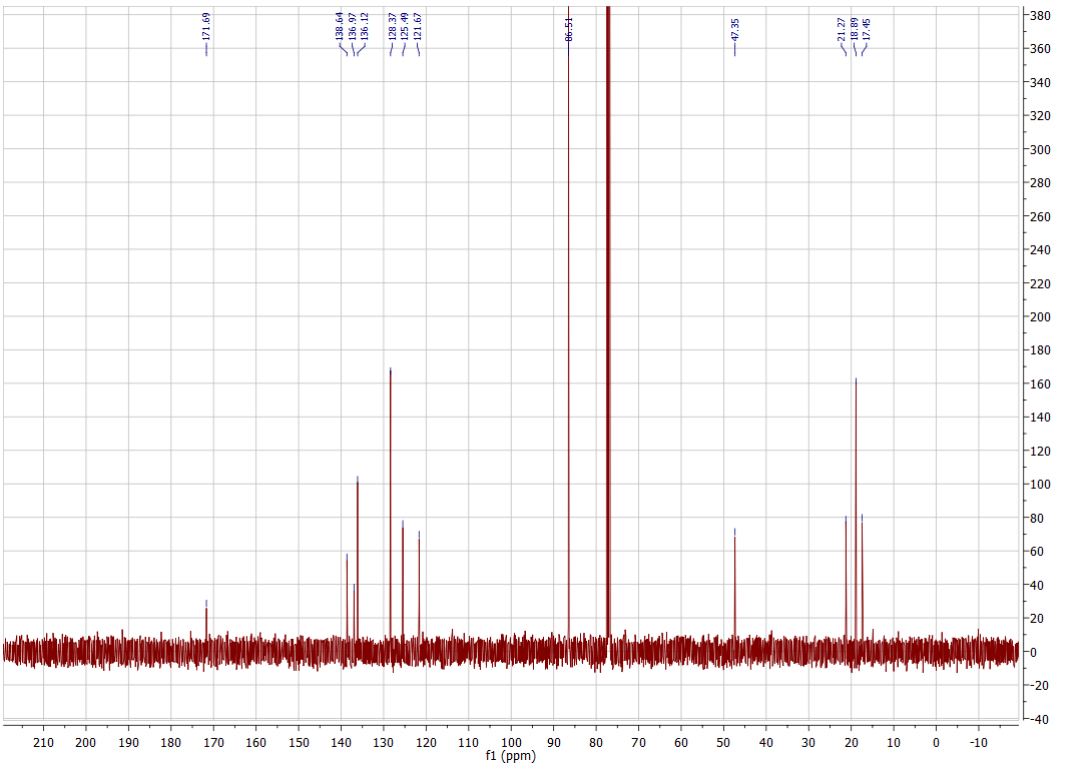

5.10. [(η^5-Cp*)IrCl$_2$(NHC-2)] 9

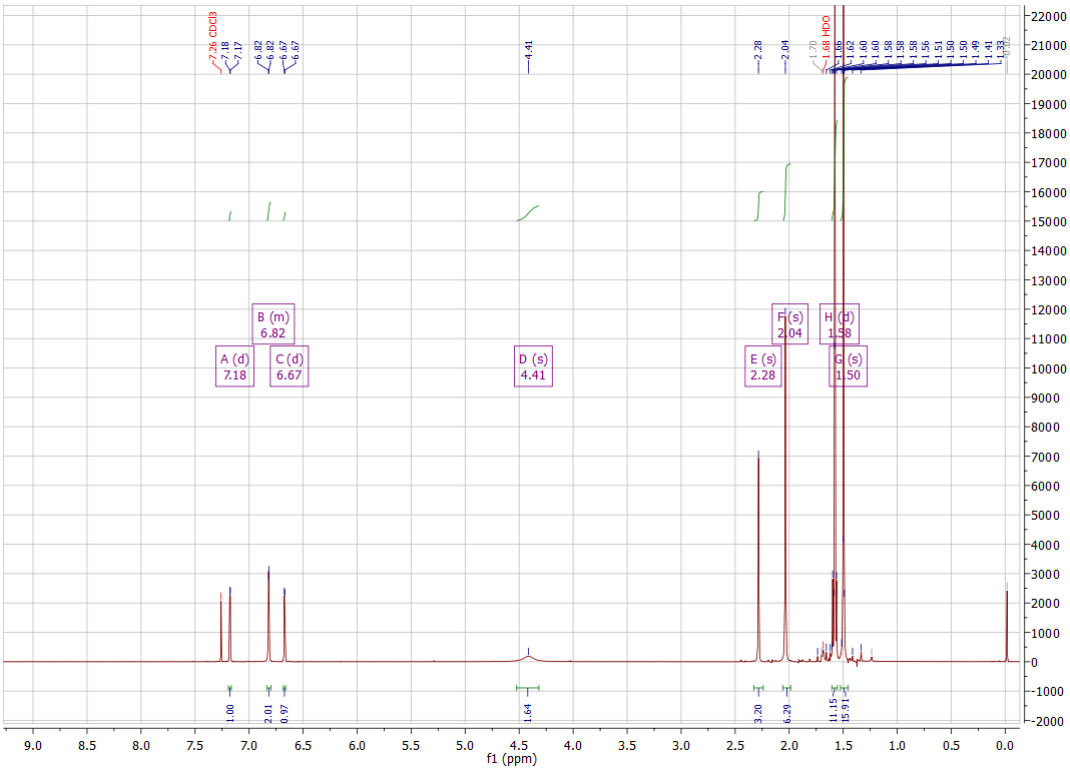

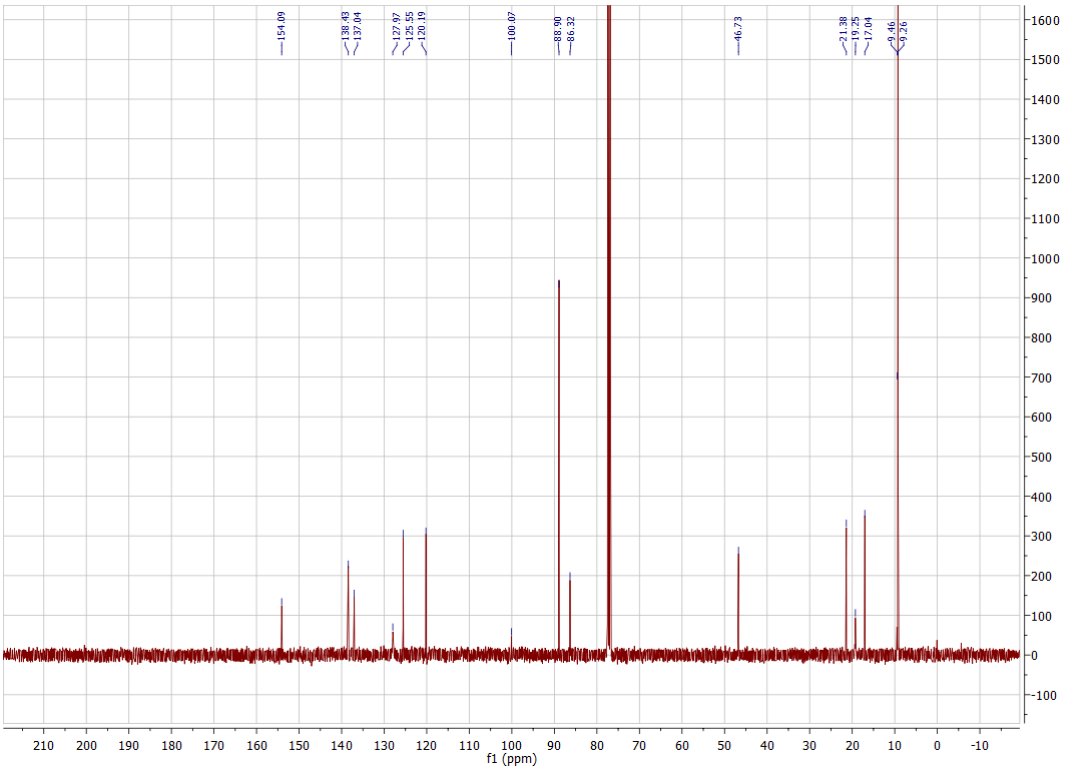

5.11. [PdCl(η^3-allyl)(NHC-2)] 10

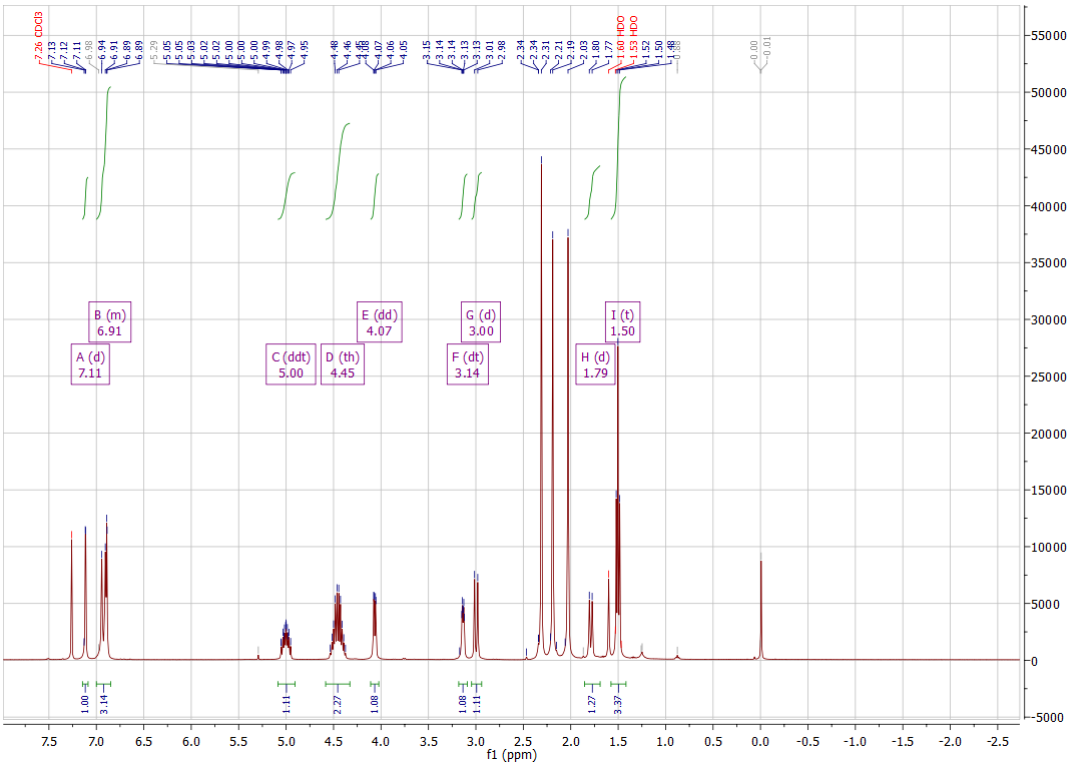

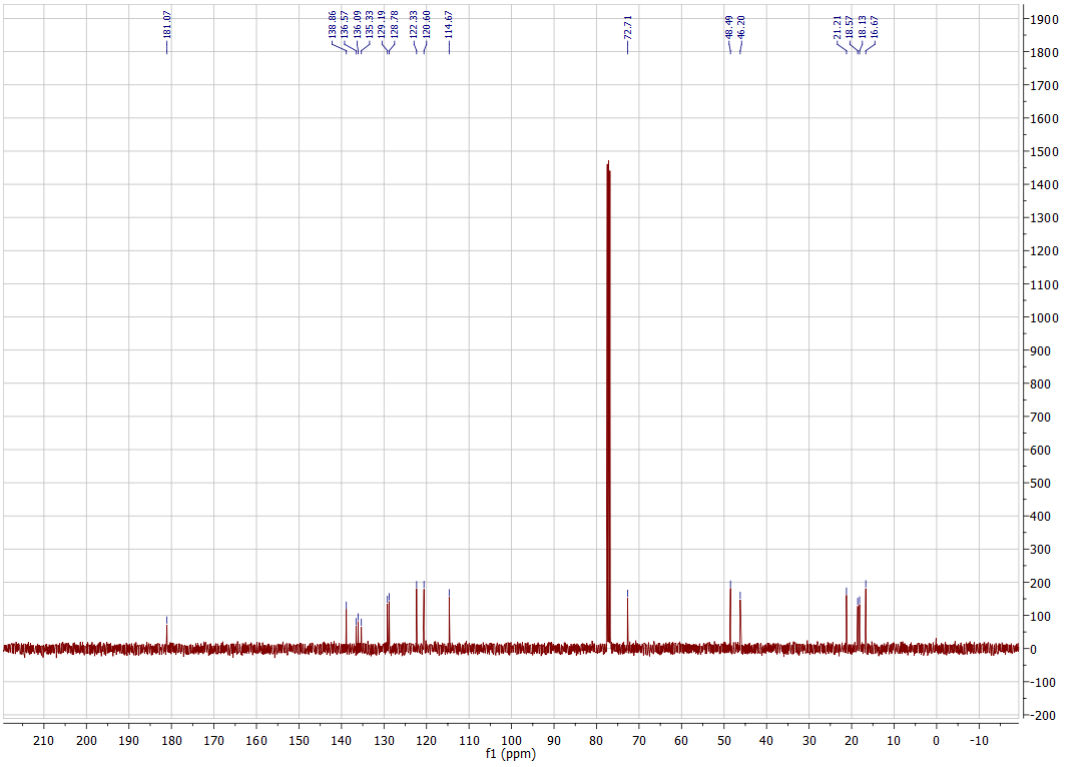

5.12. Salt (H-11)$^{+}$Br^{-}

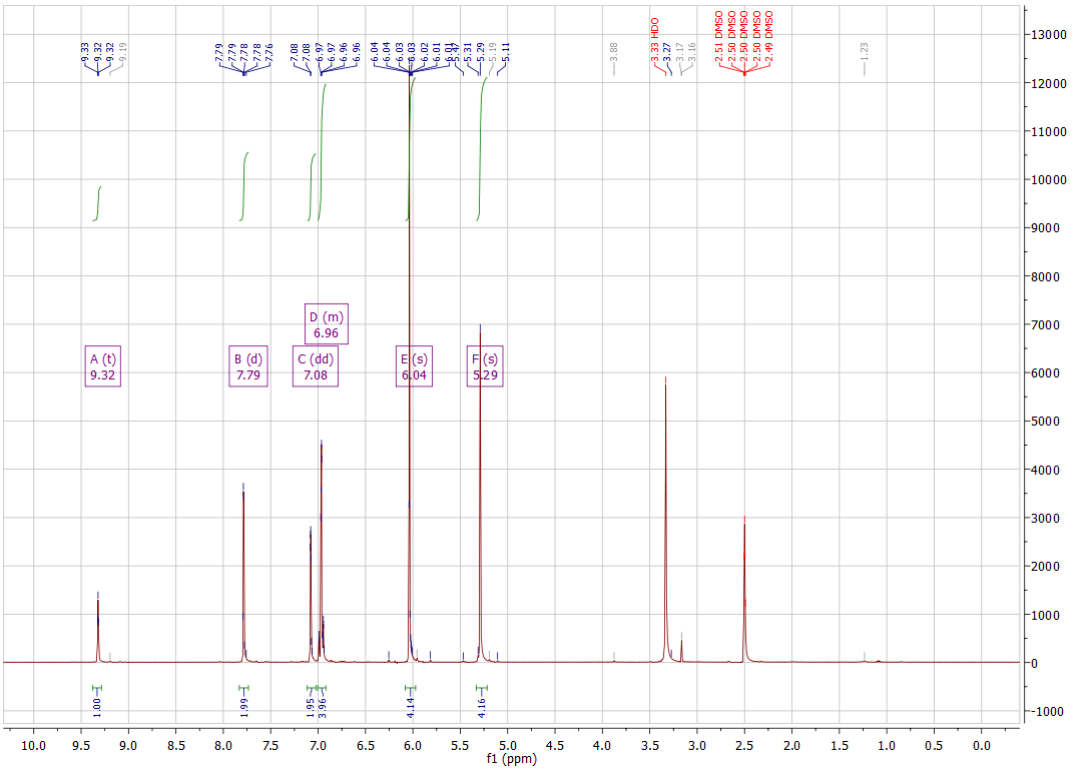

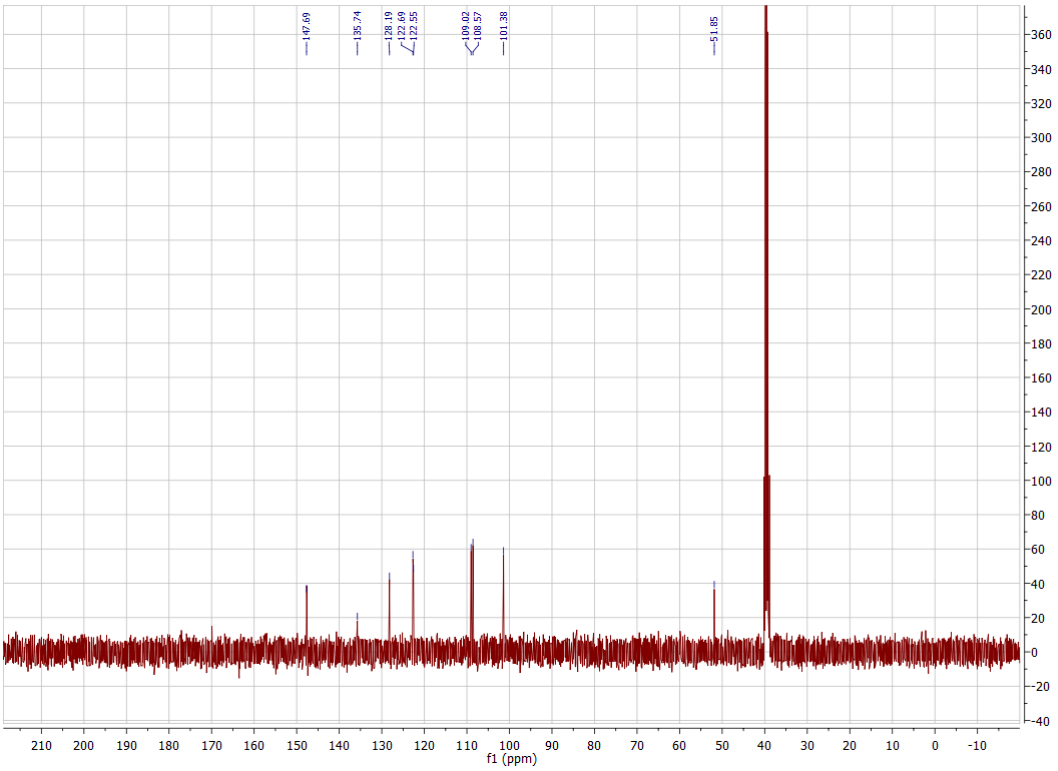

5.13. Salt $(H\text{-}13)^{+}I^{-}$

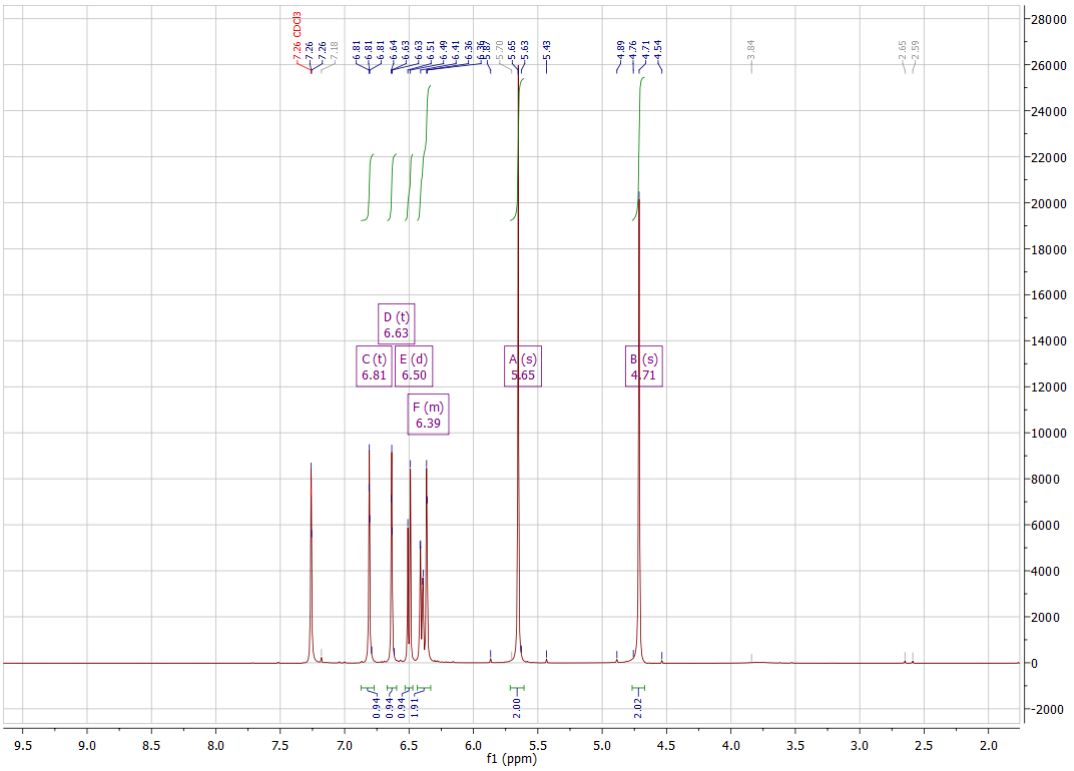

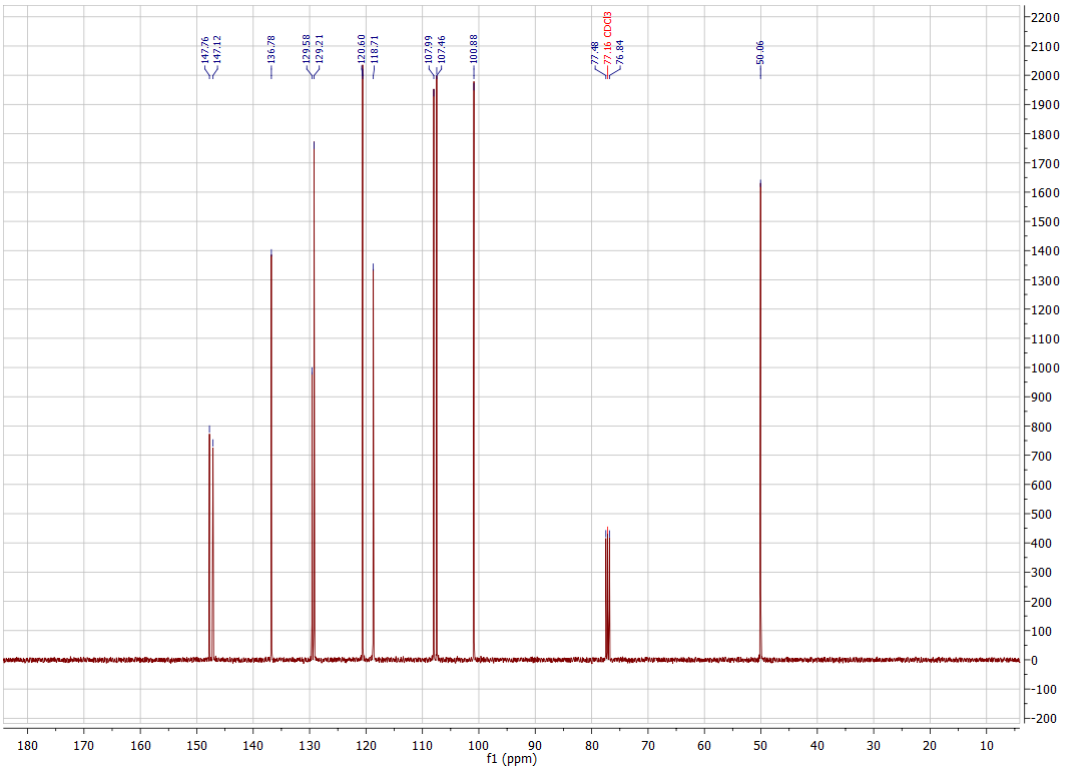

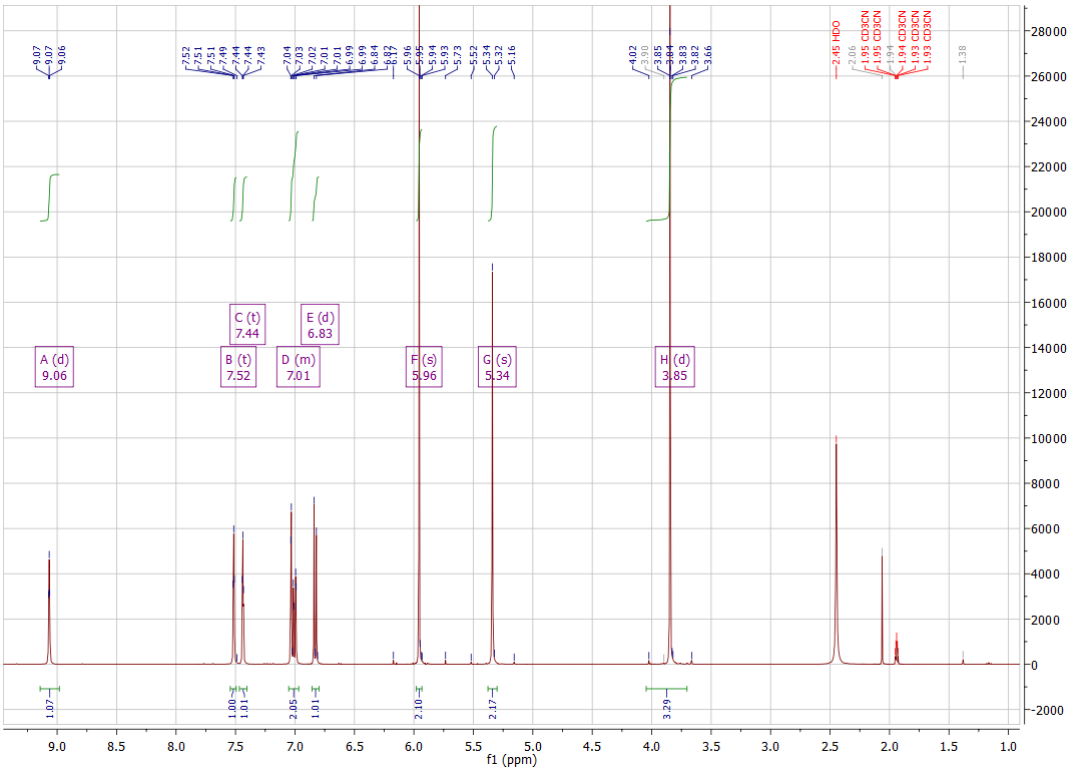
A (d)
9.06
B (t)
7.52
C (t)
7.44
D (m)
7.01
E (d)
6.83
F (s)
5.96
G (s)
5.34
H (d)
3.85
f1 (ppm)

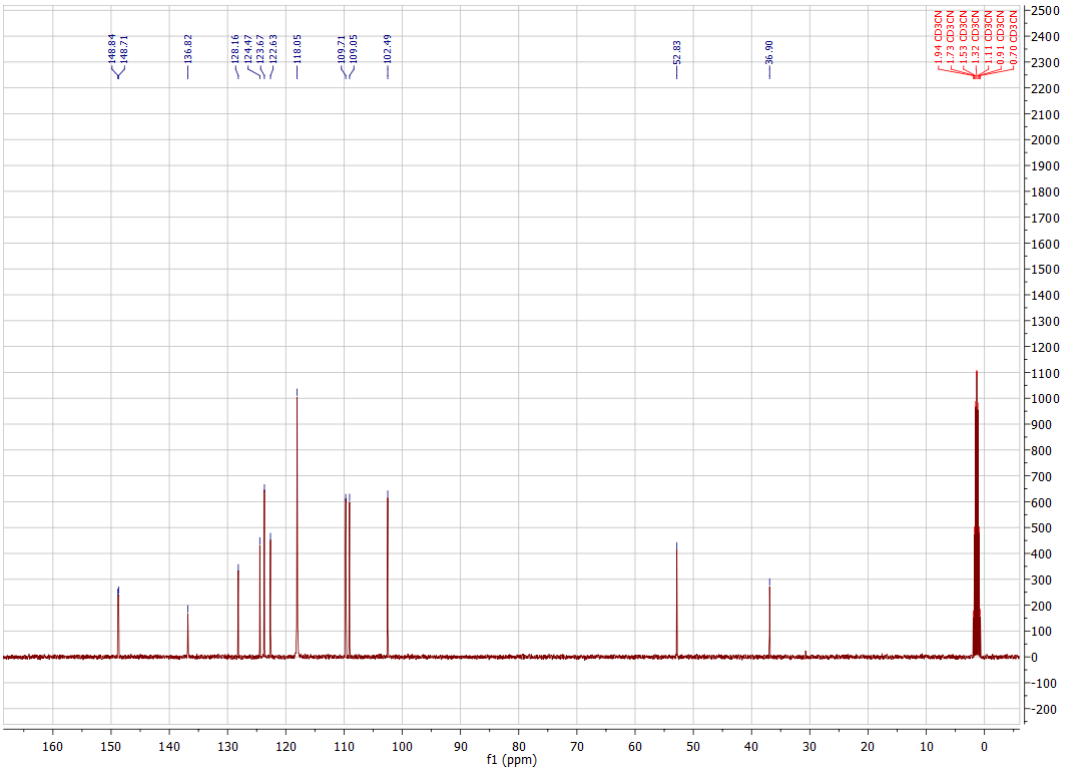
f1 (ppm)

5.14. Salt $(H_2\text{-}14)^{2+}2Br^-$

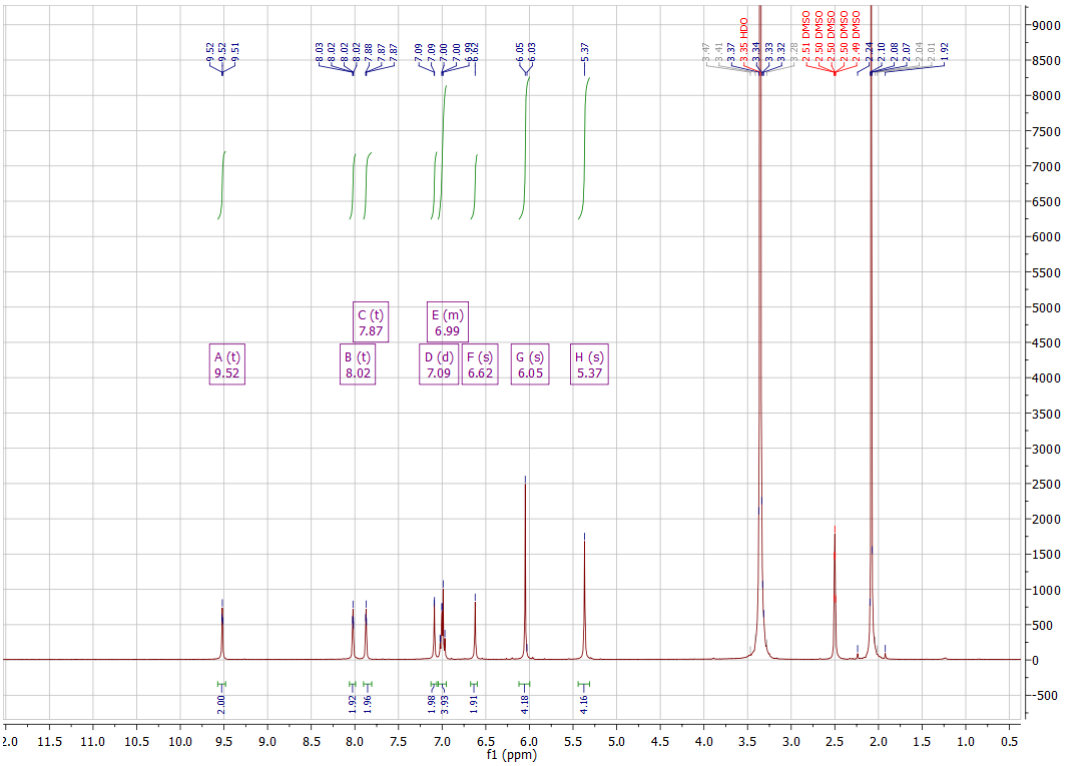

5.15. [PdCl(η^3-allyl)(NHC-11)] 19

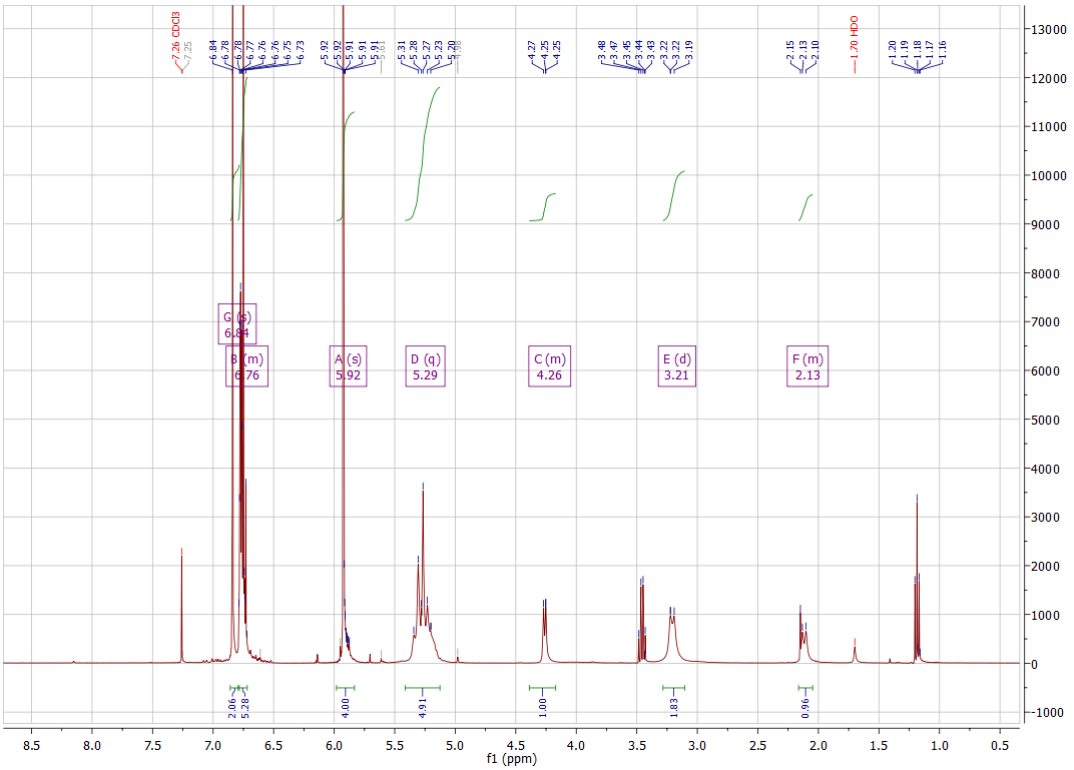

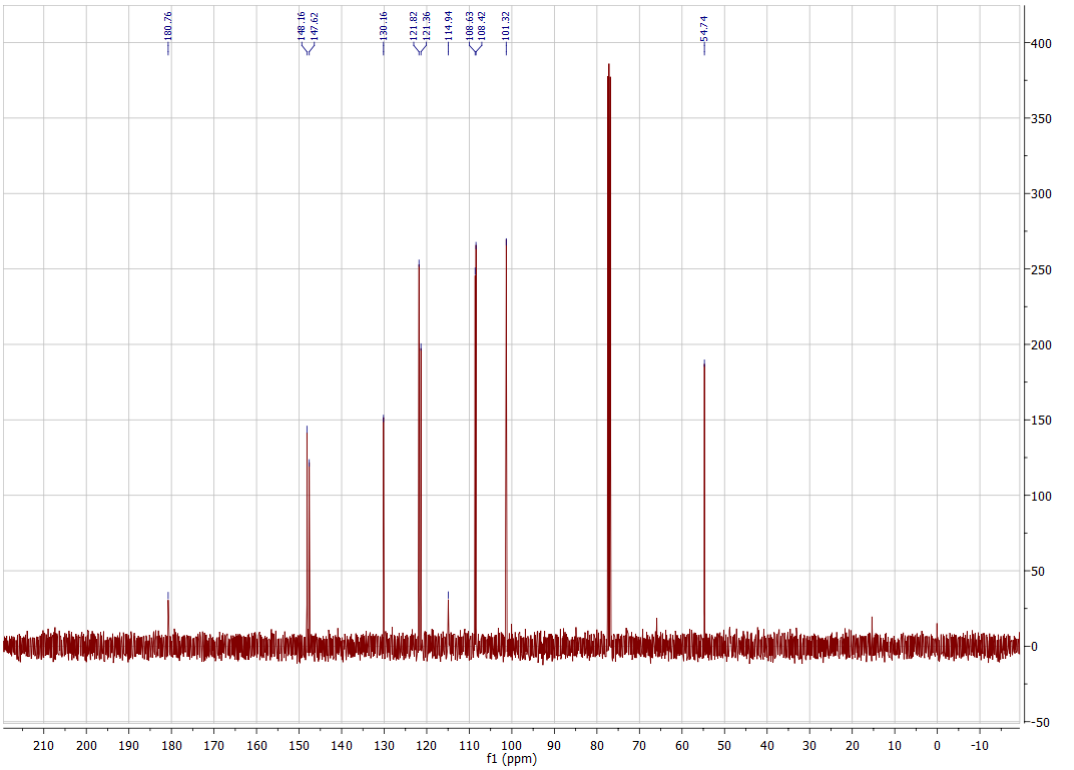

5.16. Salt (H-22)$^{+}Br^{-}$

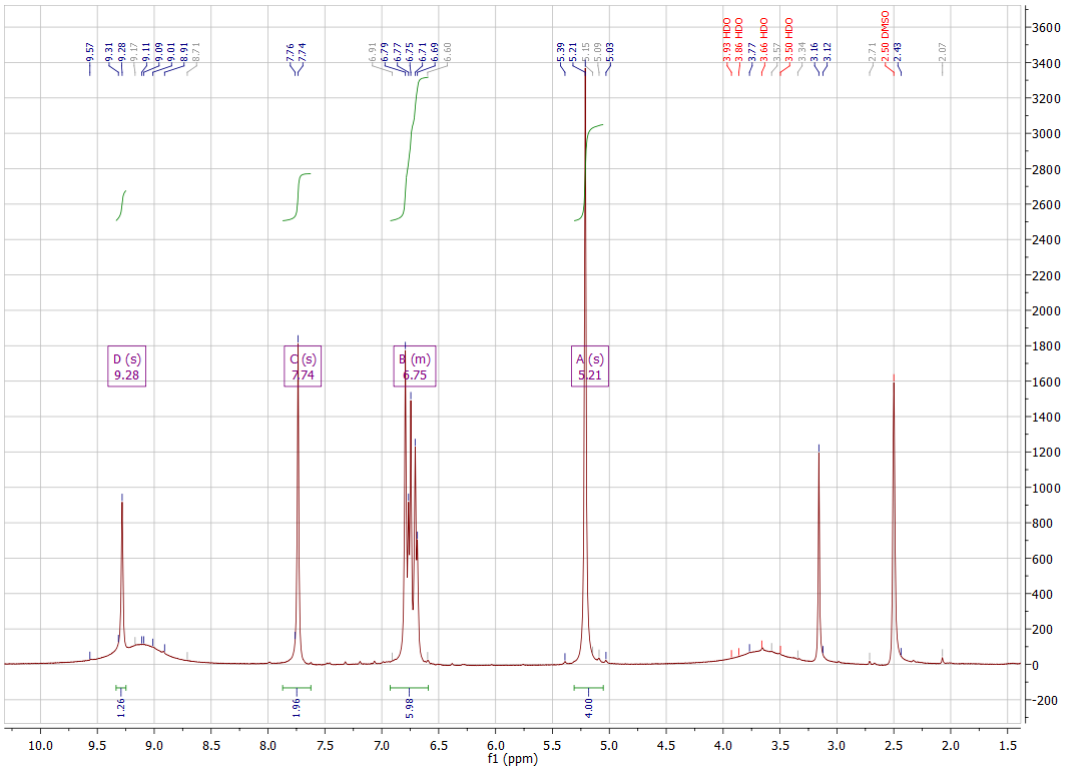

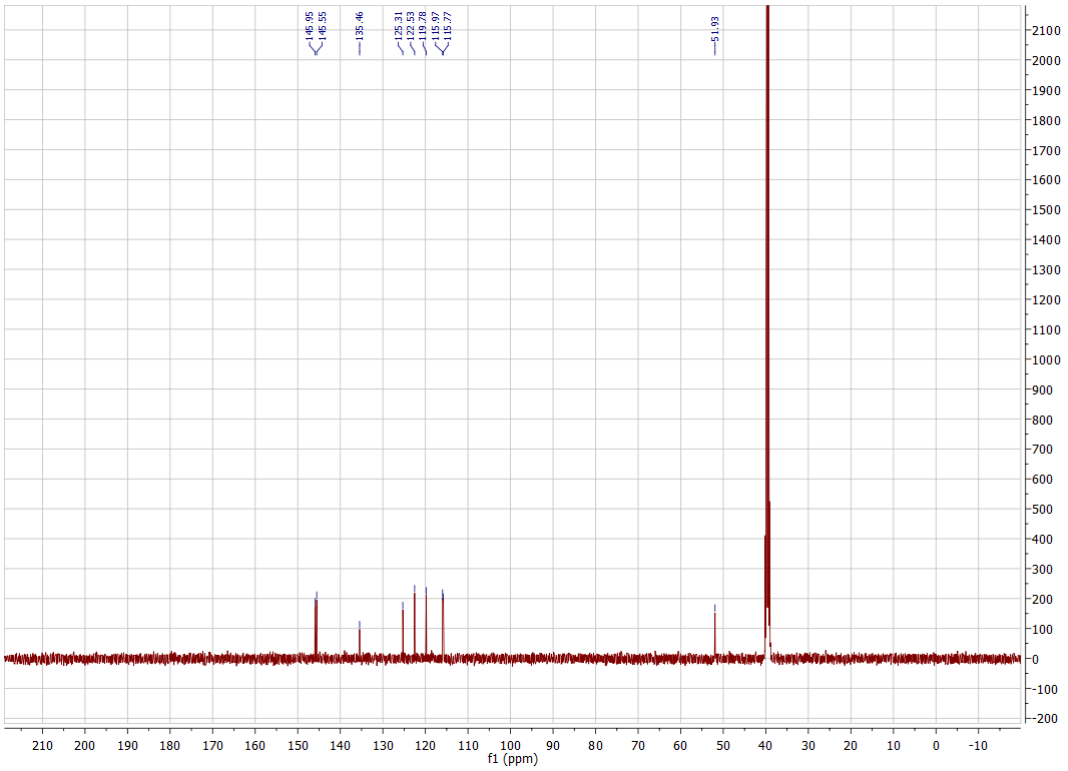

5.17. Salt (H-23)$^{+}I^{-}$

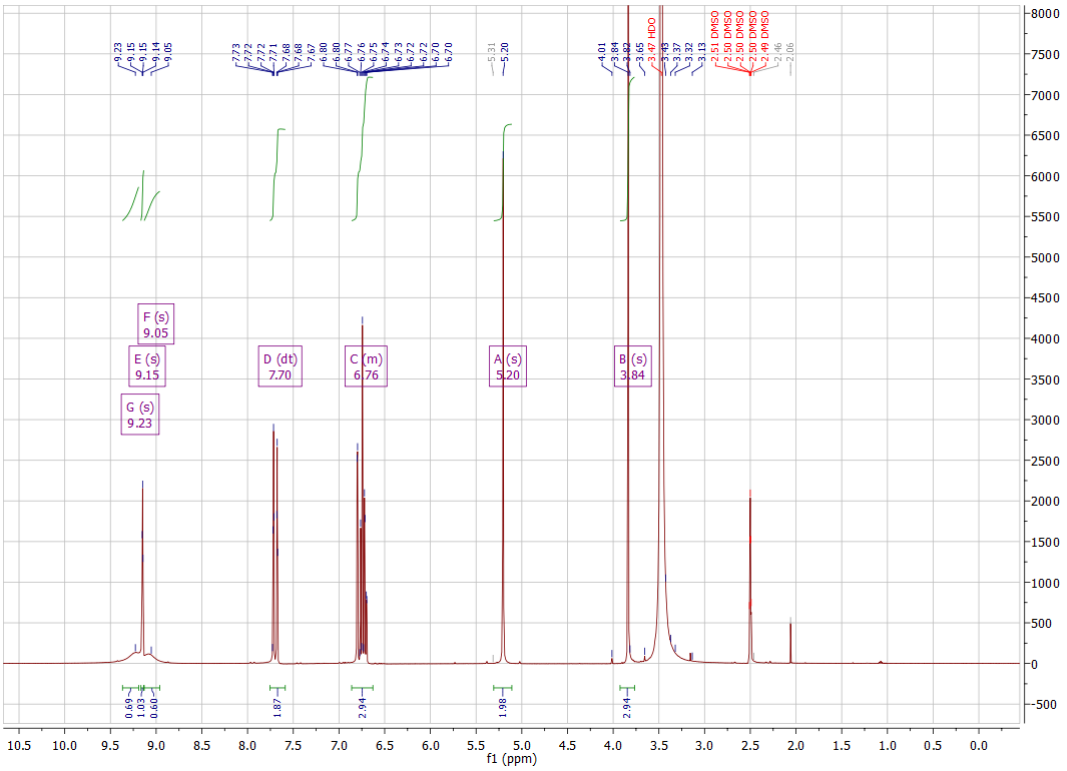

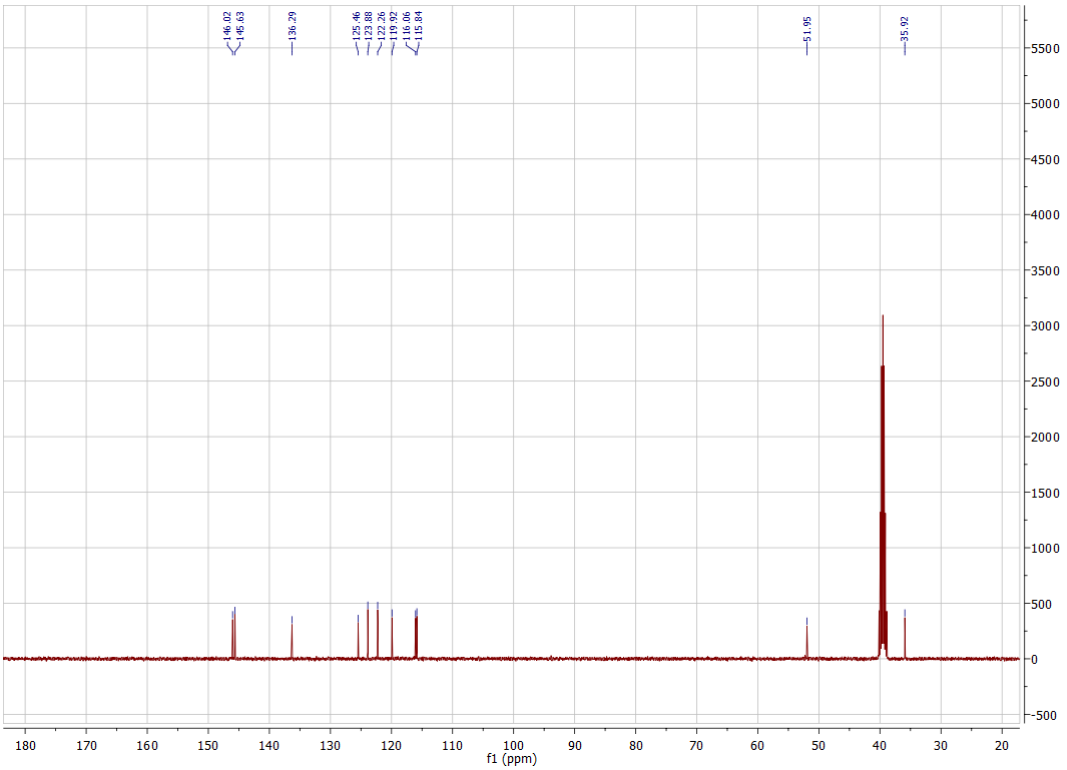

5.18. Salt (H-26)$^{+}Br^{-}$

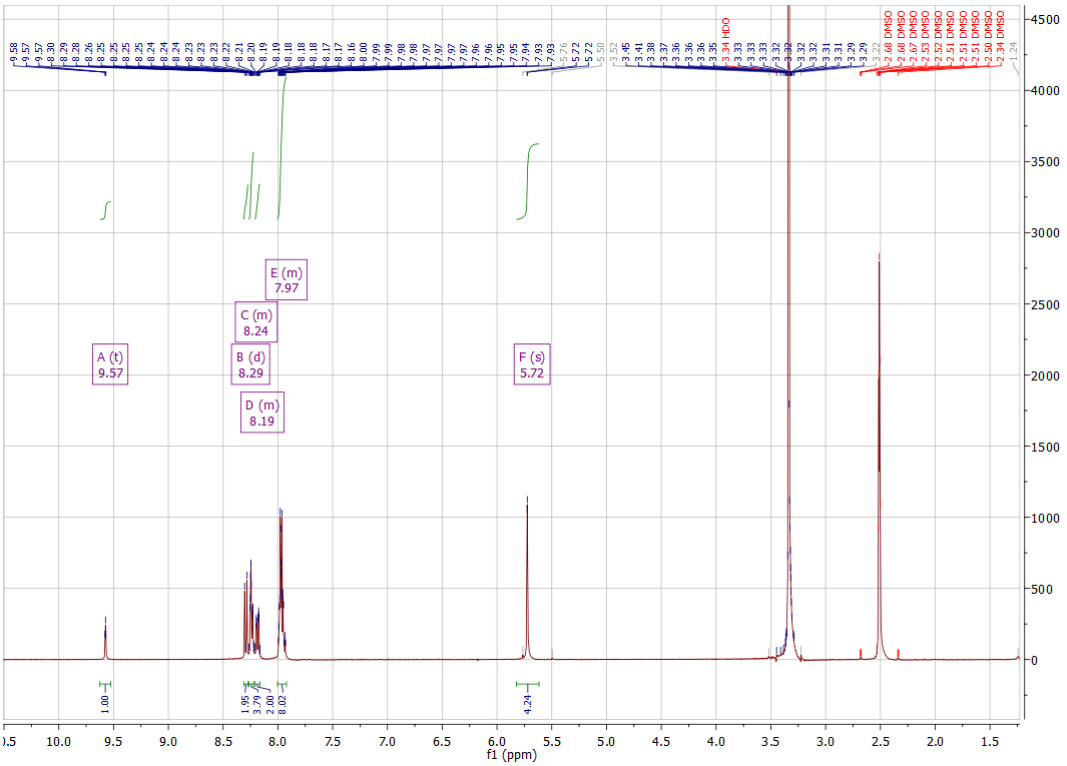

5.19. Salt (H-27)$^{+}Br^{-}$

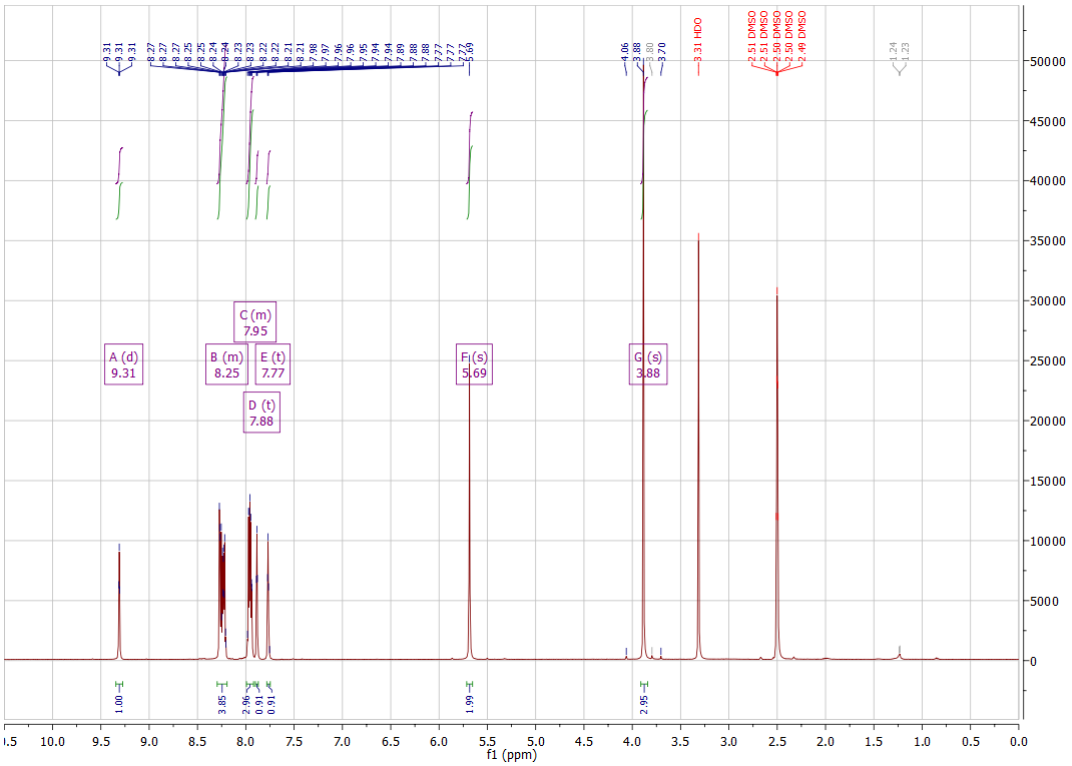

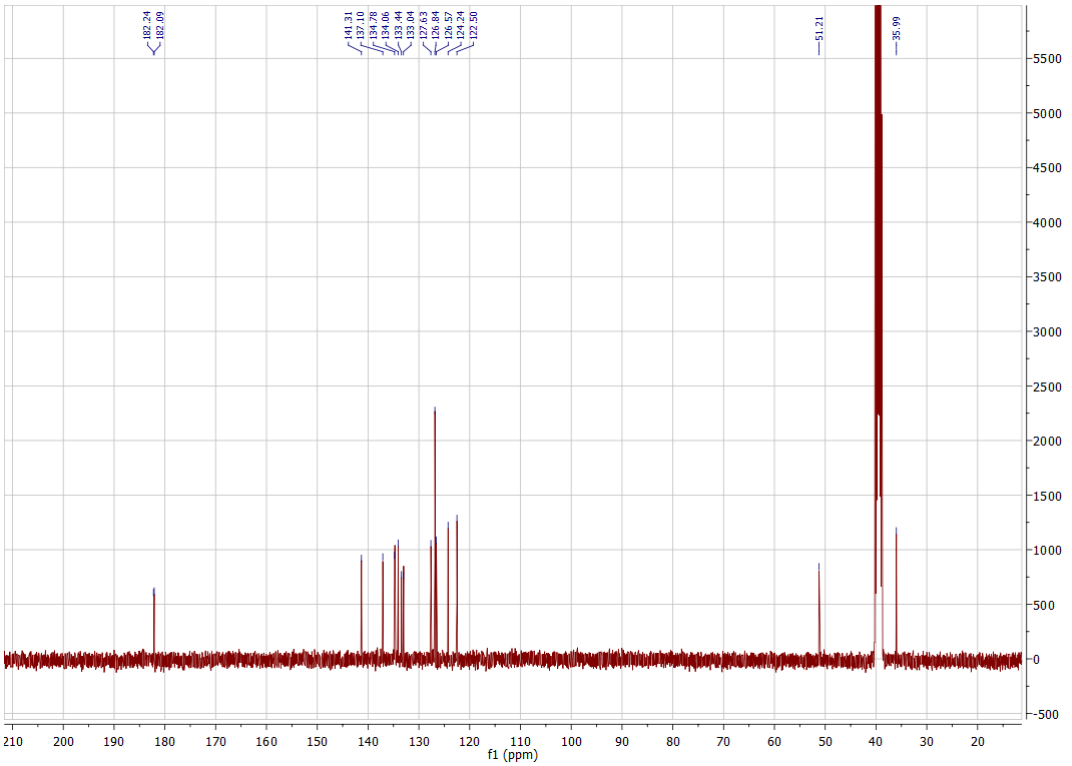

5.20. Salt (H-28)$^{+}Br^{-}$

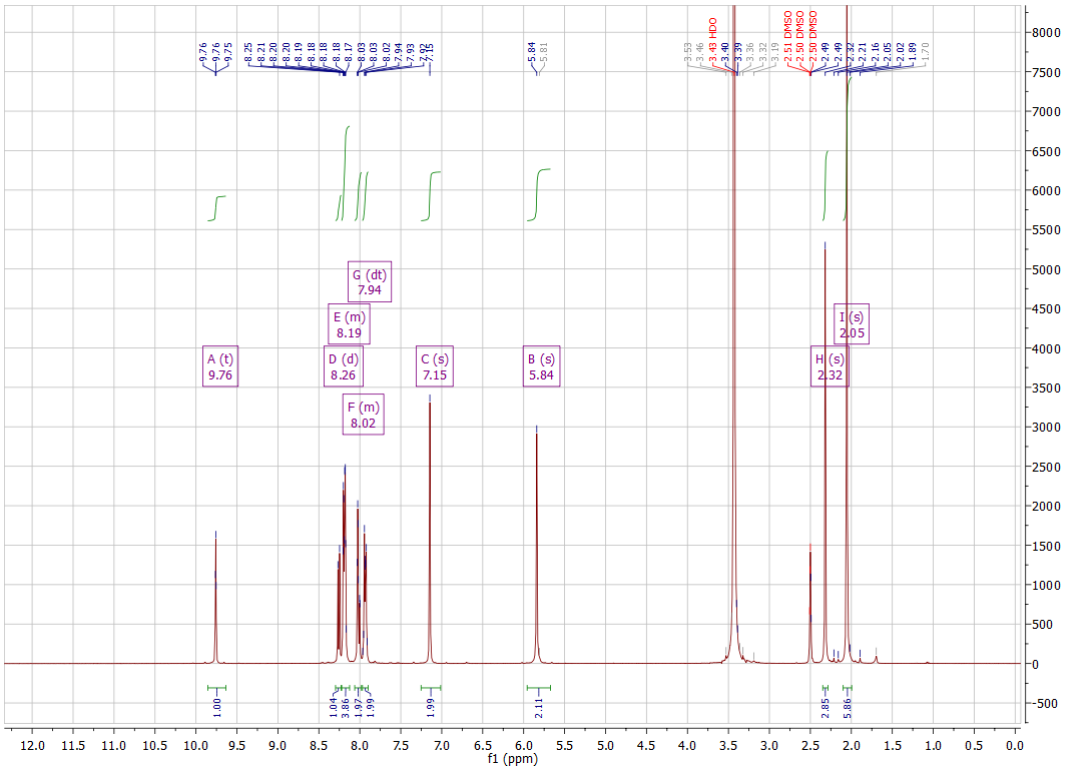

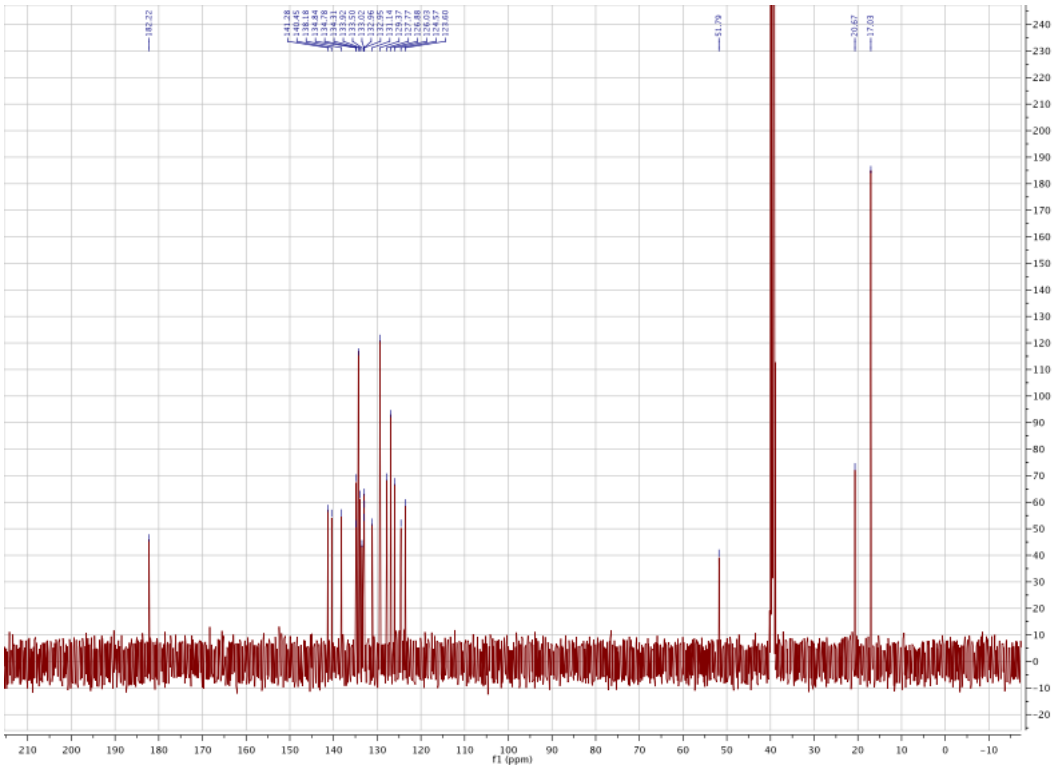

5.21. Salt (H-29)$^{+}$Br^{-}

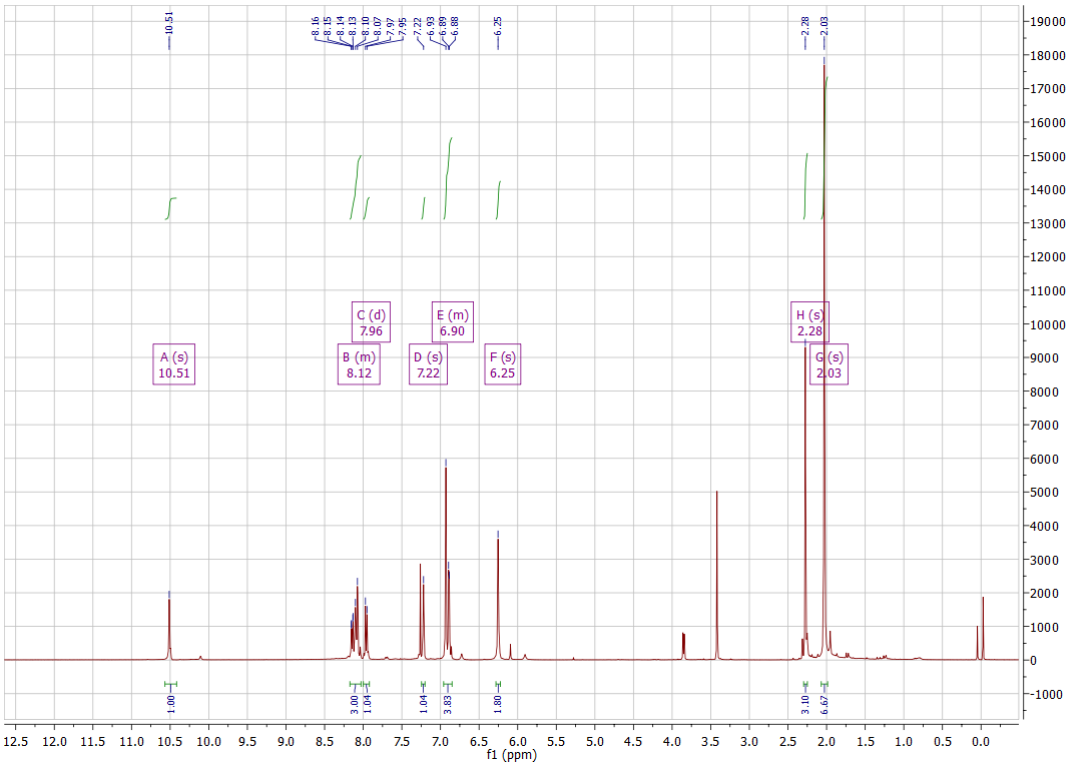

5.22. [AgBr(NHC-28)] 32

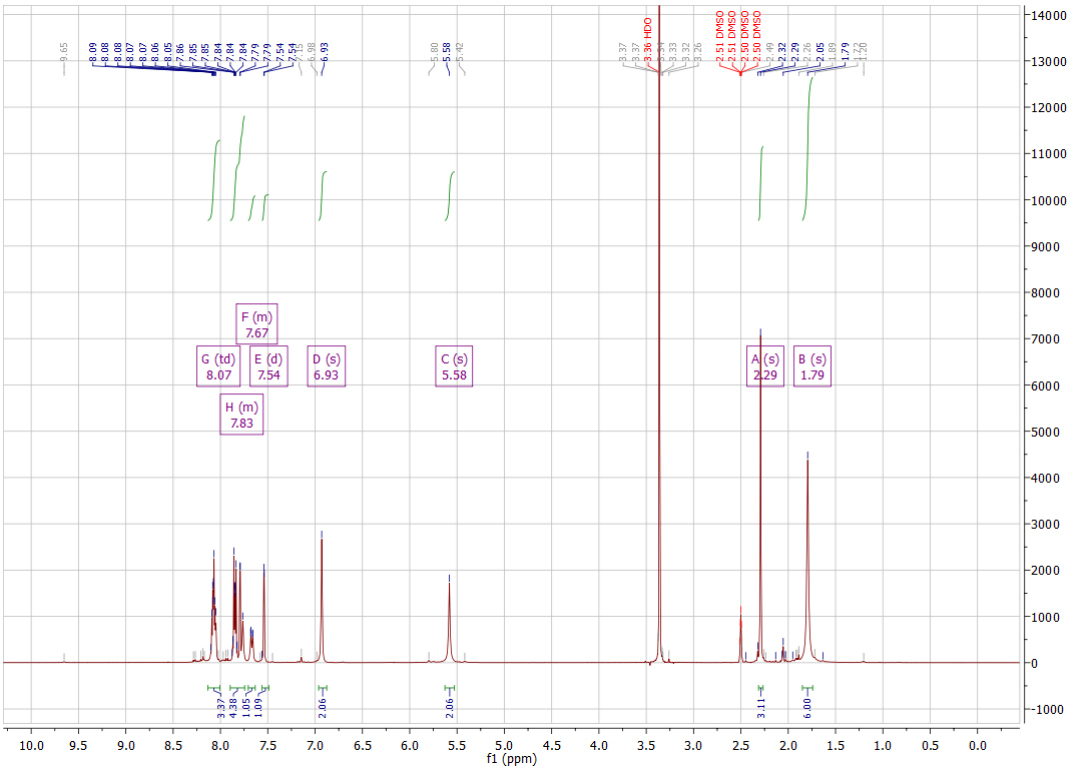

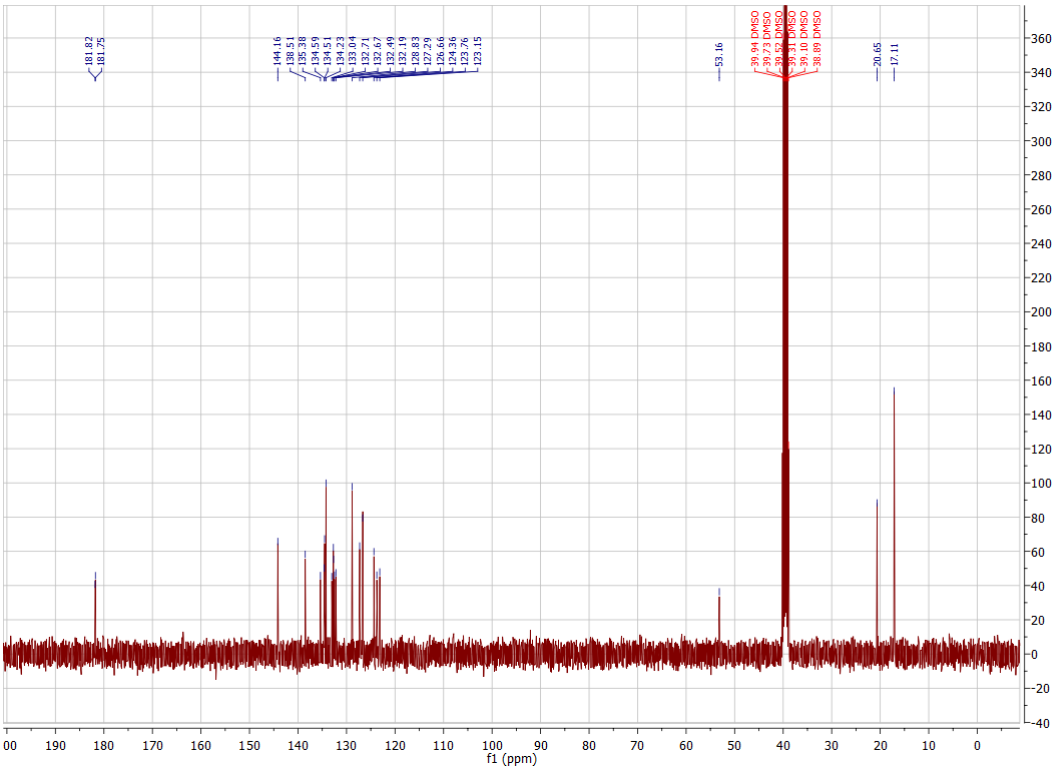

5.23. Salt (H-33)

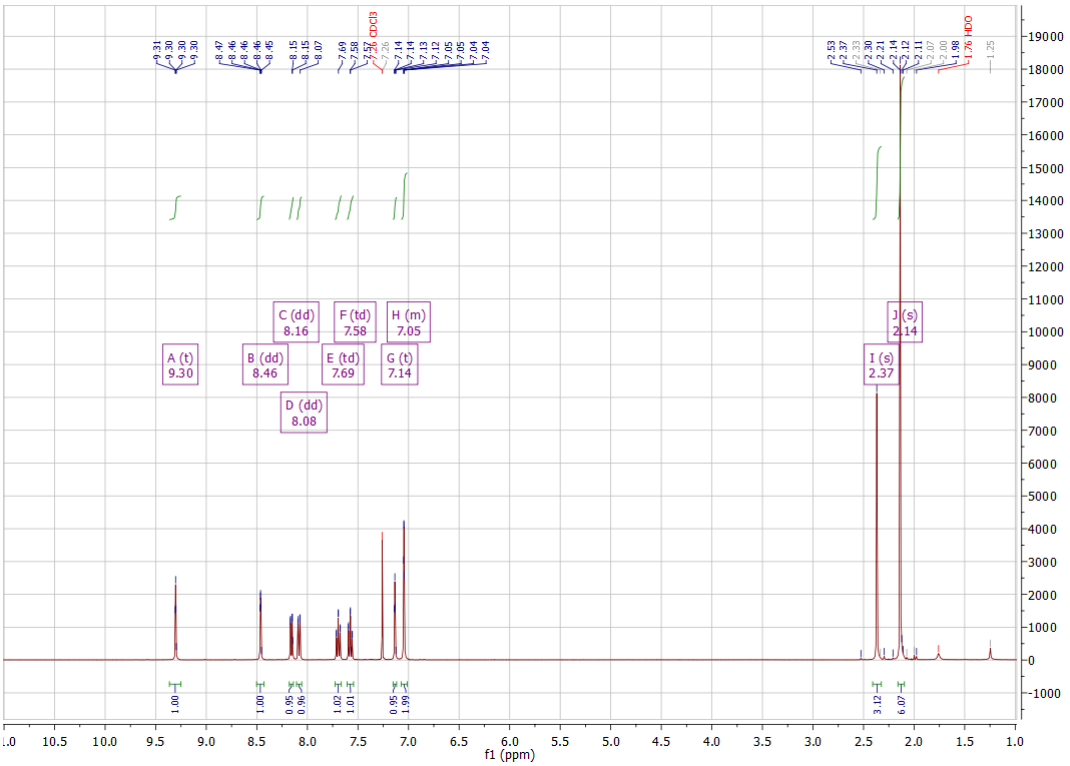
A (t) 9.30
B (dd) 8.46
C (dd) 8.16
D (dd) 8.08
E (td) 7.69
F (td) 7.58
G (t) 7.14
H (m) 7.05
I (s) 2.37
J (s) 2.14
f1 (ppm)

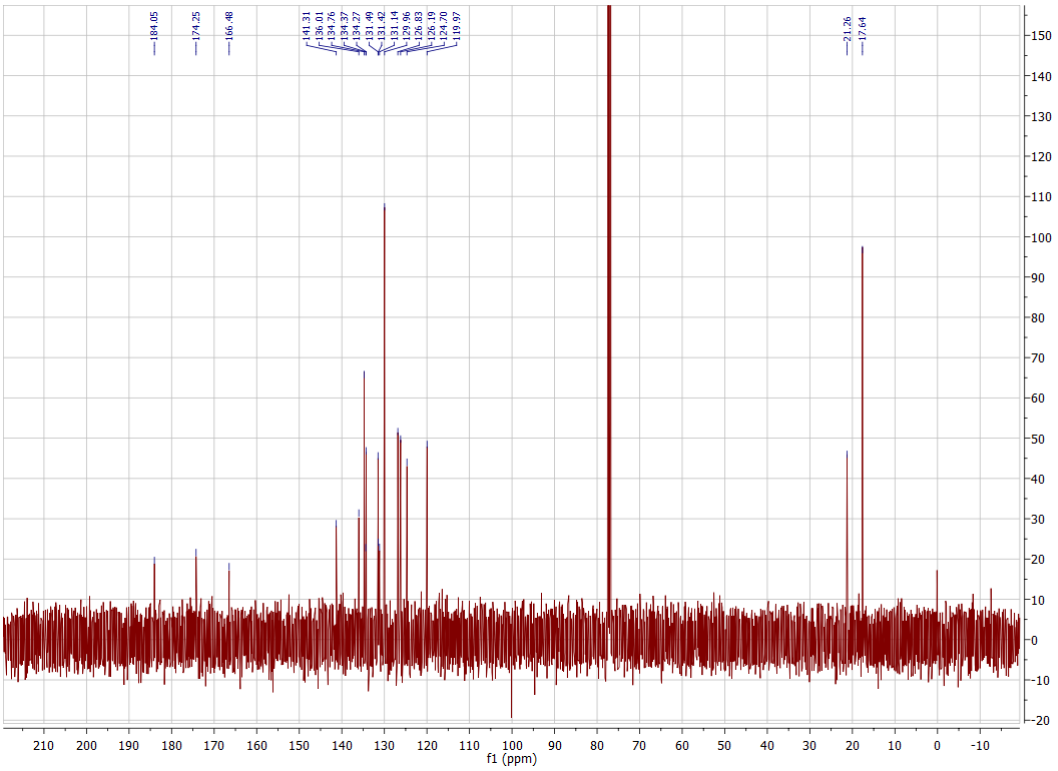
f1 (ppm)

5.24. Salt (H-34)

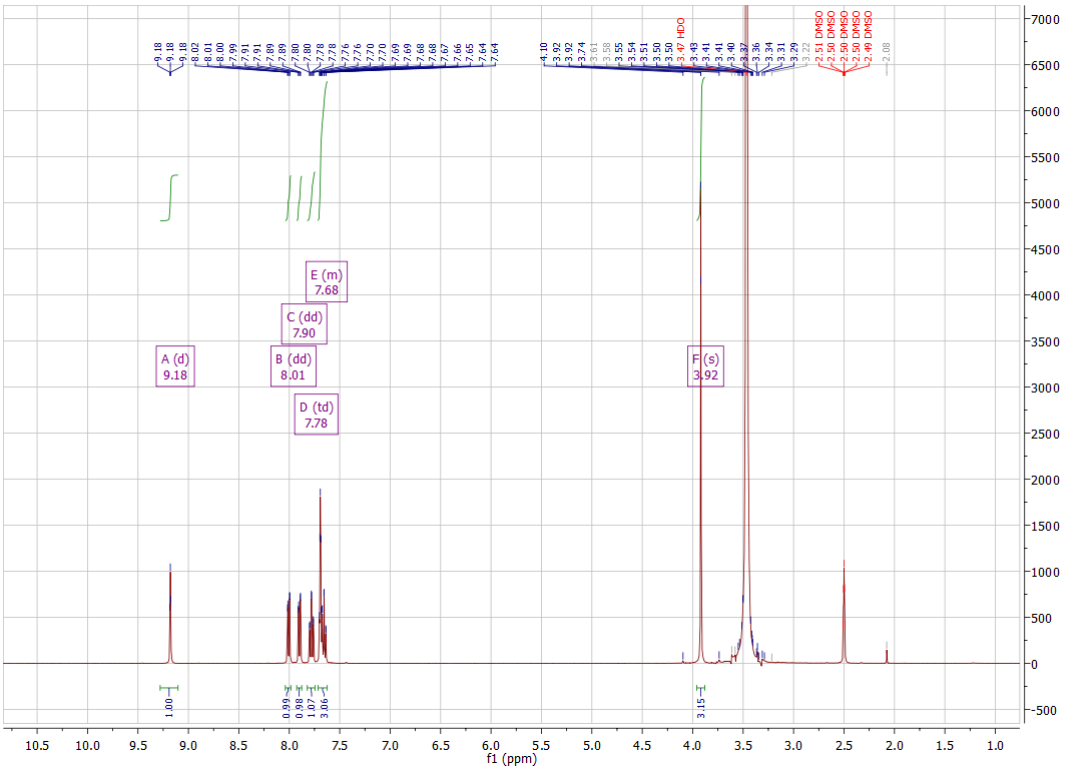

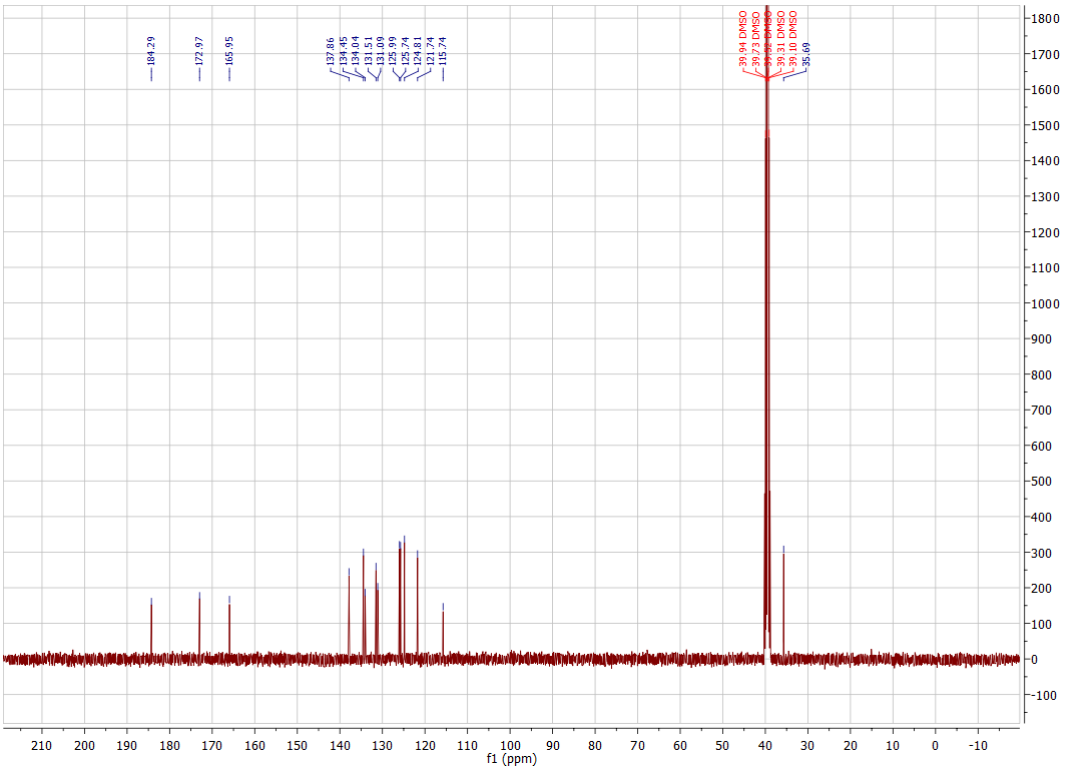

5.25. Salt (H-38)$^{+}Cl^{-}$

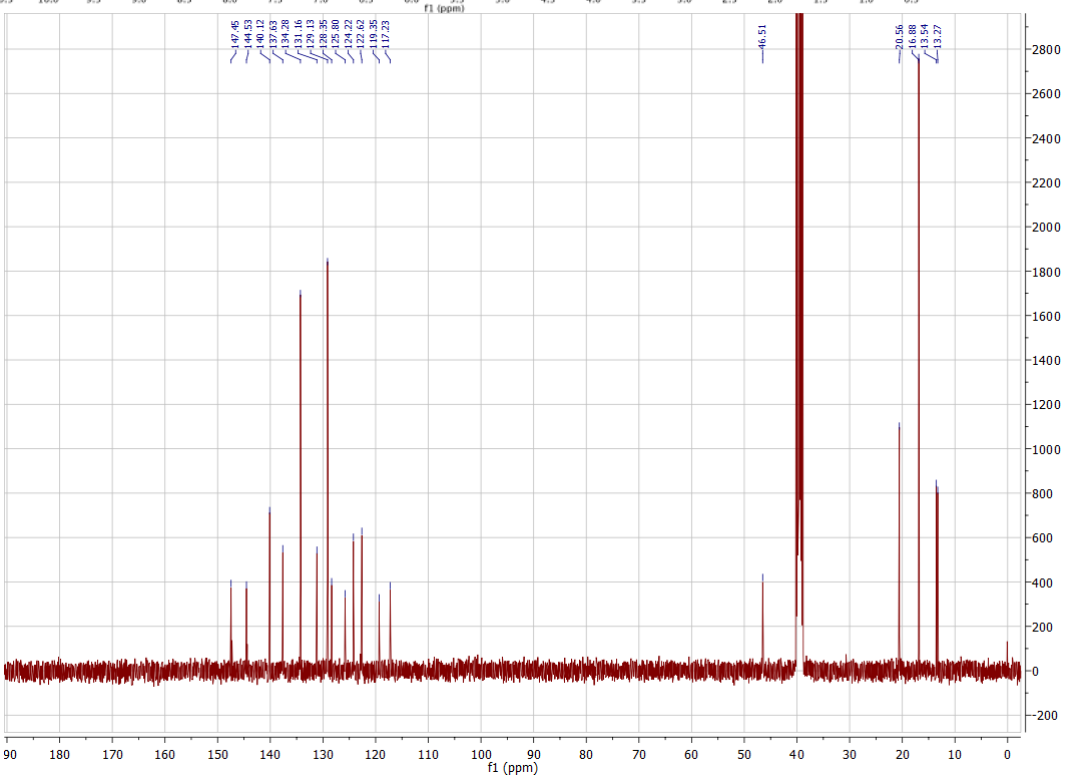

6. Appendix

6.1. [Ag(μ-Cl)(NHC-1)]$_2$ 2

Crystal data for [Ag(μ-Cl)(NHC-1)]$_2$ **2**: formula $C_{25.77}H_{25.55}Ag_1Cl_{3.55}N_3O_2$, M = 643.08, F(000) = 1298.200, orange plate, size 0.020 * 0.090 * 0.190 mm^3, triclinic, space group P -1, Z = 4, a = 13.0396(5) Å, b = 13.9638(5) Å, c = 15.2699(6) Å, α = 87.586(2)°, β = 75.500(2)°, γ = 78.590(2)°, V = 2638.54(18) Å^3, $D_{calc.}$ = 1.619 Mg * m^{-3}. The crystal was measured on a Bruker Kappa Apex2 diffractometer at 123K using graphite-monochromated Cu K_α-radiation with λ = 1.54178 Å, Θ_{max} = 68.277°. Minimal/maximal transmission 0.46/0.82, μ = 9.674 mm^{-1}. The Apex2 suite has been used for datacollection and integration. From a total of 29744 reflections, 9259 were independent (merging r = 0.047). From these, 6877 were considered as observed (I>2.0σ(I)) and were used to refine 676 parameters. The structure was solved by Other methods using the program Superflip. Least-squares refinement against F was carried out on all non-hydrogen atoms using the program CRYSTALS. R = 0.0669 (observed data), wR = 0.1064 (all data), GOF = 1.0311. Minimal/maximal residual electron density = -2.05/2.66 e Å^{-3}. Chebychev polynomial weights were used to complete the refinement. Plots were produced using Mercury.

Table 1. Crystal data for [Ag(μ-Cl)(NHC-**1**)]$_2$ **2**

formula	$C_{25.77}H_{25.55}Ag_1Cl_{3.55}N_3O_2$
formula weight	643.08
Z, calculated density	4, 1.619 Mg * m^{-3}
F(000)	1298.200
description and size of crystal	orange plate, 0.020 * 0.090 * 0.190 mm^3

absorption coefficient	9.674 mm^{-1}
min/max transmission	0.46 / 0.82
temperature	123K
radiation(wavelength)	*C*u Kα (λ = 1.54178 Å)
Crystal system, space group	triclinic, P -1
a	13.0396(5) Å
b	13.9638(5) Å
c	15.2699(6) Å
α	87.586(2)°
β	75.500(2)°
γ	78.590(2)°
V	2638.54(18) $Å^3$
min/max Θ	3.229° / 68.277°
number of collected reflections	29744
number of independent refections	9259 (merging r = 0.047)
number of observed reflections	6877 (I>2.0σ(I))
number of refined parameters	676
r	0.0669
rW	0.1064
goodness of fit	1.0311

Table 2. Coordinates for [Ag(μ-Cl)(NHC-**1**)]$_2$ **2** in SHELX-format.

[Ag(μ-Cl)(NHC-**1**)]$_2$ **2** in space group P -1

CELL 1.54178 13.0396 13.9638 15.2699 87.586 75.500 78.590

ZERR 4 0.0005 0.0005 0.0006 0.002 0.002 0.002

LATT -1

SYMM x,y,z

SYMM -x,-y,-z

SFAC C . H . Ag Cl . N O

UNIT 25 77 25 55 1 3 55 3 2

FVAR 1.0

Ag1 3 0.11219 0.39638 0.00095 11.0000 0.0388

Cl1 1 0.01665 0.43030 -0.11238 11.0000 0.0415

Cl2 1 0.15614 0.15184 -0.10784 11.0000 0.0479

N1 5 0.3196 0.3632 0.0651 11.0000 0.0429

N2 5 0.1997 0.3132 0.1687 11.0000 0.0372

N3 5 0.1085 0.0524 0.0866 11.0000 0.0361

O1 6 0.0908 -0.1303 0.1064 11.0000 0.0412

O2 6 0.2102 -0.0084 -0.2327 11.0000 0.0562

C1 1 0.2158 0.3532 0.0855 11.0000 0.0350

C2 1 0.3669 0.3294 0.1340 11.0000 0.0538

C3 1 0.2913 0.2977 0.1991 11.0000 0.0460

C4 1 0.3684 0.4017 -0.0222 11.0000 0.0425

C5 1 0.3679 0.5031 -0.0281 11.0000 0.0398

C6 1 0.4058 0.5388 -0.1142 11.0000 0.0454

C7 1 0.4429 0.4786 -0.1907 11.0000 0.0523

C8	1	0.4441	0.3796	-0.1796	11.0000	0.0561
C9	1	0.4058	0.3401	-0.0965	11.0000	0.0545
C10	1	0.3244	0.5677	0.0537	11.0000	0.0454
C11	1	0.4814	0.5208	-0.2827	11.0000	0.0694
C12	1	0.4055	0.2338	-0.0877	11.0000	0.0952
C13	1	0.0985	0.2821	0.2153	11.0000	0.0360
C14	1	0.1032	0.1741	0.1974	11.0000	0.0395
C15	1	0.1187	0.1524	0.0990	11.0000	0.0333
C16	1	0.1296	0.0007	0.0104	11.0000	0.0319
C17	1	0.1182	-0.1054	0.0280	11.0000	0.0339
C18	1	0.1426	-0.1731	-0.0483	11.0000	0.0338
C19	1	0.1307	-0.2699	-0.0322	11.0000	0.0365
C20	1	0.1553	-0.3335	-0.1053	11.0000	0.0424
C21	1	0.1953	-0.3029	-0.1915	11.0000	0.0452
C22	1	0.2061	-0.2074	-0.2080	11.0000	0.0456
C23	1	0.1781	-0.1412	-0.1366	11.0000	0.0365
C24	1	0.1843	-0.0355	-0.1559	11.0000	0.0386
C25	1	0.1564	0.0299	-0.0783	11.0000	0.0364
H1	1	0.1015	0.0180	0.1347	11.0000	0.0428
H21	1	0.4379	0.3282	0.1350	11.0000	0.0650
H31	1	0.2989	0.2706	0.2541	11.0000	0.0548
H61	1	0.4062	0.6052	-0.1214	11.0000	0.0550
H81	1	0.4711	0.3381	-0.2298	11.0000	0.0668
H101	1	0.3336	0.6333	0.0379	11.0000	0.0679
H102	1	0.2486	0.5676	0.0767	11.0000	0.0678

H103	1	0.3615	0.5443	0.0994	11.0000	0.0679
H111	1	0.5590	0.5056	-0.3008	11.0000	0.1050
H112	1	0.4572	0.5904	-0.2804	11.0000	0.1050
H113	1	0.4527	0.4931	-0.3257	11.0000	0.1051
H121	1	0.4281	0.2041	-0.1463	11.0000	0.1439
H122	1	0.4546	0.2054	-0.0520	11.0000	0.1440
H123	1	0.3341	0.2249	-0.0586	11.0000	0.1440
H131	1	0.0859	0.2921	0.2796	11.0000	0.0432
H132	1	0.0404	0.3207	0.1936	11.0000	0.0427
H141	1	0.1634	0.1364	0.2174	11.0000	0.0471
H142	1	0.0368	0.1555	0.2315	11.0000	0.0469
H151	1	0.0639	0.1965	0.0763	11.0000	0.0399
H152	1	0.1901	0.1614	0.0665	11.0000	0.0400
H191	1	0.1064	-0.2908	0.0270	11.0000	0.0438
H201	1	0.1448	-0.3974	-0.0955	11.0000	0.0512
H211	1	0.2155	-0.3471	-0.2390	11.0000	0.0541
H221	1	0.2325	-0.1875	-0.2665	11.0000	0.0550
Ag2	3	0.37020	0.33536	0.44464	11.0000	0.0367
Cl3	1	0.47655	0.21891	0.33831	11.0000	0.0598
Cl4	1	0.06624	0.28806	0.48982	11.0000	0.0367
N4	5	0.2156	0.5265	0.5287	11.0000	0.0304
N5	5	0.2236	0.4145	0.6280	11.0000	0.0308
N6	5	0.0251	0.1828	0.6836	11.0000	0.0355
O3	6	-0.0741	0.0361	0.7150	11.0000	0.0397
O4	6	-0.0561	0.2047	0.3931	11.0000	0.0352

C26	1	0.2661	0.4337	0.5406	11.0000	0.0288
C27	1	0.1436	0.5630	0.6079	11.0000	0.0310
C28	1	0.1483	0.4918	0.6700	11.0000	0.0327
C29	1	0.2382	0.5835	0.4485	11.0000	0.0299
C30	1	0.2989	0.6571	0.4485	11.0000	0.0330
C31	1	0.3140	0.7173	0.3728	11.0000	0.0323
C32	1	0.2740	0.7056	0.2998	11.0000	0.0328
C33	1	0.2169	0.6316	0.3014	11.0000	0.0329
C34	1	0.1986	0.5696	0.3744	11.0000	0.0301
C35	1	0.3434	0.6721	0.5271	11.0000	0.0431
C36	1	0.2931	0.7723	0.2180	11.0000	0.0392
C37	1	0.1322	0.4926	0.3753	11.0000	0.0385
C38	1	0.2551	0.3217	0.6747	11.0000	0.0348
C39	1	0.1980	0.2404	0.6582	11.0000	0.0323
C40	1	0.0766	0.2651	0.6926	11.0000	0.0347
C41	1	-0.0143	0.1598	0.6166	11.0000	0.0297
C42	1	-0.0761	0.0759	0.6439	11.0000	0.0320
C43	1	-0.1348	0.0477	0.5817	11.0000	0.0317
C44	1	-0.1992	-0.0214	0.6085	11.0000	0.0364
C45	1	-0.2538	-0.0502	0.5490	11.0000	0.0423
C46	1	-0.2435	-0.0093	0.4640	11.0000	0.0429
C47	1	-0.1794	0.0603	0.4377	11.0000	0.0355
C48	1	-0.1266	0.0904	0.4964	11.0000	0.0311
C49	1	-0.0616	0.1681	0.4683	11.0000	0.0288
C50	1	-0.0085	0.1984	0.5317	11.0000	0.0301

H2	1	0.0076	0.1506	0.7324	11.0000	0.0430
H271	1	0.0999	0.6247	0.6162	11.0000	0.0371
H281	1	0.1092	0.4938	0.7292	11.0000	0.0390
H311	1	0.3533	0.7663	0.3717	11.0000	0.0391
H331	1	0.1899	0.6238	0.2523	11.0000	0.0401
H351	1	0.2858	0.6994	0.5773	11.0000	0.0649
H352	1	0.3931	0.7162	0.5108	11.0000	0.0650
H353	1	0.3801	0.6107	0.5448	11.0000	0.0650
H361	1	0.2965	0.8355	0.2372	11.0000	0.0590
H362	1	0.3603	0.7461	0.1771	11.0000	0.0591
H363	1	0.2364	0.7779	0.1879	11.0000	0.0588
H371	1	0.0757	0.4980	0.4295	11.0000	0.0578
H372	1	0.1782	0.4293	0.3723	11.0000	0.0579
H373	1	0.1017	0.5012	0.3236	11.0000	0.0578
H381	1	0.2371	0.3353	0.7392	11.0000	0.0420
H382	1	0.3322	0.2992	0.6526	11.0000	0.0419
H391	1	0.2164	0.2254	0.5944	11.0000	0.0390
H392	1	0.2241	0.1829	0.6905	11.0000	0.0394
H401	1	0.0489	0.3202	0.6590	11.0000	0.0417
H402	1	0.0591	0.2828	0.7561	11.0000	0.0419
H441	1	-0.2052	-0.0487	0.6658	11.0000	0.0439
H451	1	-0.2985	-0.0960	0.5669	11.0000	0.0508
H461	1	-0.2799	-0.0278	0.4246	11.0000	0.0520
H471	1	-0.1718	0.0865	0.3802	11.0000	0.0428
Cl5	1	0.5281	0.8826	0.4582	10.7000	0.0981

Cl6 1 0.4858 0.9165 0.2796 10.7.0000 0.1117

C51 1 0.5405 0.9531 0.3617 10.7.0000 0.1043

H511 1 0.5049 1.0194 0.3790 10.7.0000 0.1252

H512 1 0.6161 0.9519 0.3345 10.7.0000 0.1249

Cl7 1 0.4126 1.0550 0.0985 10.6.0000 0.0911

Cl8 1 0.5960 1.1510 0.0287 10.6.0000 0.0897

C52 1 0.5312 1.0817 0.1134 10.6.0000 0.0905

H521 1 0.5143 1.1175 0.1700 10.6.0000 0.1091

H522 1 0.5806 1.0209 0.1169 10.6.0000 0.1089

Cl9 1 0.5209 0.8959 0.3601 10.25.0000 0.1205

Cl10 1 0.4559 1.0011 0.2075 10.25.0000 0.1232

C53 1 0.550 0.975 0.271 10.25.0000 0.1225

H531 1 0.5572 1.0359 0.2957 10.25.0000 0.1470

H532 1 0.6185 0.9455 0.2314 10.25.0000 0.1470

HKLF 4

6.2. [PdCl(η^3-allyl)(NHC-1)] 5

Crystal data for [PdCl(η^3-allyl)(NHC-**1**)] **5**: formula $C_{28}H_{29}Cl_2N_3O_2Pd_1$, M = 616.86, F(000) = 628, orange plate, size 0.010 * 0.070 * 0.220 mm^3, triclinic, space group P -1, Z = 2, a = 7.6644(5) Å, b = 13.8235(9) Å, c = 14.5683(9) Å, α = 62.491(3)°, β = 75.466(4)° γ = 76.041(4)°, V = 1310.98(15) $Å^3$, $D_{calc.}$= 1.563 Mg * m^{-3}. The crystal was measured on a Bruker Kappa Apex2 diffractometer at 123K using graphite-monochromated Cu K_α-radiation with λ = 1.54178 Å, Θ_{max} = 68.550°. Minimal/maximal transmission 0.58/0.92, μ = 7.833 mm^{-1}. The Apex2 suite has been used for datacollection and integration. From a total of 19438 reflections, 4716 were independent (merging r = 0.039). From these, 3958 were considered as observed (I>2.0σ(I)) and were used to refine 353 parameters. The structure was solved by Other methods using the program Superflip. Least-squares refinement against F was carried out on all non-hydrogen atoms using the program CRYSTALS. R = 0.0337 (observed data), wR = 0.0442 (all data), GOF = 1.1243. Minimal/maximal residual electron density = -0.61/0.96 e $Å^{-3}$. Chebychev polynomial weights were used to complete the refinement. Plots were produced using Mercury.

Table 3. Crystal data for [PdCl(η^3-allyl)(NHC-**1**)] **5**

formula	$C_{28}H_{29}Cl_2N_3O_2Pd$
formula weight	616.86
Z, calculated density	2, 1.563 Mg * m^{-3}
F(000)	628
description and size of crystal	orange plate, 0.010 * 0.070 * 0.220 mm^3

absorption coefficient 7.833 mm^{-1}

min/max transmission 0.58 / 0.92

temperature 123K

radiation(wavelength) Cu Kα (λ = 1.54178 Å)

Crystal system, space group triclinic, P -1

a 7.6644(5) Å

b 13.8235(9) Å

c 14.5683(9) Å

α 62.491(3)°

β 75.466(4)°

γ 76.041(4) °

V 1310.98(15) $Å^3$

min/max Θ 3.466° / 68.550°

number of collected reflections 19438

number of independent refections 4716 (merging r = 0.039)

number of observed reflections 3958 (I>2.0 σ (I))

number of refined parameters 353

r 0.0337

rW 0.0442

goodness of fit 1.1243

Table 4. Coordinates for [PdCl(η^3-allyl)(NHC-**1**)] **5** in SHELX-format.

TITL [PdCl(η^3-allyl)(NHC-**1**)] **5** in space group P -1

CELL 1.54178 7.6644 13.8235 14.5683 62.491 75.466 76.041

ZERR 2 0.0005 0.0009 0.0009 0.003 0.004 0.004

LATT -1

SYMM x,y,z

SYMM -x,-y,-z

SFAC C H Cl N O Pd

UNIT 28 29 2 3 2 1

FVAR 1.0

Pd1 6 0.25060 0.384989 0.416553 11.0000 0.0269

Cl1 3 -0.03462 0.33889 0.52163 11.0000 0.0405

Cl2 3 0.53497 0.65736 0.10278 11.0000 0.0501

N1 4 0.2088 0.3539 0.2279 11.0000 0.0309

N2 4 0.0417 0.50011 0.23242 11.0000 0.0283

N3 4 0.1787 0.83322 0.05069 11.0000 0.0409

O1 5 0.1918 1.0393 -0.07668 11.0000 0.0439

O2 5 0.8261 0.7709 -0.0474 11.0000 0.0439

C1 1 0.5103 0.4361 0.3553 11.0000 0.0442

C2 1 0.5101 0.3620 0.4611 11.0000 0.0459

C3 1 0.3793 0.3782 0.5371 11.0000 0.0421

C4 1 0.1638 0.4151 0.2834 11.0000 0.0277

C5 1 0.1134 0.4000 0.1442 11.0000 0.0378

C6 1 0.0084 0.4916 0.1476 11.0000 0.0350

C7 1 0.3293 0.2502 0.2590 11.0000 0.0304

C8	1	0.2562	0.1556	0.3336	11.0000	0.0344
C9	1	0.3774	0.0570	0.3674	11.0000	0.0398
C10	1	0.5619	0.0525	0.3286	11.0000	0.0421
C11	1	0.6267	0.1486	0.2522	11.0000	0.0420
C12	1	0.5135	0.2489	0.2160	11.0000	0.0364
C13	1	0.0556	0.1597	0.3762	11.0000	0.0452
C14	1	0.6891	-0.0546	0.3683	11.0000	0.0581
C15	1	0.5875	0.3514	0.1323	11.0000	0.0471
C19	1	0.3439	0.8583	0.0018	11.0000	0.0304
C20	1	0.3367	0.9794	-0.0722	11.0000	0.0284
C21	1	0.5056	1.0216	-0.1375	11.0000	0.0262
C22	1	0.5003	1.1327	-0.2077	11.0000	0.0326
C23	1	0.6567	1.1721	-0.2718	11.0000	0.0392
C24	1	0.8199	1.1014	-0.2655	11.0000	0.0445
C25	1	0.8272	0.9911	-0.1945	11.0000	0.0399
C26	1	0.6704	0.9502	-0.1307	11.0000	0.0286
C27	1	0.6782	0.8320	-0.0548	11.0000	0.0314
C28	1	0.5110	0.7935	0.0090	11.0000	0.0320
H1	2	0.0929	0.8865	0.0492	11.0000	0.0514
H11	2	0.5094	0.5126	0.3349	11.0000	0.0561
H12	2	0.5860	0.4135	0.3035	11.0000	0.0559
H21	2	0.5890	0.2894	0.4774	11.0000	0.0604
H31	2	0.3604	0.3179	0.6044	11.0000	0.0534
H32	2	0.3587	0.4466	0.5415	11.0000	0.0538
H51	2	0.1211	0.3724	0.0967	11.0000	0.0466

H61 2 -0.0707 0.5399 0.1028 11.0000 0.0443

H91 2 0.3319 -0.0079 0.4176 11.0000 0.0498

H111 2 0.7485 0.1460 0.2254 11.0000 0.0533

H131 2 0.0267 0.0865 0.4141 11.0000 0.0700

H132 2 -0.0142 0.1989 0.3209 11.0000 0.0700

H133 2 0.0226 0.1936 0.4227 11.0000 0.0696

H141 2 0.7879 -0.0429 0.3876 11.0000 0.0909

H142 2 0.7330 -0.0801 0.3151 11.0000 0.0907

H143 2 0.6249 -0.1073 0.4276 11.0000 0.0905

H151 2 0.5529 0.4098 0.1528 11.0000 0.0738

H152 2 0.7167 0.3370 0.1197 11.0000 0.0740

H153 2 0.5456 0.3743 0.0683 11.0000 0.0742

H221 2 0.3900 1.1795 -0.2114 11.0000 0.0398

H231 2 0.6534 1.2449 -0.3183 11.0000 0.0487

H241 2 0.9228 1.1291 -0.3098 11.0000 0.0551

H251 2 0.9358 0.9448 -0.1892 11.0000 0.0496

C16 1 -0.0477 0.5890 0.2650 10.833.0000 0.0299

C17 1 0.0655 0.68313 0.21721 10.833.0000 0.0324

C18 1 0.1043 0.7298 0.09775 10.833.0000 0.0341

H161 2 -0.0598 0.5570 0.3411 10.833.0000 0.0365

H162 2 -0.1661 0.6170 0.2424 10.833.0000 0.0368

H171 2 -0.0024 0.7420 0.2347 10.833.0000 0.0408

H172 2 0.1808 0.6595 0.2423 10.833.0000 0.0409

H181 2 -0.0116 0.7429 0.0738 10.833.0000 0.0461

H182 2 0.1921 0.6764 0.0771 10.833.0000 0.0463

C116 1 -0.037 0.5859 0.2704 10.167.0000 0.0302

C117 1 -0.0272 0.7014 0.1815 10.167.0000 0.0317

C118 1 0.1695 0.7220 0.1349 10.167.0000 0.0341

H1161 2 0.0374 0.5761 0.3197 10.167.0000 0.0371

H1162 2 -0.1616 0.5776 0.3052 10.167.0000 0.0371

H1171 2 -0.0863 0.7558 0.2082 10.167.0000 0.0409

H1172 2 -0.0908 0.7086 0.1285 10.167.0000 0.0410

H1181 2 0.2334 0.7115 0.1888 10.167.0000 0.0450

H1182 2 0.2279 0.6697 0.1059 10.167.0000 0.0450

HKLF 4

6.3. Imidazolium salt 33

Crystal data for imidazolium salt **33**: formula $C_{22}H_{18}N_2O_3$, M = 358.40, F(000) = 376, orange plate, size 0.040 * 0.150 * 0.270 mm^3, monoclinic, space group P 21, Z = 2, a = 7.3330(6) Å, b = 13.0242(11) Å, c = 8.9075(8) Å, α = 90°, β = 94.605(4) °, γ = 90°, V = 847.98(13) $Å^3$, Dcalc. = 1.404 Mg * $m^{-3.}$ The crystal was measured on a Bruker Kappa Apex2 diffractometer at 123K using graphite-monochromated Cu Kα-radiation with λ = 1.54178 Å, Θmax = 67.967° Minimal/maximal transmission 0.89/0.97, μ = 0.766 mm^{-1}. The Apex2 suite has been used for datacollection and integration. From a total of 6287 reflections, 2872 were independent (merging r = 0.027). From these, 2841 were considered as observed (I>2.0σ(I)) and were used to refine 245 parameters. The structure was solved by Other methods using the program Superflip. Least-squares refinement against F was carried out on all non-hydrogen atoms using the program CRYSTALS. R = 0.0264 (observed data), wR = 0.0312 (all data), GOF = 1.1180. Minimal/maximal residual electron density = -0.13/0.15 e $Å^{-3}$. Chebychev polynomial weights were used to complete the refinement. Plots were produced using CAMERON.

Table 5. Crystal data for imidazolium salt **33.**

formula	$C_{22}H_{18}N_2O_3$
formula weight	358.40
Z, calculated density	2, 1.404 Mg * m^{-3}
F(000)	376
description and size of crystal	orange plate, 0.040 * 0.150 * 0.270 mm^3
absorption coefficient	0.766 mm-1
min/max transmission	0.89 / 0.97

temperature	123K
radiation(wavelength)	*C*u Kα (λ = 1.54178 Å)
Crystal system, space group	monoclinic, P 21
a	7.3330(6) Å
b	13.0242(11) Å
c	8.9075(8) Å
α	90°
β	94.605(4)°
γ	90°
V	847.98(13) Å^3
min/max Θ	4.981° / 67.967°
number of collected reflections	6287
number of independent refections	2872 (merging r = 0.027)
number of observed reflections	2841 (I>2.0 σ (I))
number of refined parameters	245
r	0.0264
rW	0.0312
goodness of fit	1.1180

Table 6. Coordinates for imidazolium salt **33** in SHELX-format.

TITL imidazolium salt **33** in space group P 21

CELL 1.54178 7.3330 13.0242 8.9075 90 94.605 90

ZERR 2 0.0006 0.0011 0.0008 0 0.004 0

LATT -1

SYMM x,y,z

SYMM -x,y+1/2,-z

SFAC C H N O

UNIT 22 18 2 3

FVAR 1.0

C1 1 0.24047 0.26814 0.56145 11.0000 0.0229

C2 1 0.00931 0.17569 0.63009 11.0000 0.0244

C3 1 0.02859 0.25782 0.72243 11.0000 0.0239

C4 1 0.15718 0.12412 0.39367 11.0000 0.0217

C5 1 0.22872 0.02494 0.39942 11.0000 0.0234

C6 1 0.24665 -0.02332 0.26218 11.0000 0.0236

C7 1 0.19443 0.02376 0.12505 11.0000 0.0253

C8 1 0.11907 0.12171 0.12610 11.0000 0.0248

C9 1 0.09747 0.17329 0.25969 11.0000 0.0235

C10 1 0.2869 -0.02678 0.54666 11.0000 0.0300

C11 1 0.2178 -0.02785 -0.02300 11.0000 0.0314

C12 1 0.00924 0.27774 0.25945 11.0000 0.0283

C13 1 0.23649 0.41391 0.73581 11.0000 0.0225

C14 1 0.24409 0.42642 0.89575 11.0000 0.0219

C15 1 0.30877 0.52785 0.95859 11.0000 0.0229

C16	1	0.31882	0.54245	1.11415	11.0000	0.0255
C17	1	0.38591	0.63383	1.17668	11.0000	0.0282
C18	1	0.44401	0.71083	1.08422	11.0000	0.0292
C19	1	0.43240	0.69807	0.92866	11.0000	0.0271
C20	1	0.36256	0.60705	0.86484	11.0000	0.0227
C21	1	0.34432	0.59428	0.69799	11.0000	0.0232
C22	1	0.27365	0.49072	0.63163	11.0000	0.0224
N1	3	0.14385	0.18289	0.53057	11.0000	0.0220
N2	3	0.17416	0.31596	0.67748	11.0000	0.0215
O2	4	0.20336	0.35724	0.98255	11.0000	0.0287
O3	4	0.38201	0.66247	0.61270	11.0000	0.0289
O4	4	0.25575	0.48223	0.49184	11.0000	0.0282
H11	2	0.3399	0.2901	0.5082	11.0000	0.0254
H21	2	-0.0754	0.1222	0.6249	11.0000	0.0299
H31	2	-0.0390	0.2753	0.8013	11.0000	0.0282
H61	2	0.3014	-0.0882	0.2615	11.0000	0.0269
H81	2	0.0841	0.1531	0.0347	11.0000	0.0283
H101	2	0.3914	0.0063	0.5923	11.0000	0.0462
H102	2	0.3205	-0.0954	0.5297	11.0000	0.0459
H103	2	0.1890	-0.0265	0.6119	11.0000	0.0447
H111	2	0.2998	0.0117	-0.0827	11.0000	0.0495
H112	2	0.2719	-0.0947	-0.0076	11.0000	0.0485
H113	2	0.1027	-0.0318	-0.0796	11.0000	0.0486
H121	2	-0.0396	0.2942	0.1603	11.0000	0.0402
H122	2	-0.0828	0.2786	0.3307	11.0000	0.0423

```
H123  2   0.1001    0.3310    0.2879   11.0000   0.0400
H161  2   0.2805    0.4882    1.1784   11.0000   0.0311
H171  2   0.3932    0.6441    1.2849   11.0000   0.0339
H181  2   0.4964    0.7714    1.1264   11.0000   0.0352
H191  2   0.4747    0.7503    0.8632   11.0000   0.0315
HKLF  4
```

7. References

[1] O. R. Luca, R. H. Crabtree, *Chem. Soc. Rev.* **2013**, *42*, 1440

[2] V. K. K. Praneeth, M. R. Ringenberg, T. R. Ward, *Angew. Chem. Int. Ed. Engl.* **2012**, *51*, 10228

[3] A. G. Tennyson, R. J. Ono, T. W. Hudnall, D. M. Khramov, J. A. V. Er, J. W. Kamplain, V. M. Lynch, J. L. Sessler, C. W. Bielawski, *Chem. Eur. J*. **2010**, *16*, 304

a) A. G. Tennyson, V. M. Lynch, C. W. Bielawski, *J. Am. Chem. Soc.* **2010**, *132*, 9420

b) E. L. Rosen, C. D. Varnado Jr., A. G. Tennyson, D. M. Khramov, J. W. Kamplain, D. H. Sung, P. T. Cresswell, V. M. Lynch, C. W. Bielawski, *Organometallics* **2009**, *28*, 6695

c) R. J. Ono, Y. Suzuki, D. M. Khramov, M. Ueda, J. L. Sessler, C. W. Bielawski, *J. Org. Chem*. **2011**, *76*, 3239

[4] A. I. O. Suarez, V. Lyaskovskyy, J. N. H. Reek, J. I. van der Vlugt, B. de Bruin, *Angew. Chem. Int. Edit.* **2013**, *52*, 12510

[5] F. Lu, R. A. Zarkesh, A. F. Heyduk, *Eur. J. Inorg. Chem.* **2011**, *2012*, 467

[6] A. M. Tondreau, C. Milsmann, A. D. Patrick, H. M. Hoyt, E. Lobkovsky, K. Wieghardt, P. J. Chirik, *J. Am. Chem. Soc.* **2010**, *132*, 15046

[7] B. Gnanaprakasam, J. Zhang, D. Milstein, *Angew. Chem.* **2010**, *122*, 1510

[8] A. E. Wendlandt, S. S. Stahl, *J. Am. Chem. Soc.* **2014**, *136*, 506

[9] K. G. Caulton, *Eur. J. Inorg. Chem.* **2011**, *2012*, 435

[10] D. Sieh, M. Schlimm, L. Andernach, F. Angersbach, S. Nückel, J. Schöffel, N. Šušnjar, P. Burger, *Eur. J. Inorg. Chem.* **2012**, *2012*, 444

[11] S. Blanchard, E. Derat, M. Desage-El Murr, L. Fensterbank, M. Malacria, V.

Mouriès-Mansuy, *Eur. J. Inorg. Chem.* **2011**, *2012*, 376

[12] J. DePasquale, I. Nieto, L. E. Reuther, C. J. Herbst-Gervasoni, J. J. Paul, *Inorg. Chem.* **2013**, *52*, 9175

[13] D. F. Chodosh, Y. Rahamim, D. Czarkie, Y. Shvo, *J. Am. Chem. Soc.* **1986**, *108*, 7400

[14] A. McSkimming, S. B. Colbran, *Chem. Soc. Rev.* **2013**, *42*, 5439

[15] T. Ikariya, N. Y. M. Iha, R. Noyori, *Org. Biomol. Chem*. **2006**, 4, 393

[16] J. I. van der Vlugt, *Eur. J. Inorg. Chem.* **2011**, *2012*, 363

[17] M. D. Sanderson, J. W. Kamplain, C. W. Bielawski, *J. Am. Chem. Soc.* **2006**, *128*, 16514

[18] R. E. Rodríguez-Lugo, M. Trincado, M. Vogt, F. Tewes, G. Santiso-Quinones, H. Grützmacher, *Nature Chem.* **2013**, *5*, 342

[19] K. Tanaka, H. Isobe, S. Yamanaka, K. Yamaguchi, *Proc. Natl. Acad. Sci, U. S. A.* **2012**, 109, *39*, 15600

[20] X. Liu, Q. Xia, Y. Zhang, C. Chen, W. Chen, *J. Org. Chem.* **2013**, *78*, 8531

[21] S. Saravanakumar, M. K. Kindermann, J. Heinicke, M. Köckerling, *Chem. Commun.* **2006**, 640

[22] E. V. Johnston, E. A. Karlsson, S. A. Lindberg, B. Åkermark, J.-E. Bäckvall, *Chem. Eur. J.* **2009**, *15*, 6799

[23] M. D. Kärkäs, T. Åkermark, E. V. Johnston, S. R. Karim, T. M. Laine, B.-L. Lee, T. Åkermark, T. Privalov, B. Åkermark, *Angew. Chem. Int. Ed.* **2012**, *51*, 11589

[24] L. A. Berben, D. C. Craig, C. Gimbert-Suriñach, A. Robinson, K. H. Sugiyarto, S. B. Colbran, *Inorg. Chim. Acta.* **2011**, *370*, 374

[25] B. L. Ryland, S. S. Stahl, *Angew. Chem. Int. Ed*. **2014**, *53*, 8824

[26] A. Dijksman, A. Marino-González, A. M. Payeras, I. W. C. E. Arends, R. A.

Sheldon, *J. Am. Chem. Soc.* **2001**, *123*, 6826

[27] Z. An, X. Pan, X. Liu, X. Han, X. Bao, *J. Am. Chem. Soc.* **2006**, 128, *50*, 16028

[28] P. Teo, Z. K. Wickens, G. Dong, R. H. Grubbs, *Org. Lett.* **2012**, *14*, 3237

[29] B. W. Purse, L.-H. Tran, J. Piera, B. Åkermark, J.-E. Bäckvall, *Chem. Eur. J.* **2008**, *14*, 7500

[30] J.-E. Bäckvall, R. L. Chowdhury, U. Karlsson, *J. Chem. Soc., Chem. Commun.* **1991**, 473

[31] G.-Z. Wang, U. Andreasson, J.-E. Bäckvall, *J. Chem. Soc., Chem. Commun.* **1994**, 1037

[32] Á. Zsigmond, F. Notheisz, G. Csjernyik, J.-E. Bäckvall, *Topics in Catalysis* **2002**, *19*, 119

[33] J. T. Muckerman, D. E. Polyansky, T. Wada, K. Tanaka, E. Fujita, *Inorg. Chem.* **2008**, *47*, 1787

[34] H. Isobe, K. Tanaka, J. Shen, K. Yamaguchi, *Inorg.Chem.* **2014**, *53*, 397

[35] J. Piera, J.-E. Bäckvall, *Angew. Chem. Int. Ed.* **2008**, *47*, 3506

[36] S. Hong, D. P. Sanders, C. W. Lee, R. H. Grubbs, *J. Am. Chem. Soc*. **2005**, *127*, 17160

[37] G. Glocker, *J. Phys. Chem*. **1958**, *62*, 1049

[38] A. D. Walsh, *Trans. Faraday Soc*. **1971**, *67*, 1

[39] S. T. Lee, Model Studies of the Cu_B-Histidine-Tyrosine Centre in Cytochrome *c*

oxidase, The University of New South Wales, 2005

[40] B. V. Popp, J.L. Thorman, S. S. Stahl, *J. Mol. Catal. A: Chem*. **2006**, *251*, 2

[41] K. Yamaguchi, *J. Am. Chem. Soc.* **2011**, *133*, 14208

[42] B. J . Truscott, R. Klein, P. T. Kaye, *Tetrahedron Lett.* **2010**, *51*, 5041

Chapter 3

Synthesis and coordination chemistry of *N*-Heterocyclic carbene ligands bearing a pyrdinone moiety

1. Introduction

Non-innocent ligands have become a very fertile ground of research in the past years.[1-3] These ligands can be formally considered as redox neutral and can exist as tautomers.[2] The second feature is especially interesting in the context of switchable catalysis. The most known representative of the group is Shvo's ruthenium complex **1**, which has found applications in many organic transformations.[4,5] Its iron analogue **2,** which was introduced by Knölker[6] followed the success and is reminiscent to the Iron HmD hydrogenase.[7-9] Ligands can exist in two stable forms, which suggest that they can act as an electron reservoir (Scheme 1).[2] Thanks to this feature, the use of cheap metals has become possible for catalyzing organic reactions which involve two electron processes.[3,10]

a)

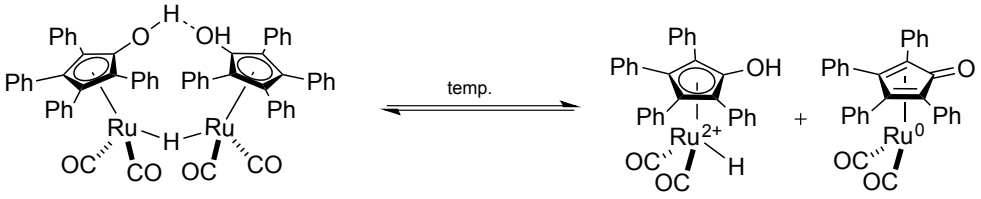

1

b)

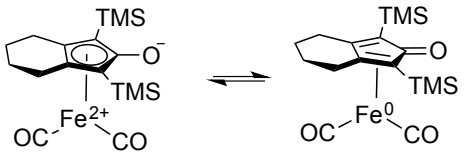

2

Scheme 1. Typical complexes bearing non-innocent ligands: a) Shvo's Ru catalyst, b) Knölker Fe catalyst.

Milstein and co-workers have introduced several pincer complexes that catalyse multi-electron reactions.[11-18] The ruthenium pincer complex **3** displays an interesting ability to split water.[19] The release of H_2 occurs at the elevated temperature and is catalysed by the de-aromatized ruthenium complex **3** (Scheme 2). This complex reacts with water and generates a hydrido-hydroxo complex **4**, which subsequently reacts with water at 100 °C and releases hydrogen. Irradiation of the complex **5** releases the O_2 and regenerates the complex **4**.

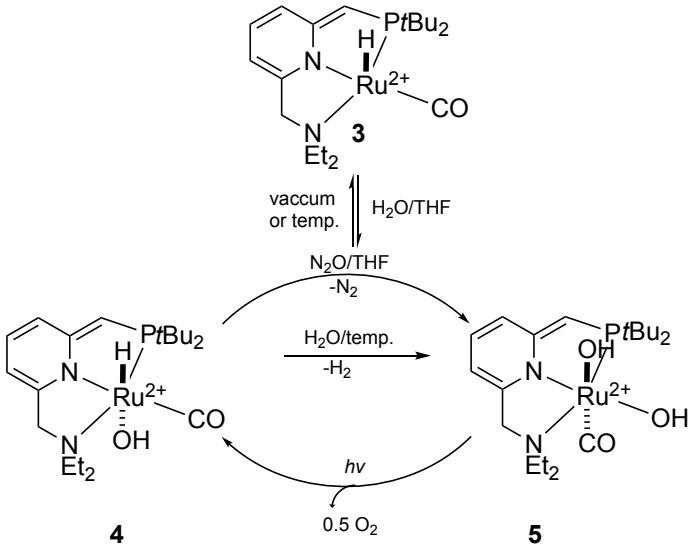

Scheme 2. Milstein's ruthenium pincer catalyst **3** catalyzes water splitting via a two-step process.

Non-innocent ligands have also found applications in the conversion of CO_2 into formic acid, which can thus act as hydrogen-storage vector.[20-22]

For example in 2007 Himeda[23] reported complex **6** (Scheme 3) as an efficient catalyst for CO_2 hydrogenation proceeding under very mild conditions: 30 °C with a TOF of 3.5 h^{-1}. The cooperation between Himeda

and Fujita[24] in 2012 resulted in a reaction proceeding at room temperature with a TOF of 64 h^{-1}. This significant improvement was achieved by replacing the dihydroxy-phenantroline ligand in **6** by a bipyridinone ligand Thbpym (4, 4', 6, 6'-tetrahydroxy-2,2' bipyrimidine) in complex **7** (Scheme 3). The enhancement was achieved thanks to presence of four hydroxyl groups, positioned near the catalytic centre, allowing the ligand act as a Brönsted base thus facilitating the heterolysis of H_2.

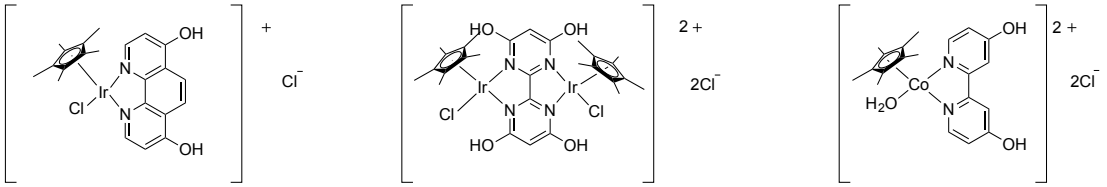

6 **7** **8**

Scheme 3. Versatile catalyst precursors used for the hydrogenation of carbon dioxide.

The dixydroxybipyridine ligand was also combined with Co(III). The resulting complex **8** catalyzed carbon dioxide hydrogenation in water to yield formate at 100 degrees with TOF = 39 h^{-1}.[25]

Iridium complexes bearing a pyridinone-type of ligand were also employed in reactions such as: acceptorless alcohol dehydrogenation (AAD),[26] water oxidation[27,28] or reversible hydrogenation of nitrogen heterocycles.[29]

As mentioned earlier, non-innocent ligands act as an electron reservoir. An example of AAD is presented in Scheme 4.[30]

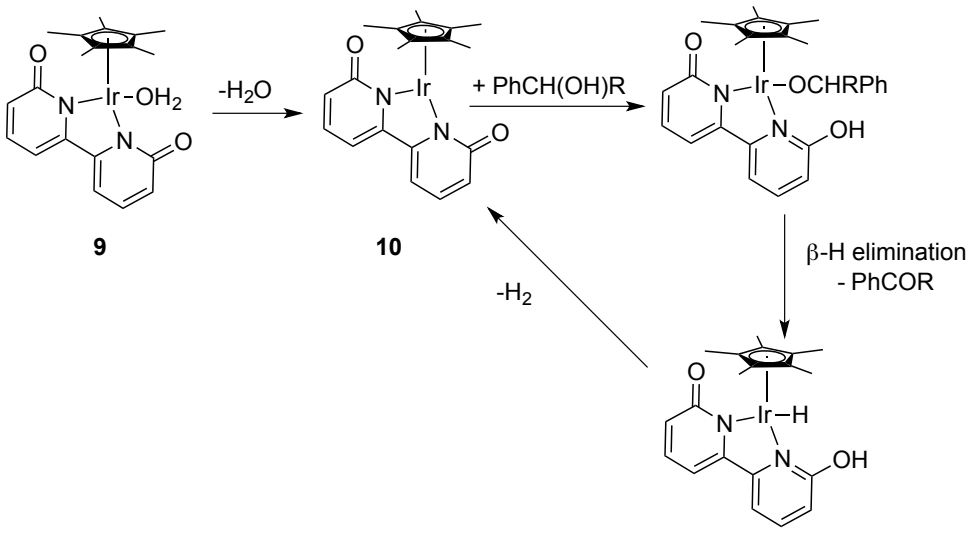

Scheme 4. A non-innocent ligand acting as an electron reservoir in an acceptorless alcohol dehydrogenation.

The oxidation state of iridium(III) **9** remains the same during the entire catalytic cycle. The coordination of the alcohol results in the ligand protonation and β-hydrogen abstraction of the coordinated alkoxide. The oxidized product is released allowing for the formation of an Ir-H moiety. Hydrogen evolution occurs in the final step, which regenerates the catalyst **10.**[30]

N-heterocyclic carbenes are known to be good ligands as they ensure a very stable and inert bond with metal irrespective of their oxidation state.[31-35] Thanks to this feature they have found multiple applications in homogeneous catalysis.[31]

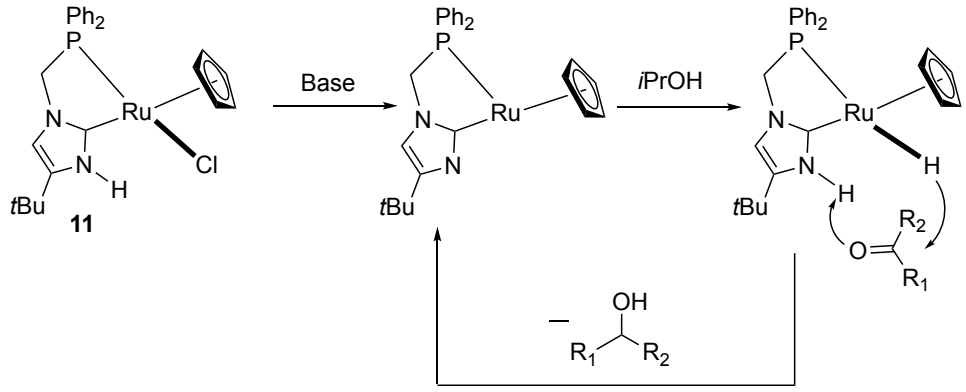

Scheme 5. Ruthenium complex **11** bearing protic NHC in ketones reduction

Several groups have recently exploited the use of NHC in switchable catalysis. Bielawski and Nelson introduced a catalyst for transestrification prompted by electronically-modulated NHC.[36] The electron donating abilities of the ligand have also been modified by changing the pH during ring opening metathesis polymerization.[37] Grotjhan reported notable results presenting the use of a ruthenium catalyst bearing a protic *N*-heterocyclic carbene for the reversible transfer-hydrogenation of acetophenone (Scheme 5).[38]

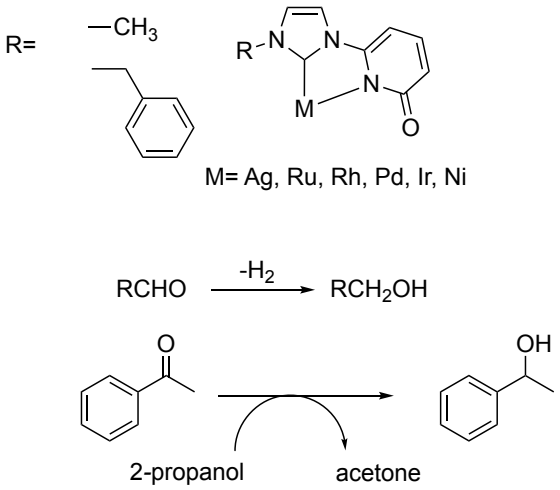

Scheme 6. Metals bearing NHC ligand with an appended pyridinol for the mild oxidation of alcohols and acetophenone reduction.

In the contex of non-innocent ligands, we have designed an NHC ligand bearing a pyridinol moiety (Scheme 6). We hypothesized that the strong donating properties of the *N*-heterocyclic moiety coupled with the acido-basic properties of the pyridinol may afford organometallic complexes with interesting properties. Herein, we describe our efforts on the synthesis and coordination properties of *N*-heterocyclic carbene ligands with an appended pyridinone moiety.

2. Results and discussion

2.1. Synthesis of an imidazolium salt flanked with a pyridinol and its coordination properties with Ru, Ir, Rh and Pd

2.1.1. Synthesis of imidazolium salt (H-14)$^+$Br$^-$ and complex [(p- cymene)RuCl(NHC-14)] 15- methods comparison

The imidazolium salt (H-**14**)$^+$Br$^-$ was synthesized by coupling imidazole with 2-bromo-6-methoxypyridine. This step was followed by an alkylation with Bz-Br and subsequent deprotection of methyl group in CH_3COOH-HBr mixture. The salt (H-**14**)$^+$Br$^-$ was obtained in an overall yield of 71% (Scheme 7).

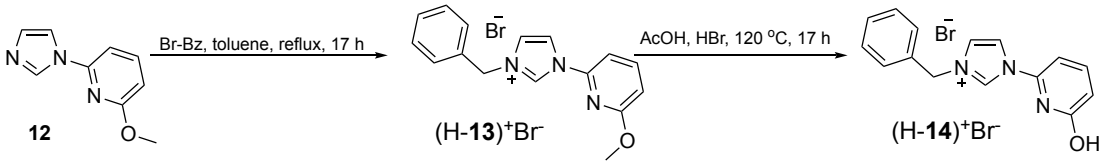

Scheme 7. The synthesis of imidazolium salt (H-**14**)$^+$Br$^-$.

Having synthesized and fully characterized the imidazolium salt, the next step was to study its coordination properties to various transition metal complexes.

To identify the best way to generate complexes with an NHC flanked with a pyridinol, we tested several methods described in the literature, including: formation of the free carbene[39] followed by addition of a metal source, b) transmetallation from a silver complex to the desired metal source,[40] or c) stirring of the (H-**14**)$^+$Br$^-$ with a metal source in the presence of base[41] (Scheme 8). In all tested reactions we benchmarked for the preparation of [(η^6-*p*-cymene)RuCl(NHC-**14**)] **15**.

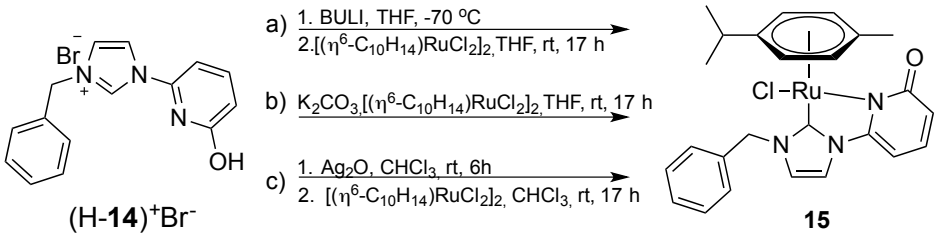

Scheme 8. Preparation of complex **15** following different routes.

The traditional method with formation of the free carbene in THF with 2.1 equivalents of BuLi, resulted in the formation of [(η^6-*p*-cymene)RuCl(NHC-**14**)] in 16% isolated yield. The modest yield may be due to the fact that, the pKa of the hydroxyl group is lower than the pKa of the imidazolium hydrogen. The strong base thus deprotonates the hydroxyl group and leads to an additional charge on the molecule, thus contributing to decrease its solubility. As a consequence, only a small amount of the free carbene was formed and could react with the metal to afford the desired complex [(η^6-*p*-cymene)RuCl(NHC-**14**)] **15** (Scheme 8a). However, the (H-**14**)$^+$Br$^-$ salt could

not be recovered at the end of reaction, which suggests that after deprotonation another process occurs that leads to decomposition of the imidazolium salt.

To investigate the transmetallation process, the (H-**14**)$^{+}$Br^{-} salt was reacted in CH_2Cl_2 with Ag_2O followed by filtration and addition of [(η^6-*p*-cymene)$RuCl_2$]$_2$. The reaction mixture was stirred for 6 hours and filtered. The filtrate was concentrated and Et_2O was added, which resulted in the formation of a brown solid. To obtain a pure complex, silicagel column chromatography (1-5% MeOH in CH_2Cl_2) was used. The [(η^6-*p*-cymene)RuCl(NHC-**14**)] **15** was isolated in 65% yield.

As third method, the dimeric ruthenium(II) complex was placed with (H-**14**)$^{+}$Br^{-} and potassium carbonate in a Schlenk flask. The reaction mixture was stirred in dry THF at room temperature for 17 hours. The reaction mixture was filtered and the solvent was evaporated. The residue was purified by silicagel column chromatography and the product was isolated in 85% yield.

We thus identified two methods to synthesise complex [(η^6-*p*-cymene)RuCl(NHC-**14**)] **15** in reasonable yields. Next, we attempted the coordination of NHC-**14** to other metals including Ir, Rh and Pd.

2.1.2. Synthesis of the complexes 15-20 bearing NHC-14

The imidazolium salt (H-**14**)$^{+}$Br^{-} and (H-**13**)$^{+}$Br^{-} were reacted with Ag_2O and added to the dimeric metal sources: $[(\eta^6\text{-}p\text{-cymene})RuCl_2]_2$, $[(\eta^5\text{-Cp*})IrCl_2]_2$, $[(\eta^5\text{-Cp*})RhCl_2]_2$, $[Pd(\eta^3\text{-allyl})Cl]_2$. This led to the formation of the corresponding monomeric complexes: [(*p*-cymene)RuCl(NHC-**14**)] **15**, [(η^5-Cp*)IrCl(NHC-**14**)] **16**, [(η^5-Cp*)IrCl(NHC-**13**)] **17**, [(η^5-Cp*)RhCl(NHC-**14**)] **18** and [Pd(η^3-allyl)(NHC-**14**)] **19** (Figure 1).

The characterization of the silver intermediate proved to be challenging. The ^{1}HNMR was very complicated, particularly in the aromatic region, suggesting formation of multiple products. Since the H_i proton was not visible in the ^{1}HNMR, we hypothesize that Ag-NHC-**14** is formed quantitatively. The crude mixture was used for transmetallation reactions to yield complexes **15**, **16**, **17,** **18** and **19** The reasonable yields obtained for these reactions suggest that [Ag(NHC-**14**)]$^{+}$ is indeed formed, thus allowing the transmetallation with various metal precursors to proceed.

Complexes [(η^5-Cp*)RhCl(NHC-**14**)] **18** and [Pd(η^3-allyl)(NHC-**14**)] **19** were purified by precipitation from CH_2Cl_2 by addition of Et_2O. In cases of complexes [(η^6-*p*-cymene)RuCl(NHC-**14**)] **15**, [(η^5-Cp*)IrCl(NHC-**14**)] silicagel column chromatography was required.

Complex [Ir(ppy)$_2$(NHC-**14**)] **20** was synthesized following the procedure reported for a related compound[42] and isolated as a bright yellow solid.

To check whether the pyridinol deprotection is possible on the metal, we attempted the synthesis of the protected version of Iridium complex [(η^5-Cp*)Ir(NHC-**13**)Cl] **17**.

The protected (H-**13**)$^+$Br$^-$ salt was reacted in CH_2Cl_2 with Ag_2O followed by filtration and addition of the dimeric [(η^5-Cp*)$IrCl_2$]$_2$. We confirmed formation of Ag-NHC complex by ESI-MS with expected m/z 637.2. We were also able to isolate the [(η^5-Cp*)Ir(NHC-**13**)Cl] **17** and characterize it by ^{1}HNMR and ESI-MS. Next we attempted the deprotection of complex [(η^5-Cp*)Ir(NHC-**13**)Cl] **17** in a CH_3COOH-HBr mixture. Unfortunately the reaction led to the complex decomposition.

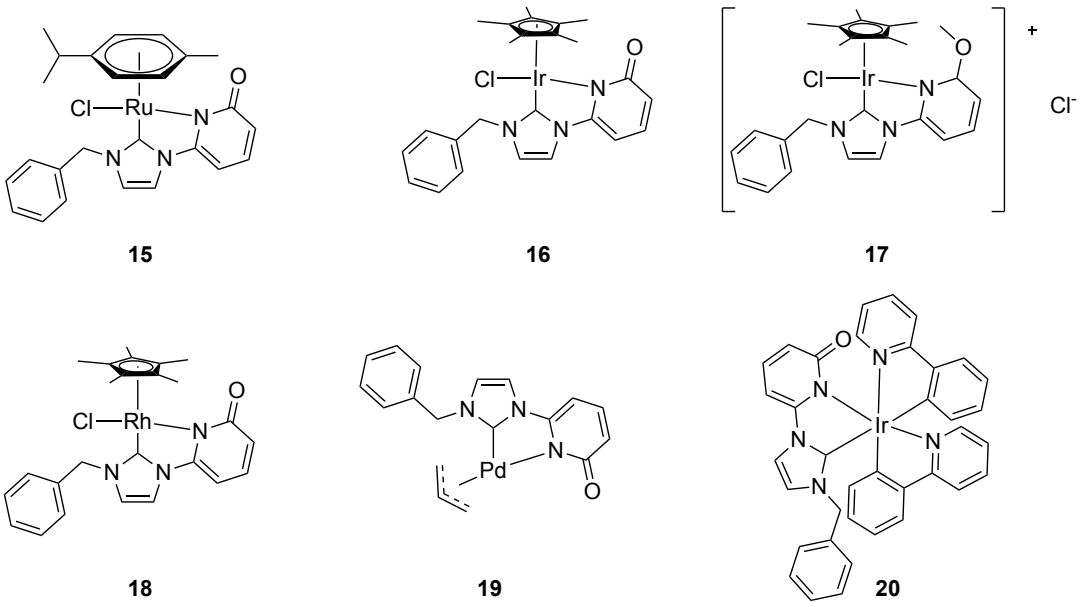

Figure 1. Synthesis of an *N*-heterocyclic carbene ligand bearing a pyridinone (NHC-**14**) and complexes thereof. The following metal dimer sources were used: [(η^6-*p*-cymene)$RuCl_2$]$_2$, [(η^5-Cp*)$IrCl_2$]$_2$, [(η^5-Cp*)$RhCl_2$]$_2$, [Pd(η^3-allyl)Cl]$_2$.

2.2. Structural characterization

2.2.1. X-ray analysis

In order to gain structural insight on the coordination properties and geometry of the resulting complexes, crystals of the NHC-bearing complexes were grown. For this purpose, slow diffusion of diethylether into a concentrated dichloromethane solution of the desired complex, afforded crystals suitable for X-Ray analysis.

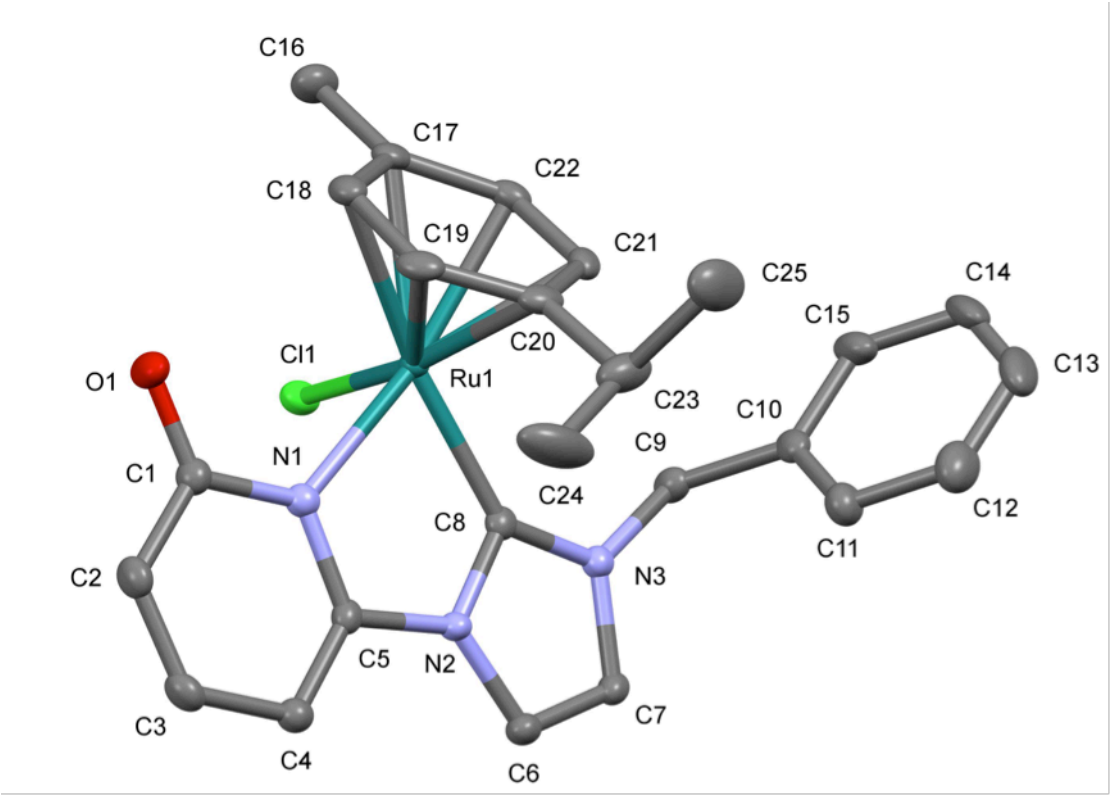

Figure 2. X-ray crystal structure of complex [(η^6-*p*-cymene)RuCl(NHC-**14**)] **15**. The heavy atoms are depicted as thermal ellipsoids (50% probability). H- atoms and residual solvent molecules are omitted for clarity.

Both the ruthenium complex [(η^6-*p*-cymene)RuCl(NHC-**14**)] **15** (Figure 2) and iridium complex [(η^5-Cp*)IrCl(NHC-**14**)] **15** (Figure 3**)** share some similarities, therefore will be described together. The similarities are particularly evident in coordination geometries around the metal. For both complexes, the η^n-bound aromatic moieties (n = 5, 6) are nearly planar and display very similar C-M distances (M = Ru, Ir) varying batween 2.166(2) to 2.302(2) Å (Ru) and 2.155(5) Å and 2.242(5) Å (Ir).

In complex [(η^6-*p*-cymene)RuCl(NHC-**14**)] **15** the NHC ligand is almost planar, no bending can be observed.

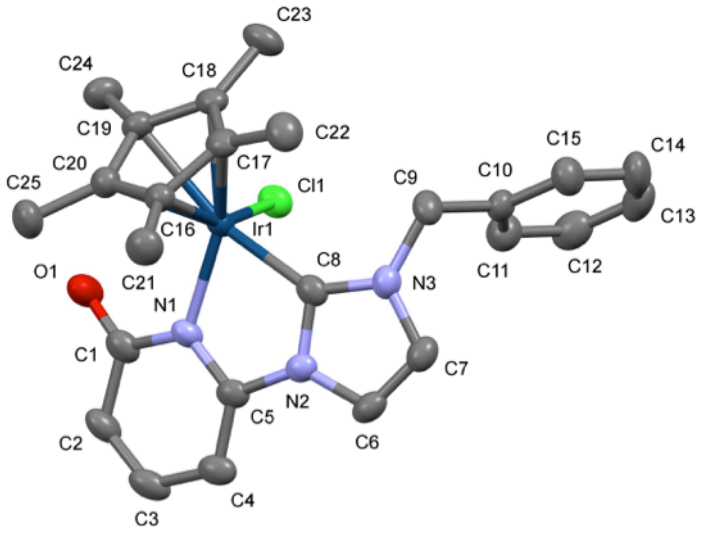

Figure 3. Crystal structure of complex [(η^5-Cp*)IrCl(NHC-**14**)] **16**. The heavy atoms are depicted as thermal ellipsoids (50% probability). H-atoms and residual solvent molecules are omitted for clarity.

In structure of the complex [(η^5-Cp*)IrCl(NHC-**14**)] **16**, the NHC-**14** ligand is bent. The angle between the best planes through the six-membered ring N1-

C1-C2-C3-C4-C5 and the five-membered NHC ring N2-C6-C7-N3-C8 is 14° while the corresponding angle in the two structures with the same ligand are 6.33° (Ru) and 4.24° (Pd) respectively. Examining the crystal packing, a number reasons for this pronounced bending can be identified: there are short contacts between C3 and C23 (3.61 Å) and C7 and C2 (3.28 Å), while both C23 and C2 are generated by symmetry.

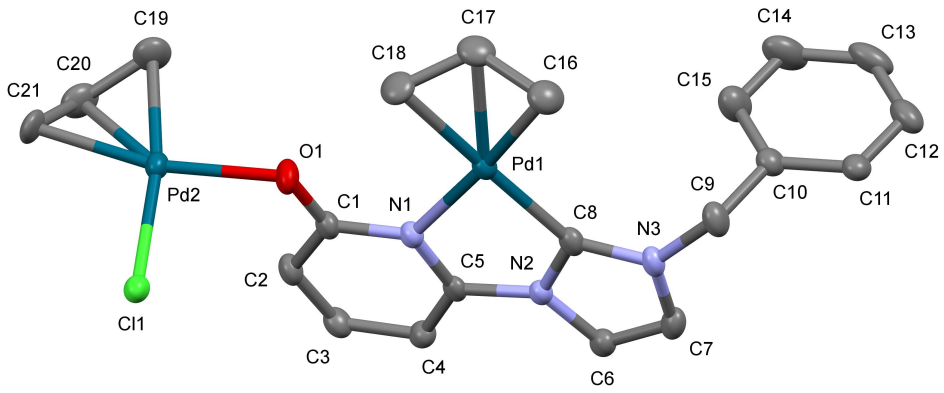

Figure 3. Crystal structure of complex [Pd(η^3-allyl)(NHC-**14**)] **19** showing all non-hydrogen atoms. The heavy atoms are depicted as thermal ellipsoids (50% probability). H-atoms and residual solvent molecules are omitted for clarity.

The structure of complex [Pd(η^3-allyl)(NHC-**14**)] **19** displays the expected square planar coordination geometry with the allyl ligand occupying two coordination sites around the Pd. The allyl group is disordered and was modeled.

The structure of [Pd(η^3-allyl)(NHC-**14**)] **19** is particular as the ligand

coordinates one more PdCl-allyl group. The bond length Pd2-O1 indicates coordination.

The bond lengths C1-O1and N1-C1 in all complexes (Table 1) indicate that ligand exists in its pyridinone form. This assumption is also confirmed by IR soectroscopy (section 2.2.2).

[(*p*-cymene)Ru(NHC-14)Cl] 15		[(η^5-Cp*)Ir(NHC-14)Cl] 16		[Pd(η^3-allyl)(NHC-14)] 19	
Angles [°]		**Angles [°]**		**Angles [°]**	
C_8-Ru-N_1	76.20(8)	C_8-Ir-N_1	76.12(17)	C_8-Pd_1-N_1	78.50(8)
C_8-Ru-Cl	86.55(6)	C_8-Ir-Cl	87.93(13)	C_8-Pd_1-C_{18}	173.1(2)
N_1-Ru-Cl	88.01(5)	N_1-Ir-Cl	87.84(11)		
Bond length [Å]		**Bond length [Å]**		**Bond length [Å]**	
C_8-Ru	2.019(2)	C_8-Ir	2.005(5)	C_8-Pd_1	2.022(2)
N_1-Ru	2.127(1)	N_1-Ir	2.098(4)	Pd_1-N_1	2.138(19)
Ru-Cl	2.423(7)	Ir-Cl	2.412(5)	C_1-O_1	1.268(4)
C_1-N_1	1.381(3)	C_1-N_1	1.378(6)	O_1-Pd_2	2.102(7)
C_1-O_1	1.257(3)	C_1-O_1	1.245(6)	N_1-Pd_1	2.124(2)
				N_1-C_1	1.375(3)

Table 1. Selected angles and bond lengths characterizing complexes [(η^6-*p*-cymene)RuCl(NHC-**14**)] **15**, [(η^5-Cp*)IrCl(NHC-**14**)] **16** and [Pd(η^3-allyl)(NHC-**14**)] **19**.

2.2.2. Analysis of the complexes by IR

X-ray structural analysis revealed that during the two step reaction, the pyridinol is deprotonated to form the corresponding pyridinone. We have further confirmed this by measuring IR of the complexes. A broad band characteristic of hydroxyl groups can be usually found in region between

3200 cm^{-1} and 3700 cm^{-1}. The spectrum of (H-**14**)$^{+}Br^{-}$, displayed in Figure 4, exhibits a broad and intense band at 3231 cm^{-1}, which is typical for a hydroxyl group. The spectra of complexes **15-20** do not contain any broad band in this region. Ideally, when hydroxyl group is transformed into carbonyl group, in the region of 1700 cm^{-1} appears new sharp band corresponding to C=O. Unfortunately we do not observe this situation in the spectra presented in Figure 4. This situation may be explained by the fact that in this region exist also bands coming from vibrations of other groups of atoms.

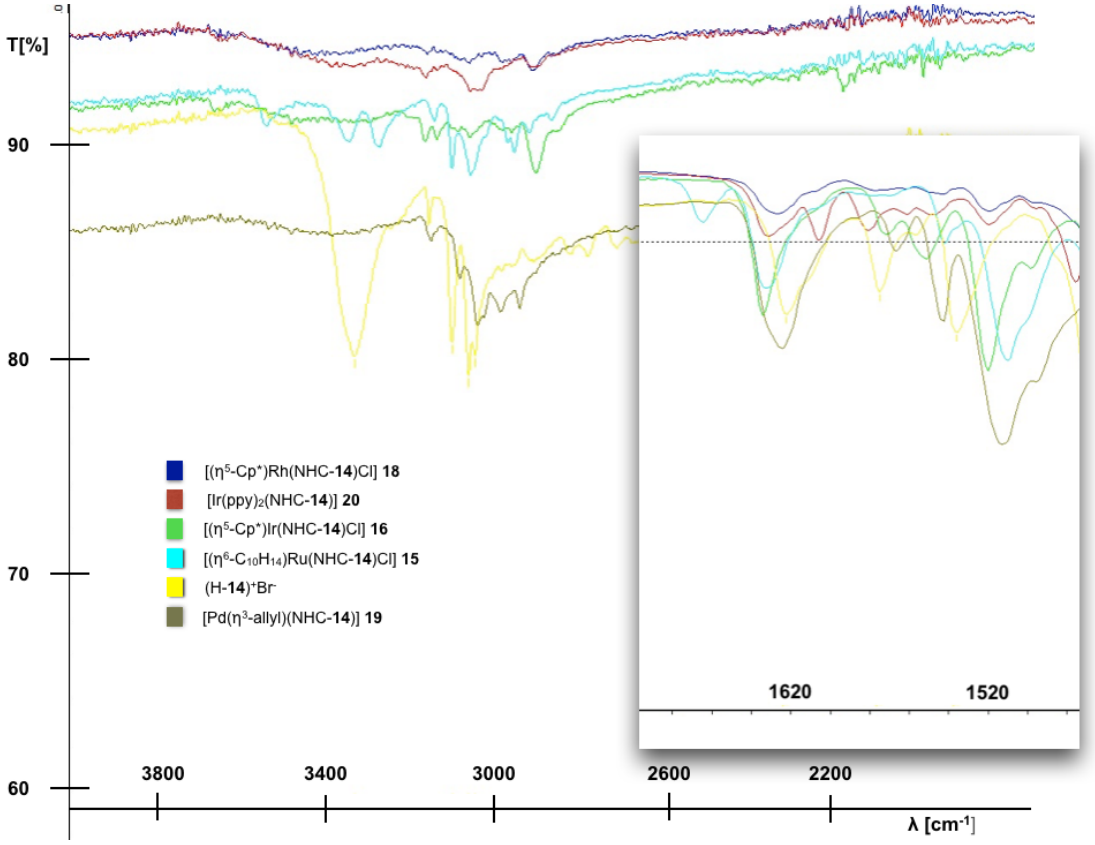

Figure 4. Superimposed IR spectra of complexes and (H-**14**)$^{+}Br^{-}$ highlighting the absence of a hydroxyl group in the complexes.

2.3. Coordination properties of the NHC-14 with the first row metals

2.3.1. Attempted synthesis of [Fe(II)-NHC-14] complexes

To obtain an iron(II) complex with NHC-**14**, all reagents were dried under vaccum and transferred to a glovebox. The reactions are summarized in Scheme 9.

We carried out the transmetallation reaction from the Ag-NHC-**14** complex to an anhydrous $FeBr_2$ source. The formation of a white precipitate was observed which suggested that a reaction had occurred. The reaction mixture was filtered and the solvent was evaporated using strict Schlenk techniques. Analysis of the ^{1}HNMR spectrum revealed the presence of the imidazolium proton as well as unidentified compounds. The reaction mixture was subjected to ESI-MS analysis. No peak indicating the formation of the desired product [Fe(NHC-**14**$)_2$] **21** (Scheme 9) could be identified. We conclude that upon mixing the Ag-NHC-**14** complex with $FeBr_2$, the complex undergoes decomposition. We also attempted transmetallation of the silver complex to [(η^5-C_5H_5)FeI$(CO)_2$] to obtain iron complexes [(η^5-C_5H_5)Fe(NHC-**14**)CO] **22**. Aanalysis of the crude reaction mixture by ^{1}HNMR and MS-ESI showed that [(η^5-C_5H_5)Fe(NHC-**14**)CO] **22** was not formed.

Since the reaction of transmetallation reaction failed, we investigated another method whereby (H-**14**)$^+Br^-$, $FeBr_2$ and K_2CO_3 were placed in a flask and dry THF was added. The reaction mixture was stirred for 3 days at ambient temperature. A white solid was separated from the solution. ^{1}HNMR of both the solid and the filtrate were recorded. The white solid proved to be

unreacted (H-**14**)$^{+}$Br^{-} salt. No peak, other than solvent was visible by ^{1}HNMR analysis of the filtrate. Because the solvent was orange, we suspect that the filtrate contained unreacted $FeBr_2$.

Following the procedure by Warratz whereby iron-NHC complexes are prepared upon reacting of $Fe_3(CO)_{12}$ with an imidazolium precursor,[43] we applied the same protocol with our ligand. Unfortunately, no formation of the desired complex [FeBr(NHC-**14**)$(CO)_3$] **23** could not be observed by ESI-MS and ^{1}HNMR analysis.

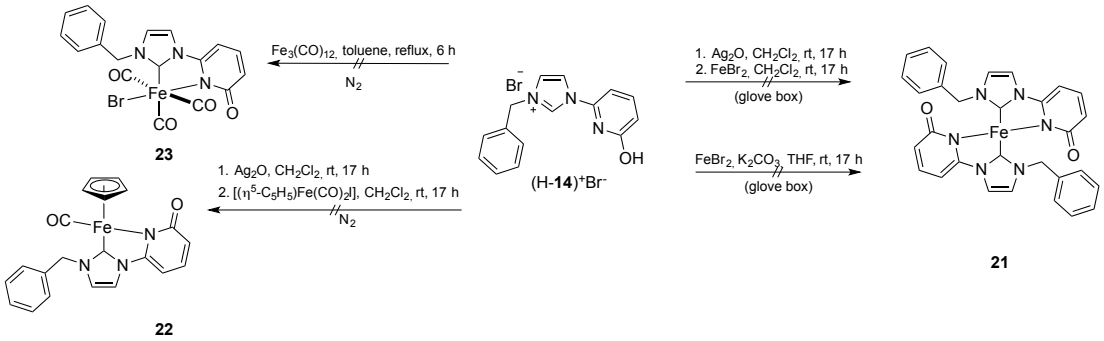

Scheme 9. Attempted synthesis of iron complexes bearing NHC-**14.**

2.3.2. Attempted synthesis of [Cu(I)-(NHC 14)] complexes synthesis

Procedures investigated for the preparation of Cu-NHC complexes were inspired from the literature.[44] Transmetallation[45] reactions were attempted from Ag-NHC-**14** complexes to either CuCl or Cu-S-Ph (Scheme 10). Copper(I) chloride was recrystallized from HCl before use. The reaction of transmetallation was performed in dry CH_2Cl_2. During the reaction, the formation of white precipitate was observed. The reaction mixture was filtered and solution was concentrated. The addition of Et_2O to the solution resulted

in the formation of a green precipitate. The ^{1}HNMR spectrum displayed broad peaks in the aromatic region. However the characteristic peak from H_i of the imidazolium salt was not present. ESI-MS analysis did not reveal the expected mass m/z 315.0 for [Cu(NHC-**12**)]$^{+}$. Instead an intense peak assigned to (H-**14**)$^{+}$ was observed. This suggest the decomposition of the complex [CuBr(NHC-**14**)] **24**. We attempted crystallization by slow diffusion of the Et_2O to [CuBr(NHC-**14**)] **24** solution in MeOH. We also prepared a saturated solution [CuBr(NHC-**14**)] **24** in MeOH at the 50 °C and slowly reduced to ambient temperature. In all cases, we observed the formation of precipitate. Unfortunately no structural characterization either by ^{1}H-NMR, MS or X-ray was possible.

Attempted direct reaction with Cu(0),[46] lead to the decomposition of the substrate.

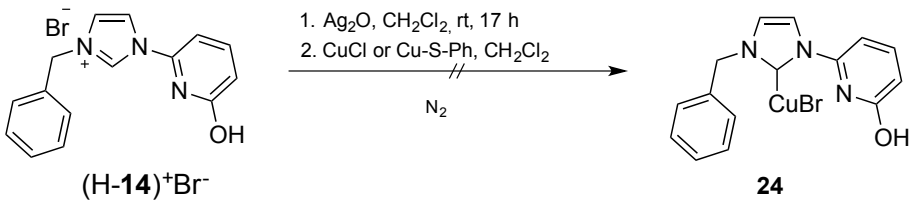

(H-**14**)$^{+}$Br^{-} **24**

Scheme 10. Attempted synthesis of the complex [CuBr(NHC-**14**)] **24.**

2.3.3. Synthesis of Ni(II)-(NHC-14) complexes

To obtain Ni(II)-NHC-**14** we attempted transmetallation reactions using Ag-NHC-**14** in the presence of either 0.5 eq. or 1 eq. of $[NiCl_2(PPh_3)_2]$ (Scheme 11).

Addition of the silver complex to a solution of $[NiCl_2(PPh_3)_2]$ caused immediate formation of a large precipitate. The solid slowly changed colour from white to dark grey, highlighting the formation of AgCl (Scheme 10). The, ESI-MS analysis revealed peak m/z 559.4 corresponding to the desired complex [Ni(NHC-**14**$)_2$] **25** and peak at m/z 631.4 corresponding to $[Ag(PPh_3)_2]^+$ (Figure 5). In the ^{1}HNMR spectrum we see peaks in the aromatic area arising from the $[Ag(PPh_3)_2]X$, which was also confirmed by the ESI-MS (Figure 5). We observe also broadened peaks what suggest that the sample contains paramagnetic compounds probably belonging to the Ni(II)-NHC-**14** complex. Indeed, depending on the bulkiness of ancillary ligands, four-coordinate Ni(II) complexes may adopt either a diamagnetic square planar or a paramagnetic tetrahedral geometry, We thus hypothesize that the four coordinate complex [Ni(NHC-**14**$)_2$] **25** is tetrahedral.

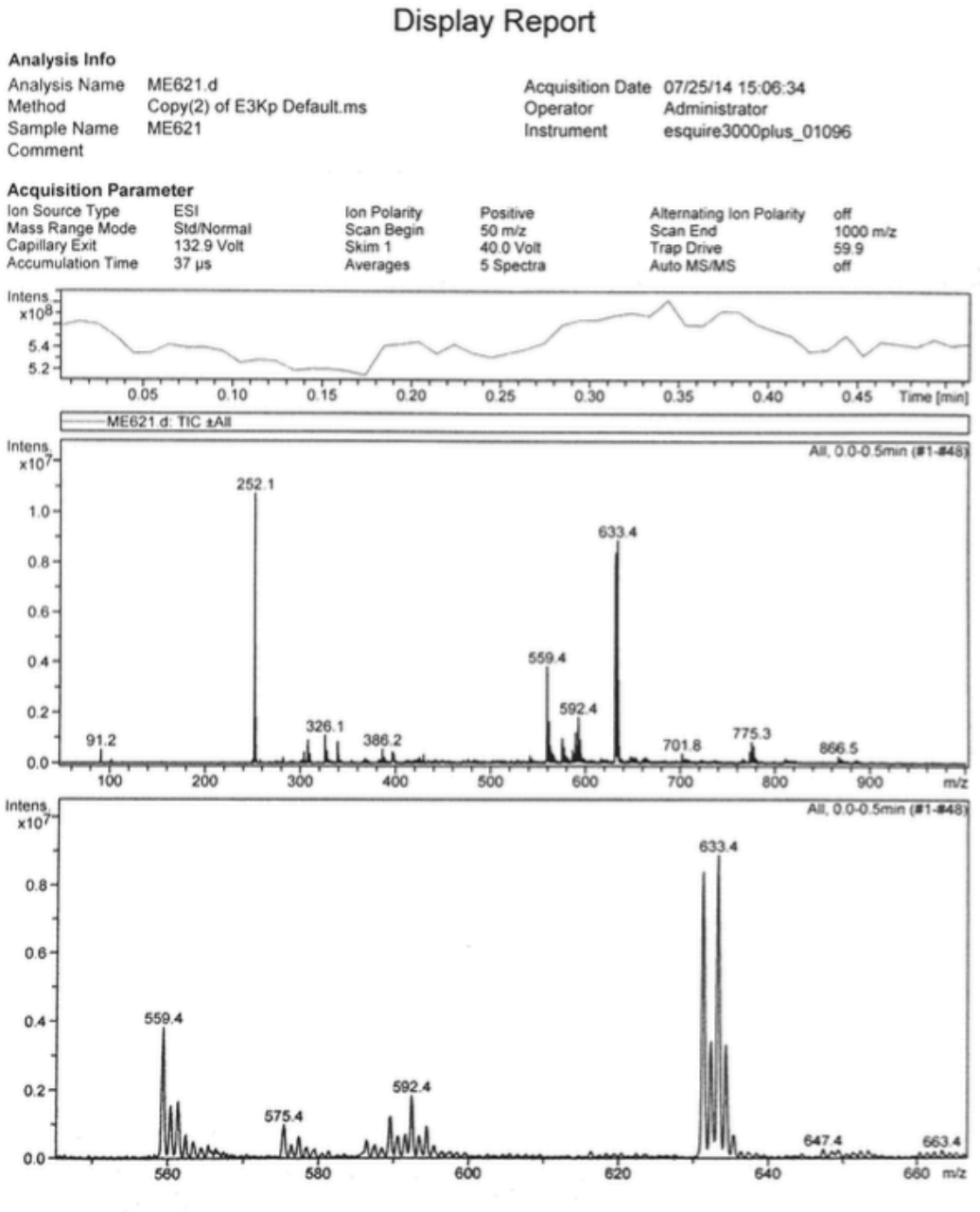

Figure 5. The ESI-MS spectrum of green precipitate obtained in a reaction of imidazolium salt **14** and 0.5 eq of $[NiCl_2(PPh_3)_2]$.

When 1 eq. $[NiCl_2(PPh_3)_2]$ was used, two peaks at m/z 252.1 and m/z= 631.4, assigned respectively to imidazolium salt and $[Ag(PPh_3)_2]^+$ were present (Figure 6).

We conclude that transmetallation from silver to nickel occurred but the formation of the desired [NiCl(NHC-**14**)PPh_3] **26** could not be confirmed. In both cases green solids were precipitated from the saturated solution of MeOH by addition of the Et_2O. Unfortunately, we were unable to separate $[Ag(PPh_3)_2]^+$ from the green precipitate. In the ESI-MS spectra, we observed peak assigned to both complex [Ni(NHC-**14**)$_2$] **25** and $[Ag(PPh_3)_2]^+$. In case of [NiCl(NHC-**14**)PPh_3] **26** we could observe only the peak belonging to $[Ag(PPh_3)_2]^+$ and imidazolium salt.

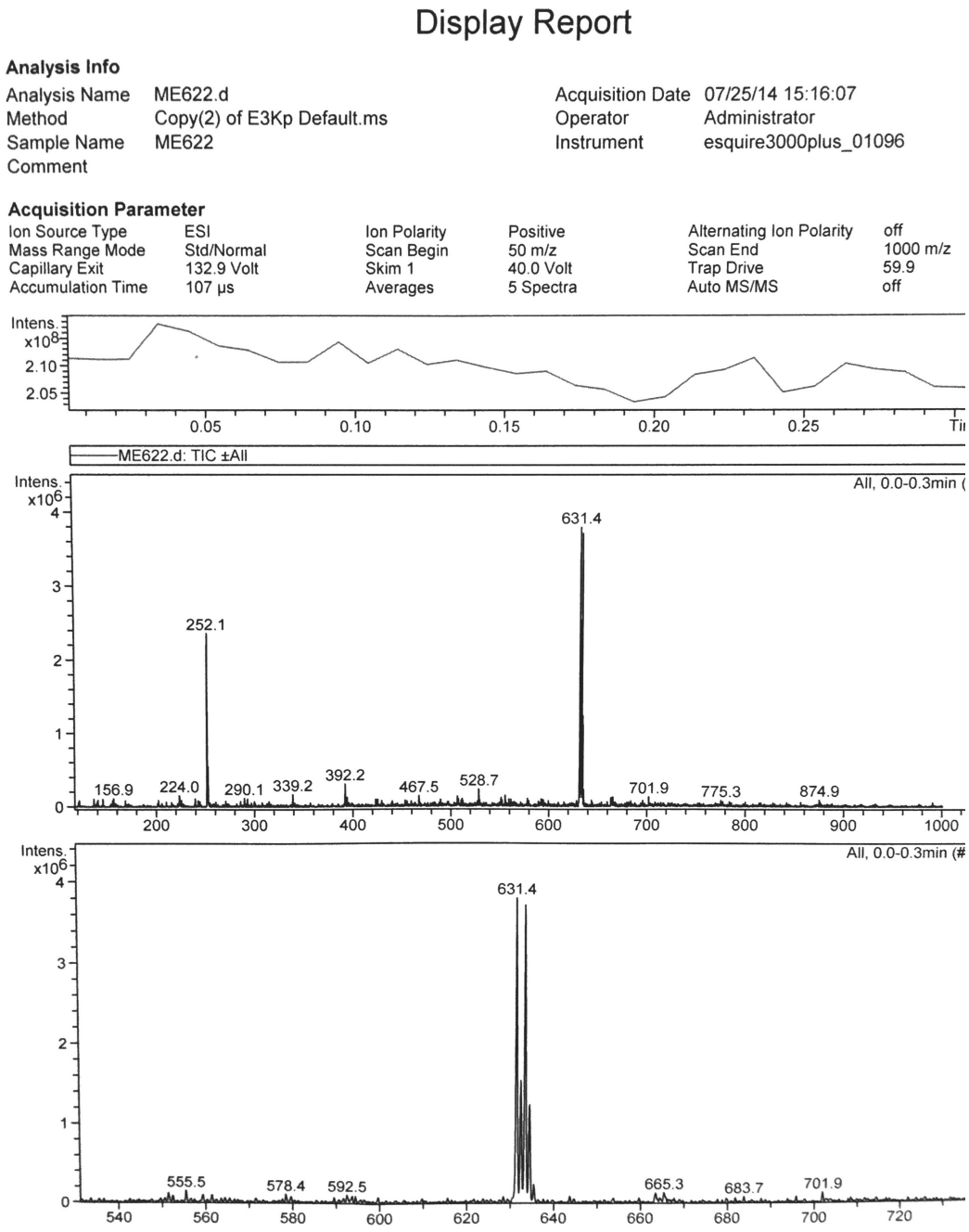

Figure 6. The ESI-MS spectrum of green precipitate obtained in a reaction of imidazolium salt **14** and 1 eq of $[NiCl_2(PPh_3)_2]$.

In the literature, 0.5 eq of $Ni(OAc)_2$ has been used as a metal source and internal base to promote the formation of the Ni-NHC complexes.[47] Reaction

of the (H-**14**)$^{+}$Br^{-} with 0.5 eq of Ni(OAc)$_2$ did not lead to the formation of Ni(II)-NHC-**14** complex. We speculate that the acetate ligand deprotonates the hydroxyl group but does not lead to the deprotonation of the imidazolium proton H$_i$. Next, we attempted this reaction in the presence of 2 eq. *t*-BuOK. The crude was analysed by ESI-MS, which suggests that the desired complex [Ni(NHC-**14**)$_2$] **25** was not formed. The corresponding mas spectrum reveals mainly (H-**14**)$^{+}$. A very similar situation results from the reaction of [NiCp$_2$] with 1 eq of imidazolium salt.[48,49] Literature reports suggest that reaction of the twenty electron [NiCp$_2$] precursor with imidazolium salt leads to release of cyclopentadiene with the concomitant formation of the [(η^5-Cp)NiX(NHC)] complex.[49] Since the (H-**14**)$^{+}$Br^{-} contains an additional acidic proton coming from pyridinol moiety that competes with imidazolium H$_i$, this strategy could not be employed in the synthesis of Ni-NHC-**14** complexes.

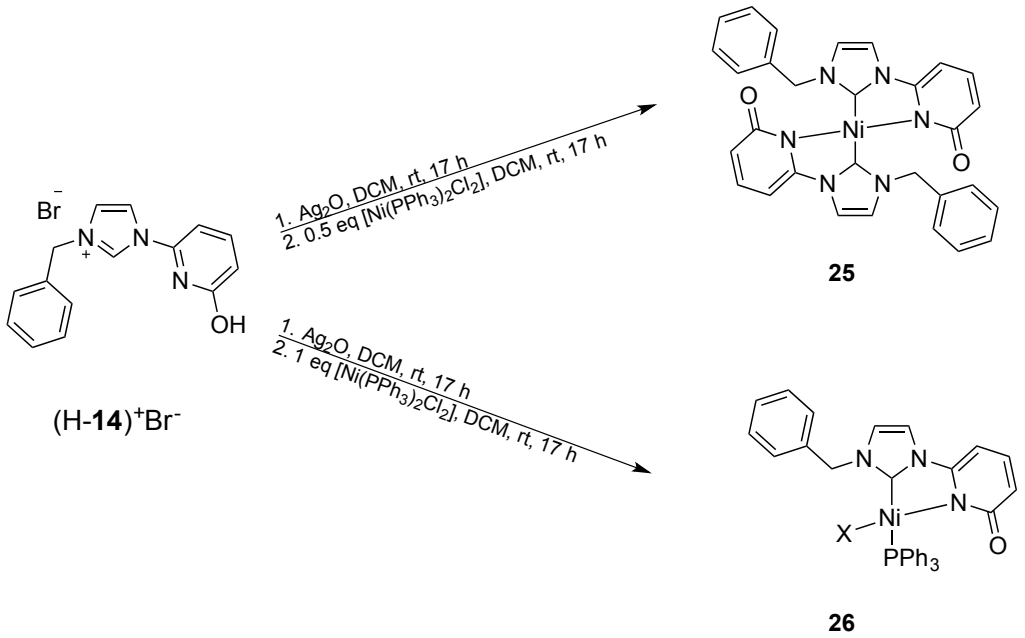

Scheme 11. Attempted synthesis of Ni(II)-NHC-**14** complexes.

3. Synthesis of the imidazolium salt (H-24)$^+I^-$ and its coordination properties.[1]

The imidazolium salt (H-**28**)$^+I^-$ (Figure 7) was synthesized in an analogous way to the imidazolium salt (H-**14**)$^+Br^-$ with the difference that compound 2-2-(1*H*-imidazol-1-yl)-6-methoxypyridine **12** was refluxed with CH_3I instead of benzyl bromide. Subsequently, the obtained salt (H-**27**)$^+I^-$ was deprotected in a mixture of CH_3COOH-HBr to yield [(H-**28**)$^+I^-$. The [(H-**28**)$^+I^-$ is a white solid that exhibits a very low solubility in common organic solvents except MeOH.

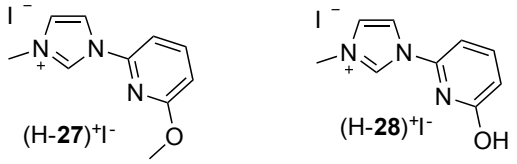

Figure 7. Imidazolium salt (H-**27**)$^+I^-$ precursor of salt (H-**28**)$^+I^-$ bearing pyridinol and methyl group on the NHC moiety.

We treated the salt (H-**28**)$^+I^-$ with Ag_2O in a different solvents: $CHCl_3$, CH_2Cl_2, MeOH, MeCN and DMSO. In every case, the imidazolium salt was isolated. The silver carbene complex could not be synthesized and therefore, we could not use the transmetallation strategy to prepare various NHC complexes bearing ligand **28**.

The reaction of imidazolium salt **28** with a strong base in dry THF and a dimeric pianostool precursor also did not result in the formation of the corresponding complex. During purification by precipitation from MeOH by

[1] Synthesized by S. Keller and J. Schaetti

slow addition of Et_2O, the imidazolium salt was isolated in 95% yield.

The reaction of (H-**28**)$^+I^-$ with K_2CO_3 and [(η^6-*p*-cymene)$RuCl_2$]$_2$ left the imidazolim salt unreacted.

To identify a suitable route for the synthesis of complexes bearing NHC-**28**, we attempted to prepare the chloroform adduct of NHC-**28**. For this purpose, the imidazolium salt was reacted with $CHCl_3$, KOH in toluene under a nitrogen atmosphere. The progress of the reaction was monitored by TLC. When reaction was complete, the solvent was evaporated and residue was dissolved in CH_2Cl_2. The solution was washed several times with a saturated solution of NaCl and evaporated. The residue was purified by silicagel column chromatography. The isolated fractions were analyzed by ^{1}HNMR. None of them corresponded to the desired chloroform adduct. The analysis revealed that each of the spots contained several unidentified compounds. Importantly, the imidazolium salt (H-**28**)$^+I^-$ could not be recovered. This suggests that during reaction, the imidazolium salt decomposes.

4. Catalysis

The obtained complexes **15**-**18** were tested in typical reactions relying on a hydrogen-borrowing strategy such as: alcohol oxidation, ketone and imine reduction.[47,48] For the alcohol oxidation and ketone reduction as model reactions, benzyl alcohol and acetophenone were selected as substrates respectively. The alcohol oxidation was carried out without a hydrogen acceptor either in an open flask or in sealed flask. Hydrogen borrowing reactions typically require high temperatures and often are performed in toluene. In both cases, the loading of the catalyst was set to 5% and reaction mixture was refluxed in toluene.

Analysis of the reactions mixtures revealed that the catalysts were not active toward alcohol oxidation. Further attempts including the addition of base or Ag_2SO_4 and solvent variations did not promote the activity. Next we tested the reduction of acetophenone. The reaction was carried out in the presence of isopropanol acting as source of dihydrogen. In this reaction we tested three complexes [(η^6-*p*-cymene)RuCl(NHC-**14**)] **15**, [(η^5-Cp*)IrCl (NHC-**14**)] **16** and [(η^5-Cp*)RhCl(NHC-**14**)] **18** as catalyst. The most active turned out to be a rhodium complex [(η^5-Cp*)RhCl(NHC-**14**)] **18** where the conversion of the acetophenone to the phenylethanol reached 67% (TON = 13.5). No activity was observed for [(η^5-Cp*)IrCl(NHC-**14**)] **15**. The results collected in Table 2 reveal an inverse dependence of activity of the iridium and rhodium complex against addition of base. Upon addition of KOH the activity of [(η^5-Cp*)IrCl(NHC-**14**)] **15** is improved. In case of the complexes [(η^6-*p*-cymene)RuCl(NHC-**14**)] **15** and [(η^5-Cp*)RhCl(NHC-**14**l] **18** the activity decreased. To investigate the activity of [(η^5-Cp*)IrCl(NHC-**14**)] **15** in the

presence of base, the reaction was also performed in the presence a stoichiometric of KOH. The analysis revealed that higher concentration of the base does not have significant impact on alcohol conversion. We also evaluated alternative source of dihydrogen including formic acid or formate using water as a solvent. Using formic acid or formate, no reduction could be detected with either complex. The reduction of imines was evaluated in the presence of isopropanol in a sealed tube. Analysis of the reaction mixtures revealed no product formation. The three catalysts tested turned out to be active only in the reaction of acetophenone reduction and the most active was [(η^5-Cp*)RhCl(NHC-**14**)] **18**.

Nr.	Complex	Loading [%]	KOH [%]	T [°C]	Yield [%|
1	**13**	5	-	90	20
2	**15**	5	-	90	67
3	**14**	5	-	90	-
4	**13**	5	33	90	17
5	**14**	5	33	90	45
6	**15**	5	33	90	20

Table 2. The table summarizing the initial results of the catalysis of the acetophenone reduction using isopropanol as dihydrogen source.

5. Summary

In this this chapter, we reported on the synthesis of two imidazolium salts, precursors of *N*-heterocyclic carbene, flanked with a non-innocent group, salt (H-**14**)$^{+}$Br^{-} rand (H-**28**)$^{+}$I^{-}. The coordination properties of the deprotonated imidazolium salts towards various metal salts were evaluated. The following complexes could be isolated and characterized [(η^6-*p*-cymene)RuCl(NHC-**14**)] **15**, [(η^5-Cp*)IrCl(NHC-**14**)] **16**, [(η^5-Cp*)IrCl(NHC-**13**)] **17**, [(η^5-Cp*)RhCl(NHC-**14**)] **18**, [Pd(η^3-allyl)(NHC-**14**)] **19** and [Ir(ppy)$_2$(NHC-**14**)] **20**. The formation of the [Ni(NHC-**14**)$_2$] **25** was confirmed by ESI-MS but the compound could not be isolated and further characterized by any other means. EPR spectroscopy may be useful to further characterize the paramagnetic nickel complex and determine its coordination geometry. These experiments were not performed however. The purification of the [Ni(NHC-**14**)$_2$] **25** from [Ag(PPh$_3$)$_2$]X could be accomplished by separation of the white crystals from the greenish precipitate under microscope. Although the formation of the Cu(I)-NHC-**14** complex was not confirmed, the formation of the white precipitate upon the filtration of the silver complex to the copper source and the recorded ^{1}HNMR could suggest that the reaction was accomplished successfully.

For the future of the project, synthesis of the ligand with protective silyl groups would be recommended. The main problem of the coordination of the (H-**28**)$^{+}$I^{-} turned out to be solubility, which in comparison to the (H-**14**)$^{+}$Br^{-} was much lower. Synthesis of the imidazolium salts flanked with non-innocent pyridinol as well as a solubilizing group could be worth of further investigation.

6. Experimental part

6.1. Synthesis and characterization

6.1.1. $(H\text{-}14)^+Br^-$

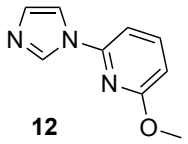

12

The following compounds: Imidazole (3.58 g, 2 eq.), 2-bromo-6-methoxypyridine (4.9 g, 1 eq.), K_3PO_4 (13.8 g, 2.5 eq.), Me_4*t*-butylXphos (0.25 mg, 0.02 eq.) and $Pd_2(dba)_3$ (0.238 g, 0.02 eq.) were placed in an oven dried Schlenk flask. The air was evacuated three times and dmso was added under nitrogen atmosphere. The reaction mixture was heated to 120 ^oC and stirred at that temperature for 2 days.

The reaction mixture was cooled and filtered. DMSO was evaporated under vacuum and CH_2Cl_2 was added. The resulting solution was washed 3 times with water, dried with Na_2SO_4 and evaporated. Silicagel column chromatography with EtOAc as eluent afforded the pure compound **12** as yellow oil (3.2 g, y = 70%). Compound **12** can be also synthesized in an alternative way described in the literature.[49]

^{1}**HNMR** (250 MHz, Chloroform-d) δ 8.33 (t, *J* = 1.1 Hz, 1H), 7.77 – 7.51 (m, 2H), 7.17 (dd, *J* = 1.4, 1.0 Hz, 1H), 6.89 (dd, *J* = 7.6, 0.6 Hz, 1H), 6.66 (dd, *J* = 8.2, 0.6 Hz, 1H), 3.97 (s, 3H).

^{13}**CNMR** (101 MHz, $CDCl_3$) δ 163.82, 147.15, 141.09, 135.10, 130.61, 116.19, 108.82, 103.71, 53.80.

HRMS(MeOH): m/z 176.0821 [M+H]

HRMS calculated: m/z 176.0824 [M+H]

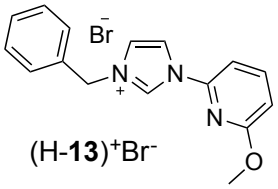

(H-**13**)$^{+}$Br^{-}

Compound **12** 2-(1*H*-imidazol-1-yl)-6-methoxypyridine (113 mg, 0.65 mmol) was placed in round-bottomed flask and an excess of benzyl bromide (2.23 g, 13 mmol, 1.5 eq.) was added followed by addition of toluene (3 mL). The reaction mixture was brought to 100 °C and stirred overnight. Upon cooling the reaction to the room temperature, a yellow oil formed. The solvent was removed and the oil was washed several times with toluene. Subsequently the oil was dissolved in a small amount of CH_2Cl_2. Addition of Et_2O led to the precipitation of the compound (H-**14**)$^{+}$Br^{-}] as beige solid (205 mg, y = 92%).

^{1}**HNMR** (400 MHz, $CDCl_3$) δ 11.51 (d, *J* = 1.6 Hz, 1H), 8.17 (t, *J* = 1.9 Hz, 1H), 7.80 – 7.70 (m, 2H), 7.67 (t, *J* = 1.9 Hz, 1H), 7.64 – 7.59 (m, 2H), 7.32 – 7.27 (m, 2H), 6.77 (dd, *J* = 7.7, 1.1 Hz, 1H), 5.81 (s, 2H), 3.94 (s, 3H).

^{13}**CNMR** (101 MHz, $CDCl_3$) δ 163.77, 143.65, 142.11, 135.11, 133.09, 129.51, 129.38, 129.33, 122.68, 118.93, 112.44, 106.13, 54.54, 53.54.

HRMS(MeOH): m/z 266.1290 [M-Br]

HRMS calculated: m/z 266.1288 [M-Br]

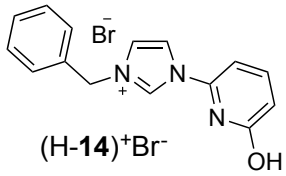

(H-**14**)$^{+}$Br^{-}

Imidazolium salt (H-**13**)$^{+}$Br^{-} (193 mg, 0.56 mmol) was placed in round bottomed flask and dissolved in acetic acid (3 ml). Ten equivalents of HBr were added and the reaction was brought to 120 ^{o}C and stirred at that temperature for 20 hours. The reaction mixture was concentrated to a small volume. Addition of CH_2Cl_2 resulted in the precipitation of a white solid. Filtration and washing the solid with Et_2O yielded pure (H-**14**)$^{+}$Br^{-} (93 mg, y = 50%)

^{1}**HNMR** (400 MHz, DMSO-d6) δ 12.29 – 11.08 (m, 1H), 10.06 (t, *J* = 1.6 Hz, 1H), 8.41 (t, *J* = 2.0 Hz, 1H), 8.03 – 7.94 (m, 2H), 7.56 – 7.36 (m, 7H), 6.86 (d, *J* = 8.2 Hz, 1H), 5.54 (s, 2H).

^{13}**CNMR** (101 MHz, DMSO) δ 163.44, 144.60, 142.93, 134.83, 134.49, 129.11, 128.99, 128.61, 123.53, 119.75, 110.93, 105.10, 52.56.

HRMS(MeOH): m/z 252.1130 [M- Br]

HRMS calculated: m/z 252.1131 [M- Br]

6.1.2. Procedure for the preparation of complexes 15-20

All reactions were performed under a nitrogen atmosphere using Schlenk techniques,

The salt (H-**14**)$^{+}Br^{-}$ and 0.65 eq. of Ag_2O were placed in the Schlenk flask and air was evacuated. Under a nitrogen atmosphere, $CHCl_3$ was added and the reaction was stirred at room temperature for 6 hours under exclusion of light. The reaction mixture was filtered off and the filtrate was added under nitrogen to a Schlenk flask containing 0.5 eq. of the dimer complex of the desired metal ($[(\eta^5\text{-Cp*})IrCl_2]_2$, $[(\eta^6\text{-}p\text{-cymene})RuCl_2]_2$, $[(\eta^5\text{-Cp*})RhCl_2]_2$. The reaction mixture was stirred for another 17 hours and then filtered. The filtrate was concentrated and hexane was added to precipitate desired complex **15-19**. The complex was redisolved in CH_2Cl_2 and precipitated with Et_2O, filtered and dried under vacuum. If impurities where present after precipitation, silicagel column chromatography was used (5% MeOH in CH_2Cl_2). Complex **20** was synthesized following the procedure given for a related compound.[42]

6.1.3. The complex [(η^6-p-cymene)RuCl(NHC-14)] 15

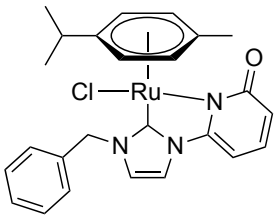

15

Column chromatography yielded pure [(η^6-*p*-cymene)RuCl(NHC-**14**)] **15** a brown solid (y = 78%)

^{1}HNMR (400 MHz, $CDCl_3$) δ 7.49 – 7.33 (m, 7H), 7.15 (dd, *J* = 8.6, 7.1 Hz, 1H), 6.91 (d, *J* = 2.1 Hz, 1H), 6.40 – 6.26 (m, 2H), 6.23 (d, *J* = 6.4 Hz, 1H), 6.08 (d, *J* = 7.1 Hz, 1H), 5.61 (d, *J* = 15.2 Hz, 1H), 5.54 – 5.40 (m, 2H), 5.10 (d, *J* = 6.0 Hz, 1H), 2.35 (s, 2H), 2.19 (s, 4H), 0.84 (dd, *J* = 6.9, 1.4 Hz, 6H).

^{13}CNMR (101 MHz, $CDCl_3$) δ 184.59, 170.72, 149.63, 137.15, 135.79, 129.43, 128.76, 127.46, 123.01, 116.50, 113.53, 91.75, 85.40, 54.51, 53.54, 50.57, 31.04, 22.62, 22.42, 19.26.

HRMS(MeOH): m/z 522.0885

HRMS calculated: m/z 522.0886

6.1.4. The complex [(η^5-Cp*)IrCl(NHC-14)] 16

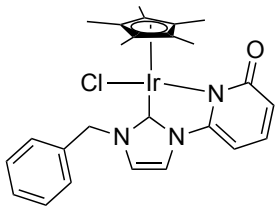

16

Column chromatography yielded pure [(η^5-Cp*)IrCl(NHC-**14)**] **16**
as a yellow solid (y = 60%)

^{1}**HNMR** (400 MHz,$CDCl_3$) δ 7.52 – 7.45 (m, 2H), 7.41 – 7.32 (m, 3H), 7.24 (d, *J* = 2.3 Hz, 1H), 7.13 (dd, *J* = 8.8, 7.0 Hz, 1H), 6.75 (d, *J* = 2.3 Hz, 1H), 6.21 (dd, *J* = 8.8, 1.1 Hz, 1H), 5.96 (dd, *J* = 7.0, 1.1 Hz, 1H), 5.59 (d, *J* = 13.8 Hz, 1H), 5.17 (d, *J* = 13.8 Hz, 1H), 1.86 (s, 14H).

^{13}**CNMR** (101 MHz, CD_2Cl_2) δ 168.55, 166.79, 150.07, 137.33, 135.71, 129.57, 129.55, 121.85, 117.28, 114.77, 91.68, 90.09, 55.01, 10.42.

HRMS(MeOH): m/z 578.1824 [M-Cl]

HRMS calculated: m/z 578.7360 [M-Cl]

6.1.5. [(η^5-Cp*)IrCl(NHC-13)] 17

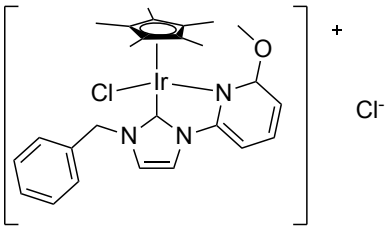

17

Complex [(η^5-Cp*)IrCl(NHC-**13**)] **17** was obtained as yellow solid (y = 79%)[1]

[1]**HNMR** (400 MHz, $CDCl_3$) δ 11.51 (d, *J* = 1.6 Hz, 1H), 8.17 (t, *J* = 1.9 Hz, 1H), 7.80 – 7.70 (m, 2H), 7.67 (t, *J* = 1.9 Hz, 1H), 7.64 – 7.59 (m, 2H), 7.32 – 7.27 (m, 2H), 6.77 (dd, *J* = 7.7, 1.1 Hz, 1H), 5.81 (s, 2H), 3.94 (s, 3H).

ESI-MS(MeOH): m/z 628.5 [M-Cl]

ESI-MS calculated : m/z 628.2

6.1.6. The complex [(η^5-Cp*)RhCl(NHC-14)] 18

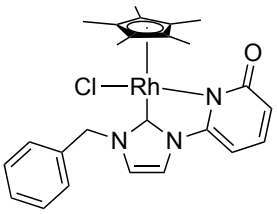

18

Complex [(η^5-Cp*)RhCl(NHC-**14**)] **18** was obtained as light brown solid (y = 65%)

^{1}HNMR (400 MHz, CD_2Cl_2) δ 7.53 – 7.46 (m, 2H), 7.43 – 7.33 (m, 3H), 7.31 (d, *J* = 2.3 Hz, 1H), 7.14 (dd, *J* = 8.7, 7.0 Hz, 1H), 6.77 (d, *J* = 2.3 Hz, 1H), 6.08 (dd, *J* = 8.7, 1.2 Hz, 1H), 6.02 (dd, *J* = 7.1, 1.1 Hz, 1H), 5.56 (d, *J* = 13.8 Hz, 1H), 5.19 (d, *J* = 13.9 Hz, 1H), 1.79 (s, 15H).

^{13}CNMR (101 MHz, CD_2Cl_2) δ 168.55, 166.79, 150.07, 137.33, 135.71, 129.57, 129.19, 121.85, 117.28, 114.77, 91.68, 90.09, 55.01, 10.42.

HRMS(MeOH): m/z 488.1201 [M-Cl]

HRMS calculated: m/z 488.1287

6.1.7. The complex [Pd(η^3-allyl)(NHC-14)] 19

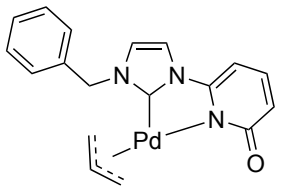

19

Complex [Pd(η^3-allyl)(NHC-**14**)] **19** was obtained as yellowish powder (y = 70%)

^{1}**HNMR** (400 MHz, $CDCl_3$) δ 7.37 – 7.30 (m, 4H), 7.24 – 7.17 (m, 3H), 6.89 (d, *J* = 2.1 Hz, 1H), 6.45 (d, *J* = 8.7 Hz, 1H), 6.04 (dd, *J* = 7.0, 1.0 Hz, 1H), 5.36 (dt, *J* = 7.7, 1.7 Hz, 1H), 5.31 – 5.19 (m, 3H), 3.71 (dt, *J* = 6.9, 2.0 Hz, 1H), 3.59 (dd, *J* = 14.0, 1.4 Hz, 1H), 2.63 – 2.54 (m, 1H).

^{13}**CNMR** (101 MHz, $CDCl_3$) δ 179.64, 168.77, 149.83, 137.92, 135.35, 129.17, 128.64, 127.30, 120.98, 117.09, 116.33, 114.71, 89.73, 73.52, 55.51, 47.56, 26.97.

HRMS(MeOH): m/z 398.0483

HRMS calculated: m/z 398.0485

6.1.8. The complex [Ir(ppy)$_2$(NHC-14)] 20

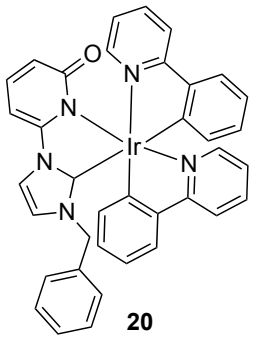

20

Complex [Ir(ppy)$_2$(NHC-**14**)] **20** was obtained as yellowish solid (y = 70%)

^{1}**HNMR** (400 MHz, CD_3CN) δ 8.13 – 8.00 (m, 2H), 7.98 (dt, *J* = 5.8, 1.1 Hz, 1H), 7.95 – 7.80 (m, 3H), 7.81 – 7.74 (m, 2H), 7.71 (ddd, *J* = 8.4, 1.7, 0.8 Hz, 1H), 7.49 – 7.37 (m, 1H), 7.34 (dd, *J* = 7.8, 1.4 Hz, 1H), 7.18 – 6.94 (m, 7H), 6.86 (td, *J* = 7.3, 1.2 Hz, 1H), 6.77 (td, *J* = 7.5, 1.3 Hz, 1H), 6.70 (td, *J* = 7.4, 1.5 Hz, 1H), 6.38 – 6.30 (m, 2H), 6.25 – 6.20 (m, 1H), 6.08 (dd, *J* = 7.6, 1.2 Hz, 1H), 4.69 – 4.54 (m, 2H).

^{13}**CNMR** (151 MHz, CD_3CN) δ 179.12, 169.73, 167.62, 154.09, 151.91, 151.13, 143.88, 138.95, 138.02, 137.73, 132.79, 130.98, 130.58, 130.53, 129.15, 128.27, 126.70, 125.46, 125.15, 124.72, 124.46, 123.85, 122.03, 120.59, 120.48, 119.19, 53.02.

HRMS(MeOH): m/z 752.1998

HRMS calculated: m/z 752.2001

6.1.9. Synthesis of the (H-27)$^{+}$I^{-}

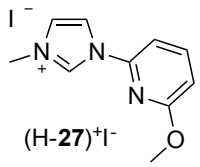

(H-**27**)$^{+}$I^{-}

The compound **12** 2-(1*H*-imidazol-1-yl)-6-methoxypyridin (150 mg, 0.85 mmol) was placed in round bottomed flask and an excess of CH_3I (2.42 g, 17 mmol, 1.1 mL) was added followed by addition of toluene (3 mL). The reaction mixture was stirred overnight at 100 ^{o}C. Subsequently the reaction mixture was cooled to room temperature and the precipitate was filtered off. The solid was washed several times with toluene and dissolved in a small amount of CH_2Cl_2. Addition of Et_2O to the solution yielded a pure white solid compound (H-**24**)$^{+}$I^{-} (255 mg, y = 98 %)

^{1}**HNMR** (400 MHz, DMSO) δ 10.03 (td, *J* = 1.6, 0.8 Hz, 1H), 8.51 (t, *J* = 1.9 Hz, 1H), 8.07 (dd, *J* = 8.3, 7.7 Hz, 1H), 7.97 (t, *J* = 1.9 Hz, 1H), 7.63 – 7.52 (m, 1H), 7.04 (d, *J* = 8.2 Hz, 1H), 3.99 (s, 3H), 3.99 – 3.97 (m, 3H).

^{13}**CNMR** (101 MHz, DMSO) δ 163.12, 144.08, 142.78, 135.39, 124.82, 118.92, 111.58, 105.72, 54.12, 36.42.

HRMS(MeOH): m/z 190.0976 [M-I]$^{+}$

HRMS calculated: m/z 190.0975

6.1.10. Synthesis of the (H-28)$^{+}$I^{-}

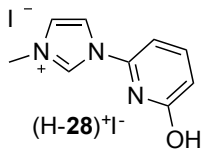

(H-**28**)$^{+}$I^{-}

Imidazolium salt (H-**27**)$^{+}$I^{-} (120 mg, 0.38 mmol) was placed in round-bottomed flask and dissolved in acetic acid (3 mL). Ten equivalents of HBr were added and reaction was brought to 120 ^{o}C and stirred at that temperature for 20 hours. The reaction mixture was concentrated to a small volume and addition of CH_2Cl_2, resulted in precipitation of a white solid. Filtration and washing with Et_2O gave clean product (82 mg, y = 71%)

^{1}**HNMR** (400 MHz, DMSO) δ 11.66 (s, 1H), 10.07 – 9.85 (m, 1H), 8.37 (t, *J* = 1.9 Hz, 1H), 8.10 – 7.89 (m, 2H), 7.46 (d, *J* = 7.7 Hz, 1H), 6.87 (d, *J* = 8.2 Hz, 1H), 3.98 (s, 3H).

^{13}**CNMR** (101 MHz, DMSO) δ 163.39, 144.56, 142.86, 135.28, 124.72, 118.84, 110.73, 104.86, 36.39.

HRMS(MeOH): m/z 176.0819 [M-I]

HRMS calculated: m/z 176.0818 [M-I]

6.1.11. Attempted synthesis of [Ni(NHC-14)$_2$] 25 and of [NiCl(NHC-14)PPh$_3$] 26

Two Schlenk flasks containing (H-**14**)$^+$Br$^-$ X (55 mg, 0.17mmol) and Ag_2O (24.9 mg, 0.11 mmol). The air was evacuated and 3 mL of dry CH_2Cl_2 were added under nitrogen. The reaction mixtures were protected from light and stirred over night in room temperature. Two clean Schlenk flasks were prepared with respectively a) 1 eq (108 mg, 0.17 mmol) and b) 0.5 eq (54 mg, 0.083 mmol) of [$NiCl_2(PPh_3)_2$].

The reaction mixtures containing silver species Ag-NHC-**14** were added under nitrogen to Schlenk flask a and b with [$NiCl_2(PPh_3)_2$]. Upon this addition, immediately appeared green-blue precipitate. The reactions were stirred for another 6 hours in room temperature and filtered. The solids were dissolved in MeOH/DMSO and precipitated with Et_2O.

6.2. Catalysis preparation

Reactions were set up according to the following procedure. The solution of the substrate (1 mL, 4 mM) and catalyst (0.5 mL, 0.38 mM) were placed in the flask and filled up with solvent to the volume of 4 mL. In case of addition of solution of KOH (4 mM) the volume of solvent was changing.

For the alcohol oxidation and ketone reduction as model reactions, benzyl alcohol and acetophenone were selected as substrates respectively (1 mM, 4 mL). Alcohol oxidation was performed in toluene and ketone reduction in isopropanol.

The catalyst loading was set to 5%. In case of alcohol oxidation all stock solutions were prepared in toluene with addition of 1% DMSO to the catalyst solutions. For ketone reduction, the stock solutions were prepared in isopropanol.

The alcohol oxidation was carried out without a hydrogen acceptor either in an open flask or in a sealed flask.

To analyse the catalysis results, reaction mixtures (1 mL) were mixed with 1,3,5- trimethoxy benzene (1 mL, 0.5 mM, as internal standard) and analysed by reversed phase HPLC using Dr. Maisch Reprospher C18-DE column (150 x 4,6 mm, 5 µm particle size).

7. ^{1}HNMR and ^{13}CNMR

7.1. Compound 12

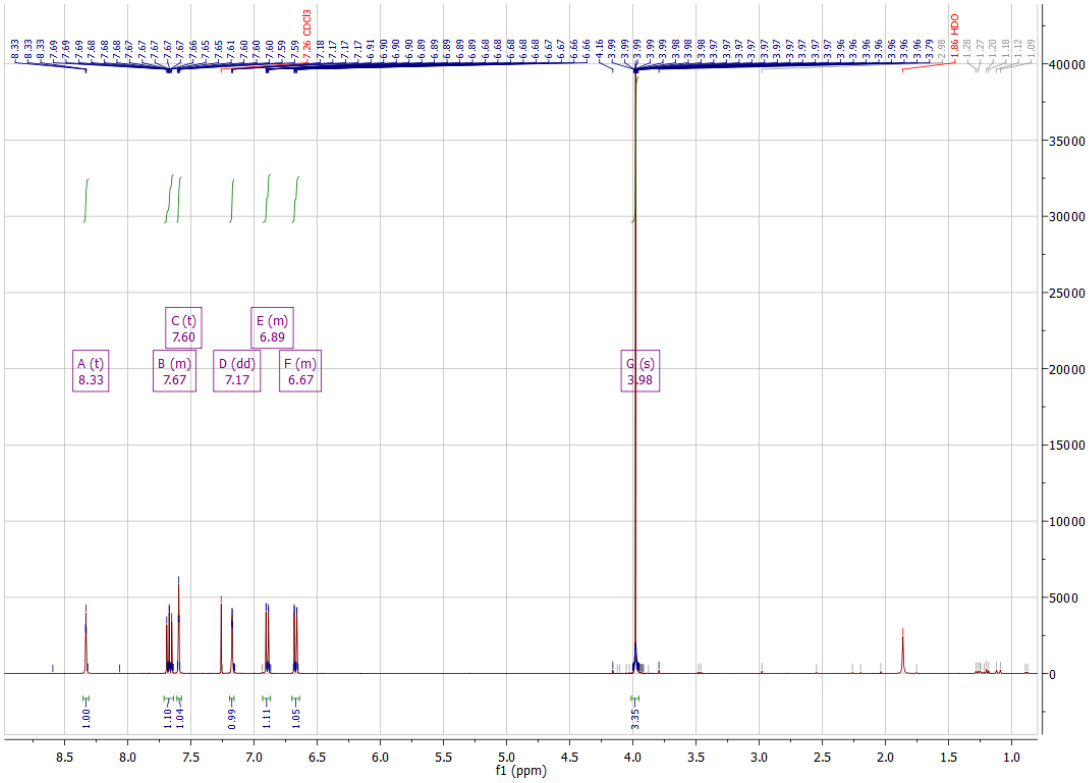

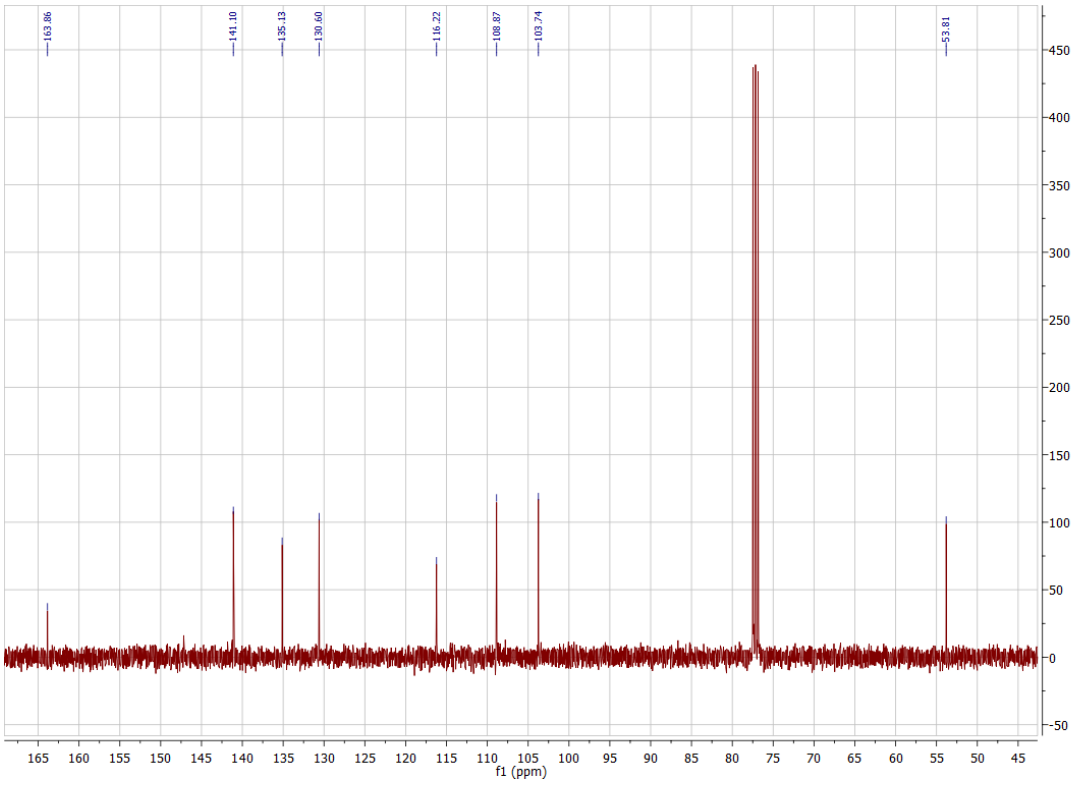

7.2. Compound $(H\text{-}13)^{+}Br^{-}$

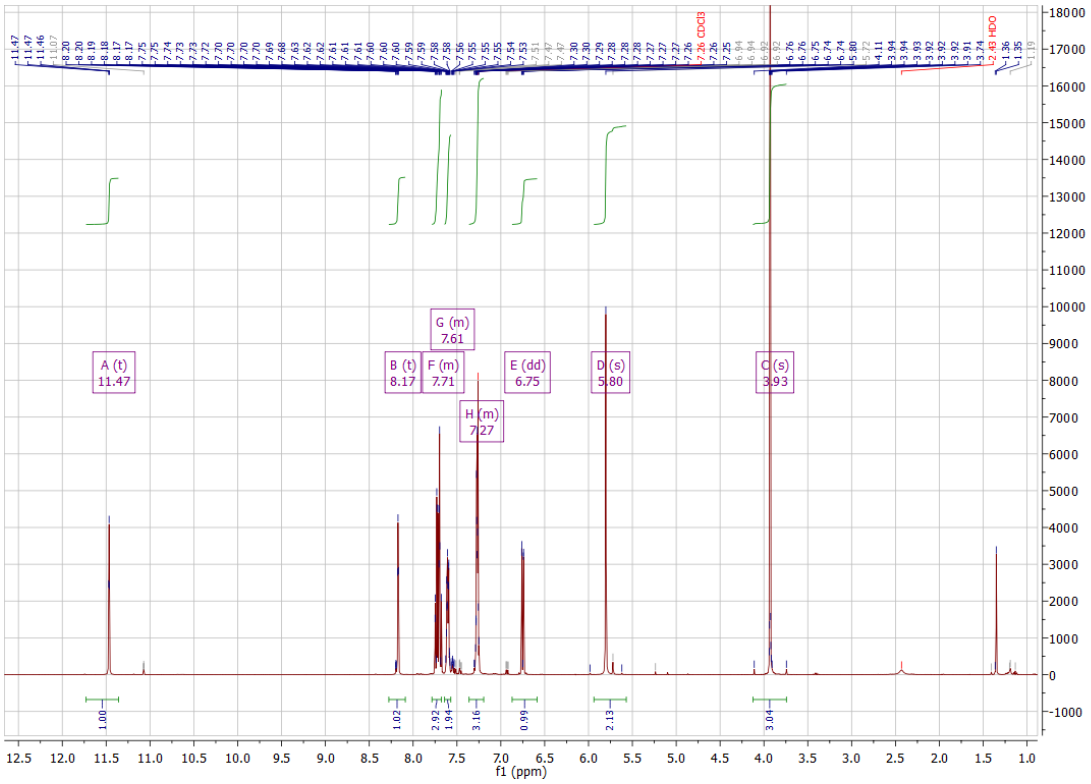

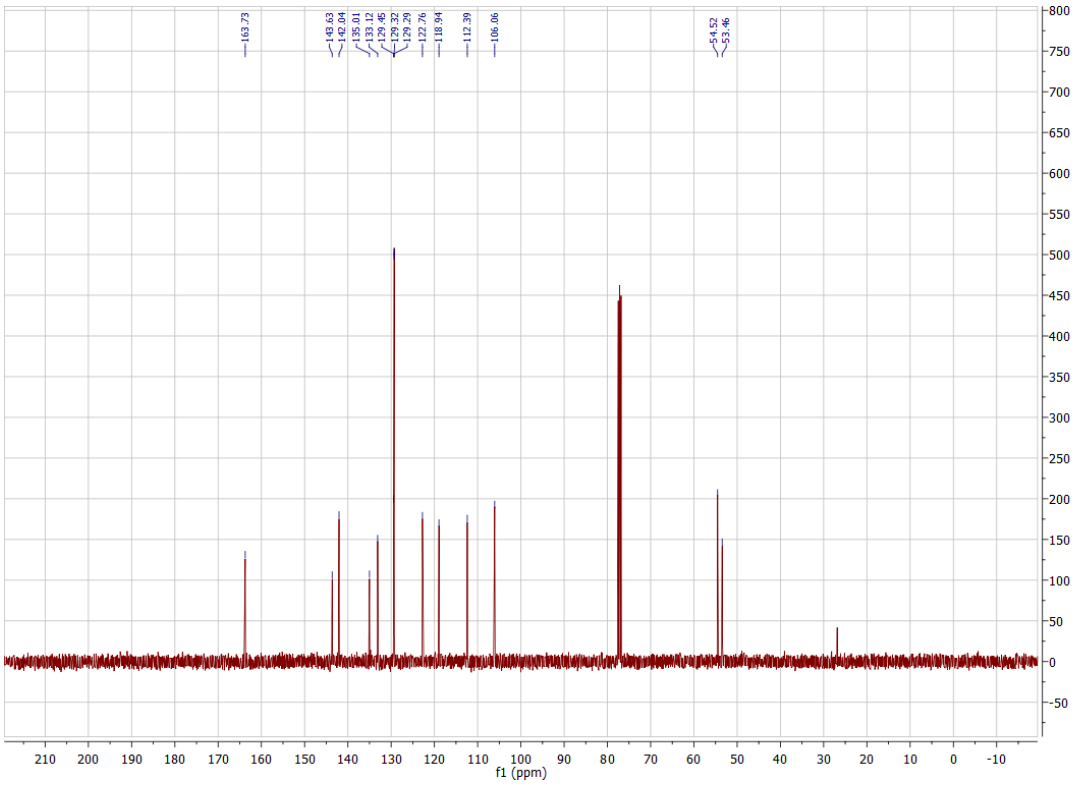

7.3. Compound $(H\text{-}14)^{+}Br^{-}$

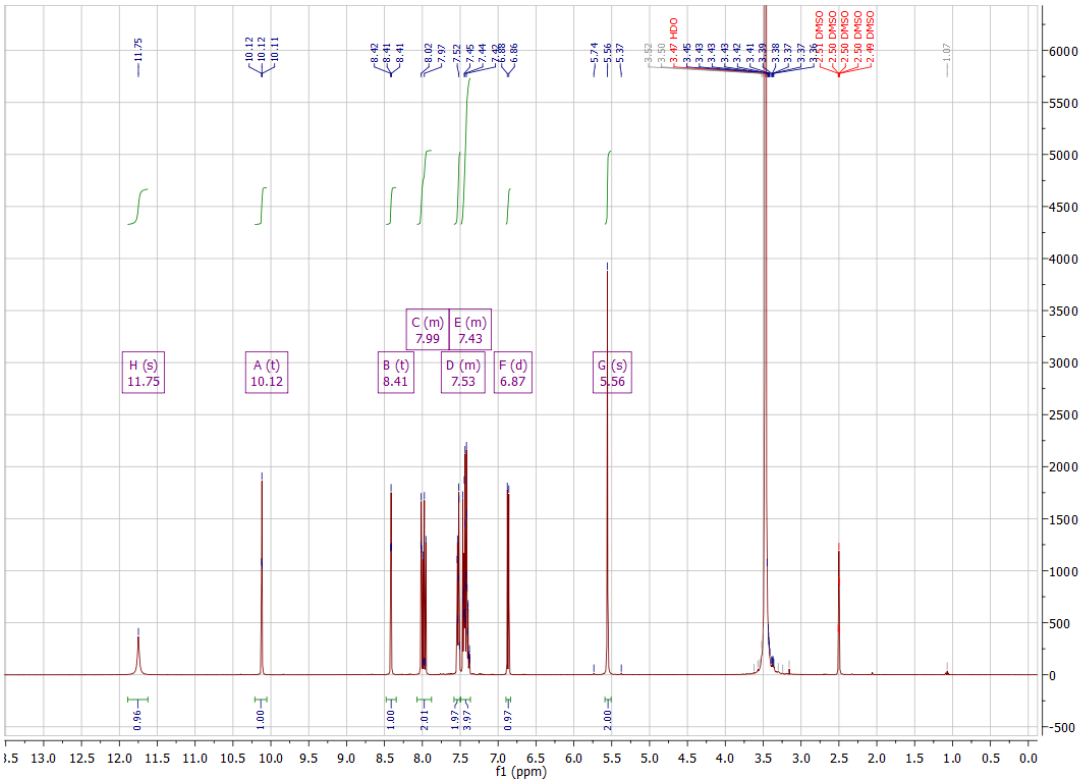

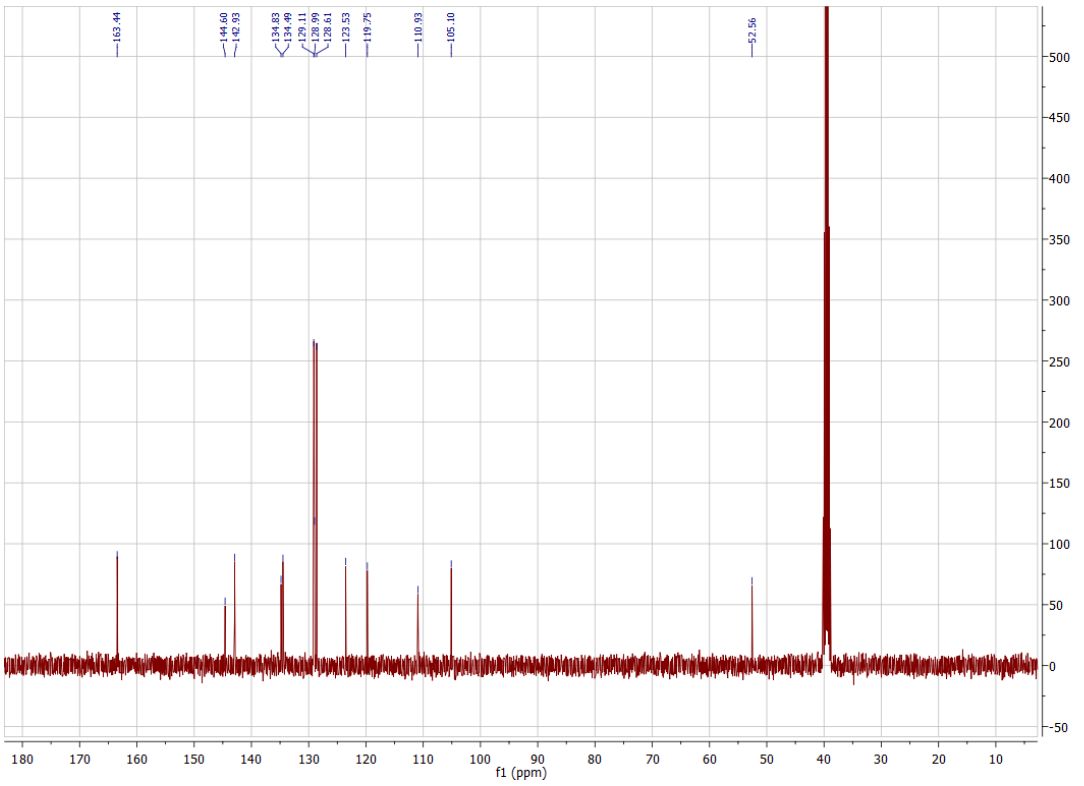

7.4. Complex [(η^6-$C_{10}H_{14}$)Ru(NHC-14)Cl] 15

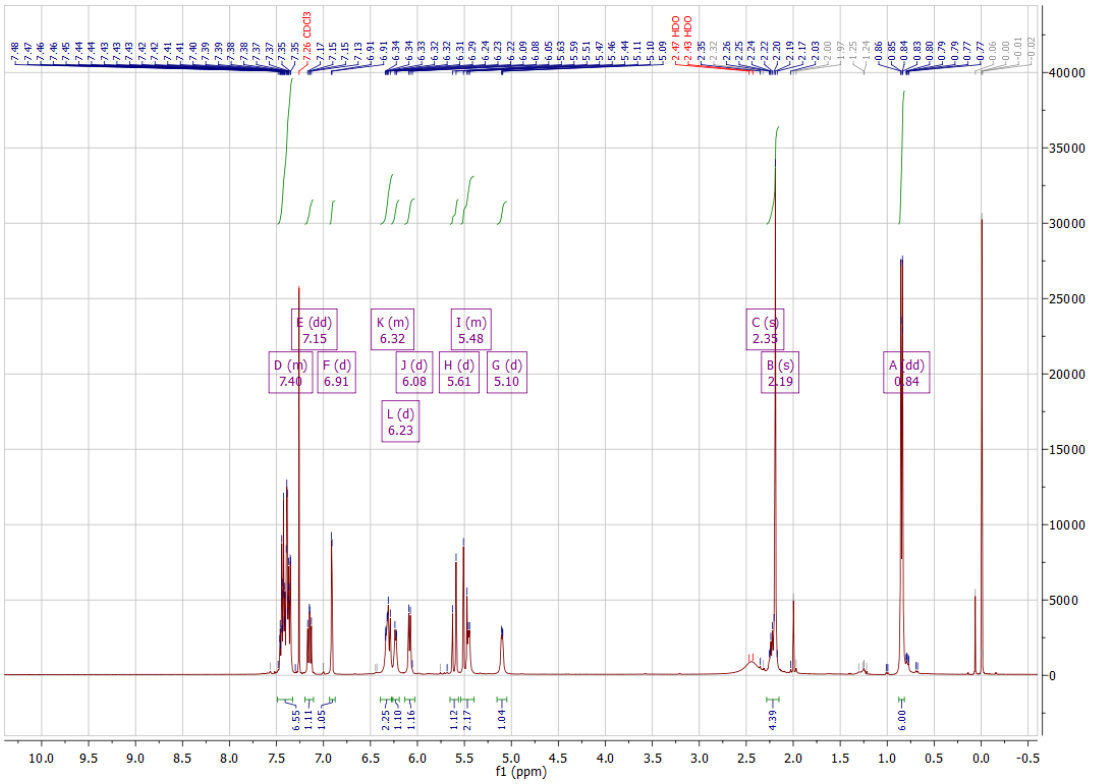

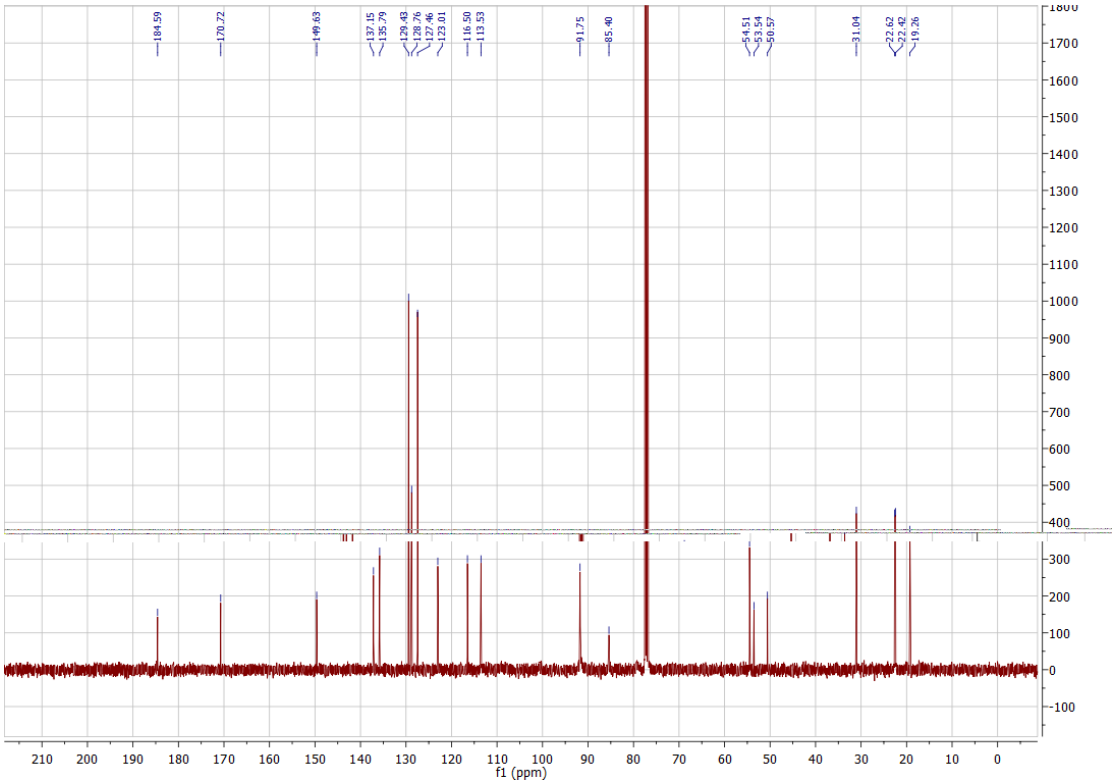

7.5. Complex [(η^5-Cp*)Ir(NHC-14)Cl] 16

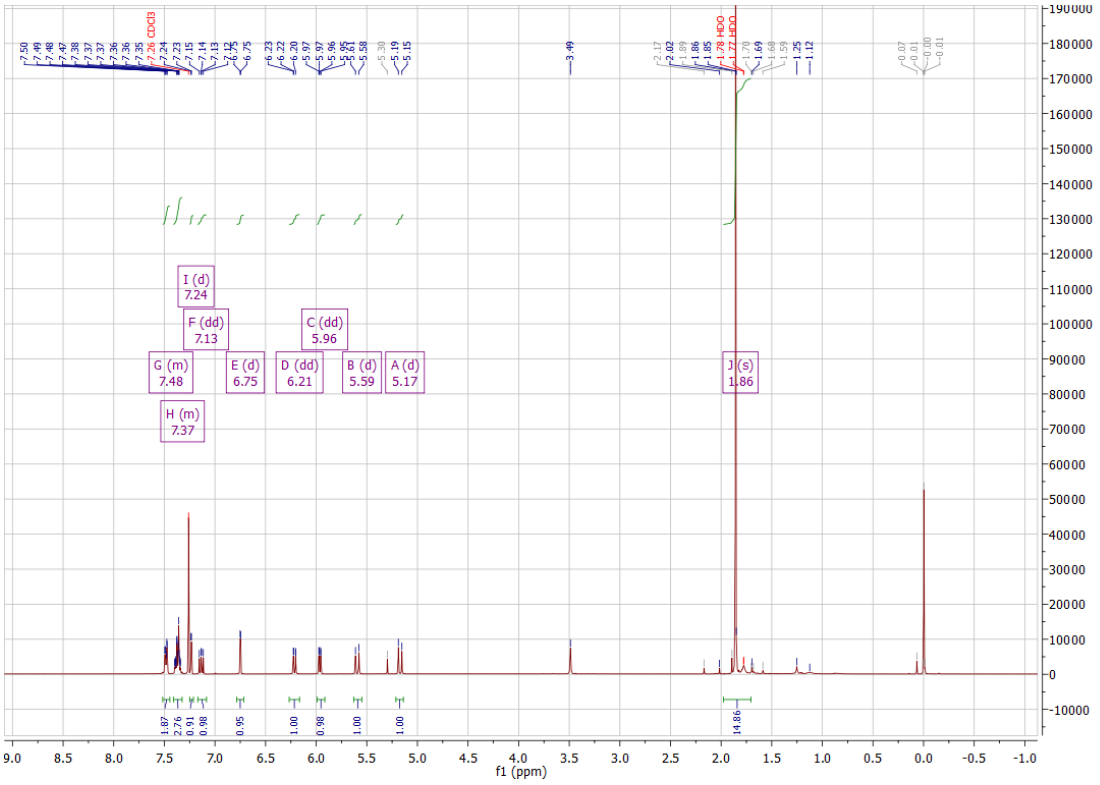

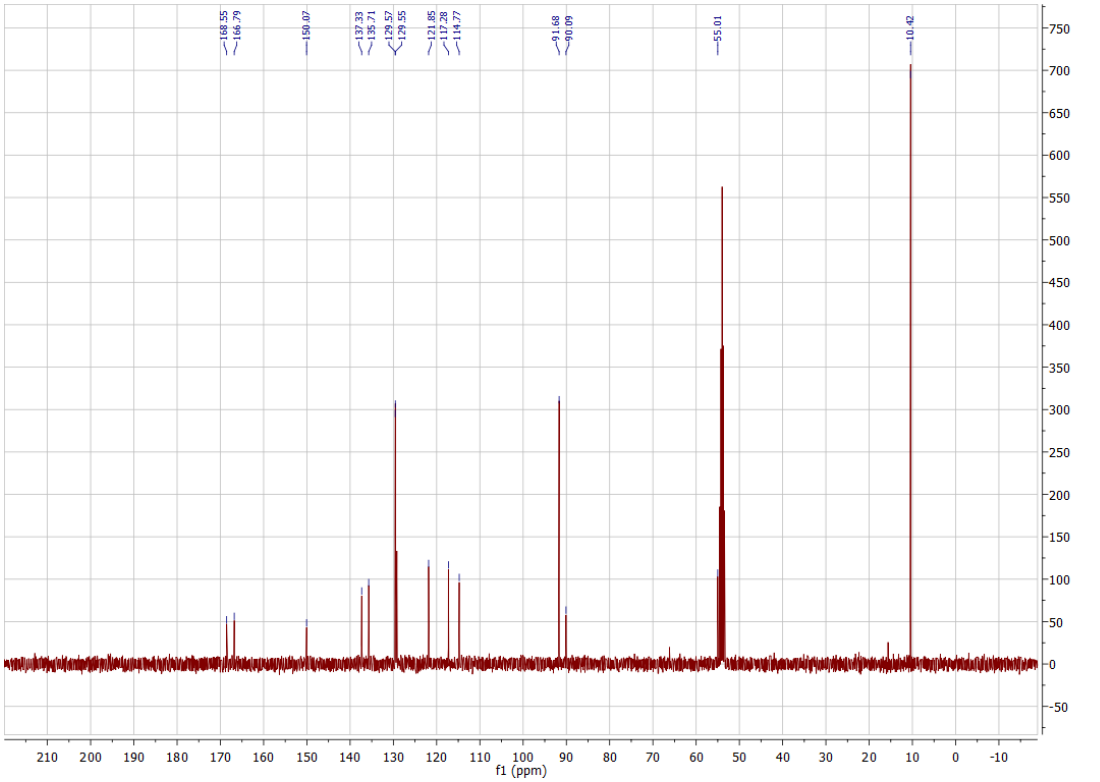

7.6. Complex [(η^5-Cp*)Ir(NHC-13)Cl] 17

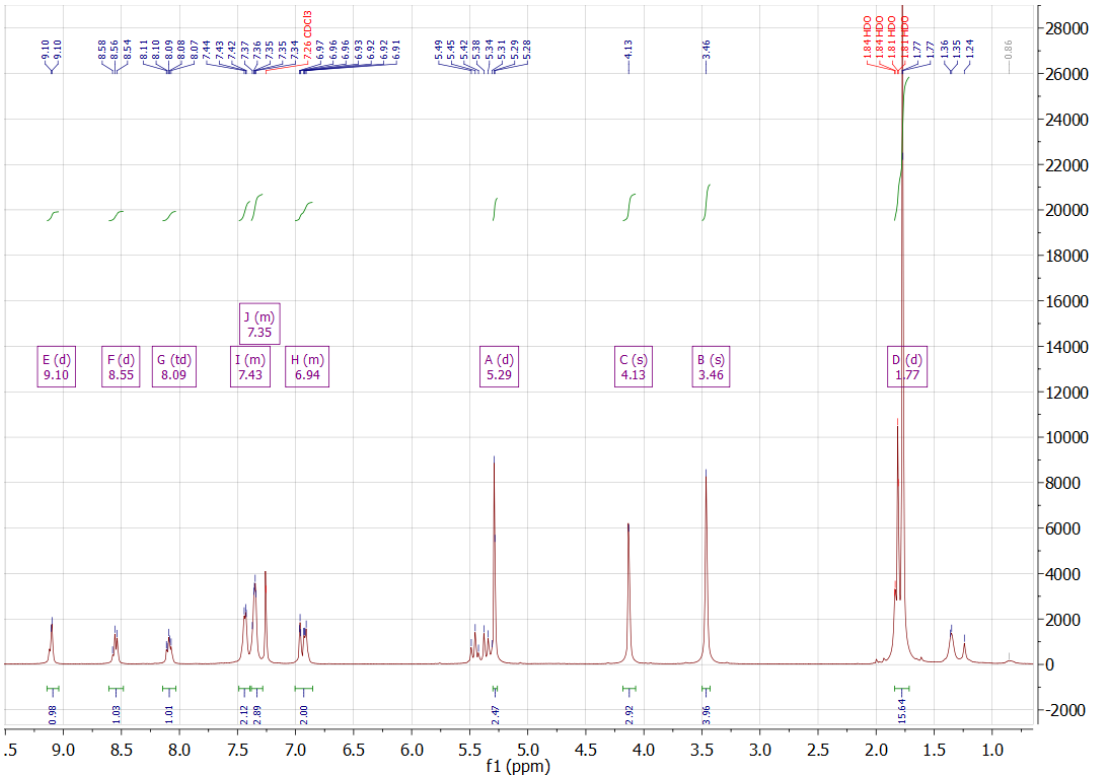

7.7. Complex [(η^5-Cp*)Rh(NHC-14)Cl] 18

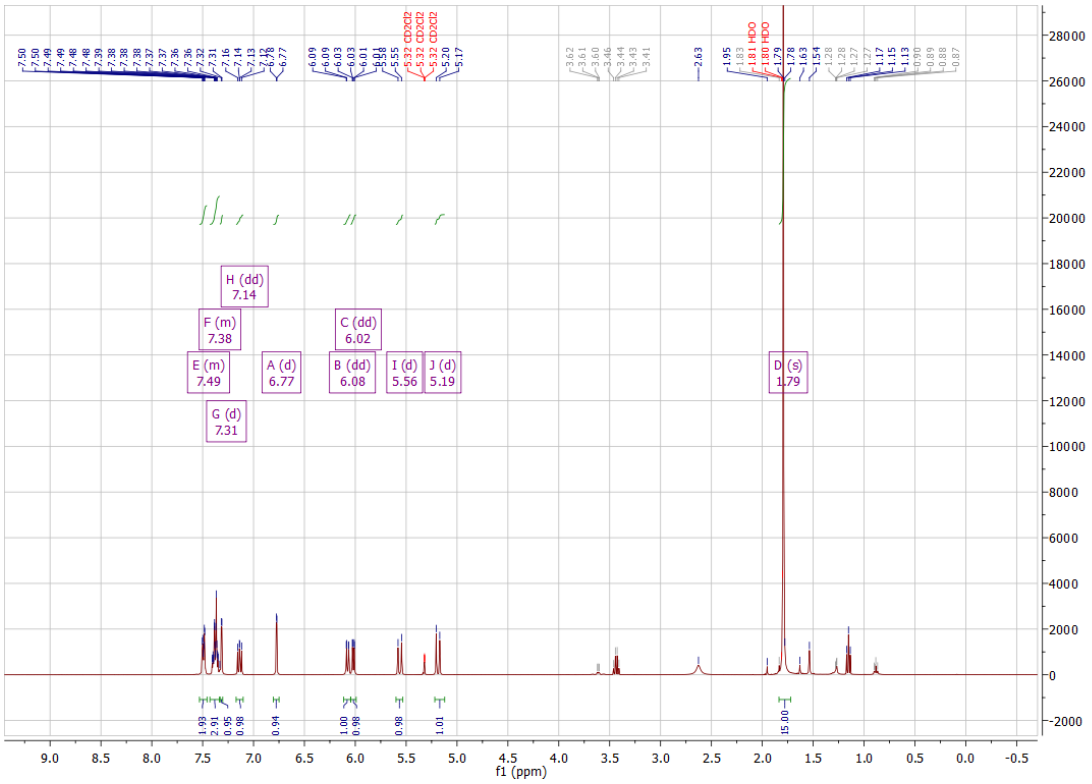

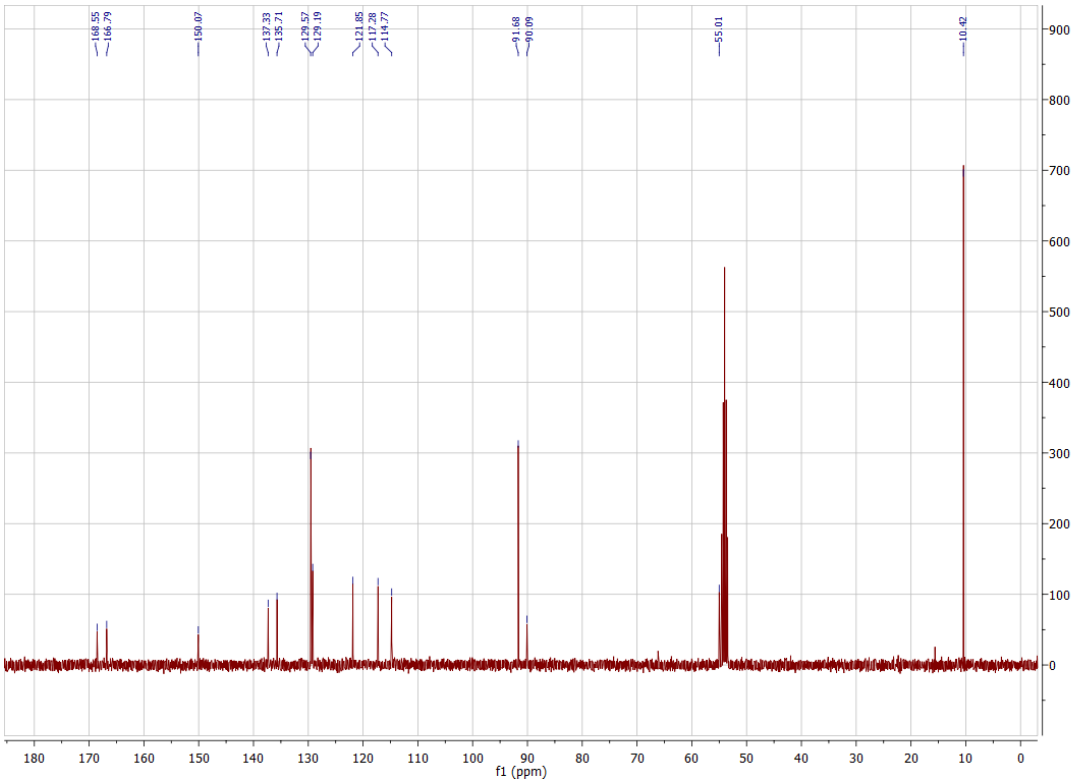

7.8. [Pd(η^3-allyl)(NHC-14)] 19

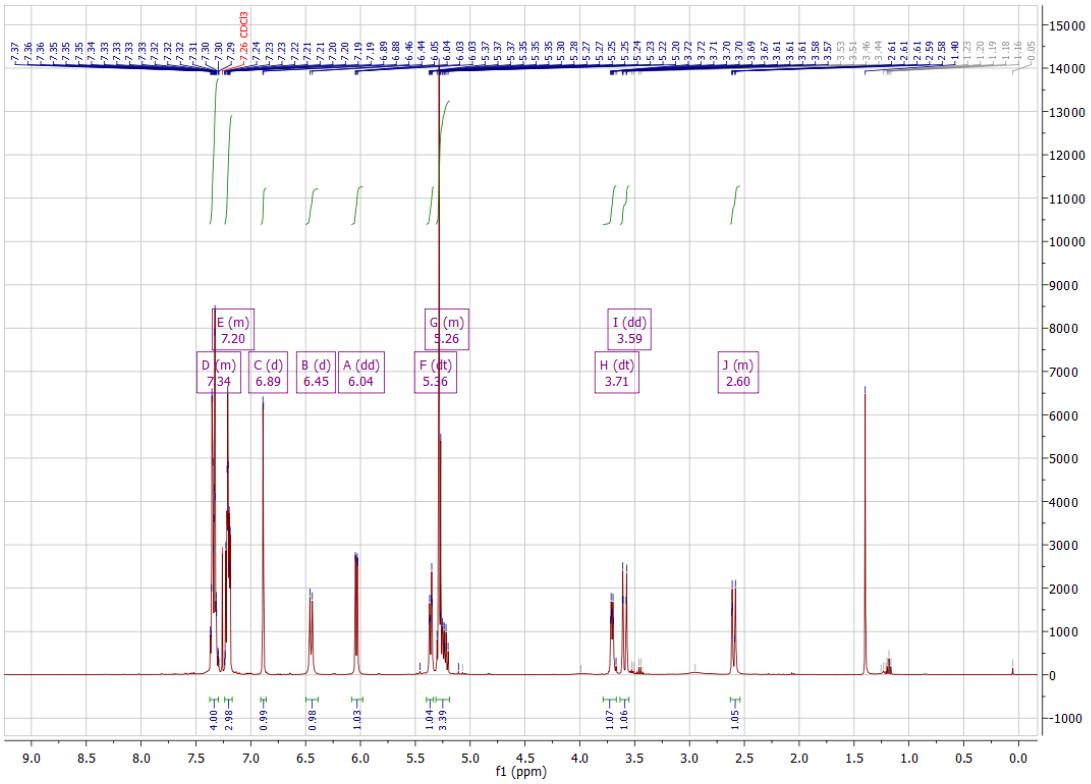

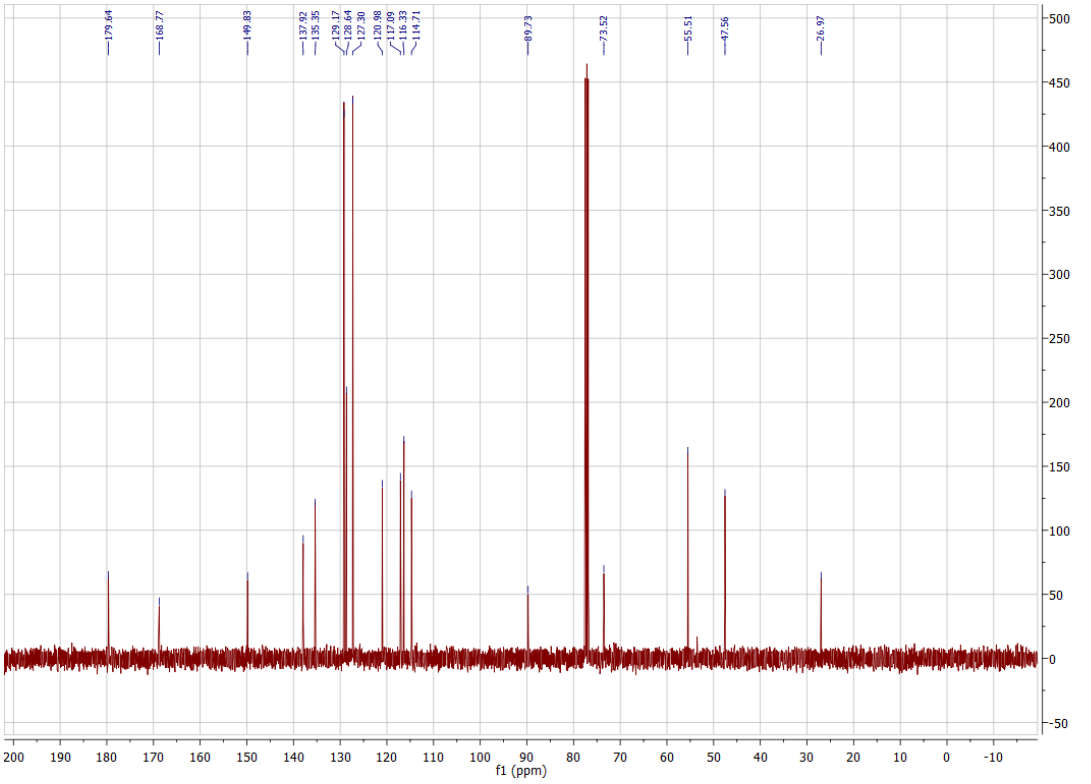

7.9. Complex [Ir(ppy)$_2$(NHC-14)] 20

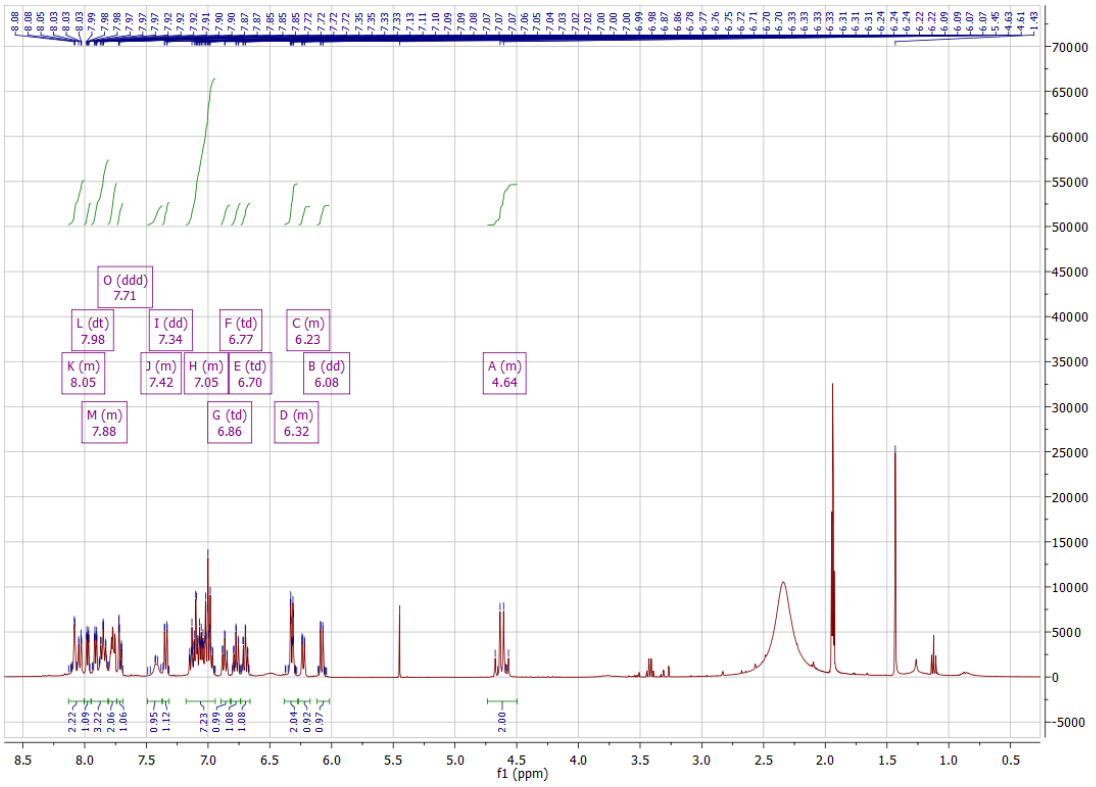

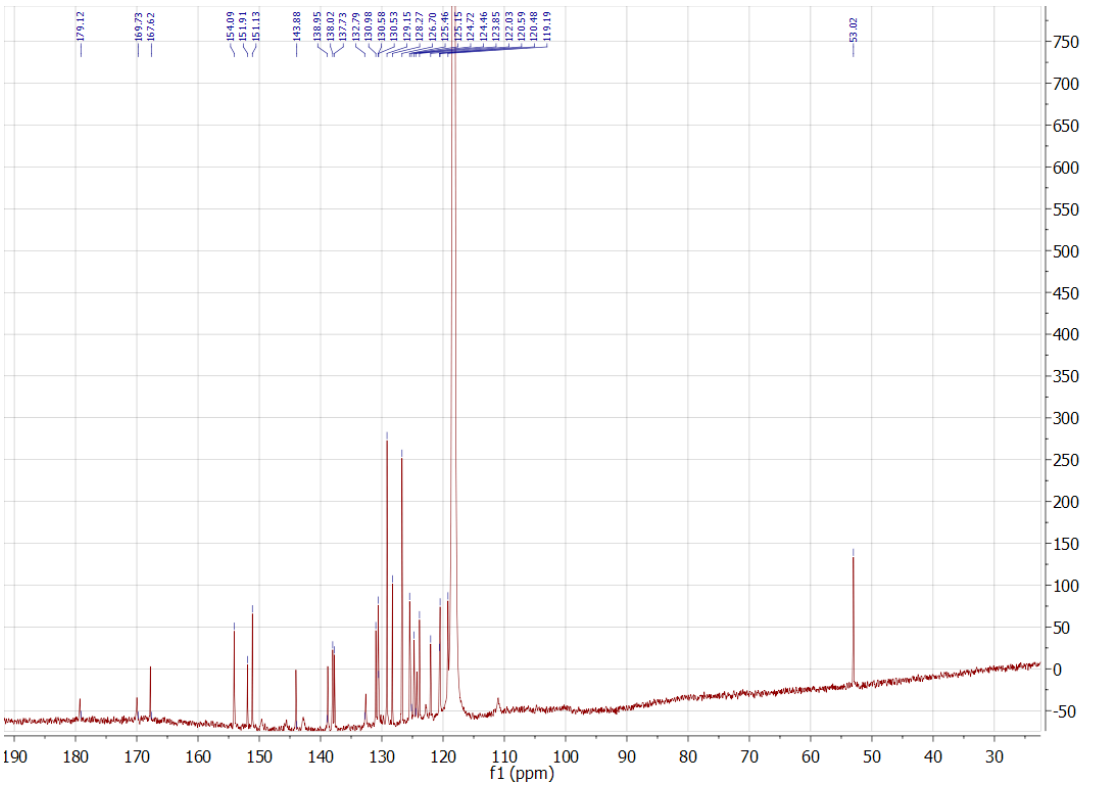

7.10. $(H\text{-}27)^{+}I^{-}$

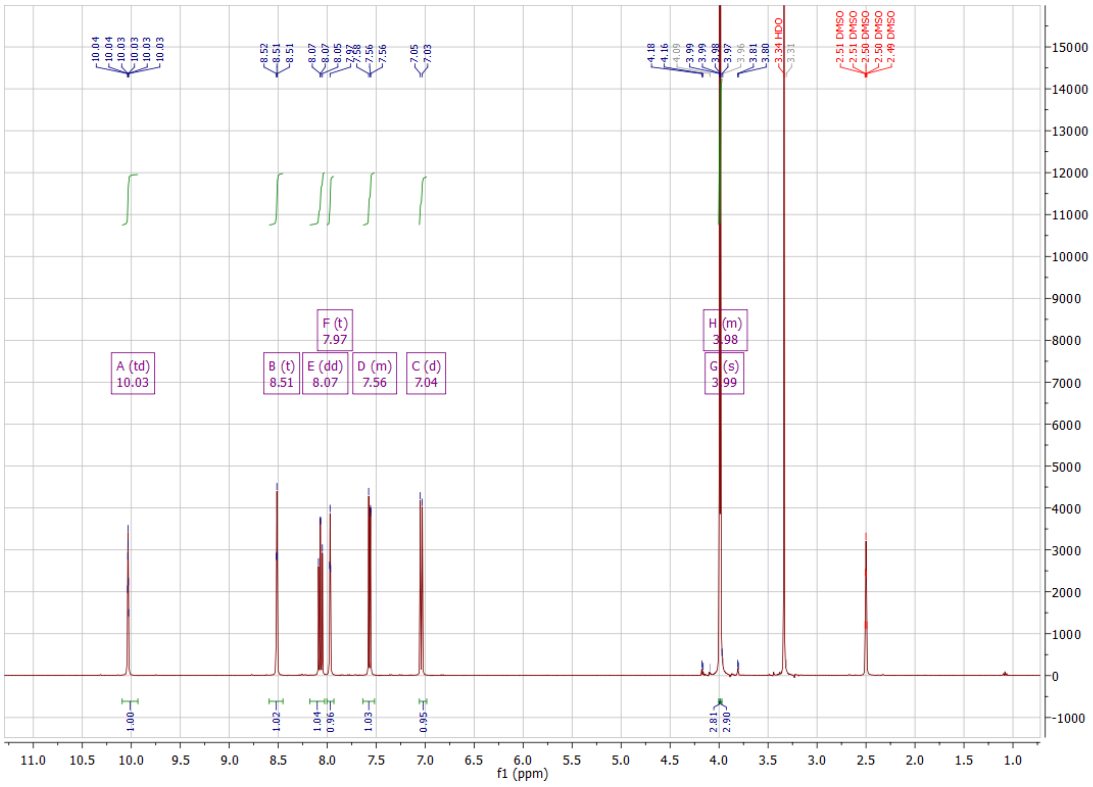

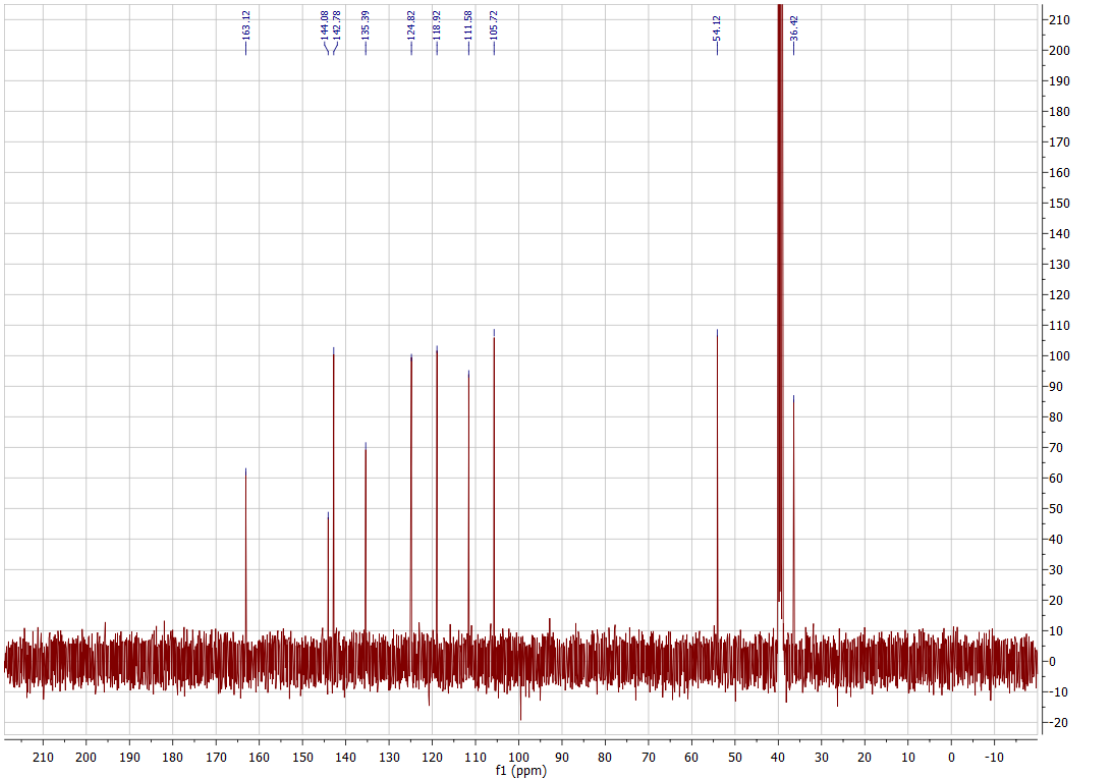

7.11. $(H\text{-}28)^{+}I^{-}$

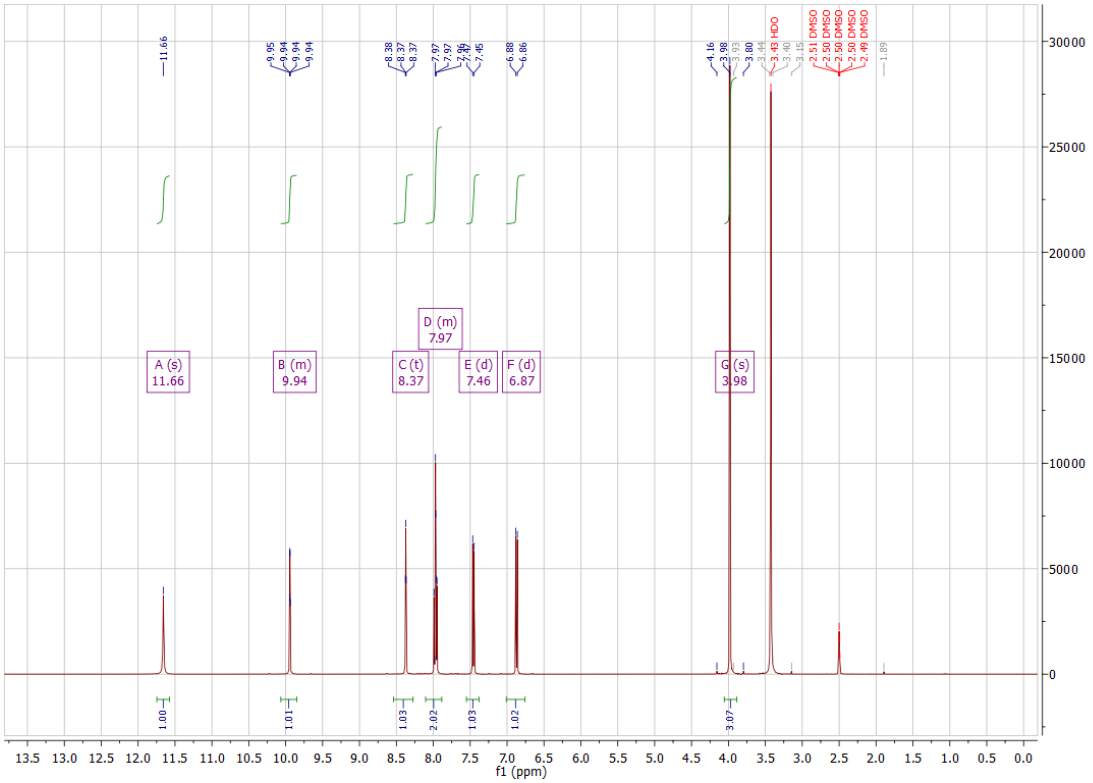

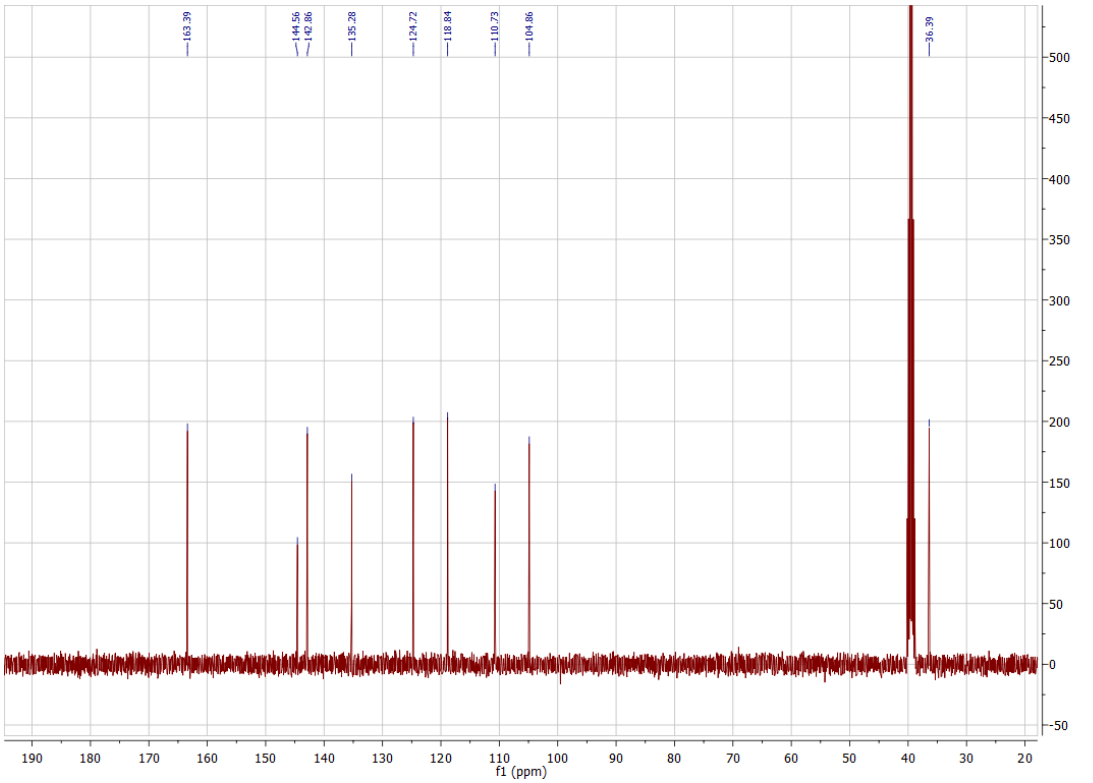

8. Appendix

8.1. Data for [(η^6-*p*-cymene)RuCl(NHC-14)] 15

Crystal data for [(η^6-*p*-cymene)RuCl(NHC-**14**)] **15**: formula $C_{25}H_{28}ClN_3O_2Ru$, M = 539.04, F(000) = 552, orange plate, size 0.020 * 0.110 * 0.160 mm^3, triclinic, space group P -1, Z = 2, a = 9.7520(7) Å, b = 10.7151(8) Å, c = 11.7536(8) Å, α = 92.110(3)°, β = 98.450(3)°, γ = 106.150(3)°, V = 1163.00(8) $Å^3$, Dcalc. = 1.539 Mg * m^{-3}. The crystal was measured on a Bruker Kappa Apex2 diffractometer at 123K using graphite-monochromated Cu Kα-radiation with λ = 1.54178 Å, Θmax = 69.079°. Minimal/maximal transmission 0.48/0.87, μ = 6.730 mm^{-1}. The Apex2 suite has been used for datacollection and integration. From a total of 12741 reflections, 4229 were independent (merging r = 0.027). From these, 3789 were considered as observed (I>2.0 σ (I)) and were used to refine 295 parameters. The structure was solved by Other methods using the program Superflip. Least-squares refinement against F was carried out on all non-hydrogen atoms using the program CRYSTALS. R = 0.0250 (observed data), wR = 0.0315 (all data), GOF = 1.0676. Minimal/maximal residual electron density = -0.38/1.02 e $Å^{-3}$. Chebychev polynomial weights were used to complete the refinement. Plots were produced using Mercury.

Table 1. Crystal data for [(η^6-*p*-cymene)RuCl(NHC-**14**)] **15**

formula	$C_{25}H_{28}ClN_3O_2Ru$
formula weight	539.04
Z, calculated density	2, 1.539 Mg * m^{-3}
F(000)	552
description and size of crystal	orange plate, 0.020 * 0.110 * 0.160 mm^3
absorption coefficient	6.730 mm^{-1}
min/max transmission	0.48 / 0.87
temperature	123K
radiation(wavelength)	*C*u Kα (λ = 1.54178 Å)
Crystal system, space group	triclinic, P -1
a	9.7520(7) Å
b	10.7151(8) Å
c	11.7536(8) Å
α	92.110(3)°
β	98.450(3)°
γ	106.150(3)°
V	1163.00(8) $Å^3$
min/max Θ	3.815° / 69.079°
number of collected reflections	12741
number of independent reflections	4229 (merging r = 0.027)
number of observed reflections	3789 (I>2.0σ(I))
number of refined parameters	295
r	0.0250

rW 0.0315

goodness of fit 1.0676

Table 2. Coordinates for [(η^6-*p*-cymene)RuCl(NHC-**14**)] **15** in SHELX-format.

[(η^6-*p*-cymene)RuCl(NHC-**14**)] **15** in space group P -1

CELL 1.54178 9.7520 10.7151 11.7536 92.110 98.450 106.150

ZERR 2 0.0007 0.0008 0.0008 0.003 0.003 0.003

LATT -1

SYMM x,y,z

SYMM -x,-y,-z

SFAC C H Cl N O Ru

UNIT 25 28 1 3 2 1

FVAR 1.0

Ru1 6 0.337693 0.303889 0.755166 11.0000 0.0118

Cl1 3 0.42045 0.53901 0.79245 11.0000 0.0175

N1 4 0.24567 0.33128 0.58567 11.0000 0.0151

N2 4 0.46986 0.33024 0.54856 11.0000 0.0139

N3 4 0.64372 0.33069 0.68321 11.0000 0.0151

O1 5 0.02659 0.33797 0.63012 11.0000 0.0224

C1 1 0.1064 0.3394 0.55513 11.0000 0.0171

C2 1 0.0579 0.3478 0.4352 11.0000 0.0199

C3 1 0.1444 0.3459 0.35409 11.0000 0.0196

C4 1 0.2864 0.3388 0.38646 11.0000 0.0172

C5 1 0.3292 0.33354 0.50226 11.0000 0.0143

C6	1	0.5909	0.3417	0.49524	11.0000	0.0172
C7	1	0.7001	0.3418	0.57997	11.0000	0.0161
C8	1	0.5019	0.32312	0.66441	11.0000	0.0139
C9	1	0.7302	0.3356	0.79660	11.0000	0.0176
C10	1	0.7578	0.2079	0.82676	11.0000	0.0191
C11	1	0.7390	0.1062	0.7441	11.0000	0.0244
C12	1	0.7690	-0.0092	0.7755	11.0000	0.0349
C13	1	0.8174	-0.0220	0.8891	11.0000	0.0406
C14	1	0.8352	0.0779	0.9719	11.0000	0.0395
C15	1	0.8058	0.1924	0.9419	11.0000	0.0290
C16	1	0.2319	0.3881	1.0097	11.0000	0.0262
C17	1	0.2489	0.2859	0.92672	11.0000	0.0182
C18	1	0.1373	0.2217	0.83757	11.0000	0.0186
C19	1	0.1597	0.1300	0.75575	11.0000	0.0199
C20	1	0.2880	0.0930	0.76744	11.0000	0.0199
C21	1	0.4010	0.1593	0.85969	11.0000	0.0182
C22	1	0.3842	0.2561	0.93632	11.0000	0.0186
C23	1	0.3125	-0.0105	0.6870	11.0000	0.0326
C24	1	0.2155	-0.0337	0.5706	11.0000	0.0509
C25	1	0.2945	-0.1365	0.7479	11.0000	0.0417
H21	2	-0.0355	0.3544	0.4130	11.0000	0.0247
H31	2	0.1095	0.3509	0.2774	11.0000	0.0237
H41	2	0.3478	0.3407	0.3345	11.0000	0.0207
H61	2	0.5940	0.3498	0.4181	11.0000	0.0207
H71	2	0.7946	0.3492	0.5737	11.0000	0.0194

H91 2 0.8215 0.3995 0.7992 11.0000 0.0214

H92 2 0.6785 0.3613 0.8513 11.0000 0.0218

H111 2 0.7066 0.1143 0.6675 11.0000 0.0298

H121 2 0.7552 -0.0757 0.7194 11.0000 0.0428

H131 2 0.8384 -0.0976 0.9102 11.0000 0.0490

H141 2 0.8677 0.0688 1.0488 11.0000 0.0490

H151 2 0.8199 0.2602 0.9980 11.0000 0.0351

H161 2 0.3139 0.4636 1.0176 11.0000 0.0416

H162 2 0.2228 0.3548 1.0834 11.0000 0.0408

H163 2 0.1466 0.4130 0.9821 11.0000 0.0411

H181 2 0.0502 0.2469 0.8237 11.0000 0.0225

H191 2 0.0833 0.0924 0.6894 11.0000 0.0253

H211 2 0.4961 0.1442 0.8659 11.0000 0.0231

H221 2 0.4667 0.3077 0.9905 11.0000 0.0228

H231 2 0.4123 0.0185 0.6733 11.0000 0.0394

H241 2 0.2408 -0.0940 0.5219 11.0000 0.0783

H242 2 0.1156 -0.0680 0.5787 11.0000 0.0788

H243 2 0.2265 0.0456 0.5334 11.0000 0.0787

H251 2 0.3090 -0.2023 0.6978 11.0000 0.0649

H252 2 0.3654 -0.1210 0.8165 11.0000 0.0645

H253 2 0.1980 -0.1658 0.7674 11.0000 0.0648

O2 5 0.0877 0.5410 0.80194 11.0000 0.0337

H1 2 0.178 0.559 0.812 11.0000 0.0527

H2 2 0.066 0.482 0.750 11.0000 0.0528

HKLF 4

8.2. [(η^5-Cp*)IrCl(NHC-14)] 16

Crystal data for [(η^5-Cp*)IrCl(NHC-**14**)] **16**: formula $C_{26}H_{31}Cl_2IrN_3O_2$, M = 704.91, F(000) = 2776, yellow needle, size 0.030 * 0.040 * 0.150 mm^3, orthorhombic, space group P b c a, Z = 8, a = 13.8421(5) Å, b = 15.7414(5) Å, c = 25.9700(10) Å, α = 90°, β = 90°, γ = 90°, V = 5658.7(3) $Å^3$, Dcalc. = 1.655 Mg * m^{-3}. The crystal was measured on a Bruker Kappa Apex2 diffractometer at 123K using graphite-monochromated Cu Kα-radiation with λ = 1.54178 Å, Θmax = 70.112°. Minimal/maximal transmission 0.63/0.71, = 70.1126 mm^{-1}. The Apex2 suite has been used for datacollection and integration. From a total of 41431 reflections, 5287 were independent (merging r = 0.046). From these, 4028 were considered as observed (I>2.0 σ (I)) and were used to refine 334 parameters. The structure was solved by Other methods using the program Superflip. Least-squares refinement against F was carried out on all non-hydrogen atoms using the program CRYSTALS. R = 0.0355 (observed data), wR = 0.0437 (all data), GOF = 1.0553. Minimal/maximal residual electron density = -0.79/1.47 e $Å^{-3}$. Chebychev polynomial weights were used to complete the refinement. Plots were produced using Mercury.

Table 3. Crystal data for [(η^5-Cp*)IrCl(NHC-**14**)] **16.**

formula	$C_{26}H_{31}Cl_2IrN_3O_2$
formula weight	704.91
Z, calculated density	8, 1.655 Mg * m^{-3}
F(000)	2776

description and size of crystal yellow needle, 0.030 * 0.040 * 0.150 mm^3

absorption coefficient 11.526 mm^{-1}

min/max transmission 0.63 / 0.71

temperature 123K

radiation(wavelength) *C*u Kα (λ = 1.54178 Å)

Crystal system, space group orthorhombic, P b c a

a 13.8421(5) Å

b 15.7414(5) Å

c 25.9700(10) Å

α 90°

β 90°

γ 90°

V 5658.7(3) $Å^3$

min/max Θ 4.582° / 70.112°

number of collected reflections 41431

number of independent reflections 5287 (merging r = 0.046)

number of observed reflections 4028 (I>2.0σ(I))

number of refined parameters 334

r 0.0355

rW 0.0437

goodness of fit 1.0553

Table 4. Coordinates for [(η^5-Cp*)IrCl(NHC-**14**)] **16** in SHELX-format.

(η^5-Cp*)IrCl(NHC-**14**)] **16** in space group P b c a

CELL 1.54178 13.8421 15.7414 25.9700 90 90 90

ZERR 8 0.0005 0.0005 0.001 0 0

LATT -1

SYMM x,y,z

SYMM -x,-y,-z

SYMM -x+1/2,y+1/2,z

SYMM x+1/2,-y+1/2,-z

SYMM x,-y+1/2,z+1/2

SYMM -x,y+1/2,-z+1/2

SYMM -x+1/2,-y,z+1/2

SYMM x+1/2,y,-z+1/2

SFAC C . H . Cl . Ir N O

UNIT 26 50 31 50 2 50 1 3 2

FVAR 1.0

Ir1 4 0.720001 0.630849 0.683067 11.0000 0.0246

Cl1 1 0.61289 0.52054 0.71306 11.0000 0.0330

N1 5 0.6075 0.7177 0.69565 11.0000 0.0291

N2 5 0.6844 0.7337 0.77272 11.0000 0.0279

N3 5 0.7853 0.6400 0.79856 11.0000 0.0305

O1 6 0.5229 0.6813 0.62409 11.0000 0.0418

C1 1 0.5314 0.7289 0.6621 11.0000 0.0336

C2 1 0.4657 0.7969 0.6736 11.0000 0.0366

C3	1	0.4732	0.8430	0.7177	11.0000	0.0385
C4	1	0.5468	0.8264	0.7530	11.0000	0.0343
C5	1	0.6108	0.7632	0.74001	11.0000	0.0272
C6	1	0.7003	0.7493	0.82455	11.0000	0.0330
C7	1	0.7630	0.6915	0.8405	11.0000	0.0343
C8	1	0.7373	0.6660	0.75671	11.0000	0.0290
C9	1	0.8469	0.5636	0.80152	11.0000	0.0343
C10	1	0.8209	0.5076	0.84634	11.0000	0.0309
C11	1	0.7247	0.4875	0.8580	11.0000	0.0418
C12	1	0.7037	0.4366	0.8997	11.0000	0.0480
C13	1	0.7770	0.4038	0.9297	11.0000	0.0519
C14	1	0.8718	0.4222	0.9187	11.0000	0.0537
C15	1	0.8945	0.4750	0.8771	11.0000	0.0425
C16	1	0.8292	0.6903	0.63610	11.0000	0.0311
C17	1	0.8699	0.6143	0.65848	11.0000	0.0323
C18	1	0.8138	0.5432	0.64190	11.0000	0.0304
C19	1	0.7415	0.5752	0.60554	11.0000	0.0318
C20	1	0.7532	0.6637	0.60094	11.0000	0.0317
C21	1	0.8727	0.7773	0.6393	11.0000	0.0431
C22	1	0.9594	0.6134	0.6907	11.0000	0.0427
C23	1	0.8296	0.4527	0.6560	11.0000	0.0446
C24	1	0.6706	0.5208	0.5772	11.0000	0.0414
C25	1	0.7021	0.7225	0.5650	11.0000	0.0442
H21	1	0.4173	0.8095	0.6503	11.0000	0.0441
H31	1	0.4298	0.8859	0.7247	11.0000	0.0460

H41	1	0.5519	0.8569	0.7835	11.0000	0.0407
H61	1	0.6732	0.7924	0.8441	11.0000	0.0399
H71	1	0.7872	0.6847	0.8730	11.0000	0.0419
H91	1	0.8395	0.5312	0.7706	11.0000	0.0420
H92	1	0.9140	0.5809	0.8052	11.0000	0.0420
H111	1	0.6751	0.5089	0.8382	11.0000	0.0498
H121	1	0.6405	0.4236	0.9068	11.0000	0.0590
H131	1	0.7622	0.3702	0.9582	11.0000	0.0616
H141	1	0.9215	0.3996	0.9389	11.0000	0.0650
H151	1	0.9586	0.4879	0.8696	11.0000	0.0511
H211	1	0.8939	0.7889	0.6738	11.0000	0.0659
H212	1	0.8245	0.8194	0.6298	11.0000	0.0660
H213	1	0.9267	0.7828	0.6168	11.0000	0.0659
H221	1	0.9592	0.6568	0.7164	11.0000	0.0647
H222	1	0.9671	0.5601	0.7072	11.0000	0.0647
H223	1	1.0144	0.6222	0.6691	11.0000	0.0647
H231	1	0.8757	0.4468	0.6830	11.0000	0.0701
H232	1	0.7697	0.4259	0.6660	11.0000	0.0698
H233	1	0.8535	0.4229	0.6262	11.0000	0.0699
H241	1	0.6167	0.5540	0.5669	11.0000	0.0639
H242	1	0.7010	0.4982	0.5471	11.0000	0.0639
H243	1	0.6503	0.4743	0.5987	11.0000	0.0639
H251	1	0.7445	0.7342	0.5366	11.0000	0.0677
H252	1	0.6455	0.6952	0.5522	11.0000	0.0678
H253	1	0.6867	0.7742	0.5828	11.0000	0.0678

```
Cl2   1   0.9032     0.4348     0.52734  10.5.0000   0.1061
Cl3   1   1.0709     0.4009     0.46651  10.5.0000   0.1492
Cl4   1   0.8975     0.3146     0.44617  10.5.0000   0.0948
C26   1   0.9656     0.3593     0.4893   10.5.0000   0.0759
H261  1   0.9858     0.3146     0.5122   10.5.0000   0.0789
O2    6   0.3996     0.7157     0.54872  11.0000   0.0689
C27   1   0.3913     0.6441     0.5194   11.0000   0.0726
H1    1   0.4468     0.7185     0.5752   11.0000   0.0828
H271  1   0.3881     0.6598     0.4842   11.0000   0.1130
H272  1   0.4479     0.6097     0.5245   11.0000   0.1129
H273  1   0.3331     0.6149     0.5291   11.0000   0.1131
HKLF  4
END
```

8.3. Data for [Pd(η^3-allyl)(NHC-14)] 19

Crystal data for [Pd(η^3-allyl)(NHC-**14**)] **19**: formula $C_{21}H_{22}ClN_3OPd_2$, M = 580.68, F(000) = 572, colourless block, size 0.070 * 0.110 * 0.160 mm^3, triclinic, space group P -1, Z = 2, a = 9.1531(9) Å, b = 10.9083(10) Å, c = 11.9753(11) Å, α = 80.933(3)°, β = 71.012(3)°, γ = 68.349(3)°, V = 1049.89(10) $Å^3$, Dcalc. = 1.837 Mg * m^{-3}. The crystal was measured on a Bruker Kappa Apex2 diffractometer at 123K using graphite-monochromated Cu Kα-radiation with λ = 1.54178 Å, Θmax = 69.069°. Minimal/maximal transmission 0.19/0.35, μ = 15.119 mm^{-1}. The Apex2 suite has been used for datacollection and integration. From a total of 12342 reflections, 3781 were independent (merging r = 0.025). From these, 3584 were considered as observed (I>2.0 σ (I)) and were used to refine 309 parameters. The structure was solved by Other methods using the program Superflip. Least-squares refinement against F was carried out on all non-hydrogen atoms using the program CRYSTALS. R = 0.0215 (observed data), wR = 0.0243 (all data), GOF = 1.0837. Minimal/maximal residual electron density = -0.55/0.84 e $Å^{-3}$. Chebychev polynomial weights were used to complete the refinement. Plots were produced using Mercury.

Table 5. Crystal data for [Pd(η^3-allyl)(NHC-**14**)] **19.**

formula	$C_{21}H_{22}ClN_3OPd_2$
formula weight	580.68
Z, calculated density	2, 1.837 Mg * m^{-3}

F(000) 572

description and size of crystal colourless block, 0.070 * 0.110 * 0.160 mm^3

absorption coefficient 15.119 mm^{-1}

min/max transmission 0.19 / 0.35

temperature 123K

radiation(wavelength) *C*u Kα (λ = 1.54178 Å)

Crystal system, space group triclinic, P -1

a 9.1531(9) Å

b 10.9083(10) Å

c 11.9753(11) Å

α 80.933(3)°

β 71.012(3)°

γ 68.349(3)°

V 1049.89(10) $Å^3$

min/max Θ 3.907° / 69.069°

number of collected reflections 12342

number of independent reflections 3781 (merging r = 0.025)

number of observed reflections 3584 (I>2.0σ(I))

number of refined parameters 309

r 0.0215

rW 0.0243

goodness of fit 1.0837

Table 6. Coordinates for [Pd(η^3-allyl)(NHC-**14**)] **19** in SHELX-format.

[Pd(η^3-allyl)(NHC-**14**)] **19** in space group P -1

CELL 1.54178 9.1531 10.9083 11.9753 80.933 71.012 68.349

ZERR 2 0.0009 0.001 0.0011 0.003 0.003 0.003

LATT -1

SYMM x,y,z

SYMM -x,-y,-z

SFAC C H Cl N O Pd

UNIT 21 22 1 3 1 2

FVAR 1.0

Pd1 6 0.541645 0.744491 0.473141 11.0000 0.0182

Pd2 6 0.75812 0.689045 0.848820 11.0000 0.0204

Cl1 3 0.91934 0.46439 0.80962 11.0000 0.0235

N1 4 0.4690 0.66097 0.64591 11.0000 0.0185

N2 4 0.2987 0.61898 0.56278 11.0000 0.0180

N3 4 0.2959 0.66606 0.38306 11.0000 0.0211

O1 5 0.6474 0.70126 0.71685 11.0000 0.0267

C1 1 0.5283 0.6597 0.7380 11.0000 0.0203

C2 1 0.4515 0.6130 0.8521 11.0000 0.0235

C3 1 0.3259 0.5664 0.8681 11.0000 0.0238

C4 1 0.2720 0.5630 0.7722 11.0000 0.0222

C5 1 0.3471 0.6120 0.6658 11.0000 0.0180

C6 1 0.1825 0.5741 0.5489 11.0000 0.0227

C7 1 0.1809 0.6038 0.4363 11.0000 0.0241

C8	1	0.3701	0.6768	0.4599	11.0000	0.0199
C9	1	0.3191	0.7235	0.2623	11.0000	0.0257
C10	1	0.1738	0.8460	0.2534	11.0000	0.0231
C11	1	0.0974	0.8577	0.1680	11.0000	0.0241
C12	1	-0.0386	0.9687	0.1612	11.0000	0.0334
C13	1	-0.0959	1.0684	0.2387	11.0000	0.0391
C14	1	-0.0191	1.0576	0.3235	11.0000	0.0437
C15	1	0.1152	0.9472	0.3309	11.0000	0.0358
H21	2	0.4879	0.6133	0.9149	11.0000	0.0285
H31	2	0.2747	0.5390	0.9427	11.0000	0.0286
H41	2	0.1909	0.5308	0.7806	11.0000	0.0271
H61	2	0.1216	0.5318	0.6065	11.0000	0.0268
H71	2	0.1185	0.5864	0.3986	11.0000	0.0295
H91	2	0.4175	0.7449	0.2397	11.0000	0.0308
H92	2	0.3298	0.6591	0.2107	11.0000	0.0307
H111	2	0.1341	0.7906	0.1161	11.0000	0.0286
H121	2	-0.0899	0.9746	0.1053	11.0000	0.0400
H131	2	-0.1873	1.1413	0.2356	11.0000	0.0474
H141	2	-0.0582	1.1236	0.3755	11.0000	0.0517
H151	2	0.1663	0.9400	0.3876	11.0000	0.0427
C16	1	0.6381	0.8227	0.3038	10.622.0000	0.0323
C17	1	0.6612	0.8854	0.3866	10.622.0000	0.0303
C18	1	0.7439	0.8087	0.4663	10.622.0000	0.0290
H161	2	0.5629	0.8772	0.2597	10.622.0000	0.0397
H162	2	0.7328	0.7597	0.2527	10.622.0000	0.0403

H171	2	0.6003	0.9792	0.4001	10.622.0000	0.0372
H181	2	0.7347	0.8493	0.5353	10.622.0000	0.0354
H182	2	0.8513	0.7467	0.4377	10.622.0000	0.0359
C116	1	0.7200	0.8348	0.4803	10.378.0000	0.0299
C117	1	0.7477	0.8036	0.3649	10.378.0000	0.0318
C118	1	0.6152	0.8477	0.3166	10.378.0000	0.0328
H1161	2	0.8016	0.7861	0.5204	10.378.0000	0.0371
H1162	2	0.6762	0.9265	0.5006	10.378.0000	0.0369
H1171	2	0.8495	0.7349	0.3265	10.378.0000	0.0382
H1181	2	0.5544	0.9411	0.3137	10.378.0000	0.0402
H1182	2	0.6324	0.8101	0.2429	10.378.0000	0.0401
C19	1	0.6465	0.8835	0.8991	10.544.0000	0.0351
C20	1	0.6971	0.8007	0.9912	10.544.0000	0.0349
C21	1	0.8619	0.7199	0.9700	10.544.0000	0.0307
H191	2	0.5293	0.9246	0.9072	10.544.0000	0.0431
H192	2	0.7034	0.9443	0.8594	10.544.0000	0.0431
H201	2	0.6153	0.7869	1.0636	10.544.0000	0.0423
H211	2	0.8915	0.6496	1.0270	10.544.0000	0.0379
H212	2	0.9479	0.7576	0.9367	10.544.0000	0.0384
C119	1	0.8174	0.7194	0.9984	10.456.0000	0.0360
C120	1	0.7482	0.8398	0.9447	10.456.0000	0.0346
C121	1	0.5930	0.8699	0.9307	10.456.0000	0.0447
H1191	2	0.9319	0.6919	0.9948	10.456.0000	0.0447
H1192	2	0.7565	0.6938	1.0754	10.456.0000	0.0452
H1201	2	0.8130	0.8972	0.9070	10.456.0000	0.0412

```
H1211 2   0.5544     0.9457     0.8796   10.456.0000   0.0549
H1212 2   0.5021     0.8638     0.9991   10.456.0000   0.0550
HKLF  4
END
```

8. References

[1] O. R. Luca, R. H. Crabtree, *Chem. Soc. Rev*. **2013**, *42*, 1440.

[2] V. K. K. Praneeth, M. R. Ringenberg, T.R. Ward, *Angew. Chem. Int. Ed. Engl*. **2012**, *51*, 10228.

[3] S. Blanchard, E. Derat, M. Desage-El Murr, L. Fensterbank, M. Malacria, V. Mouriès-Mansuy, *Eur. J. Inorg. Chem.* **2012**, 376.

[4] R. Karvembu, R. Prabhakaran, K. Natarajan, *Coord. Chem. Rev.* **2005**, *249*, 911.

[5] Y. Shvo, D. Czarkie, Y. Rahamim, *J. Am. Chem. Soc.* **1986**, *108*, 7402.

[6] H.- J. Knölker, E. Baum, H. Goesmann, R. Klauss, *Angew. Chem. Int. Ed. Engl.* **1999**, *38*, 2064.

[7] D. Chen, R. Scopelliti, X. Hu, *Angew. Chem. Int. Ed.* ***2010***, *49* 7512.

[8] T.R. Simmons, G. Berggren, M. Bacchi, M. Fontecave, V. Artero, *Coord. Chem. Rev*. **2014**, *271*, 127.

[9] S. Dey, P.K. Das, A. Dey, *Coord. Chem. Rev*. **2013**, *257*, 42.

[10] K. Wieghart, P.J. Chirik, Science **2010**, *237*, 794.

[11] J. Zhang, G. Leitus, Y. Ben-David, D. Milstein, *J. Am. Chem. Soc.* **2005**, *127*, 10840.

[12] B. Gnanaprakasam, J. Zhang, D. Milstein, *Angew. Chem*. **2010**, *122*, 1510.

[13] B. Butschke, K.L. Fillman, T. Bendikov, L.J.W. Shimon, Y. Diskin-Posner, G. Leitus, *Inorg. Chem.* **2015**, *54*, 4909.

[14] E. Balaraman, B. Gnanaprakasam, L.J.W. Shimon, D. Milstein, *J.*

Am. Chem. Soc. **2010**, *132*, 16756.

[15] B. Gnanaprakasam, Y. Ben-David, D. Milstein, *Adv. Synth. Catal.* **2010**, *352,* 3169.

[16] T. Zell, R. Langer, M.A. Iron, L. Konstantinovski, L.J.W. Shimon, Y. Diskin-Posner, et al., *Inorg. Chem.* **2013**, *52,* 9636.

[17] D. Srimani, Y. Ben-David, D. Milstein, *Chem. Commun.* **2013**, *49* 6632.

[18] C. Gunanathan, D. Milstein, *Chem. Rev*. **2014**, *114,* 12024.

[19] S.W. Kohl, L. Weiner, L. Schwartsburd, L. Konstantinovski, L.J.W. Shimon, Y. Ben-David, *Science* **2009**, *324*, 74.

[20] S. Enthaler, J. von Langermann, T. Schmidt, *Energy Environ. Sci.* **2010**, *3*, 1207.

[21] T.C. Johnson, D.J. Morris, M. Wills, *Chem. Soc. Rev.* **2010**, *39*, 81.

[22] B. Loges, A. Boddien, F. Gärtner, H. Junge, M. Beller, *Top. Catal.* **2010**, *53*, 902.

[23] Y. Himeda, Eur. J. *Inorg. Chem*. **2007**, 3927.

[24] W.-H. Wang, J.F. Hull, J.T. Muckerman, E. Fujita, Y. Himeda, *Energy Environ. Sci*. **2012**, *5*, 7923.

[25] Y.M. Badiei, W.-H. Wang, J.F. Hull, D.J. Szalda, J.T. Muckerman, Y. Himeda, *Inorg. Chem.* **2013**, *52,* 12576.

[26] R. Kawahara, K.-I. Fujita, R. Yamaguchi, *Angew. Chem. Int. Ed.* **2012**, *51,* 12790.

[27] T. Zhang, K.E. deKrafft, J.-L. Wang, C. Wang, L. Wenblin, *Eur. J. Inorg. Chem.* **2014**, 698.

[28] J. DePasquale, I. Nieto, L.E. Reuther, C.J. Herbst-Gervasoni, J.J.

Paul, V. Mochalin, *Inorg. Chem.* **2013**, *52,* 9175.

[29] K.-I. Fujita, Y. Tanaka, M. Kobayashi, R. Yamaguchi, *J. Am. Chem. Soc.* **2014**, *136*, 4829.

[30] G. Zeng, S. Sakaki, K.-I. Fujita, H. Sano, R. Yamaguchi, *ACS Catal.* **2014**, *4,* 1010.

[31] F. Glorius, N-Heterocyclic Carbenes in Catalysis—An Introduction, in: Topics in Organometallic Chemistry, Springer Berlin Heidelberg, **2007**: pp. 1–20.

[32] H. Clavier, S.P. Nolan, *Chem. Commun.* **2010**, *46,* 841.

[33] W.A. Herman, C. Kocher, *Angew. Chem. Int. Eng.* **1997**, *36,* 2162.

[34] S. Zlatogorsky, C. A. Muryn, F. Tuna, D. J. Evans, M. J. Ingleson, *Organometallics* **2011**, *30*, 4974.

[35] S. J. Hock, L.-A. Schaper, W. A. Herrmann, F. E. Kühn, *Chem. Soc. Rev.* **2013**, *42*, 5073.

[36] B. M. Neilson, C. W. Bielawski, *J. Am. Chem. Soc.* **2012**, *134*,12693.

[37] S. L. Balof, S. J. P'Pool, N. J. Berger, E. J. Valente, A. M. Shiller, H.-J. Schanz, *Dalton Trans.* **2008**, 5791.

[38] V. Miranda-Soto, D. B. Grotjahn, A. L. Cooksy, J. A. Golen, C.E. Moore, A. L. Rheingold, *Angew. Chem. Int. Ed*. **2010**, *50*, 631.

[39] A. J. Arduengo, R.L. Harlow, M. Kline, *J. Am. Chem. Soc.* **1991**, *113*, 361.

[40] J. C. Garrison, W. J. Youngs, *Chem. Rev.* **2005**, *105*, 3978.

[41] H. Lebel, M.K. Janes, A.B. Charette, S.P. Nolan, *J. Am. Chem. Soc.* **2004**, *126*, 5046.

[42] F. Monti, F. Kessler, M. Delgado, J. Frey, F. Bazzanini, G. Accorsi, *Inorg. Chem.* **2013,** *52*, 10292.

[43] S. Warratz, L. Postigo, B. Royo, *Organometallics* **2013**, *32*, 893.

[44] O. Santoro, A. Collado, A.M.Z. Slawin, S.P. Nolan, C.S.J. Cazin, *Chem. Commun.* **2013**, *49*, 10483.

[45] F. Cisnetti, P. Lemoine, M. El-Ghozzi, D. Avignant, A. Gautier, Tetrahedron Lett. **2010**, *51,* 5226

[46] X. Liu, Q. Xia, Y. Zhang, C. Chen, W. Chen, *J. Org. Chem*. **2013**, *78*, 8531

[47] T. D. Nixon, M. K. Whittlesey, J. M. J. Williams, *Dalton Trans*. **2009**, 753.

[48] M. H. Hamid, M. H. Slatford, J. M. J. Williams. *Adv. Synth. Catal*. **2007**, *349*, 1555.

[49] J. M. Keith, *J. Org. Chem.* **2008**, *73,* 327.